TIME-DEPENDENT RESPONSE OF REINFORCED CONCRETE ELEMENTS NEAR COLLAPSE

A Dissertation presented to

the Faculty of the Graduate School at

the University of Missouri – Columbia

In Partial Fulfillment of the Requirements for the Degree

of Doctor of Philosophy

---

by

MOHAMMED SHUBAILI

Dr. Sarah Orton, Dissertation Supervisor

May 2021

The undersigned, appointed by the dean of the Graduate School, have examined the thesis entitled:

TIME-DEPENDENT RESPONSE OF REINFORCED CONCRETE ELEMENTS NEAR COLLAPSE

Presented by Mohammed Shubaili,

a candidate for the degree of degree of Doctor of Philosophy in Civil Engineering,

and hereby certify that, in their opinion, it is worthy of acceptance.

_____

Professor Sarah Orton

_____

Professor Hani Salim

_____

Professor Zhen Chen

_____

Professor Sanjeev Khanna

DEDICATION

I would like to thank my wonderful parents, my wife, my child, and my siblings. Their love and support have lightened up my spirit to finish this work.

ACKNOWLEDGEMENTS

Alhamdulillah, I praise and thank the Almighty God for his greatness and for giving me the strength and courage to complete this dissertation.

First, I would like to express my gratitude to my supervisor Dr. Sarah Orton for her inspiration, tolerance, excellent guidance, unwavering confidence, and support throughout this work. It has been an honor to be one of her Ph.D. students. She has provided countless helpful suggestions and has pushed me to be my best. I appreciate all her contributions of time, ideas, and funding to make my Ph.D. experience productive and stimulating.

Also, I would like to thank the rest of my thesis committee: Dr. Hani Salim, Dr. Zhen Chen, and Dr. Sanjeev Khanna, for their acceptance to serve in my thesis committee. I would also like to thank Michael Carraher, Ghassan Al Bahhash, and Richard Oberto for their technical support. Moreover, I would like to thank Ali Elawadi, Russell Clark, Philip Swoboda, David Treece, and Kellen Senor for their great help during my experimental works in the RTF. I would like to thank Dr. Hossam Sallam, Professor of Materials Engineering at Zagazig University, Egypt, for his help and support.

Finally, I wish to express my gratitude for the government of Saudi Arabia and Jazan University for financing my studies and providing me with a generous scholarship.

TABLE OF CONTENTS

LIST OF FIGURES

LIST OF TABLES

Time-Dependent Response of Reinforced Concrete Elements Near Collapse

Mohammed Shubaili

Dr. Sarah Orton, Dissertation Supervisor

ABSTRACT

Reinforced Concrete (RC) structures may experience collapse under high levels of sustained gravity load. High levels of load are possibly due to errors in design and construction, material degradation, and abnormal loading. The evolution from local damage to large-scale collapse is time-dependent, and there is a lack of knowledge of the strength and stiffness characteristics of RC members under high levels of sustained loads.

This research focuses on the impact of high levels of sustained gravity loads on the time-dependent strength and stiffness characteristics of RC isolated slab column connections and RC beams. Concrete is experiences creep under compressive load, and plain concrete has experienced compressive failure at load levels of 80% of its short-term strength (Rusch 1960). However, the behavior of reinforced concrete members under high levels of the sustained load is not well studied, yet there have been several previous collapses of RC structures under constant gravity loads.

This research investigated the time-dependent behavior of RC beams and flat-plate connections under high sustained stresses through experimental testing of shear and flexure-controlled RC beams as well as punching shear in flat-plat connections. Two beam series consisting of 4 and 6 beams were tested at concrete ages of 67 to 543 under sustained

loads ranging from 82% to 98% of the short-term capacity for time periods from 24 to 52 days, with one beam failing under sustained load within 84 minutes. Ten isolated slab-column connections with reinforcement ratios of 0.64% and 1% were tested. The specimens were 0.47 scale and tested at concrete ages from 175 to 402 days at load intensities of 83% to 97%, with one specimen failing under sustained load within 21 minutes.

The research found that high sustained loads can lead to eventual failure (collapse) in these systems; however, the level of load needs to be very close (~95%) to the short-term capacity. The research also found that sustained load increased the deflection at peak load with greater increases in specimens that were more brittle under short-term loading. The increase in deflection could allow for load redistribution in redundant structural systems. The rate of increase in deflection followed the material level behavior of concrete under creep. Steel reinforcement strains increased at a similar rate to the deflection. The increase in steel strain under constant load indicated the redistribution of forces from the concrete as it deforms under creep. However, the sharp increase in deflection due to the tertiary phase of creep occurred in a short time (~2 min), leading to little warning of impending failure.

Chapter 1

INTRODUCTION

This chapter contains an overview of the research in this dissertation starting with objectives and contributions of this research in Sections 1.1 and 1.2, respectively. Then, the motivation for this research is discussed in Section 1.3, followed by the organization of the dissertation in Section 1.4.

1.1 Objectives

The objective of this research is to understand the impact of high sustained gravity loads on the evolution of large-scale collapse in reinforced concrete (RC) elements. In particular, this research is investigating the time-dependent behavior of RC beams and flat-plate connections under high sustained stresses. The research program is designed to evaluate the time-dependent strength and stiffness characteristics of shear and flexure-controlled RC beams as well as punching shear in flat-plat connections. The research seeks to determine what level of high sustained load would lead to eventual failure (collapse) in these systems and what are the characteristics of impending failure.

1.2 Contributions

This research will result in the following contributions:

- Time-dependent strength and stiffness characteristics of RC beams under high levels of sustained load. Specifically, the research will identify what level of loading will lead to eventual failure under sustained loading, the behavior of beams under high sustained loads, and evaluate possible changes in failure mode under sustained loading.
- Time-dependent strength and stiffness characteristics of flat-plate connections under high levels of sustained load. Specifically, the research will identify what level of loading will lead to eventual failure under sustained loading, the behavior of slab-column connections under high sustained loads and evaluate the effect of the reinforcement ratio in the sustained loading.

1.3 Motivation

The collapse of a structure can have serious societal and economic consequences. According to Wardhana and Hadipriono (2003), 172 building failures happened in low-rise and multistory buildings in the United States from 1989 to 2000 during service life. These failures refer to two conditions: distress and collapse. Distress refers one or more of the building elements that become unserviceable. Collapses of buildings occur when an entire building or a part of it fails. Out of the 172 failures, 94% of these failures ended up with partial or total collapse, and about 45% of these failures were associated with design and construction errors, overloading, and material deficiency. Most of the collapses occurred under sustained gravity loads. Eldukair and Ayyub (1991) conducted a study showing that 604 failures occurred in the United States from 1975 to 1986, excluding those

caused by natural disasters. The study showed that 56% of the total failures were associated with collapse, and technical errors caused 78%. About 86% of the failures were attributed to a deficiency in reinforced concrete components. In addition to the impact of these failures on the economic and industry, 416 people were killed, and 2,515 people were injured in these failures. In contrast, 70 deaths occurred due to earthquakes in the United States from 1990, according to USGS 2020. These data highlight the likelihood of structural failure under sustained stresses in the U.S., where buildings are rigorously designed and constructed.

This research is further motivated by results from a test conducted by the Defense Threat Reduction Agency (DTRA) (Morrill et al. 2016), which showed that the evolution from local damage to global collapse is time-dependent. An experimental test of full-scale RC flat-plate buildings was carried out to investigate the progressive collapse resistance. In this test, the central front column was removed instantly. As shown Figure 1-1, the deflection at the missing column was 267 mm (10.5 in.) after 15 minutes, and the structure seemed safe and obtained an alternative load path to carry the gravity loads. However, the slab continued to deform under gravity loads. After 4 hours, the deflection was 1486 mm (58.5 in.) and punching failures occurred at two neighboring slab-column connections. The system at this stage was still able to tolerate the local failures and maintain stability. Observers thought the structure was stable, and no collapse would occur. At some point overnight, the test structure completely collapsed. This test is of significance – it revealed that, after the survival of an RC building from the failure of a critical component such as a column, sustained high stresses on other components can still gradually lead to a catastrophic collapse. The evolution from local damage to global collapse is time

dependent. In fact, the applied load was high enough to cause the collapse, but it took more than 4 hours to collapse. The current knowledge to predict the time-dependent collapse of structures and to know the capacity of a concrete member under high sustained loads is not sufficient, and this research seeks to provide the experimental basis to address this lack of knowledge.

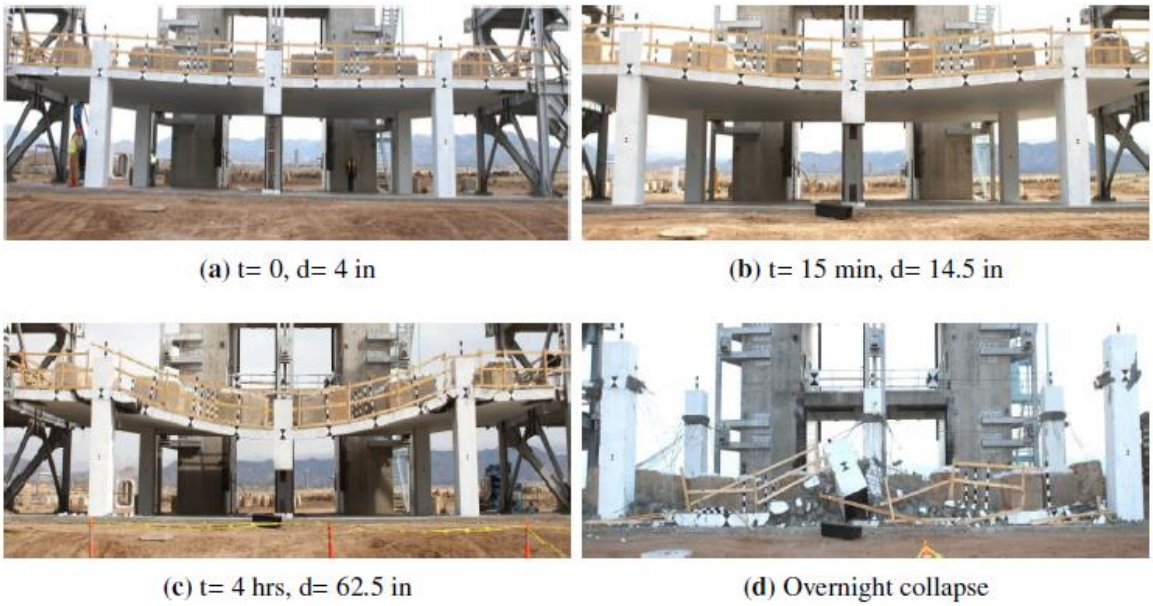

Figure 1-1. Full-scale experiment of a flat-plate structure subjected to losing a column (Morrill et al. 2016).

1.4 Organization of the Dissertation

The dissertation contents are as follows:

- Chapter 1 contains the objectives, contributions, and motivation of the research.
- Chapter 2 presents literature reviews of time-dependent behavior of concrete and RC, beams, flat plates.

- Chapter 3 investigated the time-dependent behavior of RC beams under high sustained stresses. Two beam series were tested.
- Chapter 4 investigated the time-dependent behavior of flat-plate connections under high sustained stresses.
- Chapter 5 presents the conclusions and recommendations.

Chapter 2

LITRATURE REVIEW

2.1 Consequences of High Sustained Loading

The collapse of a structure can have serious societal and economic consequences. RC parking garage structures appear to be particularly vulnerable to failure. Material deterioration can lead to collapse like the collapse of the New York Wilson Hospital parking garage, a flat-plate structure, as seen in Figure 2-1a (Gabrielle Lucivero 2015). The partial collapse of the Pipers Row Car Park in the UK in 1997 is another failure example, as shown in Figure 2-1b (Wood 2003). Although the garage was empty, the collapse occurred under only the dead load in the night. The punching shear failure of one column overstressed the neighboring columns resulted in a progressive collapse in seven adjacent columns with the same manner of failure — the deterioration of the slab materials on the top floor and creep.

(a) Wilson Hospital parking garage (b) Pipers Row Car Park

Figure 2-1. Parking garage failures.

In other cases, the structural collapse was temporarily averted, such as in the Dolphin Tower condominium, a 15-story RC flat-plate building in Sarasota, Florida (Hill et al. 2011). Buckling and tile floor cracking occurred on the fourth floor; then, the building was evacuated and shored. Failure was determined to be punching shear failure due to poor concrete and inadequate reinforcing steel detailing. It took nearly five years to rehabilitate because the functionality and safety condition could not be judged based on available knowledge since the building was built about 35 years ago. Furthermore, there was extensive and time-consuming litigation on who would cover the costs of building.

Many more failures occurred worldwide. Several notable failures demonstrated the time-dependent effects of high sustained loading on RC buildings. One such failure is the collapse of the Sampoong Department Store, a 5-story flat-plate relatively young building in Seoul, Korea, in 1995 as shown in Figure 2-2 (Gardner et al. 2002).

Figure 2-2. North wing collapse of Sampoong Department Store.

The building was occupied at the collapse, and 502 people were killed. Two months before the collapse, abnormal slab cracking initiated on the fifth floor and propagated dramatically

about 10 hours before the collapse. Several factors led to overloading in slab column connections, including not obeying the specified design during construction and the change of use of the fifth floor, which led to an increase in the dead load by 35%.

2.2 Time-Dependent of Concrete

Concrete undergoes three main types of time-dependent deformations that may cause stresses, deflection, and cracking that affect the serviceability of reinforced concrete structures. These types are shrinkage, creep, and thermal expansion or contraction. Many materials like concrete undergo an increase in strains, when the stress is applied to these materials and this stress is kept constant. This phenomenon is called creep. For these materials exhibiting creep, another phenomenon, which is referred to as relaxation, can take place when strain is applied and is kept constant. Two types of time-dependent strains of concrete under a constant temperature can be distinguished: creep, which is dependent on stress, and shrinkage, which is independent of the stress and at constant temperature. When a concrete specimen is exposed to a drying environment, the specimen shrinks with time at a gradually decreasing rate until it approaches a finite bound.

2.3 Shrinkage

Shrinkage is the time-dependent deformation of non-stressed specimens during drying and hardening under constant temperature. When a concrete specimen is exposed to a dry atmosphere, the specimen undergoes shrinkage, and the magnitude of this shrinkage strain is a function of time. Surfaces of elements exposed to drying have larger

shrinkage than their inner part. The shrinkage occurs at a high rate first, and this rate is gradually decreasing with time (Figure 2-3). Shrinkage leads to a reduction in concrete volume if the concrete is not restricted. If concrete is restricted, shrinkage produces stresses that may lead to deflections or cracking. The primary type of shrinkage is called drying shrinkage or simply shrinkage. It occurs due to the increase of the capillary tension of pore water and the solid surface tension of pore walls, as well as thinning of multimolecular hindered adsorbed water layers in cement gel micropores. Drying shrinkage occurs as diffusion of water out of pores. Several factors affect the shrinkage. When the relative humidity is 40% or less, the shrinkage is the largest. High temperature speeds the evaporation of water and, consequently, increases shrinkage. The smaller the size of aggregate particles, the greater the shrinkage. The greater the aggregate content, the smaller the shrinkage. Shrinkage strains are dependent on the composition of the concrete mix-the more cement or water content in the concrete mix, the greater the shrinkage. Autogenous shrinkage is another type of shrinkage. It occurs without the loss of moisture due to the chemical reactions of cement hydration inside the cement matrix. For normal-strength concrete, autogenous shrinkage is considered to be a small fraction of the drying shrinkage and is usually ignored. However, for the high-strength concretes with a low water/cement ratio (0.4 or less), the autogenous shrinkage may comprise a significant percentage of the total shrinkage, and this type only occurs on sealed specimens. Therefore, it must be taken into account in calculations. Since the chemical reaction of hydration virtually halts when the relative humidity is below 60%, autogenous shrinkage does not take place in this situation. The last type of shrinkage is called carbonation shrinkage. It occurs when the concrete is exposed to air containing carbon dioxide. The largest effect occurs in a dry

environment with 50% relative humidity, and carbonation shrinkage could be equaled to the drying shrinkage, effectively doubling the total amount of shrinkage. The carbonation shrinkage decreases at higher and lower humidity.

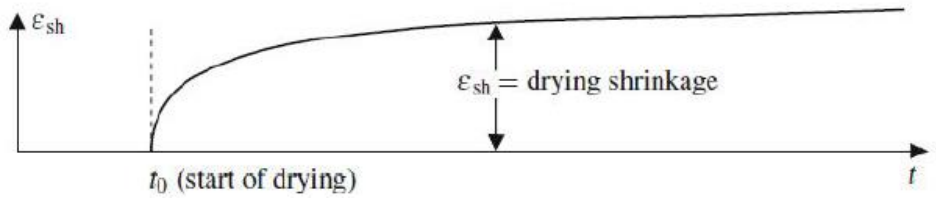

Figure 2-3. Shrinkage.

2.4 Creep

The creep phenomenon is the increase in strain when the stress is held at a constant level. For materials undergoing creep, stress tends to decrease when the strain is constant. This phenomenon is known as relaxation. Creep and relaxation are connected and have a common source in viscous deformation processes in the material microstructure. Such time-dependent behavior could result in undesirable effects on the structural level, such as causing stresses, cracking, and deflection. Excessive deflection can lead to the failure of the element or even the entire structure. Unlike metals, concrete undergoes time-dependent deformation even if the applied stress is much smaller than the concrete strength. The time-dependent deformations of concrete play a significant role in the serviceability and durability of structures. Creep occurs due to the application of loading. When a concrete specimen is loaded in compression, an instantaneous elastic strain develops. Then, creep strains develop with time at a gradually decreasing rate if the load remains. Creep strains

take place at a constant moisture content of concrete is called the basic creep, which occurs due to breakage and reformation of atomic bonds at various highly stressed sites within the colloidal microstructure of the calcium-silicate-hydrate gels in the hardened cement paste. Concurrently, an additional creep called the drying creep occurs if the specimen is exposed to drying. The drying creep develops with time alike to shrinkage. Unlike the basic creep, the drying creep depends on cross-sectional thickness. Drying creep occurs both for drying and wetting. The development of drying creep is attributed to complex physical reasons. One reason is that drying elevates the local stress peaks within the microstructure of calcium silicate hydrates and consequently increases the rate of bond breakages (Bažant and Jirásek 2018). Another reason is apparent, due to the fact that a large part of the observed drying creep in compression has its origin in cracking and is treated as creep only for convenience. If the load after time is removed from the specimen, an instantaneous strain recovery occurs, and this strain recovery is less than the instantaneous elastic strain that took place when the specimen was first loaded. Another strain recovery develops by creep strain at a gradually decreasing rate. However, residual strain remains due to the bonding of the calcium-silicate-hydrate gels particles in the deformed position. The increase in concrete compression strains due to creep will result in an increase in deflections with time. This increase may lead to a redistribution of stresses within cross-sections and cause a decrease in prestressing forces. A significant property of concrete creep is aging that is different from the aging of concrete. The aging of concrete leads to an increase in strength and modulus of elasticity with time, and the rate of the increase gradually diminishing in time. One demonstration is that the instantaneous elastic strain is bigger than the instantaneous elastic recovery, as shown in Figure 2-4. Another

manifestation is that the early loading of a concrete element will lead to higher creep strains than these occur due to late loading. One significant cause leading to the aging in creep is the process of hydration.

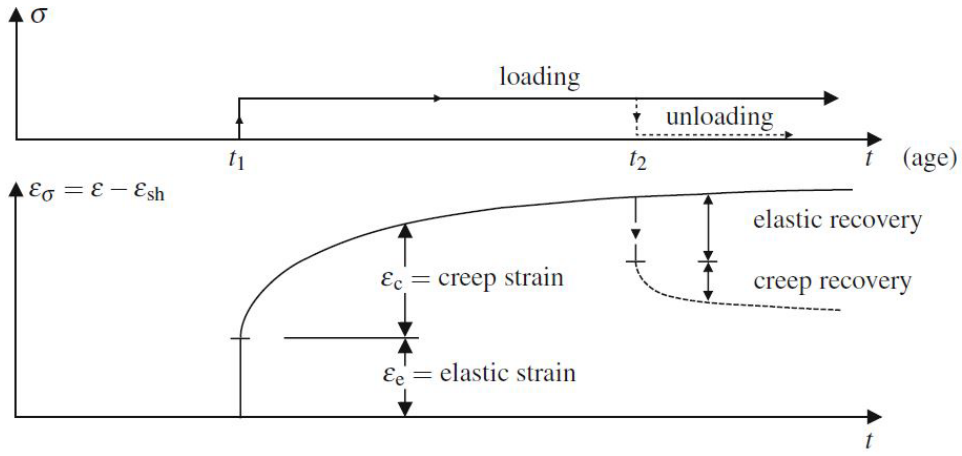

Figure 2-4. Creep and recovery after unloading.

2.4.1 Characteristics Affecting Creep Behavior

Several factors affect creep, including concrete mix, environmental, and loading conditions. In general, the increase in concrete strength, maximum aggregate size or aggregate content, and reduction in water/cement ratio (W/C) lead to a reduction in creep strain. Also, the reduction in humidity and surface-to-volume area and an increase in temperature result in an increase in creep strain. Finally, creep is dependent on stress intensity, duration of stress, and the age of the concrete to which the stress was applied. Concrete creeps more when it is loaded at an early stage, at high-intensity load.

2.4.2 Concrete Material Level Creep

Under sustained loading, creep develops in concrete under compression, and macrocrack growth develops under tension. Several parameters affect creep, including the level of stress, duration of loading, short-time strength, age of concrete, temperature,

aggregate type and size, water-cement ratio, geometry, and humidity (Bažant 1975; Iravani and MacGregor 1998; Mazzotti and Savoia 2002). Creep is fundamentally caused by the progressive propagation of internal microcracking (Shah and Chandra 1970). Two types of creep can occur. The first type is a basic creep, which is caused by breakage and reformation of atomic bonds at various highly stressed sites within the colloidal microstructure of the calcium silicate hydrate gels in the hardened cement paste (Bažant and Jirásek 2018). Another type is drying creep, defined as an excess of creep when a specimen is exposed to drying under sustained loading. This type of creep is less important since the concrete specimens have been tested at ages more than five months to reduce concrete humidity and stabilize concrete strength gain due to age. At service load, the creep of concrete has little effect on the safety against collapses except for some cases such as buckling. However, at high stresses, it can lead to collapse. Generally, when the stress is less than 0.70f'c, microcracks grow slowly, and concrete is safe. However, when the sustained stress is greater than 0.80f'c, concrete may experience a failure within finite time, preceded by a rapid crack growth and a sharply increased volume expansion. Of importance to structural behavior is the stress-strain response. As shown in Figure 2-5, sustained compressive strength is less than the short-term compressive strength. Additionally, if the sustained stress is less than 0.40f'c, creep strain is linear with respect to stress. Nonlinearity presents at higher stresses due to microcrack initiation and progress in the concrete and, once the stress becomes greater than the critical stress, the material will suffer tertiary creep characterized by accelerated permanent strain due to microcrack progression and coalescence (creation of macrocracks), leading eventually to failure. The critical stress is between 0.75f'c and 0.80f'c (Rusch 1960). A study by Iravani and

MacGregor (1998) showed that the ratio of the sustained load strength to the ultimate strength increased when concrete strength increased. The sustained load strengths were between 0.85f'c to 0.90f'c for 105 MPa (15,220 psi) and 120 MPa (17,400 psi) concrete strengths. For 65 MPa (9425 psi) and 95 MPa (13,780 psi) concrete strengths, the sustained load strengths were between 0.70f'c to 0.75f'c and 0.75f'c to 0.80f'c, respectively. Also, small eccentric loading leads to a slight improvement in sustained load strength. The ascending parts of stress-strain curves were more linear when the compressive strength increased. The derivation from linear to nonlinear occurred when specimens were load between 0.65f'c to 0.85f'c of their ultimate strengths.

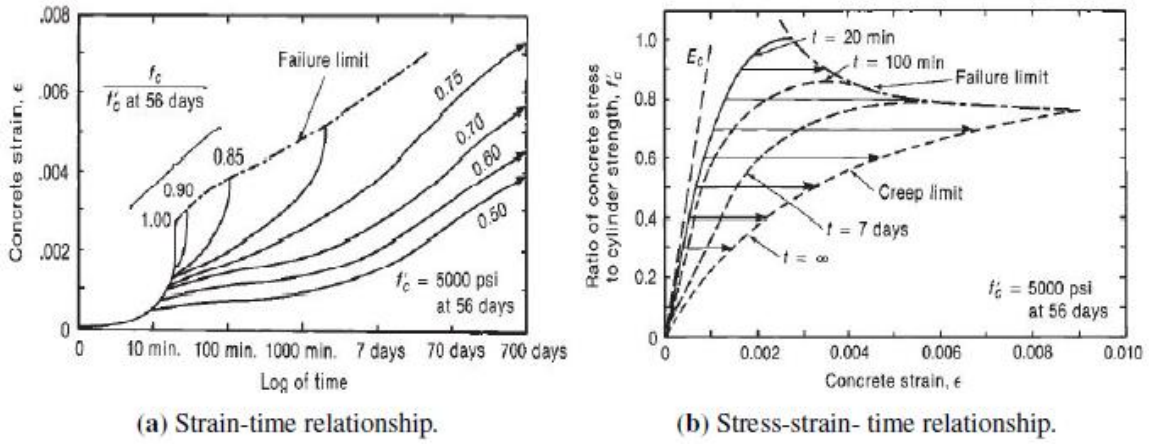

Figure 2-5. Effect of sustained loads on the behavior of concrete in uniaxial compression (Rusch 1960).

There is a strong interaction between fracture and creep in concrete; therefore, this interaction must be considered in the analysis of fracture propagation (Bazant and Gettu 1992). Concrete, as a quasi-brittle material, is also impacted by sustained loading on macrocracking-induced fracture growth. Bazant and Xiang (Bažant and Xiang 1997) demonstrated this by eccentrically loading edge-notched fracture specimens subjected to compression at one side and tension at another side under 50%, 70%, and 90% of their

peak loads for around a month. A time-dependent model was used to verify the test data. This model consists of two parts. The first part is creep which is based on linear viscoelasticity. The second one is related to the crack growth rate, which is based on q power law. The test results showed that the lifetime of a specimen could be divided into three stages, as shown in Figure 2-6. In stage I, the linear viscoelastic behavior governed the response. In stage II, both linear viscoelasticity and the time-dependent crack growth rate are significant. In the last stage, which leads to failure, the time-dependent governs the response, and linear viscoelasticity becomes insignificant. Creep was found to impact little on lifetime, for which an approach based on a time-dependent crack growth theory was explored and validated.

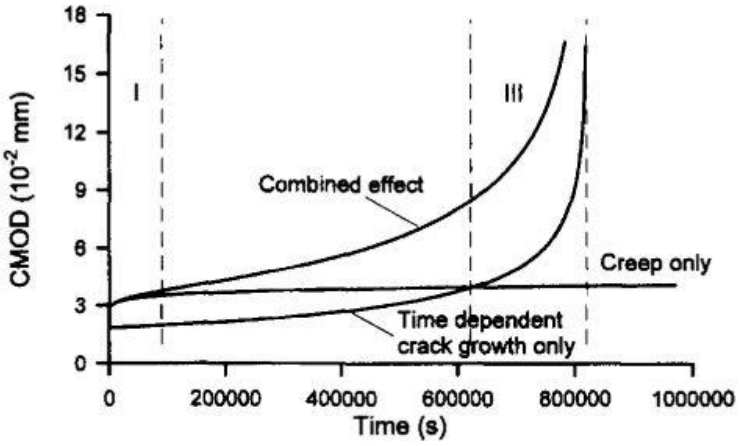

Figure 2-6. Time history of CMOD (Bazant and Gettu 1992).

Under high sustained stresses, three stages of creep can be seen, namely primary, secondary, and tertiary creep (Zhou 1992), as shown in Figure 2-7 (Tasevski et al. 2019). In the primary creep, the creep strain rate decreases steadily. The secondary creep has a relatively constant rate of strains. For the tertiary creep, the rapid rate of strains increases rapidly and eventually leads to failure. The secondary and tertiary creep development

mainly depends on the level of stresses applied to the concrete. For stresses less than 0.40f'c, the primary creep develops at a high rate at first and then decreases with time. When the stresses during loading and microcracking propagation under sustained loading. At sustained stresses higher than 0.75f'c, tertiary creep may develop due to microcrack coalescence.

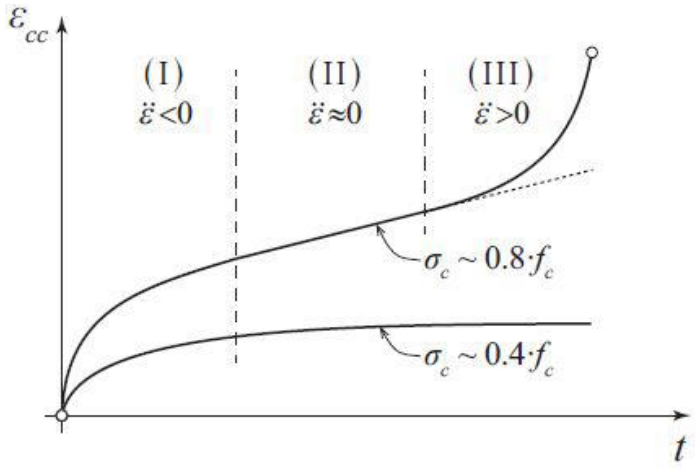

Figure 2-7. Evolution of creep strains with time (primary, secondary and tertiary stages of creep).

Ruiz et al. (2007) adopted an approach to predict the failure in plain concrete under sustained load. The approach is based on the stress-strain curve of concrete cylinders in compression. According to this approach, the failure occurs under a high level of a sustained load if accumulated inelastic strain that develops under sustained stress attains the inelastic strain capacity (Figure 2-8a) that is, the difference between instantaneous post-peak and pre-peak longitudinal strains the same level of stress (Figure 2-8b). If the level of sustained stress is equal to or higher than 0.75f'c, the inelastic strain developing within the creep process may reach the inelastic strain capacity, and failure takes place; under

sustained stresses less than 0.75f'c, inelastic strain capacity is not reached, and the failure does not occur (Figure 2-8c).

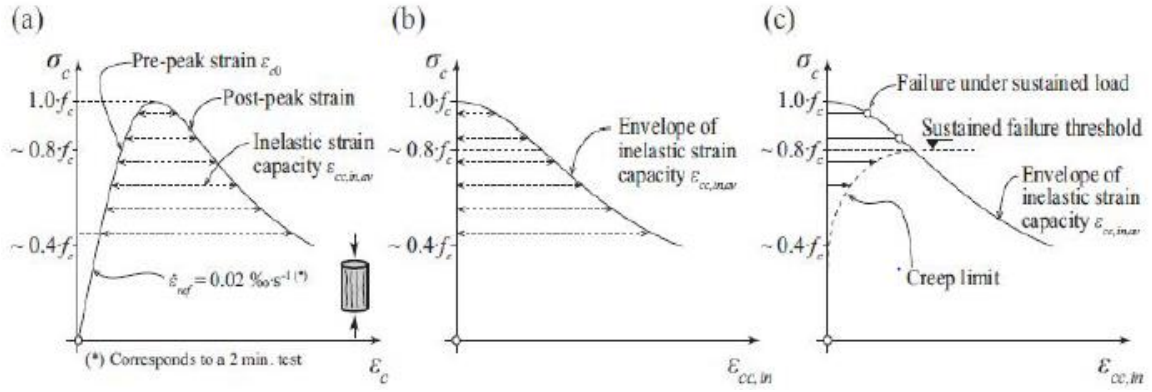

Figure 2-8. Inelastic strain capacity.

2.4.3 Reinforced Concrete Under Sustained Stresses

Considerable research has been conducted with the main concentration on long-term deflection rather than the strength of RC beams under normal conditions (Alwis 1999; Bakoss et al. 1982; Espion and Halleux 1990; Paulson et al. 1991; Samra 1997) or corrosion (Dekoster et al. 2003; Du et al. 2013; Liu et al. 2016; Yu et al. 2015). Furthermore, RC columns behave differently from that of plain concrete under sustained load due to creep and strain compatibility between steel and concrete. The load carried by steel increases with time; as a result, the creep effect on concrete is delayed. Richart and Heitman (1938) tested axially loaded RC circular columns under sustained loads, ranging from 16% to 26% of ultimate loading capacity. After one year, steel strain increased by 81% to 381% due to creep. The stress redistribution between steel and concrete was stabilized thereafter. Additionally, the sustained load did not compromise ultimate column strength; an observation was also made in testing composite columns (Han et al. 2004; Kim et al. 2017).

Only very limited studies for this loading condition are available. Viest et al. (1956) applied sustained loads, ranging from 83% to 95% of the ultimate capacity, on RC short columns with small to moderate eccentricities. Within the 500-days test duration, 6 out of 19 columns failed during a span of 48 to 274 days. Concrete failure strain averaged 0.0061 as opposed to 0.0032 in the short time loading counterparts. However, if the creep strains are deducted, the remaining strains agree well with the ultimate strain for short time loading. Due to second-order effects, the influence of sustained loading is more pronounced in eccentrically-loaded slender columns. Five RC columns tested by Green R and Breen JE (1969) under sustained loads at 50% to 60% of ultimate capacity failed within one hour to 7.7 years. Longitudinal cracking and strains in excess of 0.007 were observed prior to failure. Figure 2-9 shows deflection time history at column center height for three specimens that failed under sustained loads.

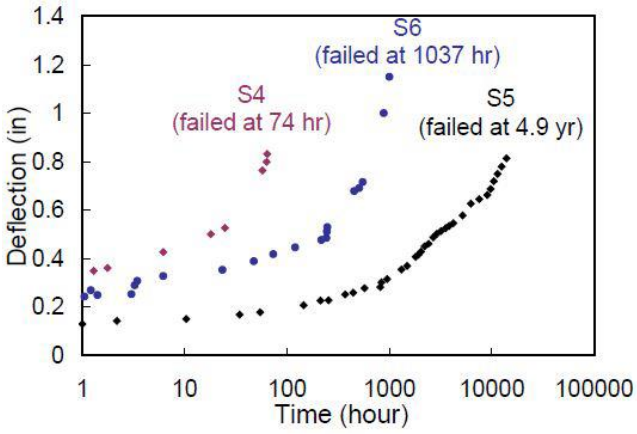

Figure 2-9. Deflection history of columns that failed under eccentric loading (Green R and Breen JE 1969).

Very few tests have been conducted on RC beams under high sustained loads. Tests focusing on beam flexural strength (Reybrouck et al. 2015; Washa and Fluck 1953) indicate that high sustained loads have a negligible impact on loading capacity. This can

be expected because beam flexural strength is controlled mainly by longitudinal bars rather than concrete. Limited experimental works have been conducted to understand the effect of high sustained loading (87% - 95% of short-term shear capacity) on the shear capacity of RC beams within a duration of up to 1113 days. The first experimental work on this field was done by Sarkhosh (2015). In this work, 42 RC beams without shear reinforcement were tested. Among the 42 RC beams, 18 RC beams were tested under high sustained loading. Among the 18 RC beams, two beams failed under sustained loads: one failed after 2.5 hours and the other one failed after 44 hours. The 16 beams not failed under sustained loading were loaded up to failure at the end of the tests. In general, the shear capacities of these 16 beams were higher than the controlled beams.

Saifullah et al. (2017) studied the effects of sustained loading on the shear strength of beams. He found that the increase in crack width under sustained load was very small, and the shear strength of concrete was not affected by creep. Maekawa et al. (2006) had done work to monitor in real underground RC box culverts of about 30 years of age to understand the mechanism of the progressive excessive deformation. It was found that the deflection was ten times greater than that expected at the design stage, accompanied by the out-of-plane shear failure. The investigation revealed that coupling of subsidence of the backfill soil and the combined creep and shrinkage of concrete after cracking is closely associated with the delayed shear failure found in the culvert in service. A laboratory test to reproduce the time-dependent shear crack propagation and modeling were conducted to prove the delayed shear failure under sustained loading. Moreover, a numerical study exhibited that high levels of sustained loading have the potential to adversely affect that arching action and direct strut action (Bugalia and Maekawa 2017).

Another study on the effect of load duration on shear strength of reinforced concrete beams was conducted by Tasevski et al. (2020). The study showed that a higher duration of the sustained load had no noticeable reduction of shear strength. However, the authors mentioned that the observation was based on limited data. Because longitudinal bars restrain crack opening and maintain aggregate interlock, the time-dependency of crack growth in a RC beam could be less pronounced than in plain concrete. Note that all the aforementioned beams were simply supported in the tests without rotational and axial restraint at ends that actually exist in beam-column frames. Building codes (ACI Committee 318 2014; CEB 2013) limit the axial load applied on a RC column to 80% to 85% of its short-time capacity due mainly to minimum eccentricity, and concrete strength is limited to 0.85fc' due to the expectation of weaker concrete at the column or beam top (Ferguson et al. 1988). However, these limits include a myriad of effects and are not specific to high sustained loads.

The flat plate system consists of a reinforced concrete slab without beams, capitals, and drop panel, which makes it widely used due to the flexibility of architectural design, reduced structural height, cost-effective, and easy formwork. Slab column connections are vulnerable to punching shear failure due to high stress at these connections. Many analytical models and code predictions were developed to predict to punching shear capacity of flat plates. Some codes take into account flexural reinforcement, and some consider size-effect and geometry and dimensions of columns. However, there are no codes that consider the effect of the clear cover in the tension zone, which could lead to an increase in punching shear capacity. One study conducted to study the effect of the clear cover in the tension zone was done by Qiuning (2014). In this study, 16 flat plates with

different clear covers that varied from 10 mm (0.39 in.) to 70 mm (2.76 in.). The study revealed that the increase in the clear cover from 10 mm (0.39 in.) to 50 mm (1.97 in.) could increase the punching shear capacity by as much as 50%. However, when the clear cover exceeds 50 mm, the increase in the capacity is not considerable. Gilbert et al. (2006) tested seven large-scale multi-flat plat specimens under a sustained load of up to 58% of collapse load for time periods ranging from 508 to 750 days. The specimens were loaded at age 14 days. The long-term deflection was found to be 5 to 9 times greater than instantaneous deflection, which was significantly larger than that predicted by ACI. For punching capacity, Rankin and Long (1987) tested an isolated slab-column specimen under a concentric load of 70% of short-time loading capacity for 12 weeks. No failure occurred. Ozden et al. (2013) conducted similar tests, where specimens were loaded up to 65% of their short-time capacity for 270 days. The width of slab inclined shear cracks doubled, but failure did not happen. However, neither of these tests applied a load high enough to trigger time-dependent effects on punching failure or considered eccentric loading that slab-column connections would experience during failure propagation.

Chapter 3

BEAMS UNDER HIGH SUSTAINED LOADING

The goal of the experimental work in this chapter is to evaluate the time-dependent strength and stiffness characteristics of RC beams under sustained high stresses. The experimental work consisted of two-beam series. In beam series I, four beams were tested under four-point bending (4PB). In beam series II, six beam specimens were tested under three-point bending (3PB). The main differences between beam series I and beam series II were the reinforcement and the test setup. In beam series I, the shear and flexural capacities of the beam were similar; in beam series II the beams were shear controlled.

3.1 Beam Series I

In this experimental series, four beam specimens were tested under four-point bending (4PB). One specimen was tested under short-term loading to serve as the control specimen, while the rest were tested under long-term loading of periods ranging from 24 to 42 days.

3.1.1 Test Specimens

The experimental work involved the testing of four simply supported beams under four-point bending (4PB). The design of the beams was chosen to be similar to the slabs cast at a 0.47 scale. The beam specimens were constructed with dimensions of 1524 mm × 140 mm × 140 mm (60 in. × 5.5 in. × 5.5 in.). All the specimens had two layers of reinforcement: one in the tension zone and another in the compression zone. The reinforcement ratios in the tension zone and compression zone were 0.86%. Two rebars

were placed in the top, and two rebars were placed in the bottom of the beam. Four stirrups were provided to hold the reinforcement in the cage but did not provide any additional shear resistance: two near the center and two near the loading points. The rebars and the stirrups used in this series were No.10 (No.3) with 9.525-mm (3/8-inch) diameter, Grade 420 (Grade 60). The clear covers were 6.35 mm (0.25 in.) for both the tension and compression flexural reinforcement rebars for all specimens. The clear cover 6.35 mm (0.25 in.) was chosen to be the same as the slab specimens. Figure 3-1 shows the reinforcement configuration.

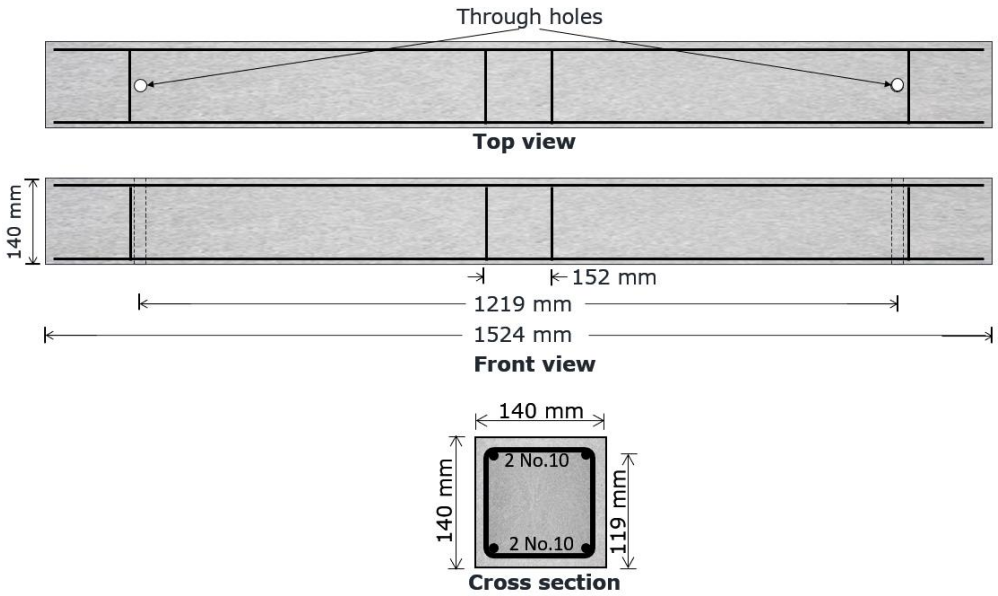

Figure 3-1. Reinforcement details of beam series I.

3.1.2 Experimental Setup

The test setup is shown in Figure 3-2. The test setup was designed to apply concentrated loading at two points. Each beam had two through holes created using PVC pipes to allow threaded rods to pass through and load the beam. Each threaded rod was

connected to the lab's strong floor, and the load was applied to the beam by turning the nuts on the top of the threaded rods. Springs with stiffness of 0.84 kN/m (4.8 kip/in) were added to help maintain a constant axial load.

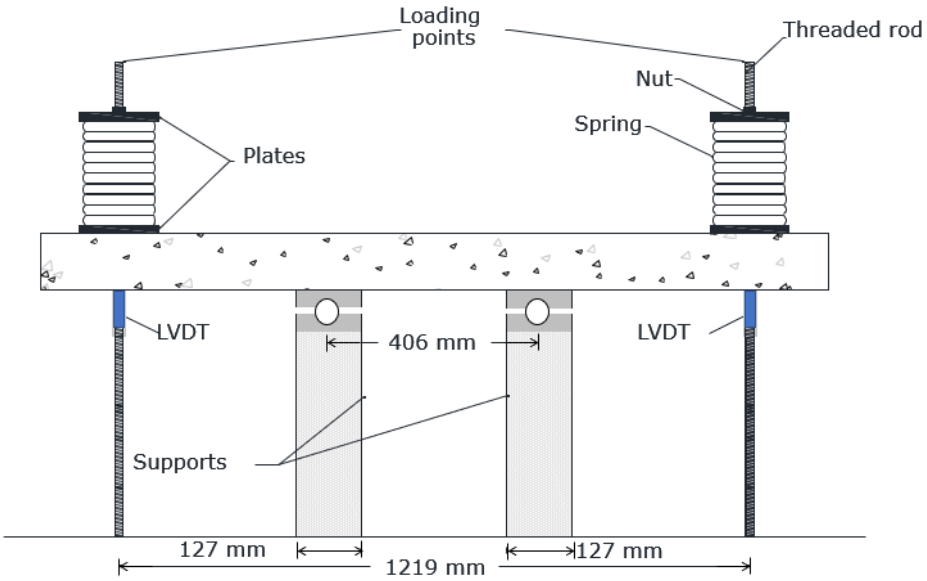

Figure 3-2. Beam series I test setup.

A load washer under the loading plate was used to measure the applied load. Beams were tested under four-point bending (4PB). Two 152 mm (6 in.) supports were set at the third span of the four-foot test setup. The loading was checked and adjusted in a short period of time (2-8 hrs) for the first three days of loading. Afterward, the load was checked and might be adjusted every 24 hours.

3.1.3 Constructions of Specimens

The formwork was constructed, and stirrups and longitudinal rebars were placed and tied inside the forms. The stirrups were rested on 6.35 mm (0.25 in.) hardwood square dowels to provide a clear cover. Each beam specimen had two through holes for loading created using PVC pipes. After casting the concrete, the top surfaces were leveled and finished. The formwork was covered by plastic sheets and moist cured for one week. The formwork was removed after two weeks. A picture of the formwork with the reinforcement is shown in appendix A.

3.1.4 Loading Histories.

Beam 1 (B1) was tested under monotonically increasing loading to failure at the age of 64 days as a control specimen. Beam 2 (B2) was tested at age 65 days under sustained loading for 25 days. The load was monotonically increased until the specified load, 16 kN (3600 lbs), was reached. At the age of 90 days, the load was increased to failure. For Beam 3 (B3), The load was applied at the age of 91 days. The sustained load was 17.13 kN (3850 lbs). The test was terminated after 42 days by loading up the beam to failure. The last specimen in this beam series was Beam 4 (B4), which was tested under sustained loading. The specimen was loaded up at the age of 135 days at a level of loading

equal to 18.24 kN (4100 lbs). The load was increased to failure after 24 days. Figure 3-3 exhibits the loading histories for the first beam series.

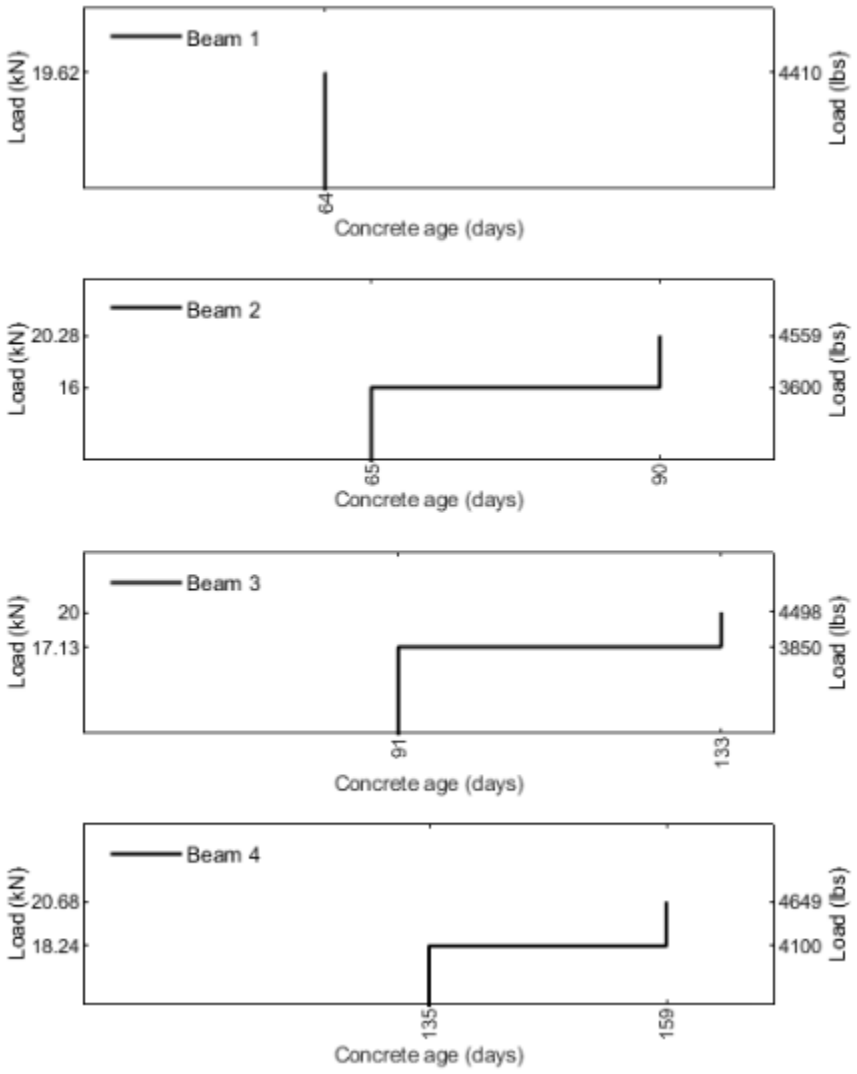

Figure 3-3. Beam series I loading histories.

3.1.5 Instrumentation and Data Collection

Each beam specimen was instrumented to provide detailed data required to understand the specimen's behavior during the entire loading history. Measurements include load, deflection, and reinforcement strains.

3.1.5.1 Load Measurement

Each beam specimen had two loading points at a four-foot span length. The 15.875 mm (5/8 in.) threaded rods going through the through-holes were connected to the lab's strong floor. Two load cells with 89 kN (20000 lbs) capacity were used in most of the tests. The load cells were placed between the plate and washer at the top of the beam specimen. Also, two calibrated strain gauges were attached to each rod underneath the beam specimen to measure the applied load. The measured load was the applied load, the self-weight not included.

3.1.5.2 Deflection Measurements

Two (LVDTs) were utilized to determine the vertical deflections of the beam at the loading points. The LVDTs were placed underneath the beam close to the through-hole and threaded rod. The measured deflections were based on the measured applied load without self-weight.

3.1.5.3 Strain Measurements on Steel Reinforcement

Each beam had two 350-ohm electrical strain gauges. One strain gauge was attached to flexural tension reinforcement, and one was attached to flexural compression reinforcement. The presence of the strain gauges was to provide information on rebar strain distribution and redistribution in reinforcement. The strain gauges were installed on the neutral plane of the rebar cross-section. In this beam series, the strain gauges were installed on two parallel rebars at 76 mm (3 in.) from the center of the beam.

3.1.6 Material Properties

The following section provides an overview of the mechanical properties of materials used to build RC beams (series I), including concrete and steel reinforcement.

3.1.6.1 Concrete

The concrete mixture was designed to obtain 27.58 MPa (4000 psi) compressive strength at age 28 days. Batch 1 was utilized to construct these beam specimens. Cylindrical specimens of dimensions 100 × 200-mm (4 × 8-in.) were tested under compressive axial loading to obtain the average compressive strength of the concrete. The compressive strength of this batch at the age of 64 days was 42.45 MPa (6157 psi). Stress-strain curves from 2 of the tested cylindrical specimens are shown in Figure 3-4. The concrete mixture of this batch is exhibited in appendix A.

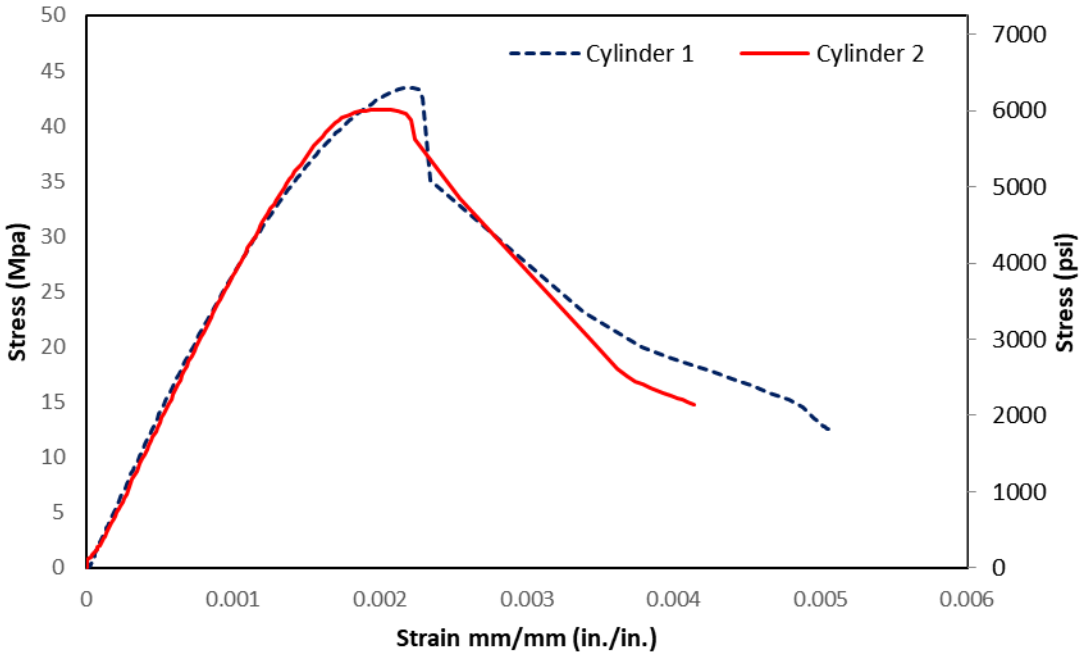

Figure 3-4. Stress-strain curves of concrete batch 1.

3.1.6.2 Steel Reinforcing Bars

Reinforcement bars used in all beam specimens were Grade 420 (Grade 60) rebar. Steel rebars were tested under uniaxial tension according to the specifications of ASTM

A370. Table 3-1 summarizes the steel rebar properties. Stress-strain curves from tested reinforcement specimens are exhibited in Figure 3-5.

Table 3-1. Material properties of steel rebars

Property	Yield strength MPa (ksi)	Tensile strength MPa (ksi)	Young's Modulus GPa (ksi)
Reinforcement bars	476 (69)	718 (104)	197 (28600)

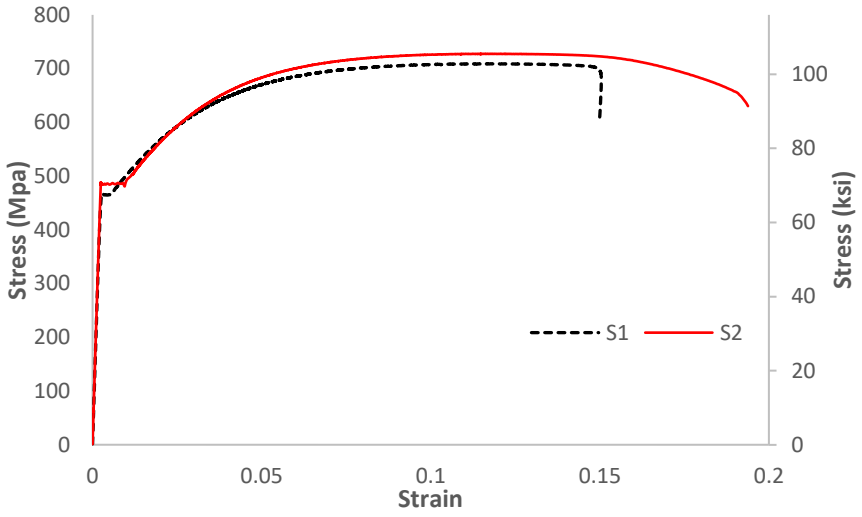

Figure 3-5. Stress-strain curves of reinforcement.

3.1.7 Results

This section presents the results of beam series I. Beam 1 (BC1) was the control specimen, tested in the short term, while the rest of the beams (Beam 2, Beam 3, and Beam 4) were tested under sustained loads at percentages of the BC1 load capacity for at least 24 days. Then, the beams were loaded up to failure. The results include deflections, mode of failure, and reinforcement strains.

3.1.7.1 Beam 1 (BC1)

As mentioned before, Beam 1 (BC1), the control specimen of this series, was loaded to failure at the age of 64 days. The load was applied monotonically. Figure 3-6 shows the measured load versus deflection. The stiffness of the beam softened when the load approached 16 kN (3600 lbs), due to yield in the reinforcement. The ultimate load was 19.62 kN (4410 lbs), while the deflections at the left and right loading points at the ultimate load were 13.07 mm (0.514 in.) and 12.44 mm (0.490 in.), respectively. The failure of the beam was caused suddenly by the formation of a brittle shear crack, as shown in Figure 3-8.

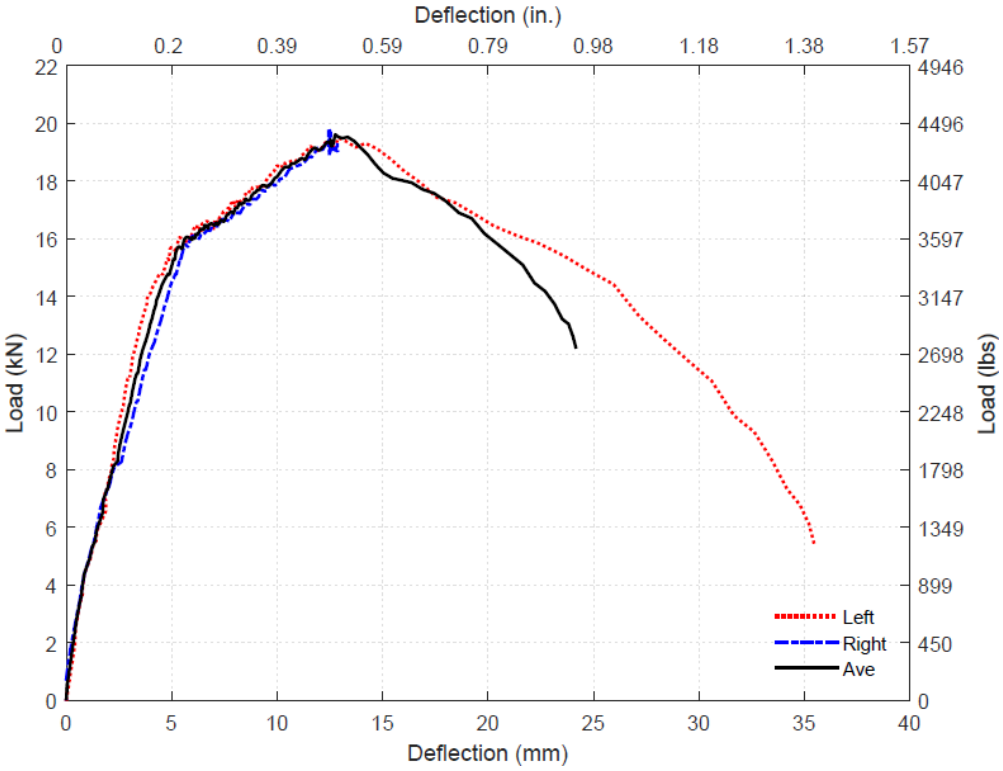

Figure 3-6. Load vs. deflection for BC1.

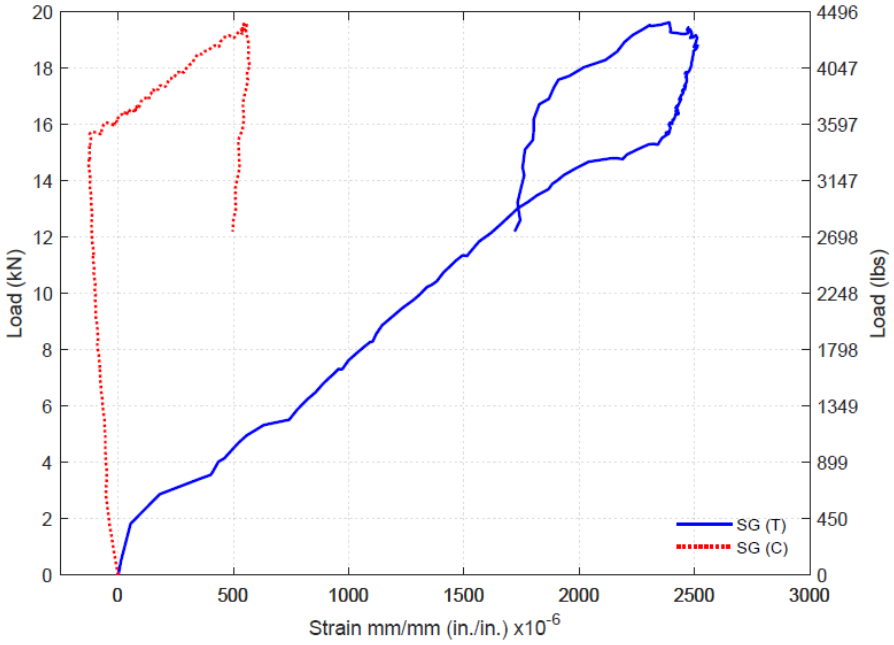

Figure 3-7. Load versus reinforcement strain responses for BC1.

Figure 3-8. Beam 1 (BC1) failure.

3.1.7.2 Beam 2 (B2-SL)

Beam 2 (B2-SL) was loaded up to the sustained load of 16 kN (3600 lbs) at the age of 65 days. The sustained load was 16 kN (3600 lbs), which is 82% of the short-term shear resistance of the control beam (BC1). This value was selected based on that stiffness degradation occurred around this value of loading in the BC1 specimen. It is noticeable that there was no reduction in the stiffness of this beam before reaching the specific value

of the sustained load. The instantaneous deflections of B2-SL at the left and right loading points were 6.13 mm (0.241 in.) and 4.50 mm (0.177 in.), respectively. The specimen was under the sustained load for 25 days. The long-term deflections at the left and right loading points were 7.20 mm (0.283 in.) and 5.63 mm (0.222 in.). The increase in deflections due to the time-dependent effect at the left and right loading points were 1.07 mm (0.042 in.) and 1.13 mm (0.045 in.), respectively, which were 17.5% and 25.2% of their instantaneous deflections. The load vs. deflection curve from the beginning of the test until the end of the sustained loading period is exhibited in Figure 3-9.

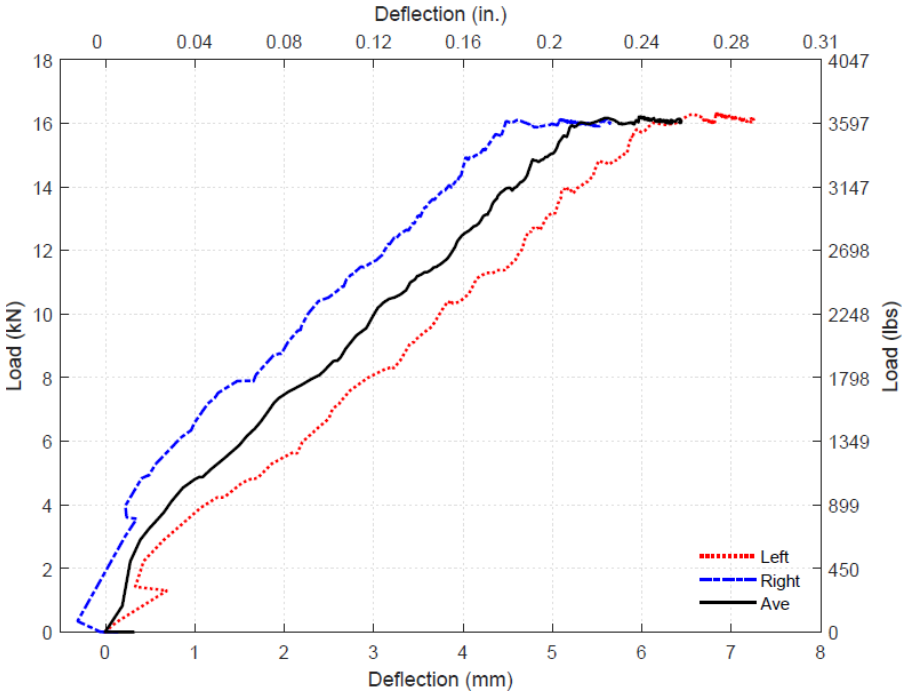

Figure 3-9. Load vs. deflection until the end of SL (B2-SL).

The increase in the deflections under sustained loading is shown in Figure 3-10. In the first 23 hours under the sustained loading, the left loading point deflection increased more than the right loading point deflection. The increase in deflections after ~24 hours at the left and right loading points were about 58% and 30% of the total increase in deflections

under sustained loading, respectively. The right load was adjusted after 24 hours because there was a reduction in load. After the adjustment of the load, there was an increase in deflection of the right side from 0.34 mm (0.0135 in.) to 0.46 mm (0.018 in.), which can be seen in Figure 3-10. This increase could be due to cracking on the right side. On the fifth day of sustained loading, the increases in deflections were 71.50% and 58% of the total increase in deflections for the left and right deflections, respectively. The increase in the right loading point deflection on the 11th,17th, and 18th day was due to adjustment in the load.

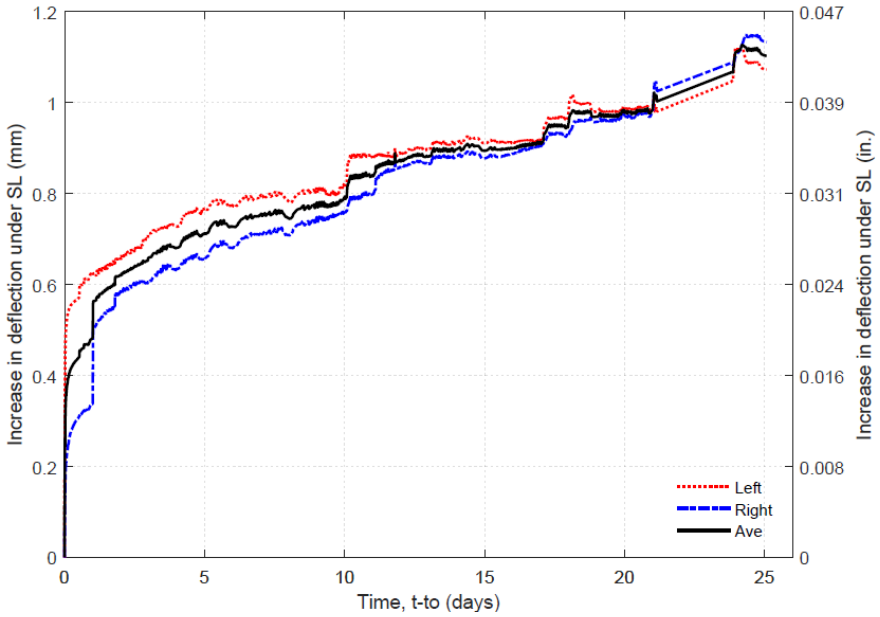

Figure 3-10. The increase in deflection under SL (B2-SL).

At the end of the sustained loading period, 25 days, the B2-SL specimen was loaded up to the failure. The peak load and the deflection at the peak load were 20.28 kN (4599 lbs) and 13.88 mm (0.547 in.), respectively. After the peak load, the applied loads dropped on average from 20.28 kN (4599 lbs) to about 18.95 kN (4261 lbs) simultaneously with an increase in the deflections in both sides, as exhibited in Figure 3-11, due to crushing of the

concrete and failure of the specimen in flexure. The specimen still resisted loads with significant increases in displacements (flexural hinge response) loads until shear failure took place on the right side while increasing loading. The crack that happened in concrete cover in tension that initiated the shear crack. When the tip of this crack entered the shear zone, the failure happened very suddenly. The failure of the specimen B2-SL is shown in Figure 3-12.

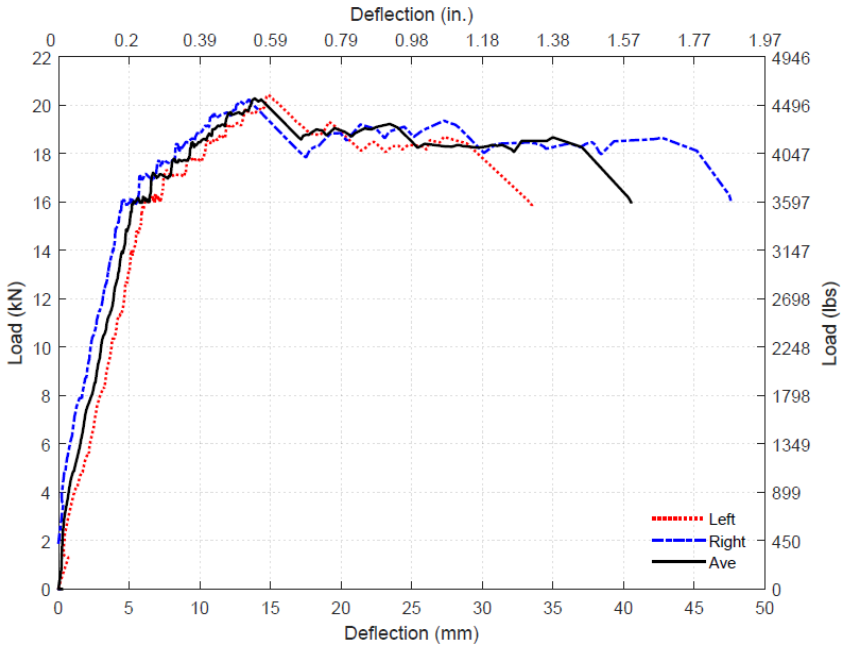

Figure 3-11. Load vs. deflection for B2-SL specimen for the entire test.

Figure 3-12. B2-SL failure.

The reinforcement strains are shown in Figure 3-13. The tension and compression reinforcement strain at the beginning of the sustained loading was 0.002537 mm/mm and 0.000041mm/mm, respectively. Figure 3-14 shows the change in strains under SL (B2-SL). At the end of the sustained load, they were 0.00304 mm/mm and -0.000704mm/mm. Both the tension and compression strains changed under sustained loading as the creep in the concrete was taken by the reinforcement.

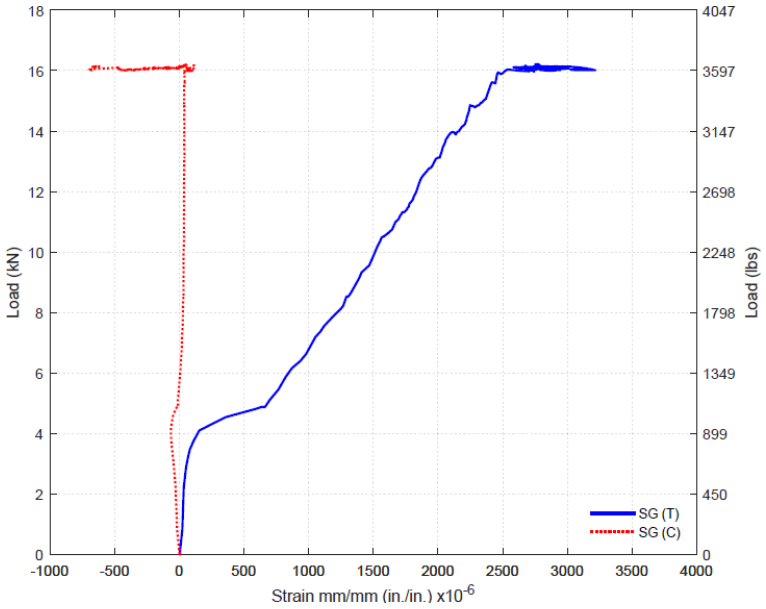

Figure 3-13. Load vs. SGs until the end of SL (B2-SL).

The change in the strain indicates more curvature in the specimen, as also evidenced by the increase in deflection with time. The strain in the tension rebar increased by 23% under the sustained loading, whereas the compression strain increased by almost eight times. The large increase in the compression strain is due to the creep deformations of the concrete in compression.

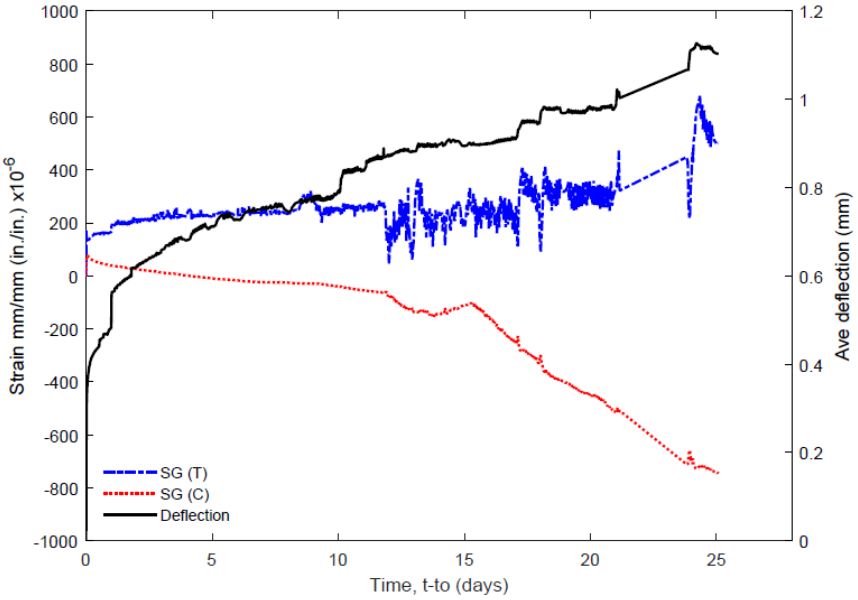

Figure 3-14. The change in strains under SL (B2-SL).

3.1.7.3 Beam 3 (B3-SL)

The third specimen, B3-SL, was tested under sustained loading at the age of 91 days for 42 days. The sustained load was 17.13 kN (3850 lbs), which is 87% of the short-term shear resistance of the control beam, BC1. Due to the lack of failure of specimen B2-SL, the sustained load of B3-SL was chosen to be higher than the sustained load in B2-SL. The stiffness reduction happened when the average load exceeded 14.83 kN (3334 lbs). The instantaneous deflections of B3-SL were 9.05 mm (0.356 in.) and 9.79 mm (0.385 in.) at the left and right loading points, respectively. At the end of the sustained loading period, the left and right loading point deflections were 12.21 mm (0.481 in.) and 13.89 mm (0.547 in.), respectively. The left and right loading point deflections increased under the sustained load by 3.16 mm (0.124 in.) and 4.11 mm (0.162 in.), respectively. The percentages of increase in deflections of the left and right loading points were 35% and 42% of the

instantaneous deflections, respectively. Figure 3-15 shows the load vs. deflection curve from the beginning of the test until the end of the sustained loading period of B3-SL.

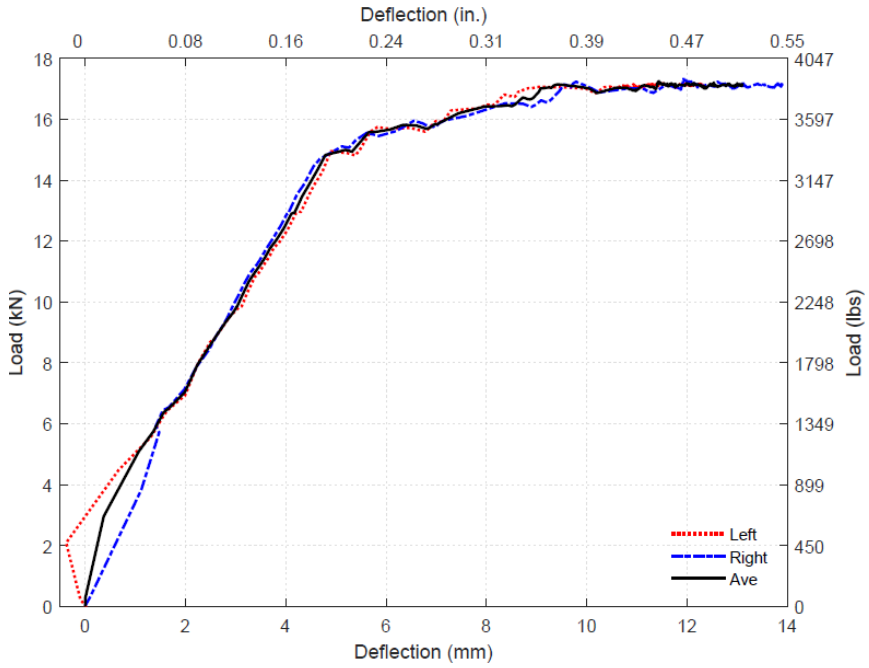

Figure 3-15. Load vs. deflection until the end of SL (B3-SL).

Figure 3-16 exhibits the increase in the deflections with time under sustained loading. At the time of about 16 hours of the sustained loading, the left and right loading point deflections were 10.63 mm (0.418 in.) and 11.32 mm (0.446 in.). Therefore, 50% and 37% of the deflection increases in the left and right loading deflections of the overall deflection increases under the sustained loading took place in the first 16 hours. Shortly after that, the loads were adjusted, which increased the deflections in the left and right loading points to 10.67 mm (0.420 in.) and 11.62 mm (0.457 in.). Also, the adjustment of the loads after nine days and 15 hours caused the deflections to increase. The increases in deflections when the time was about 16 days and 4.8 hours were due to cracking. The jumps in deflections on the day of the 21st and 29th of the sustained loading were due to load

adjustment. The increase in the right loading point deflection on the days of 33rd was due to cracking. At the end of the sustained loading period (42 days), the right loading point deflected more than the left one, and most of the load adjustment was on the right side. Fifty percent of the deflection increase under the sustained load occurred in the first 17 hours for the left loading point and about 30.50 hours for the right loading point.

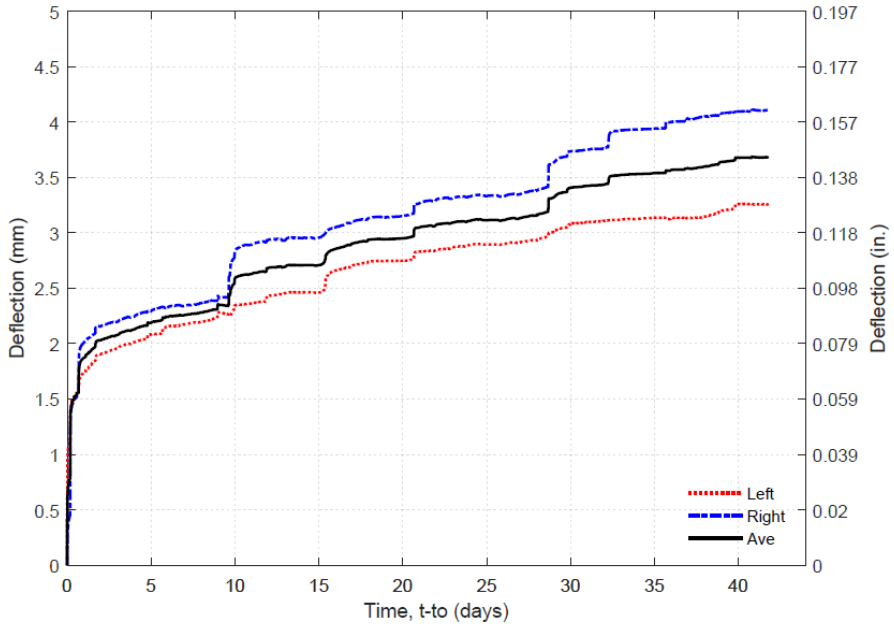

Figure 3-16. The increase in deflection under SL (B3-SL).

After about 42 days, the test was terminated by loading up the B3-SL to failure, as shown in Figure 3-17. The ultimate load was 20.01 kN (4498 lbs), and the average deflection at the ultimate load was 20.42 mm (0.804 in.). After the ultimate load, the left load dropped to 15.35 kN, and the left loading deflection increased to 28.93 mm, while the right load reduced to 17.26 kN (3880 lbs) and the right loading deflection rose to 27.57 mm due to flexural failure shown by crushing of the concrete cover. B3-SL was still able to carry loads after the ultimate loads but not higher than the peak. The deflections kept increasing with the load increases due to the flexural cracking. Then, the shear failure

happened suddenly on the left side. Besides the shear failure, there was crushing of concrete at compression between the two supports near the right support. The left and right loading deflections were 38.18 mm and 51.46 mm at the end of the test after the shear failure. Figure 3-18 shows the failure of the specimen B3-SL.

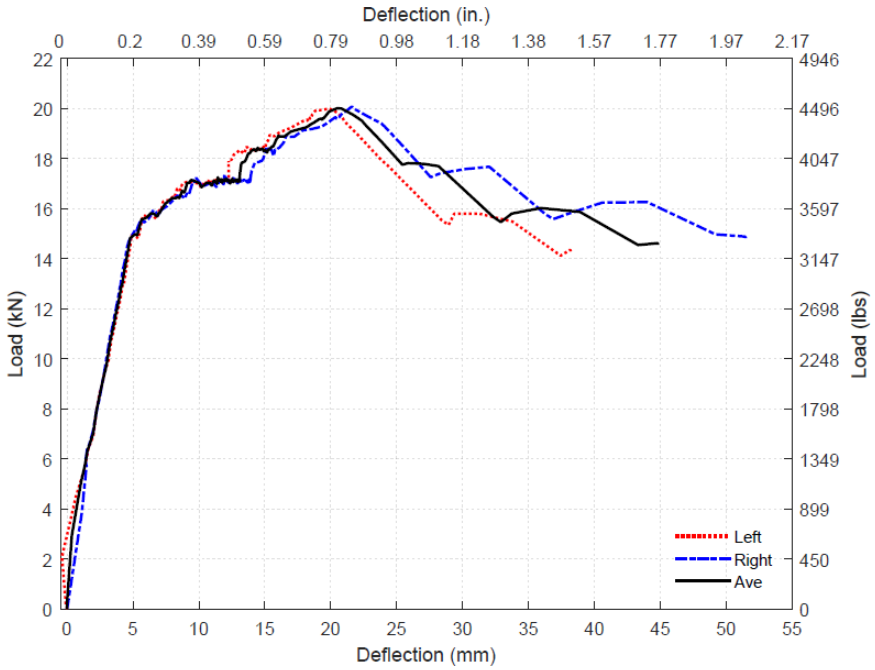

Figure 3-17. Load vs. deflection for B3-SL specimen for the entire test.

Figure 3-18. B3-SL failure.

Figure 3-19 exhibits the reinforcement strains. The tension reinforcement yielded when the load was 15.58 kN. The tension strain increased from 0.00211 mm/mm at the

load of 16.43 kN to 0.0064 mm/mm at the load of 16.65 kN. The compression strain increased as the load exceeded 14.83 kN, and the compression reinforcement became in the tension zone.

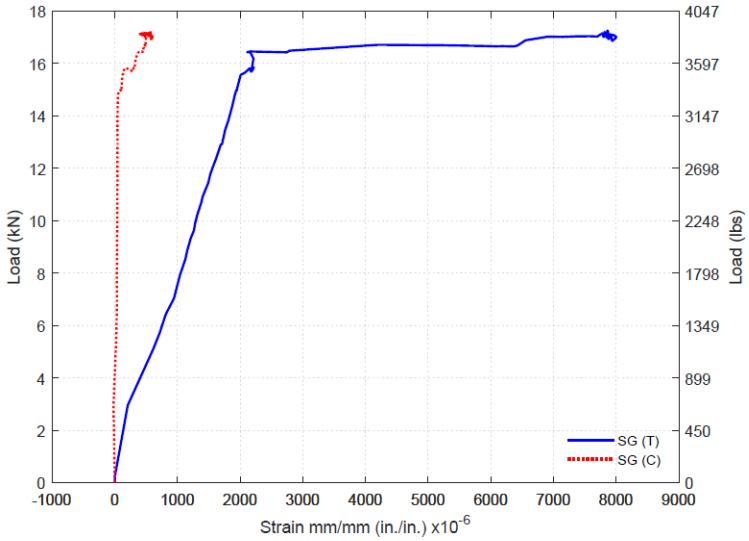

Figure 3-19. Load vs. SGs until the end of SL (B3-SL).

Figure 3-20 exhibits the reinforcement strains. At the beginning of the sustained loading, the tension and compression reinforcement strain were 0.0078 mm/mm (in./in.) and 0.00055 mm/mm (in./in.), and they became 0.0079 mm/mm (in./in.) and 0.00040 mm/mm (in./in.) at the end of the sustained loading. Thus, the tension strain increased by 0.00006 mm/mm (in./in.), which was 0.83% of the instantaneous tension strain. The compression strain decreased by 0.00014 mm/mm (in./in.), which was 25.88% of the instantaneous compression strain. The tension strain increased by 0.0002 mm/mm (in./in.) in the first 25 minutes. Then, it decreased with time until the time of 16 hours. After that it fluctuated due to load adjustment. Load adjustment could be known based on the deflection curve. The compression strain increased by 0.00004 mm/mm (in./in.) in the first 25 minutes; then it decreased unless load adjustment took place, which led to an increase in

compression strain. on the 16th day, load adjustment led to a huge decrease in tension strain and an increase in compression strain.

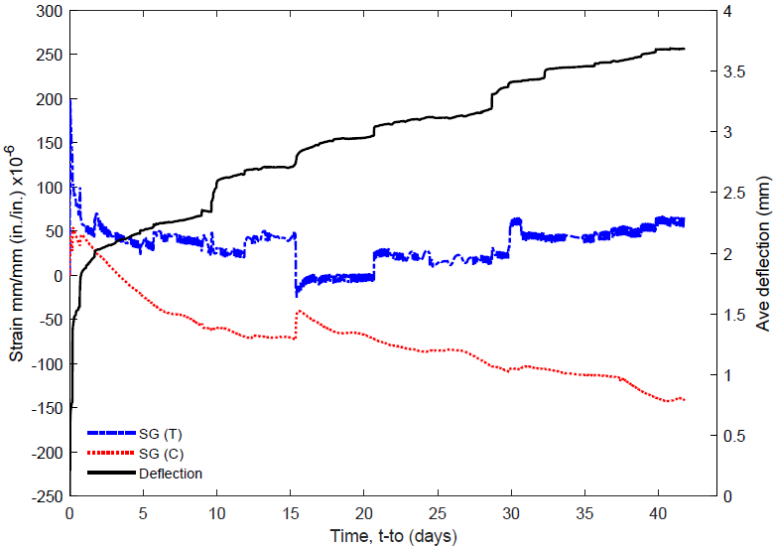

Figure 3-20. The change in strains under SL (B3-SL).

3.1.7.4 Beam 4 (B4-SL)

Beam 4 (B4-SL) was tested at the age of 135 days. The sustained load was 18.24 kN (4100 lbs), which is 93% of the short-term shear resistance of the control beam (BC1). The reduction in the stiffness of B4-SL occurred before the load reached 16 kN (3600 lbs). The left and right loading deflections at the beginning of the sustained loading were 9.90 mm (0.390 in.) and 11.42 mm (0.450 in.), respectively. At the end of the sustained loading period (24 days), the left and right loading deflections were 12.03 mm (0.474 in.) and 13.64 mm (0.537 in.), respectively. The percentages of the increase in deflections due to the sustained load were 21.55% and 19.44% of the instantaneous deflections for the left and right loading deflections. The load vs. deflection curve from the beginning of the test until the end of the sustained loading period is exhibited in Figure 3-21.

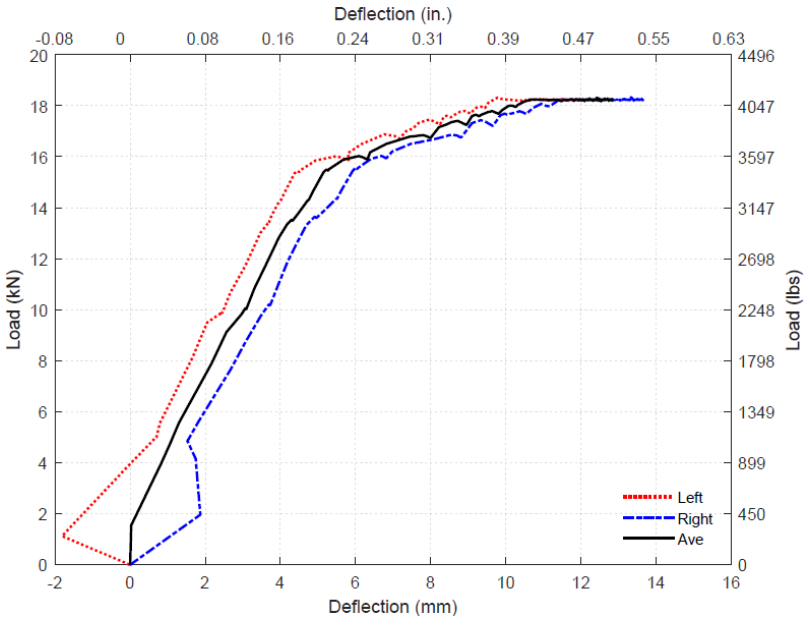

Figure 3-21. Load vs. deflection until the end of SL (B4-SL).

The increase in the deflections with time under sustained loading is shown in Figure 3-22. About 51% of the total increase under sustained in the right loading deflection took place in about 1 hour and 47 minutes, while 30% of the total deflection increase in the right loading deflection occurred in the same period. About 54.86% and 71.85% of the increases in the left and right loading deflections of the overall deflection increases under the sustained loading took place in the first 24 hours. The jumps in deflection in 16th and 20th days were due to the load adjustment. Also, the load adjustment caused a sudden increase in the deflection in the 23rd and 24th days. After seven days of the sustained loading, the percentages of increase in the left and right loading deflections of the overall deflection increases due to the time-dependent effect were 75.50% and 86%, respectively. In the beginning, there was a large difference between the left and right loading deflection increase. For example, the left loading deflection increase under sustained loading was 0.64 mm (0.025 in.), and the right loading deflection increase under sustained loading was 1.13

mm (0.045in.) at the time of one day and 47 minutes. Then at the end of the sustained loading period, this difference became small. At the end of the sustained loading period (24 days), the left and right loading deflection increases under sustained loading were 2.13 mm (0.084 in.) and 2.22 mm (0.087 in.).

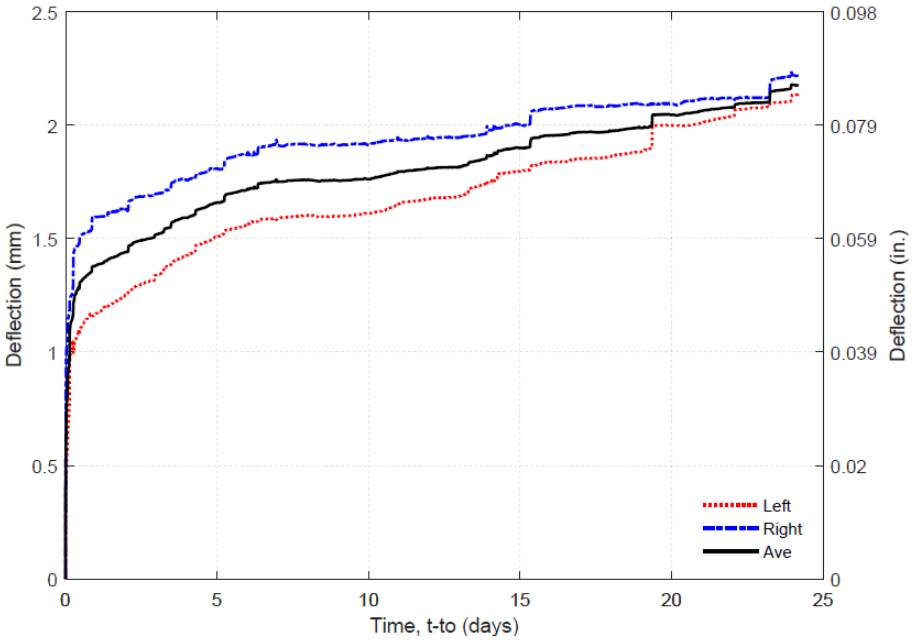

Figure 3-22. The increase in deflection under SL (B4-SL).

After 24 days, the period of sustained loading, the specimen was loaded up to failure. The peak load was 20.68 kN (4649 lbs), and the average deflection was 16.91 mm (0.666 in.). The left loading deflection was almost similar to the right loading deflection at the peak load. After the peak load, there was not much reduction in the loads. At the end of the test, the left load was 18.61 kN (4184 lbs), and the right load was 18.86 kN (4240 lbs). The left and right loading deflections were 44.48 mm (1.751 in.) and 32.04 mm (1.261 in.) at the end of the test after the shear failure. Figure 3-24 shows the failure of the specimen B4-SL. Flexural actions took place in this specimen before shear crack happened. The shear failure happened on the left side, which deflected more before the failure. It was

difficult to see the shear crack in this specimen. Crushing of concrete at the compression zone between the support took place before the shear failure.

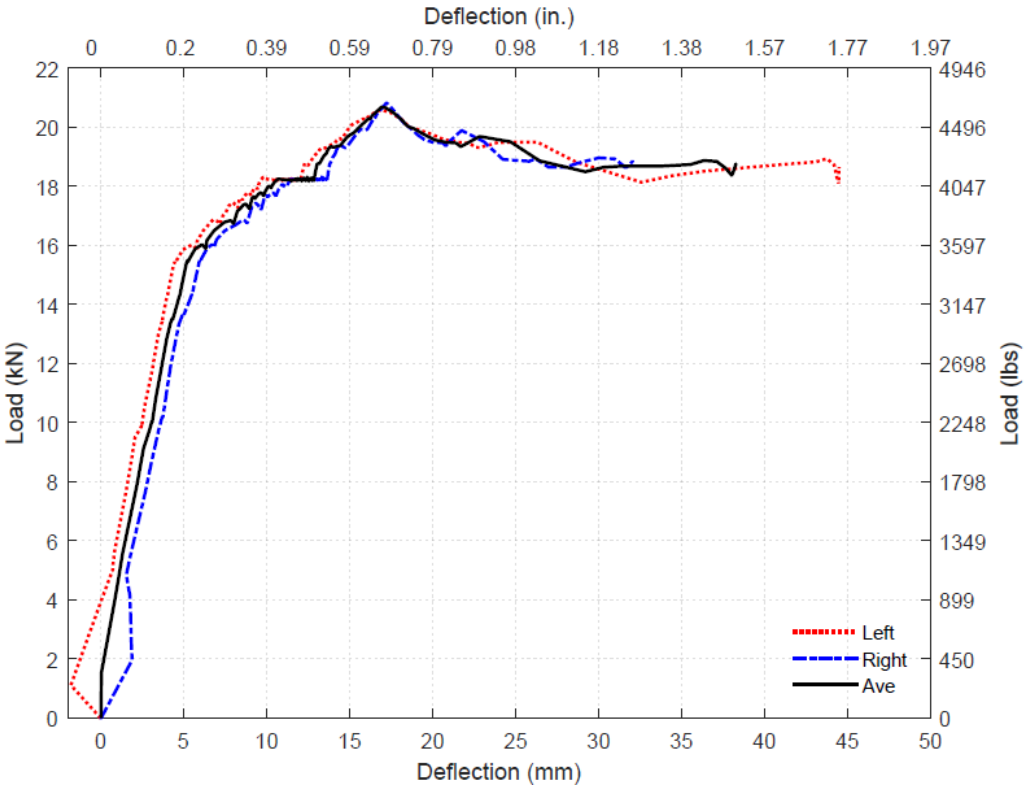

Figure 3-23. Load vs. deflection for B4-SL specimen for the entire test.

Figure 3-24. B4-SL failure.

Reinforcement strain up to the end of the sustained loading period is shown in Figure 3-25. At the beginning of the sustained loading, the tension and compression strains were 0.00265 mm/mm and 0.00062 mm/mm. The tension strain decreased a little at the

first 40 minutes. After that, the strain kept increasing with time to the end of the sustained loading period. The compression strain increased in the first 40 minutes to 0.000692 mm/mm; then, it decreased with the time until the end of the sustained loading period.

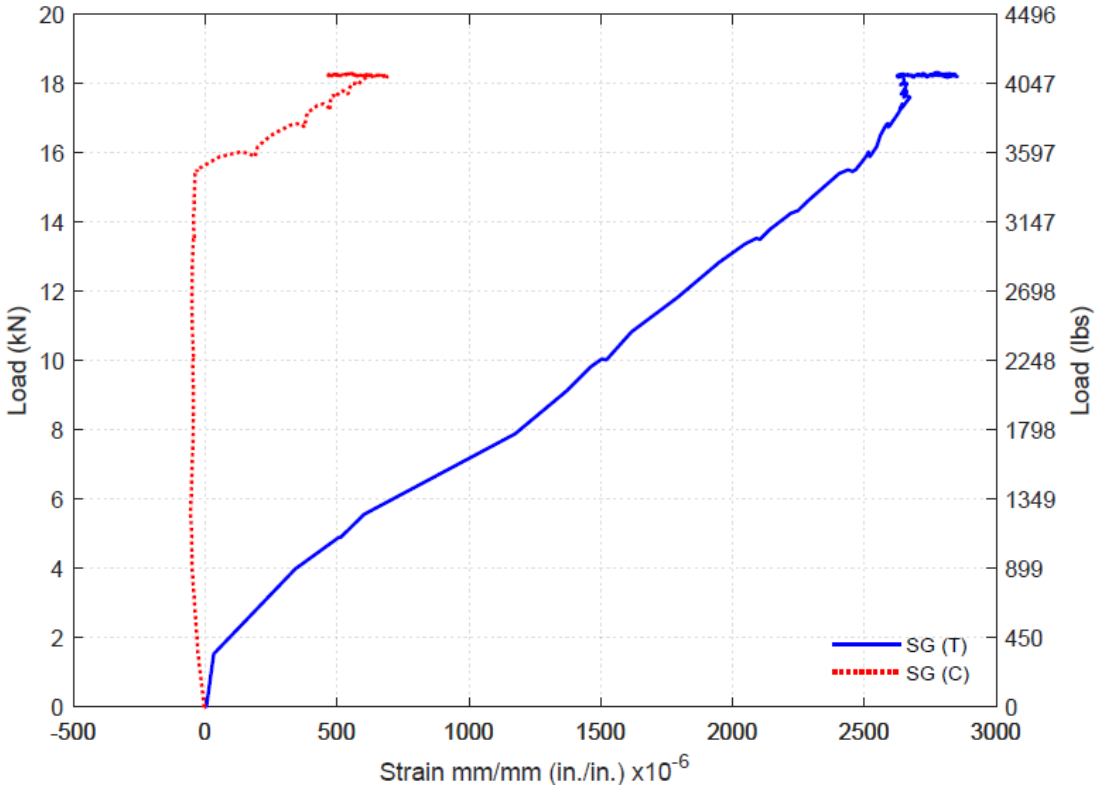

Figure 3-25. Load vs. SGs until the end of SL (B4-SL).

After ~ 62 hours, the compression strain became less than the initial value of strain (0.00062 mm/mm) at the beginning of the sustained loading. At the end of the sustained loading, the tension and compression strains were 0.00284 mm/mm and 0. 0.00046 mm/mm. The tension strain increased by 7.30%, and the compression strain decreased by 25% at the end of the sustained loading.

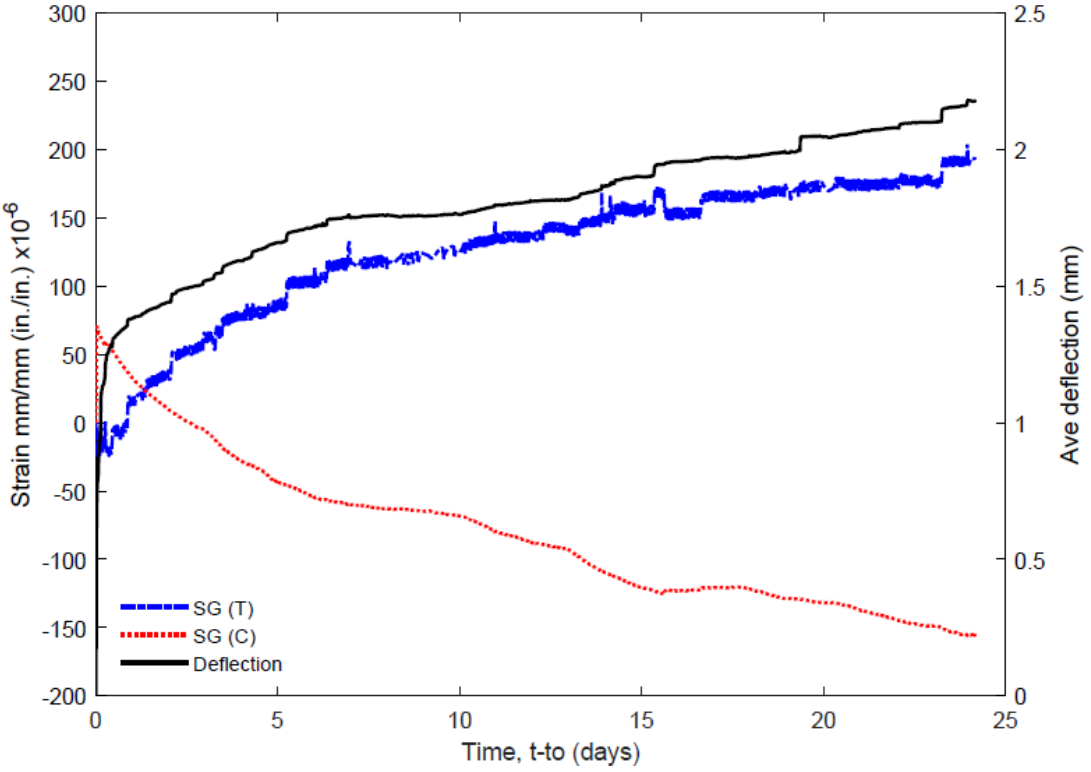

Figure 3-26. The change in strains under SL (B4-SL).

3.1.7.5 Temperature

Figure 3-27 exhibits temperature fluctuations of beam series I. Temperatures were about 60 ˚F for B2-SL and B4-SL. The temperatures of B3-SL were around 60 ˚F at the first eight days; then, they dropped to 55 ˚F. The temperature range of B2-SL was between 53 ˚F and 73 ˚F with an average of 59.65 ˚F. The temperature range was 51.15 ˚F and 68 ˚F for B3-SL. The average temperature of B3-SL was 56 ˚F. B4-SL had a temperature range of 55 ˚F and 60 ˚F with an average temperature of 61.67 ˚F.

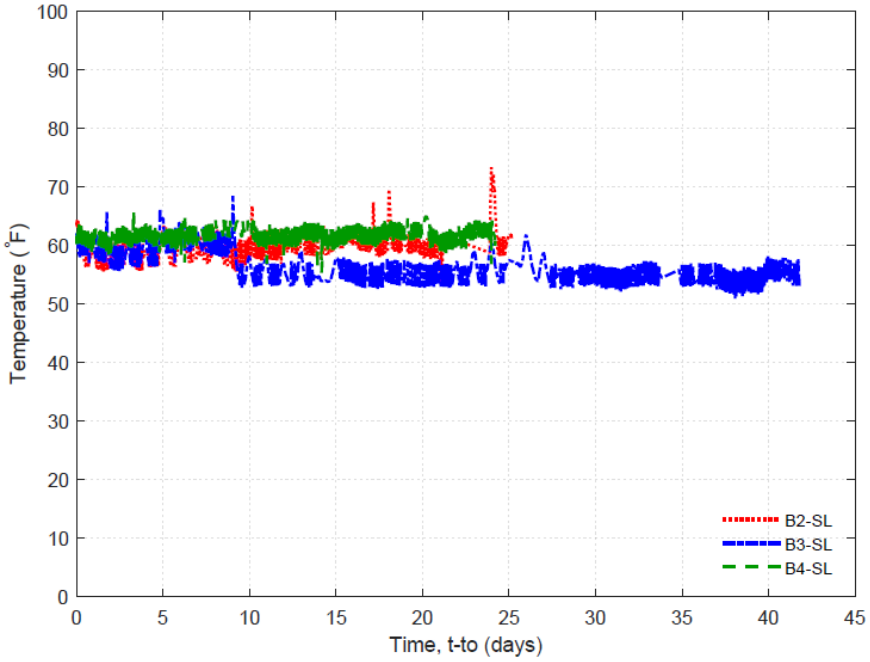

Figure 3-27. Temperature of beam series I.

3.1.8 Discussion

Figure 3-28 shows the load vs. deflection curves for beam series I, and

Table 3-2 summarizes the beam series I result. BC1 served as a control specimen, which was tested under monotonically increasing loading to failure. BC1 softened before the failure, and it failed at the load of 19.62 kN (4410 lbs) at the deflection of 12.75 mm (0.502 in.).

B2-SL was tested under the sustained load of 16 kN (3600 lbs), which was 82% of the short-term shear resistance of the control beam (BC1) for 25 days. At the end of the 25 days, the specimen was loaded up to failure. The ultimate load was 20.28 kN (4599 lbs), and the deflection at the ultimate load was 13.88 mm (0.547 in.).

B3-SL was under the sustained load of 17.13 kN (3850 lbs), which is 87% of the short-term shear resistance of the control beam, BC1, for 42 days. At the end of the

sustained load period, the load was increased to failure for B3-SL. The peak load and the deflection at the peak were 20.01 kN (4498 lbs) and 20.42 mm (0.804 in.), respectively.

B4-SL, the last specimen in this series, was tested under the sustained load of 18.24 kN (4100 lbs), which is 93% of the short-term shear resistance of the control beam (BC1) for 24 days. Then, the load was increased to failure. The ultimate load was 20.68 kN (4649 lbs), and the deflection at the ultimate load was 16.91 mm (0.666 in.).

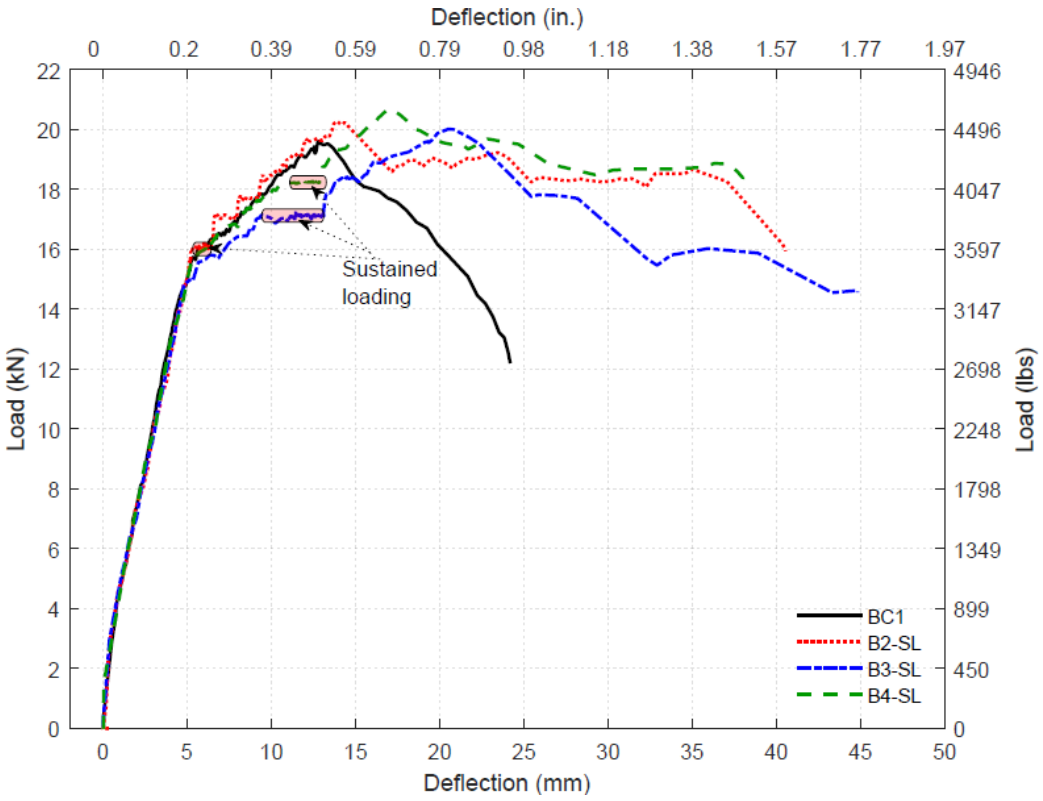

Figure 3-28. Load vs. deflection for beam series I.

The increase in the deflection of B2-SL under the sustained loading was small in comparison with B3-SL and B4-SL due to the lower level of load intensity, and the sustained load was applied before the softening of the stiffness took place. The increase in the deflection of B3-SL under the sustained loading was the highest in this series due to

initial softer stiffness and longer load duration. Also, the age of concrete at the application of the sustained load to B4-SL may be a reason why the increase in the deflection of B4-SL was less than the one in B3-SL.

The peak loads of B2-SL, B3-SL, and B4-SL were higher than the control specimen BC1 (5%, 3%, and 7%, respectively), and the failure of the specimens exhibited first flexural failure due to concrete crushing followed by shear failure at a reduced level of load. The deflections at flexural failure (peak loads) of the beams that experienced sustained load were on average 41% higher than the control specimen. The result shows the significant deflections that can occur under sustained load and may be an indicator of possible structural issues.

Figure 3-28 shows the significant increase in deflection after flexural failure for the beams that experienced sustained load. While the peak load is within the margin of variability for concrete specimens, it is clear the effect of the sustained load seemed to change the failure mode of the beams, as evidenced by significant displacements after peak load. The effect of the sustained load on the concrete compression resistance may have allowed the flexural failure to occur before the final shear failure even though the additional load was applied at a rate similar to the control specimen. The increase in peak load and delay of shear failure until after flexural failure agrees with Maekawa et al. (2006).

Table 3-2. Beam series I test matrix.

Specimen	BC1	B2-SL	B3-SL	B4-SL
Sustained load intensity	-	0.82	0.87	0.93
Loading age t_o (days)	64	65	91	135
Duration t_d (days)	-	25	42	24
Peak load kN (lbs)	19.62 (4410)	20.28 (4559)	20.01 (4498)	20.68 (4659)
Ratio of the peak load to the peak load of BC1	1	1.03	1.02	1.05
Deflection at the peak mm (in.)	12.75 (0.502)	13.88 (0.547)	20.47 (0.806)	16.91 (0.666)
Overall deflection mm (in.)	24.18 (0.952)	40.54 (1.596)	44.82 (1.765)	38.26 (1.506)
Ratio of deflection at the peak to deflection at peak of BC1	1	1.09	1.60	1.33

Figure 3-29 exhibits the increase in deflection during sustained loading and the sustained load intensity with time. All the specimens had the same general behavior. The behavior matches the behavior of concrete, as shown in Figure 2-7. In the first stage (primary), deflections increased rapidly; in the second stage (secondary), the deflections increased at a linear rate. None of the specimens reached the third stage (tertiary) during the sustained loading. Most of the jumps in deflections were due to load adjustments.

The increase in the deflection of B3-SL was the highest because it was the softest beam. B2-SL had the lowest increase in deflection because the sustained load intensity was the lowest. Figure 3-30 shows normalized sustained load & deflection with time up to 24 days. As can be seen in Figure 3-30, the increase in the deflection of B4-SL on the first day was the highest. While there are some differences with the specimens, all specimens show

a fairly similar percent increase in deflection with time. Most of the increase in deflection took place in the first week.

For reinforcement strain, the tension strain increased with the time under sustained loading in general. The increase of the tension strain with sustained loading indicates that the concrete was softening under the sustained load (as consistent with its material behavior), and due to compatibility, the reinforcement was carrying more load. The addition of the reinforcement in the tests is a likely reason the specimen did not fail under sustained load even though the load ratio was high.

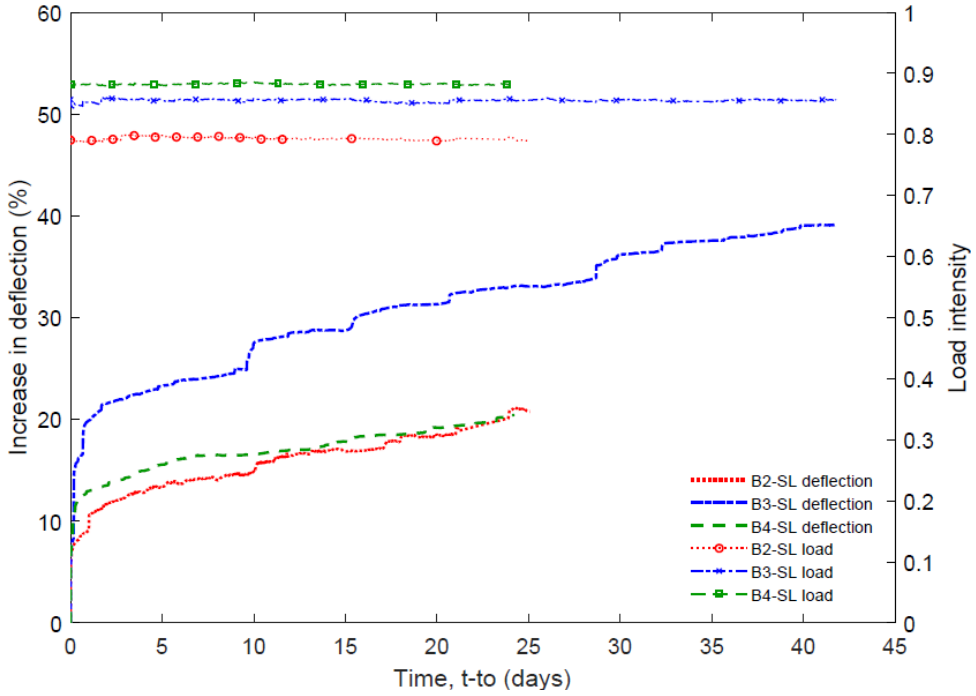

Figure 3-29. Sustained load & deflection with time.

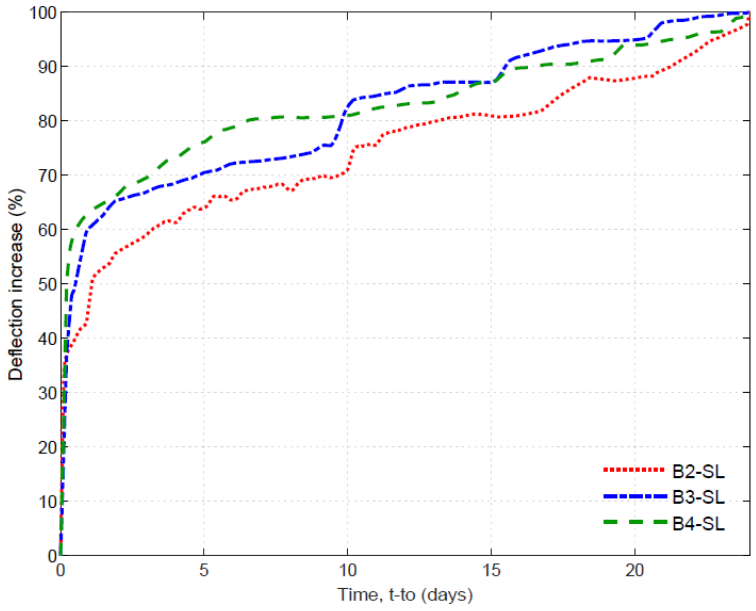

Figure 3-30. Normalized sustained load & deflection with time.

Figure 3-31 shows the increase in deflection and curvature under sustained loading. As shown, deflection and curvature increased under sustained loading. The increase in deflection in the first hours was higher than the increase in curvature. Lately, the increases in the curvature of B2-SL and B4-SL were higher.

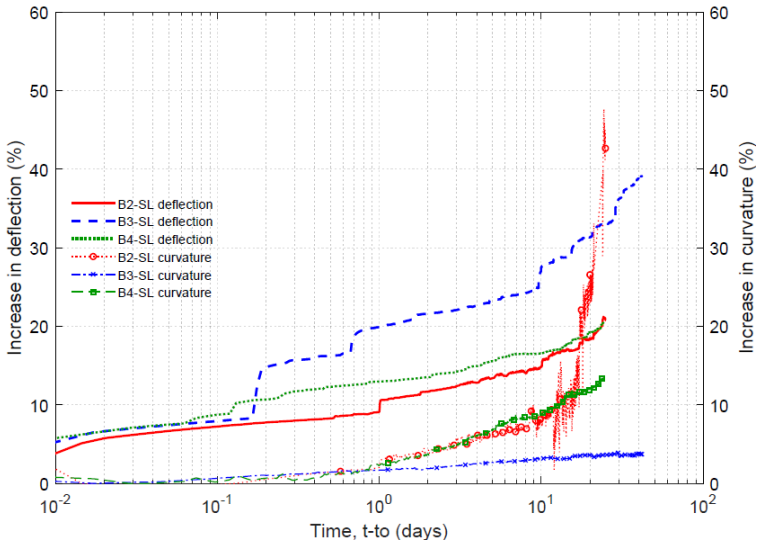

Figure 3-31. Increase in deflection and curvature under sustained loading (beam series I).

Figure 3-32 shows the beam series I failures. As can be seen, the control specimen, BC1, failed with a definite shear crack. The failure occurred suddenly without much flexural action going on the beam. The specimen was not capable of carrying loads after the failure. The rest of the beams, which were tested under sustained loading, experienced flexural failure and increases in deflection before ultimate shear failure. What can be noticed for specimens tested under sustained loads is that the shear crack became less definite when the sustained load intensity increased.

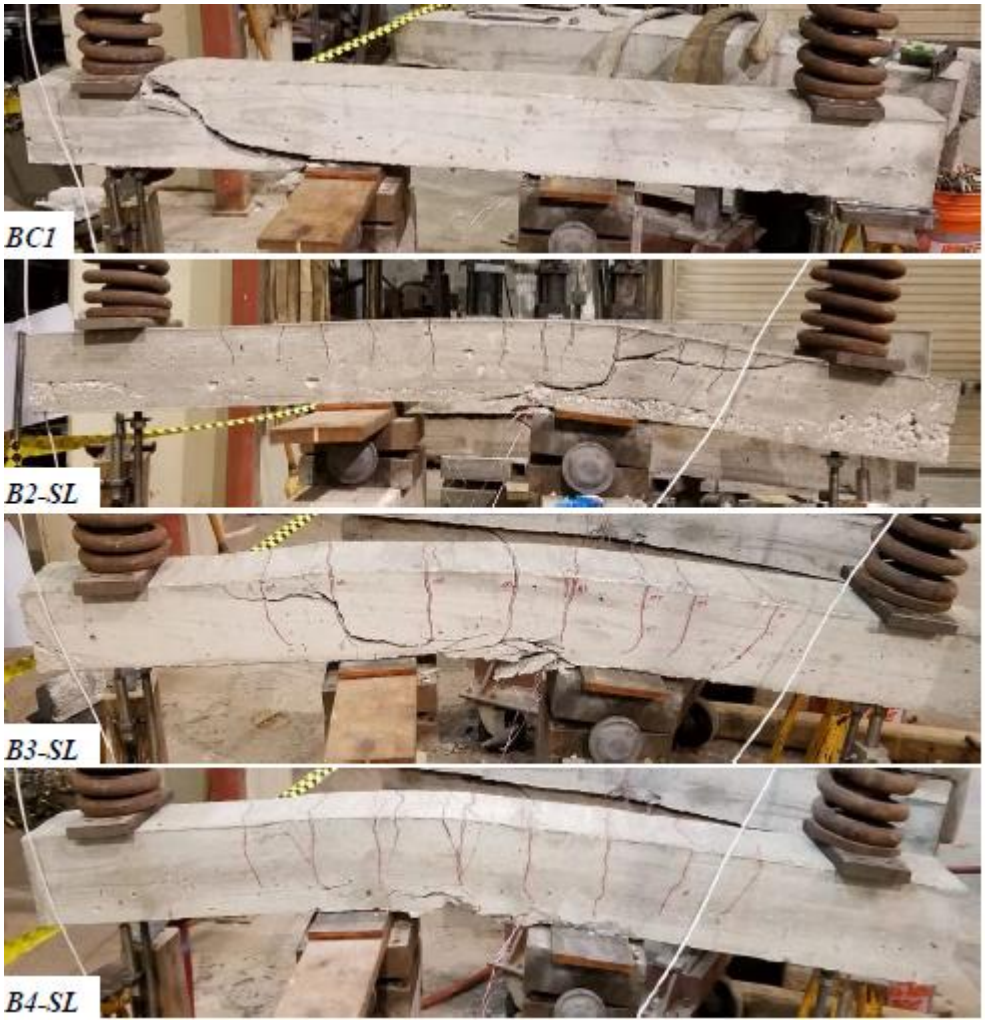

Figure 3-32. Beam series I failures.

During the sustained loading periods, energy dissipation and redistributions of stresses between the concrete and reinforcement took place. In this beam series, the specimens were loaded up to failure at the end of the sustained loading periods. When the sustained load intensity was higher, energy dissipation and redistributions of stresses under the sustained load increased. Then, when the specimen was loaded up to failure at the end of the sustained load period, the load required to make the specimen fail was the lowest for with highest sustained load intensity. Thus, the energy stored in the specimen was lowest, which led to a less definite shear crack. The opposite was true. When the load that was required to make the specimen fail was high, as what happened in B2-SL, the shear crack was very noticeable. Based on these limited data, sustained loading could change the mode of failure. This could be attributed to the that the flexural strength was close to the shear strength of this beam series, and sustained loading delayed the shear failure, as Maekawa et al. (2006) revealed.

3.2 Beam Series II

In series I, there was no failure under sustained loading, and the failure mode of specimens tested under sustained loading was flexural at first, with ultimate failure in shear. Therefore, the flexural reinforcement was increased to ensure that the specimens of series II failed in shear. In this experimental series, six beam specimens were tested under three-point bending (3PB). One specimen was tested under short-term loading serving as a control specimen, while the other five were tested under long-term loading of periods ranging from 84.5 minutes to 52 days.

3.2.1 Test Specimens

The experimental work involved the testing of six simply supported beams under three-point bending (3PB). The specimens were designed to fail in shear. The beam specimens were constructed with dimensions of 1524 mm × 140 mm × 140 mm (60 in. × 5.5 in. × 5.5 in.). All the specimens had two layers of reinforcement: one in the tension zone and another in the compression zone. The reinforcement ratios in the tension and compression zones were 1.29% and 0.86%, respectively.

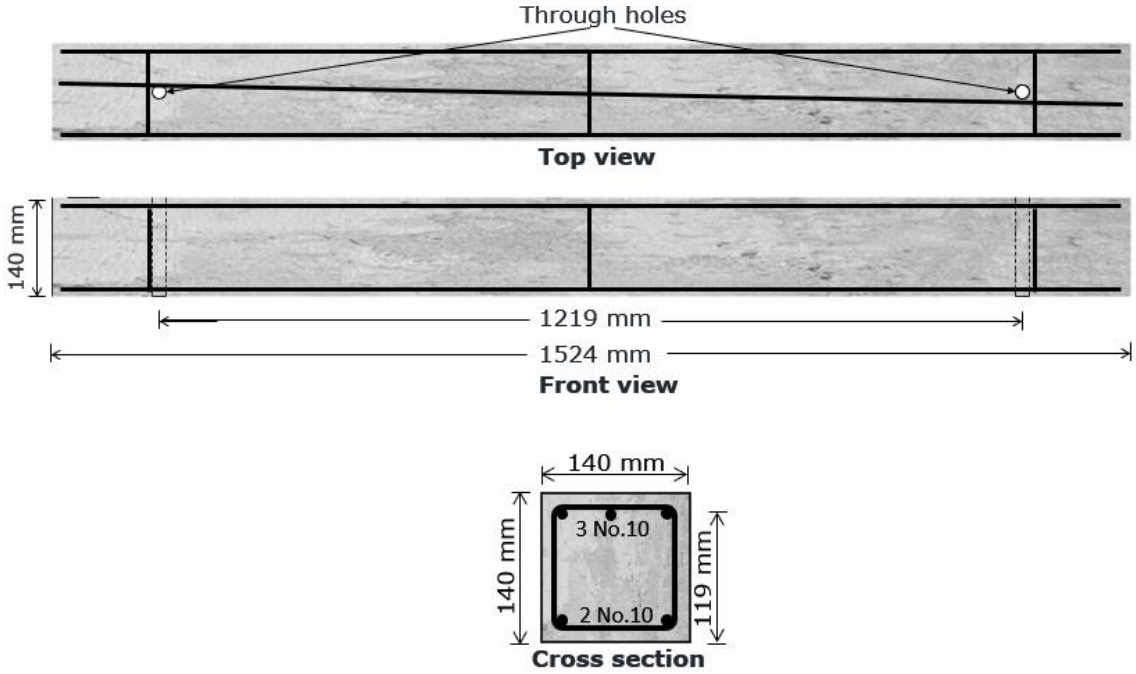

Figure 3-33. Reinforcement details of beam series II.

Three rebars were placed on the top, and two rebars were placed at the bottom of the beam. Three stirrups were provided to hold the reinforcement in the cage: one at the center and two outside the loading point, so they did not contribute to the shear strength. The rebars and the stirrups used in this series were No.10 (No.3) with 9.525-mm (3/8-inch) diameter, Grade 420 (Grade 60). The clear covers of 6.35 mm (0.25 in.) for both the tension

and compression flexural reinforcement rebars for all specimens as in the first series. Figure 3-33 shows the reinforcement configuration of this series.

3.2.2 Experimental Setup

The test setup is shown in Figure 3-34. The test setup was designed to apply concentrated loading at two points. Each beam had two through holes at (0.4 L) of the center created using PVC pipes to allow threaded rods to pass through and load the beam.

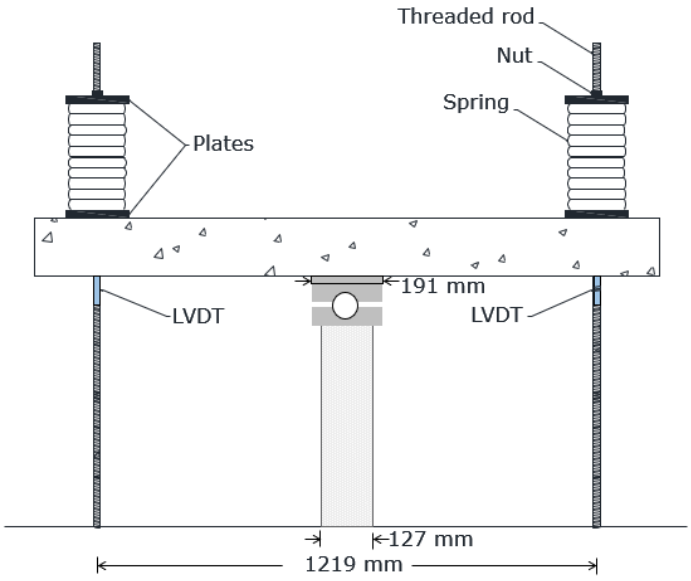

Figure 3-34. Beam series II test setup.

Each threaded rod was connected to a load cell to measure the applied load. Loads were applied to the beam by fastening the nuts on the top of the threaded rods. Beams were tested under three-point bending (3PB). One support with a thickness of 191 mm (7.5 in.) was used and set at the center span of the four-foot test setup. The loading was checked and adjusted in a short period of time (2-8 hrs) for the three days of loading. Afterward, the load was checked and might be adjusted every 24 hours.

3.2.3 Constructions of Specimens

The formwork was constructed, and stirrups and longitudinal rebars were placed and tied inside the forms. The stirrups were rested on 6.35 mm (0.25 in.) hardwood square dowels to provide a clear cover. Each beam specimen had two through holes for loading created using PVC pipes. After casting the concrete, the top surfaces were leveled and finished. The formwork was covered by plastic sheets and moist cured for one week. The formwork was removed after two weeks. Appendix A has a picture of the formwork with the reinforcement.

3.2.4 Loading Histories.

Figure 3-35 shows the loading histories for the second beam series except for the B6-SL loading history, which is exhibited in Figure 3-36. The control specimen, Beam 5 (BC5), was tested under monotonically increasing loading to failure at the age of 282 days. Beam 6 (B6-SL) was tested under the sustained load of 15.38 kN (3457 lbs) at the age of 284 days for 28 days. After that, the sustained load was increased by 0.35 kN (79 lbs) to 15.73 kN (3536 lbs) for three days. Then, the sustained load was increased by 0.35 kN (79 lbs), and the load was held for two days. The previous step was repeated nine times. In the

last step, the sustained load was 19.22 kN (4322 lbs). Then, the sustained load was increased by 0.35 kN (79 lbs) to 19.57 kN (4400 lbs), and the load was kept for ~3 hours. After that, the sustained load was increased to 19.92 kN (4479 lbs) for about 15 hours. Then, the sustained load was increased to 20.27 kN (4557 lbs) for 2 hours. Then, the test was terminated by increasing the load to failure.

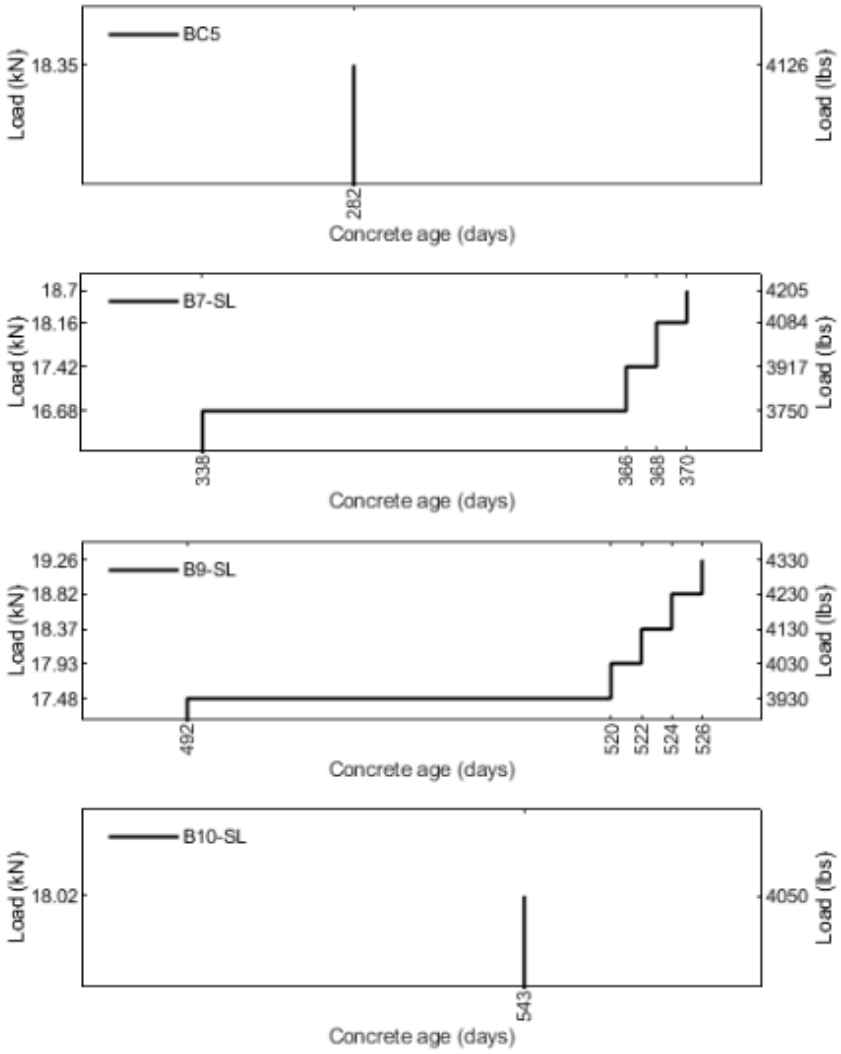

Figure 3-35. Beam series II loading histories.

Beam 7 (B7-SL) was loaded up at the age of 338 days. The sustained load was 16.68 kN (3750 lbs), and the load was held for 28 days. Then, the sustained load was

increased by 0.74 kN (166.67 lbs) to 17.42 kN (3917 lbs), and the load was kept for two days. After that, the sustained increased to 18.16 kN (4083 lbs) for two days. Then, B7-SL failed while adding additional load to it.

Beam 9 (B9-SL) was loaded up at the age of 492 days for 28 days. The sustained load was 17.48 kN (3930 lbs). After that, the sustained load was increased by 0.445 kN (100 lbs), and the load was held for two days. The previous step was repeated three times until the beam failed during the additional load of 19.26 kN (4330 lbs) after ~16 minutes.

Beam 10 (B10-SL) was the last specimen tested under sustained loading in beam series II. It was tested at the age of 543 under the sustained load of18.02 (4050 lbs) for 84.5 minutes when it failed under the sustained load.

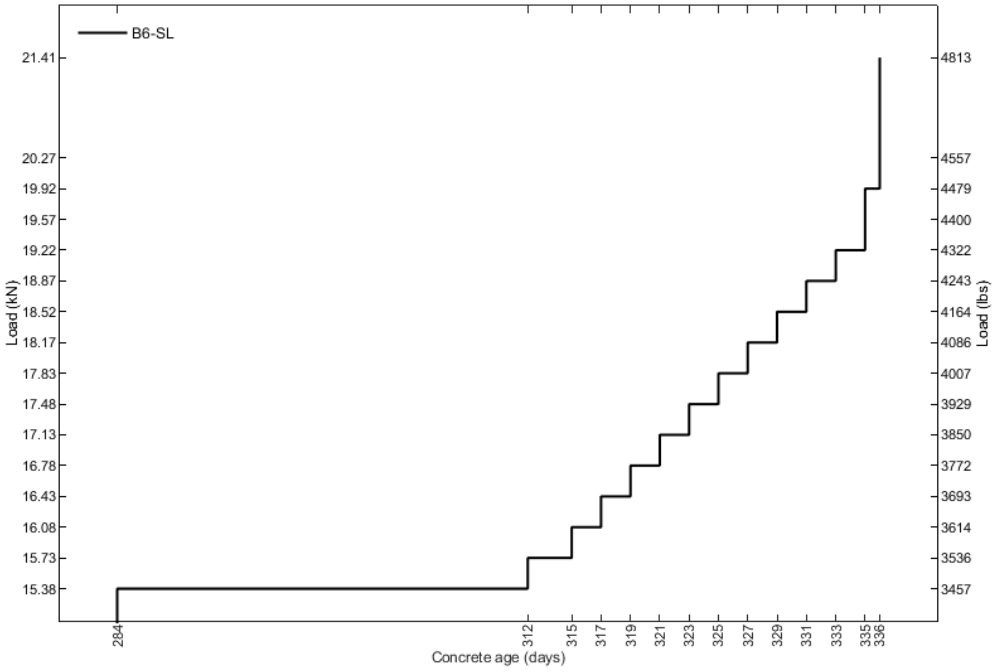

Figure 3-36. B6-SL loading history.

3.2.5 Instrumentation and Data Collection

The instrumentation and data collection used in beam series II were the same as beam series I.

3.2.6 Material Properties

The following section provides an overview of the mechanical properties of materials used to build series II beams, including concrete and steel reinforcement.

3.2.6.1 Concrete

The concrete mixture was designed to obtain 27.58 MPa (4000 psi) compressive strength at age 28 days. Batch 2 was utilized to construct these beam specimens. Cylindrical specimens of dimensions 100 × 200-mm (4 × 8-in.) were tested under compressive axial loading to obtain the average compressive strength of the concrete. The compressive strength of this batch at the age of 206 days was 35.45 MPa (5141 psi). Stress-strain curves from two of the tested cylindrical specimens are shown in Figure 3-37. The details of the concrete mixture of batch 2 are in Appendix A.

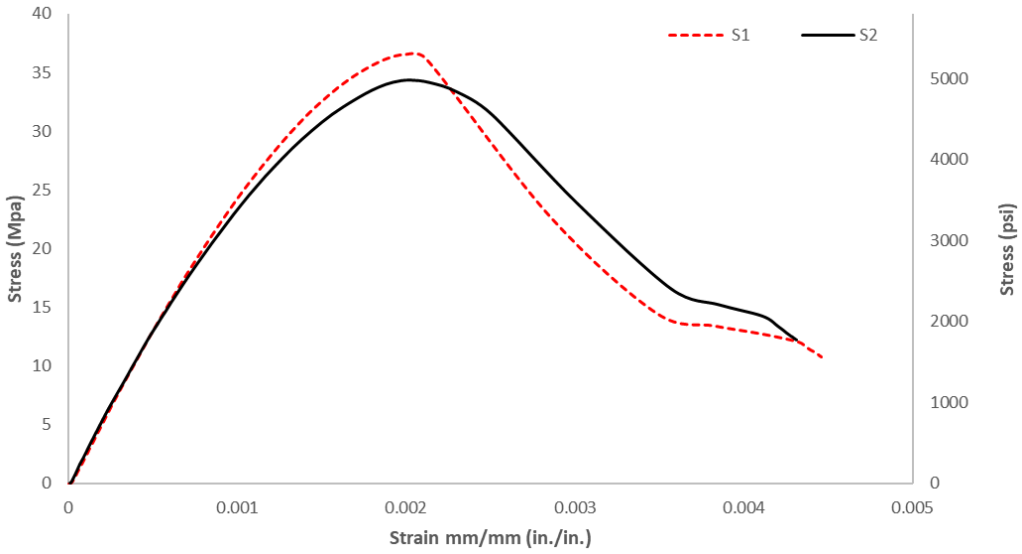

Figure 3-37. Stress-strain curves of concrete batch 2.

3.2.6.2 Steel Reinforcing Bars

The mechanical properties of reinforcement in beam series II were the same as beam series I.

3.2.7 Results

The results of beam series II are presented in this section. The control specimen was Beam 5 (BC5). The remaining beams were tested under high sustained loads. The sustained loads were ratios of the control specimen (BC5). Deflections, mode of failure, and reinforcement strains are presented.

3.2.7.1 Beam 5 (BC5)

Beam 5 (BC5) was loaded monotonically to failure at the age of 282 days as a control specimen of beam series II. The load versus the average deflection is shown in Figure 3-38. The first cracking of the concrete occurred around 4 kN (899 lbs). The applied load was increased to 18.35 kN (4126 lbs), and the specimen failed at this load when the average

deflection was 5.64 mm (0.222 in.). The design depth of all the tension reinforcement was 119 mm (4.6875 in.). However, the average depth was found to be 116 mm (4.573 in.) for this specimen.

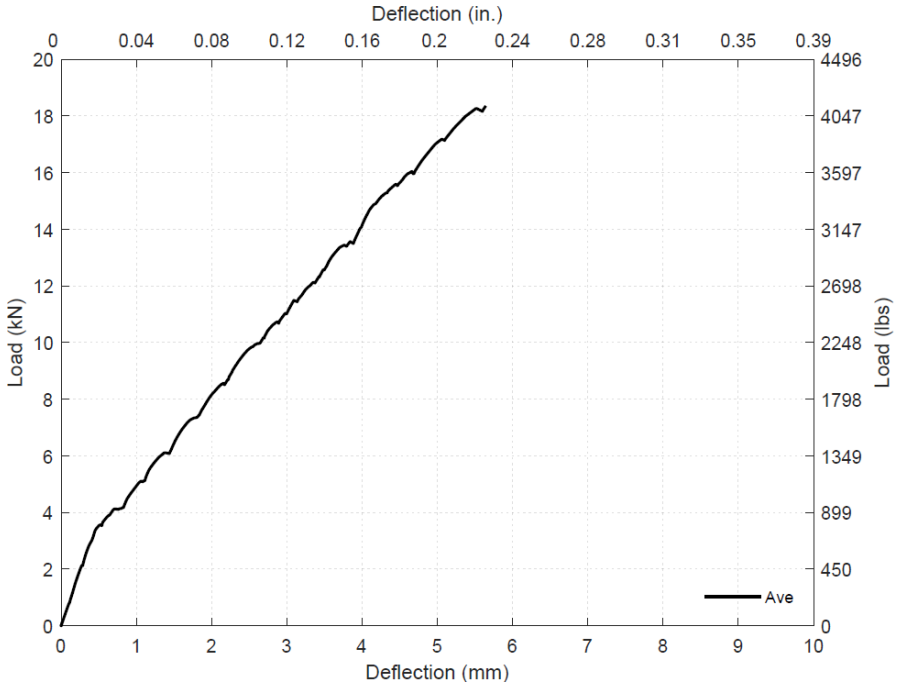

Figure 3-38. Load vs. deflection for BC5 specimen.

Reinforcement strains are shown in Figure 3-39. As can be seen, the tension reinforcement strain was linear. At the failure, the tension strain was 0.00265 mm/mm (in./in.) The compression reinforcement strain increased with the increase of the load. It reached the maximum strain of 0.00019 mm/mm (in./in.) when the load was 14.26 kN (3206 lbs). Then, the compression strain decreased with the increase of the load due to the movement of the natural axis. At the failure, the compression strain was 0.00017 mm/mm (in./in.)

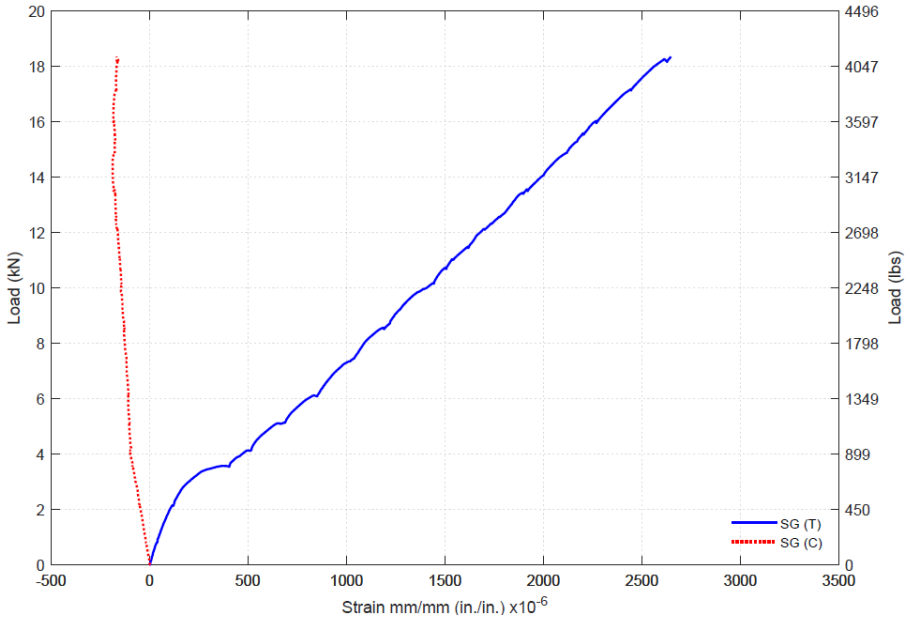

Figure 3-39. Load vs reinforcement strain responses for BC5.

BC5 failed with sudden shear failure, as can be seen in Figure 3-40. The reinforcement bars can be seen due to the concrete cover crushed on the left tension zone. The specimen had a branching crack. The flexural deflections were very small.

Figure 3-40. Beam 5 (BC5) failure.

3.2.7.2 Beam 6 (B6–SL)

Beam 6 (B6-SL) was loaded up to the sustained load of 15.38 kN (3457 lbs) at the age of 284 days. The percentage of the sustained load to short-term resistance of BC5 was 84%. Figure 3-41 shows the load vs. deflection curve of B6-SL, and load vs. reinforcement strain responses for B6-SL is exhibited in Figure 3-42. Table 3-3 and Table 3-4 summarize

the increase in deflection and the change in reinforcement strain. There were 15 sustained loading stages before loading up the specimen to failure.

The first stage of the sustained load of 15.38 kN (3457 lbs) lasted 28 days. At the beginning of the first stage of the sustained loading, the deflection was 4.98 mm (0.196 in.). The deflection was 5.75 mm (0.226 in.) at the end of the first stage of sustained loading. The total increase in deflection was 0.77 mm (0.030 in.), which was 15.43% of the instantaneous deflection. The tension and the compression reinforcement strains were 0.00236 mm/mm and -0.00088 mm/mm at the beginning of the sustained loading. At the end of the first stage, the tension and the compression reinforcement strains were 0.00016 mm/mm and -0.00040 mm/mm. The increase percent in strain was 6.57% and 45.42% for the tension and the compression reinforcement strains.

The second stage of the sustained loading was 15.73 kN (3536 lbs), and the load was kept for three days. The increase in deflection during this stage was 0.10 mm (0.004 in.). The ratio of increase in deflection to the first stage was 0.125 because the additional load in this stage to the previous stage was small, and the specimen underwent most of the load in the first stage. The increase in the tension and the compression reinforcement strains during this stage were 0.000014 mm/mm and 0.000004 mm/mm. There was a small reduction in the compression strain.

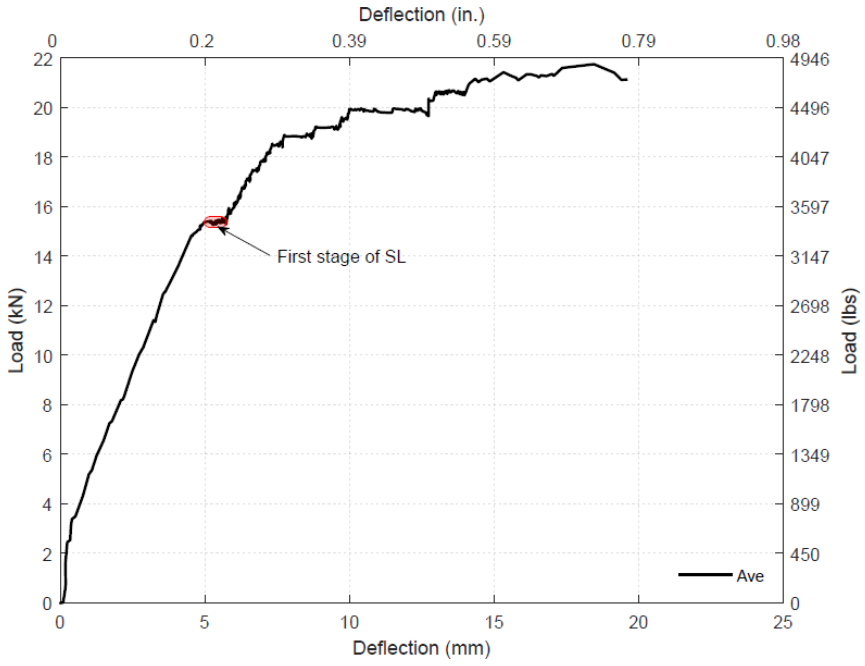

Figure 3-41. Load vs. deflection for B6-SL.

The third stage of the sustained loading was 16.08 kN (3614 lbs), and the load was held for two days. The increase in deflection during this stage was 0.07 mm (0.003 in.). The ratio of increase in deflection in this stage to the first stage was 0.086. The increase in the tension strain during this stage was 0.000008 mm/mm. The compression reinforcement strain decreased by 0.000002 mm/mm.

The 4th stage of the sustained loading was 16.43 kN (3693 lbs), and it lasted for two days. The increase in deflection in this stage was 0.05 mm (0.002 in.). The ratio of increase in deflection in this stage to the first stage was 0.063. The ratio of deflection to the first stage decreased with the increase of the load, and the lowest ratio was in the 4th stage of the sustained loading. During this stage of loading, the tension and the compression reinforcement strains increased by 0.00013 mm/mm and 0.00001 mm/mm.

The 5th stage of the sustained loading was 16.78 kN (3772 lbs), and the load was kept for two days. The increase in deflection in this stage was 0.08 mm (0.003 in.). The ratio of increase in deflection in this stage to the first stage was 0.104. The ratio of increase in deflection began to increase. In this sustained loading stage, the increases in the tension and the compression reinforcement strains were 0.00002 mm/mm and 0.00002 mm/mm.

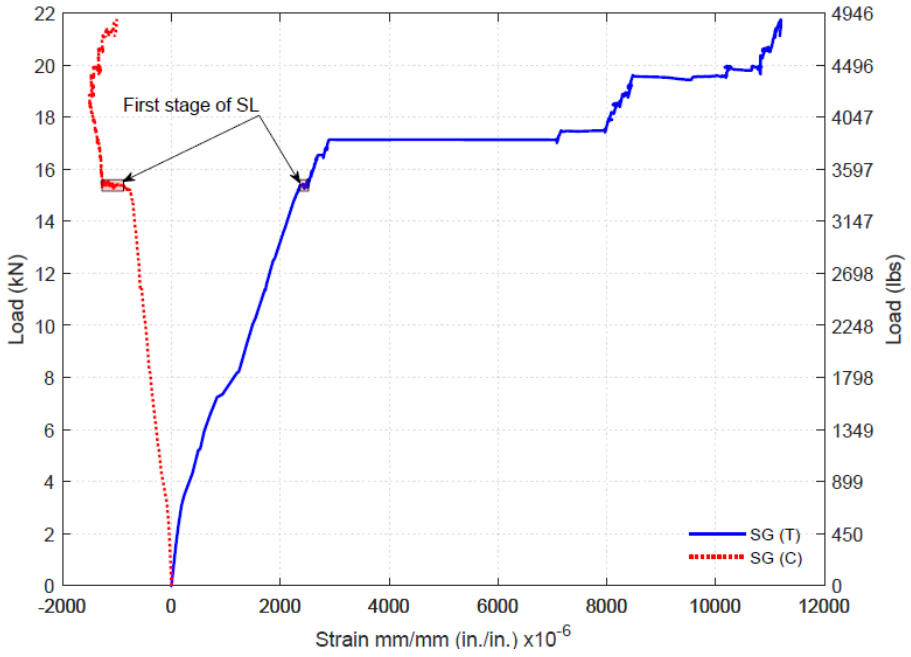

Figure 3-42. Load vs reinforcement strain responses for B6-SL.

The 6th stage of the sustained loading was 17.13 kN (3850 lbs), and the load was kept for two days. The increase in deflection in this stage was 0.11 mm (0.004 in.). The ratio of increase in deflection in this stage to the first stage was 0.146. The ratio of increase in deflection was highest so far after the first stage. The tension and the compression reinforcement strains increased by 0.00418 mm/mm and 0.00002 mm/mm. The ratio of the tension reinforcement strain to the one in the first stage was 29.98, which was high. The compression strain seemed stable in this stage.

The 7th stage of the sustained loading was 17.48 kN (3929 lbs), and the load lasted for two days. The increase in deflection in this stage was 0.19 mm (0.008 in.). The ratio of increase in deflection in this stage to the first stage was 0.251. In this sustained loading stage, the increases in the tension and the compression reinforcement strains were 0.00081 mm/mm and 0.00002 mm/mm. The ratio of increase in the tension reinforcement strain in this stage to the tension reinforcement strain in the first stage was 5.23.

Table 3-3 .Increases in deflection under all stages of sustained loading (B6-SL).

Stage	Duration (days)	Load		Increase in deflection	
		kN	lbs	mm	in.
1	27.9	15.38	3457	0.77	0.030
2	3.0	15.73	3536	0.10	0.004
3	2.0	16.08	3614	0.07	0.003
4	2.0	16.43	3693	0.05	0.002
5	2.0	16.78	3772	0.08	0.003
6	2.0	17.13	3850	0.11	0.004
7	2.1	17.48	3929	0.19	0.008
8	1.9	17.83	4007	0.15	0.006
9	2.0	18.17	4086	0.10	0.004
10	2.0	18.52	4164	0.36	0.014
11	2.0	18.87	4243	1.00	0.039
12	2.0	19.22	4322	0.83	0.033
13	0.12	19.57	4400	0.21	0.008
14	0.64	19.92	4479	2.75	0.108
15	0.08	20.27	4557	1.04	0.041

The 8th stage of the sustained loading was 17.83 kN (4007 lbs), and the load was held for two days. The increase in deflection in this stage was 0.15 mm (0.006 in.). The ratio of increase in deflection in this stage to the first stage was 0.198. The tension and the compression reinforcement strains increased by 0.00001 mm/mm and 0.00002 mm/mm. The tension reinforcement strain became stable.

In the 9th stage, the sustained loading was 18.17 kN (4086 lbs), and it lasted for two days. The increase in deflection in this stage was 0.10 mm (0.004 in.). The ratio of increase in deflection in this stage to the first stage was 0.136. In this sustained loading stage, the increases in the tension and the compression reinforcement strains were 0.00005 mm/mm and 0.00002 mm/mm.

The 10th stage of the sustained loading was 18.52 kN (4164 lbs), and the load lasted for two days. The increase in deflection in this stage was 0.36 mm (0.014 in.). The ratio of increase in deflection in this stage to the first stage was 0.462. The tension and the compression reinforcement strains increased by 0.00005 mm/mm and 0.00001 mm/mm.

In the 11th stage, the sustained loading was 18.87 kN (4243 lbs), and it was kept for two days. The increase in deflection in this stage was 1.00 mm (0.039 in.). The ratio of increase in deflection in this stage to the first stage was 1.297. In this stage, the increase in the deflection was higher than the increase in the deflection in the first stage, although the duration was just two days compared to 28 days in the first stage. The specimen was not capable of bearing the sustained load. In this stage, the tension reinforcement strain increased by 0.0001 mm/mm, while the compression reinforcement strain decreased by 0.00005 mm/mm.

The 12th stage of the sustained loading was 19.22 kN (4322 lbs), and the load lasted for two days. The increase in deflection in this stage was 0.83 mm (0.033 in.). The ratio of increase in deflection in this stage to the first stage was 1.079. The increase in deflection in this stage was also higher than the one in the first stage. The tension reinforcement strain decreased by 0.00002 mm/mm, while the compression reinforcement strains increased by 0.000003 mm/mm.

In the 13th stage, the sustained loading was 19.57 kN (4400 lbs), and it was kept for ~3 hours. The increase in deflection in this stage was 0.21 mm (0.008 in.). The ratio of increase in deflection in this stage to the first stage was 0.268. the tension reinforcement strain increased by 0.00172 mm/mm, and the compression reinforcement strain decreased by 0.00005 mm/mm in this loading stage. The ratio of tension strain to the one in the first stage was 11. The neutral axis started moving toward the compression zone due to cracking. Thus, the compression strain decreased.

The 14th stage of the sustained loading was 19.92 kN (4479 lbs), and the load was kept for two days. The increase in deflection in this stage was 2.75 mm (0.108 in.). The ratio of increase in deflection in this stage to the first stage was 3.576, although the duration of the load was ~15 hours. At this stage, the specimen seemed not able to resist the sustained load. In this stage, the tension reinforcement strain increased by 0.00060 mm/mm. The compression reinforcement decreased by 0.00009 mm/mm.

The last stage of sustained loading, which lasted two hours, was 20.27 kN (4557 lbs). The increase in deflection under sustained load in this stage was 1.04 mm (0.041 in.), and the ratio of increase to the increase in the first stage was 1.36. In this stage, the tension strain continued to increase, and compression strain continued to decrease. The tension strain increased by 0.00012 mm/mm, and the compression decreased by 0.00006 mm/mm.

Finally, the specimen was loaded to failure, and it failed due to critical shear at the load 21.13 kN (4750 lbs) at the deflection of 19.62 mm (0.772 in.). The tension and compression strains at the shear failure were 0.0112 mm/mm and -0.00106 mm/mm. The peak load was 21.75 kN (4889 lbs) at a deflection of 18.45 mm (0.727 in.). At the peak, the tension and compression strains were 0.0112 mm/mm and -0.00101 mm/mm. The ratio

B6-SL strength to BC5 strength was 1.185, while the ratio of B6-SL shear resistance to BC5 shear resistance was 1.151. Therefore, the sustained load increased the strength of the specimen. The shear failure deflection of B6-SL was 3.48 times that of the shear failure deflection of BC5. Thus, the sustained load increased the deformation of the specimen. The design depth of all the tension reinforcement was 119 mm (4.6875 in.). However, the average depth was found to be 112 mm (4.41 in.).

Table 3-4. Change in strain under all stages of sustained loading (B6-SL).

Stage	Duration (days)	Change in strain	
		Tension	Compression
1	27.9	0.00016	-0.00040
2	3.0	0.00001	-0.000004
3	2.0	0.00001	0.000002
4	2.0	0.00013	-0.00001
5	2.0	0.00002	-0.00002
6	2.0	0.00418	-0.00002
7	2.1	0.00081	-0.00002
8	1.9	0.00001	-0.00002
9	2.0	0.00005	-0.00002
10	2.0	0.00005	-0.00001
11	2.0	0.00010	0.00005
12	2.0	-0.00002	0.00000
13	0.12	0.00172	0.00005
14	0.64	0.00060	0.00009
15	0.08	0.00012	0.00006

Figure 3-43 shows the increase in strains and deflection under the first stage of the sustained load of 15.38 kN (3457 lbs). Table 3-5 summarizes the percentage of increase in strains and deflection in the first stage of sustained loading. At the beginning of the first sustained load, the average deflection was 4.98 mm (0.196 in.). After one day, the average deflection increased to 5.15 mm (0.203 in.). The increase percent in the average deflection

of the total increase under the first stage of the sustained loading was 22.69%. At the beginning of the seventh day, the average deflection increased by 64.84% of the total increase to 5.48 mm (0.216 in.). after three weeks, the average deflection became 5.72 mm (0.225 in.), which was 96.64% of the total increase in deflection under the first stage of the sustained loading. At the end of the first stage, the deflection became 5.75 mm (0.226 in.). The tension and compression reinforcement strains were 0.00236 mm/mm (in./in.) and 0.00088 mm/mm (in./in.) at the beginning of the first stage of the sustained loading. At the end of the first stage, the tension and compression strains became 0.0025141 mm/mm (in./in.) and 0.00128 mm/mm (in./in.). The increase in the compression strain was 2.58 times the increase in the tension strain. Over 92% of the increase in the strains took place in the first three weeks.

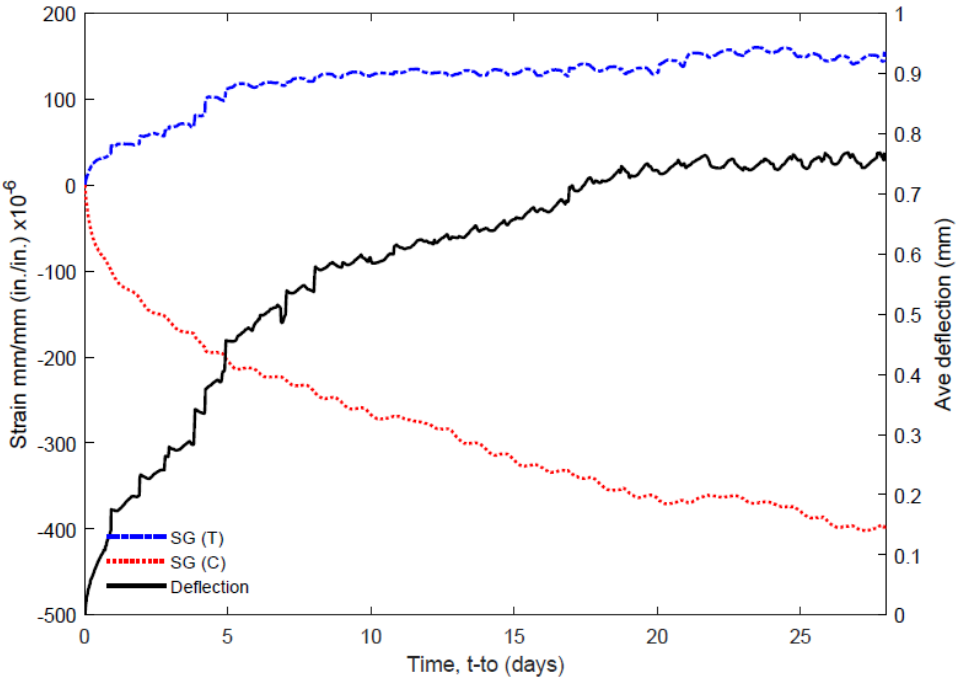

Figure 3-43. The increase in strains and deflection under 1st stage of SL (B6-SL).

Table 3-5. Percentages of the increase in strains and deflection under 1st stage of SL (B6-SL).

Time (days)	SG (T) (%)	SG (C) (%)	Ave deflection (%)
1	29.02	26.40	22.69
7	74.72	56.56	64.82
21	94.32	92.13	96.64
27.93	100	100	100

Figure 3-44 shows the failure of B6-SL. The specimen deflected more than any specimen in this series, and the strength was the highest. Although the specimen failed in shear, the shear crack is less prominent than in the other specimens. The specimen reached the flexural strength; then compression failure took place over the support, which resulted in the crack in the right side and a reduction in the load.

Figure 3-44. Beam 6 (B6-SL) failure.

3.2.7.3 Beam 7 (B7–SL)

Beam 7 (B7-SL) was tested at the age of 338 days. There were three stages of sustained loading before the specimen failed while adding load to it. The first stage of the sustained loading was 16.68 kN (3750 lbs), which was 91% of the short-term resistance of BC5. This sustained load was kept for 28 days. Figure 3-45 exhibits the average load vs. average deflection curve of B7-SL. At the beginning of the sustained load of 16.68 kN (3750 lbs), the average deflection was 6.45 mm (0.254 in.), and it became 8.03 mm (0.326)

at the end of the sustained load period (28 days). The increase in the average deflection was 1.49 mm (0.062 in.), which was 24.61% of the instantaneous deflection.

In the second stage of the sustained loads, which lasted two days, the sustained load was increased by 0.74 kN (166.67 lbs) to17.42 kN (3917 lbs). The increase in average deflection at the end of the two-day period was 0.27 mm (0.011 in.), which was 0.172 times the increase in the deflection in the first stage. The increase was not that much because the specimen experienced most of the applied load during the first stage of loading, which lasted for 28 days.

The last stage of the sustained loads was 18.16 kN (4084 lbs), which was held for two days. The average deflection was 8.65 mm (0.340 in.) at the beginning of this stage of the sustained loads, and it was 11.62 mm (0.457) at the end of this sustained load period. Thus, the increase in the average deflection was 2.97 mm (0.117 in.), which was 1.87 times the increase in the first stage, although the duration in this stage was just two days and it was 28 days in the first stage. The damage to the specimen was high, and it seemed like the specimen was close to failure.

Finally, the specimen failed while trying to add another 0.74 kN (166.67 lbs) of the load. The load failure was 18.70 kN (4205 lbs) at the average deflection of 11.76 mm (0.463 in.). The difference between the failure load and the last sustained load was 0.54 kN (121 lbs). The percentage of the last sustained load to the failure load was 97%. The strength of B7-SL was slightly higher than the strength of the control specimen, BC5. The ratio of the B7-SL failure load to BC5 failure load was 1.02. The failure deflection of B7-SL was 2.08 times that of the failure deflection of BC5. If the increase in deflection was subtracted, the ratio became 1.23. Thus, the sustained load increased the deformation of

the specimen. The design depth of all the tension reinforcement was 119 mm (4.6875 in.). However, the average depth was found to be 112 mm (4.42 in.). The depth was less than the depth of BC5.

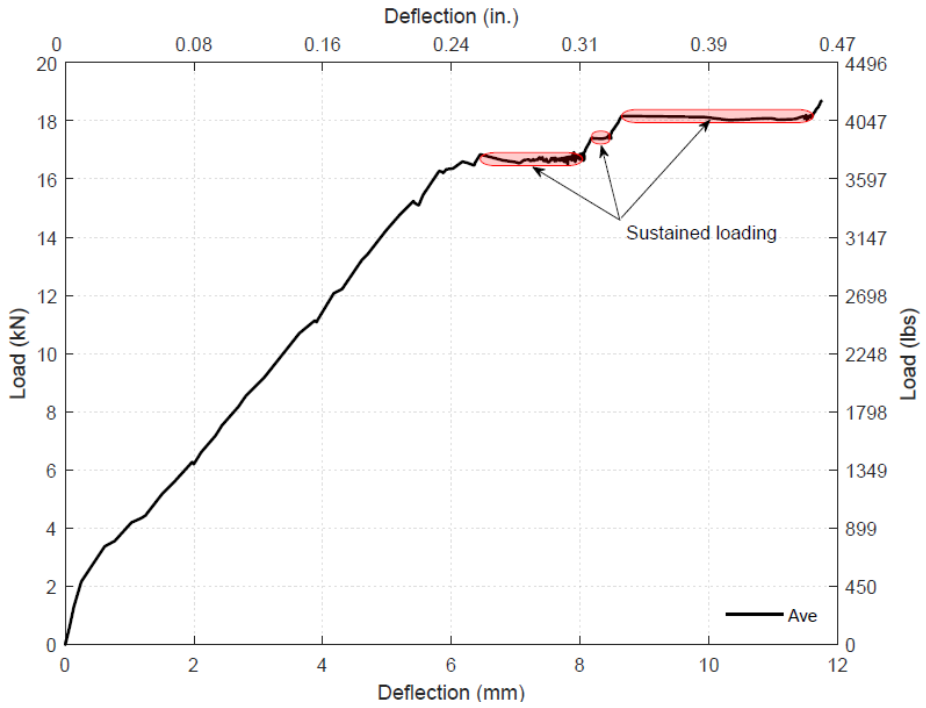

Figure 3-45. Load vs. deflection for B7-SL.

Figure 3-46 shows the increase in the average deflection under the first stage of the sustained loading, which lasted for 28 days. About 50% of the total increase in deflection took place in the 100 minutes. The average deflection after 24 hours was 1.15 mm (0.0452 in.), which was 72.32% of the total increase on the deflection 1.59 mm (0.0625 in.) under this stage of the sustained loading. At the beginning of the 8th day, the increase in the average deflection was 1.36 mm (0.0536 in.), which was 85.74% of the total increase in the average deflection. The increase percent in the average deflection on the 21st day was 101% when the average deflection was 1.60 mm (0.0631 in.). At the end of this stage of

the sustained loading, the average deflection was 1.59 mm (0.0625 in.). It is noticeable that the deflection decreased slightly at the end of the test compared to the deflection on the 21st day. This could happen due to fluctuations in the temperature. Thus, the deflection was almost constant in the last seven days of this stage. Table 3-6 summarizes the increases in deflection and percentage under the 1st stage of SL (B7-SL).

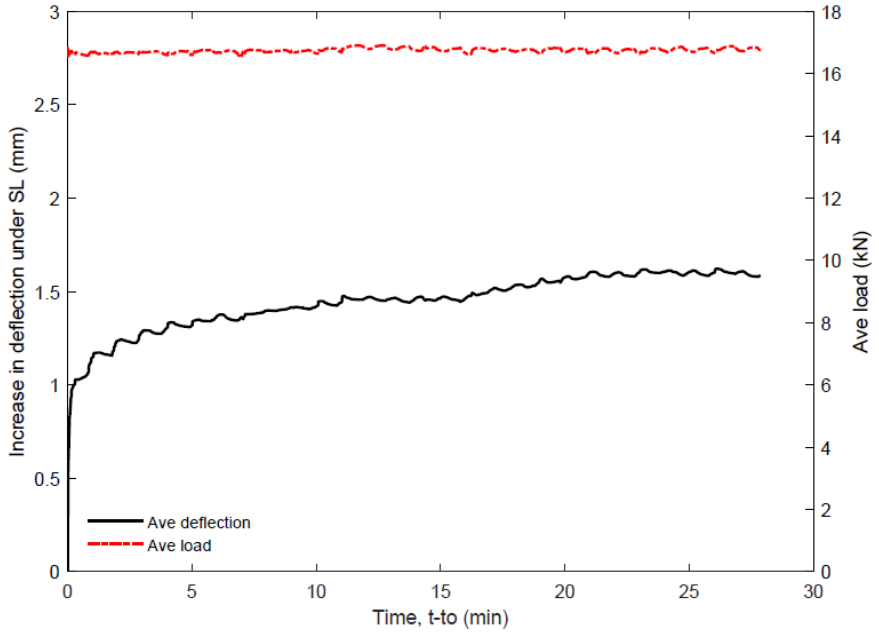

Figure 3-46. The increase in deflection under 1st stage of SL (B7-SL).

Table 3-6. The increases in deflection and percentage under 1st stage of SL (B7-SL).

Time (days)	Increase in ave deflection mm (in.)	Ave deflection (%)
1	1.15 (0.0452)	72.32
7	1.36 (0.0536)	85.74
21	1.60 (0.0631)	101
27.86	1.59 (0.0625)	100

This test had no data for reinforcement strains. The increase in average deflection in the second and third stages, which lasted two days each, is exhibited in Figure 3-47. As

mentioned before, the increase in the deflection was the highest in all three stages. As seen in Figure 3-47, most of the increase in the deflection took place in the first 4 hours.

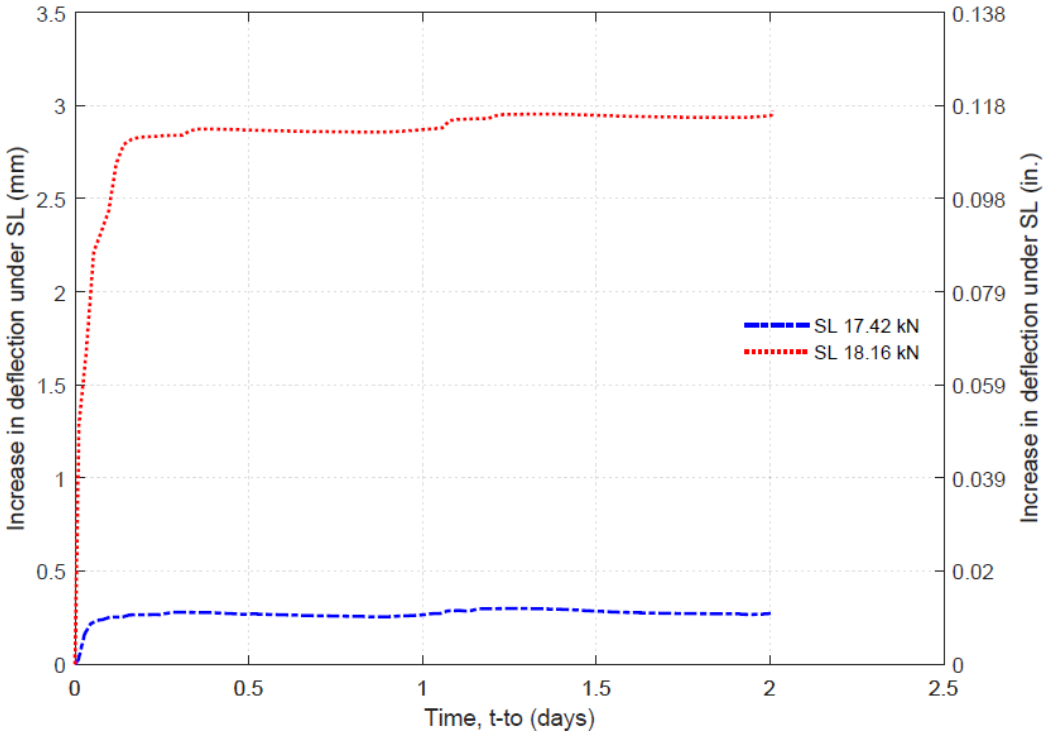

Figure 3-47. The increase in deflection under 2nd and 3rd SL (B7-SL).

The failure of B7-SL is shown in Figure 3-48. Similar to the failure of BC5, the failure was shear, and it happened suddenly on the left side of the beam.

Figure 3-48. B7-SL failure.

3.2.7.4 Beam 8 (B8–SL)

Beam 8 experienced issues with the data acquisition system and will not be reported.

3.2.7.5 Beam 9 (B9–SL)

Beam 9 (B9-SL) was loaded up to the sustained load at the age of 492 days. Five stages of sustained loading were in this test, and the specimen failed under sustained loading during the last stage. The load vs. deflection curve of B9-SL is shown in Figure 3-49, and load vs. compression reinforcement strain response for B9-SL is exhibited in Figure 3-50. The first stage of the sustained loads was 18.02 kN (3930 lbs), which is 95% of the BC5 ultimate load, and the load was kept for 28 days. At the beginning of this stage, the deflection was 6.84 mm (0.269 in.). At the end of the first stage, the average deflection became 8.80 mm (0.346 in.). The total increase in the average deflection under this stage of the sustained loading was 1.95 mm (0.0769 in.). Thus, the increase percent in average deflection to instantaneous deflection was 28.6%. The compression reinforcement strain was -0.00048 mm/mm at the beginning. It became -0.00041 mm/mm after 3.5 hours. Then, the compression strain decreased with time. At the end of the first stage, the compression strain was -0.00067 mm/mm. It decreased by -0.00019 mm/mm, which was 40.62% of the instantaneous compression strain.

In the second stage, the sustained load was increased to 17.93 kN (4030 lbs), and it was held for two days. The average deflection was 8.87 mm (0.349 in.) at the beginning of this second stage, and it was 9.56 mm (0.376 in.). The total increase in the average deflection in this stage was 0.688 mm (0.0271 in.), which was 0.25 times the increase in the deflection in the first stage. The compression reinforcement strain was -0.00068 mm/mm, and it became -0.00057 mm/mm at the end of this stage. It increased by 0.00011 mm/mm.

The sustained load of the third loading stage was 18.37 kN (4130 lbs), and it was kept for two days. The average deflection increased from 9.67 mm (0.381 in.) to 10.95 mm (0.431 in.) at the end of this stage. The total increase in the average deflection in this stage was 1.28 mm (0.0505 in.). The ratio of increase in the deflection in the third stage to the first stage was 0.66. In this stage, the compression reinforcement strain moved from -0.00058 mm/mm to -0.00049 mm/mm.

In the 4th stage, the sustained load was increased to 18.82 kN (4230 lbs) for two days. At the beginning of this stage, the average deflection was 11.07 mm (0.436 in.), and it became was 12.40 mm (0.488 in.) at the end of this stage. The total increase in the average deflection was 1.33 mm (0.0524 in.), which was 0.68 times the one in the first stage. The compression reinforcement strain at the beginning of this stage was -0.00049 mm/mm, and it moved to -0.00038 mm/mm at the end. It increased by 0.0001 mm/mm during this stage.

The last stage of the sustained loads was 19.26 kN (4330 lbs), and it lasted for only 15,83 minutes when the specimen failed under this sustained load. At the beginning of this stage, the average deflection was 12.52 mm (0.493 in.), and it became 12.75 mm (0.502 in.) just before the failure took place. During this stage, the specimen was not capable of resisting the load of 19.26 kN (4330 lbs). The reduction in the applied load happened very quickly. The compression reinforcement strain was -0.00039 mm/mm at the beginning of this stage, and it became -0.00037 mm/mm at the failure. It increased by 0.000015 mm/mm.

Table 3-7 summarizes the increase and change in deflection under different sustained loading stages. Not like the previous specimens tested under sustained loading, the increase in the average deflection during the additional load of the sustained load was less than the increase in the average in the deflection in the first loading stage. It seemed

the specimen not close to failure during the additional stages. However, it failed. The compression reinforcement strain increased under the first stage of sustained loading. However, it decreased during the additional stages of the sustained loading. The damage in the concrete was high during these stages that the neutral axis kept moving toward the compression zone fiber. Based on the compression strain reading, the failure should have been expected before taking place. B9-SL strength was higher than the strength of the control specimen, BC5. The ratio of the B9-SL failure load to BC5 failure load was 1.05, which meant the sustained loads increased the capacity of the specimen.

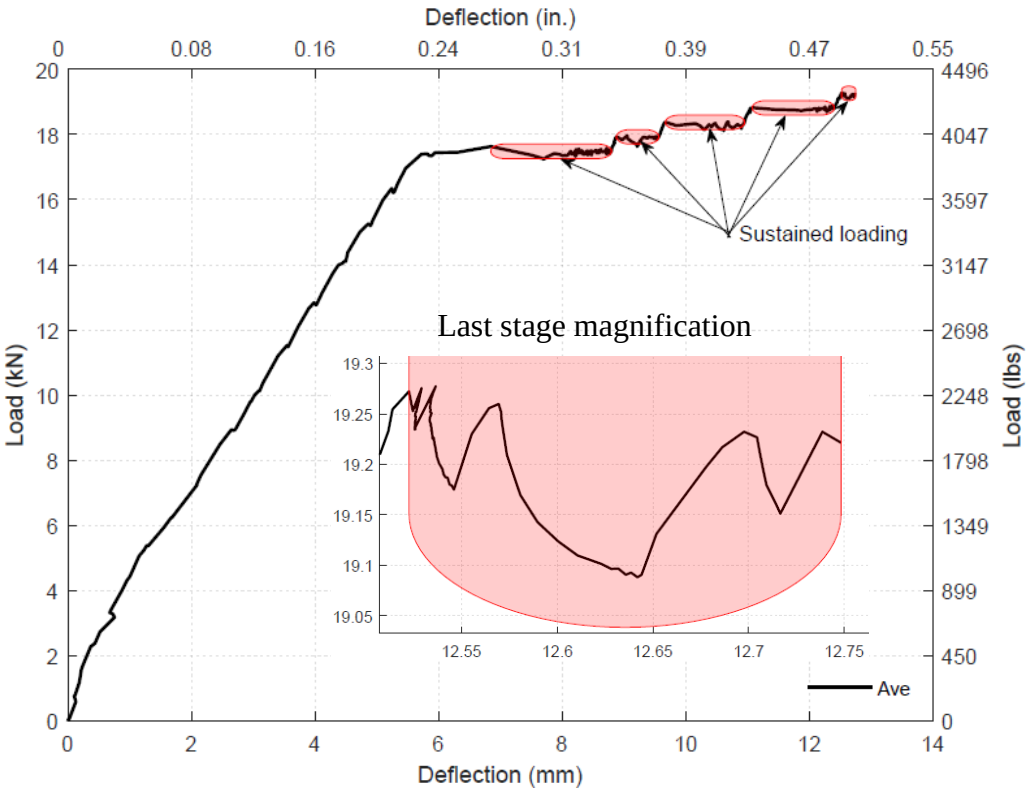

Figure 3-49. Load vs. deflection for B9-SL.

The failure deflection of B9-SL was 2.26 times that of the failure deflection of BC5. If the increase in deflection under the sustained loading stages was subtracted, the

ratio became 1.29. Therefore, the sustained load increased the deformation of the specimen. The design depth of all the tension reinforcement was 119 mm (4.6875 in.). However, the average depth was found to be 111 mm (4.35 in.). The depth was less than the depth of BC5, which was 116 mm.

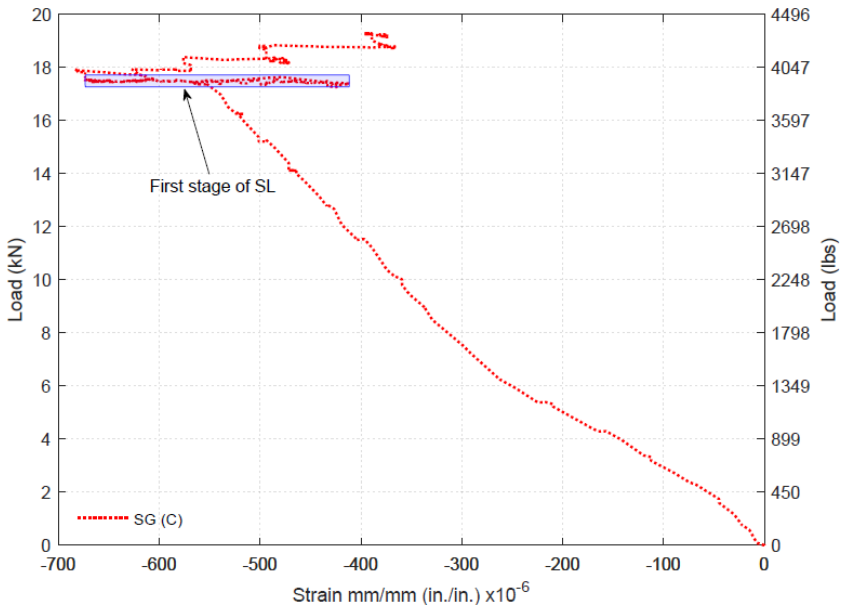

Figure 3-50. Load vs reinforcement strain responses for B9-SL.

Table 3-7. Summary of B9-SL deflection under different stages.

Duration	Load kN (lbs)	Increase in average deflection mm (in.)	Change in SG (C) mm/mm (in./in.)
28 days	17.48 (3930)	1.954 (0.077)	-0.00019
2 days	17.93 (4030)	0.688 (0.027)	0.00011
2 days	18.37 (4130)	1.283 (0.051)	0.00008
2 days	18.82 (4230)	1.331 (0.052)	0.00010
15.83 minutes	19.26 (4330)	0.226 (0.009)	0.00001

Figure 3-51 exhibits the increase in deflection and the change compression strain under the first stage of the sustained load of 15.38 kN (3457 lbs). Table 3-8 summarizes the percentage of increase in strains and deflection in the first stage of sustained loading.

Slightly above 52% of the total increase in the average deflection took place in about 115 minutes. At the beginning of the second day, the average deflection was 8.20 mm (0.3229 in.), which was 69.53% of the total increase on the deflection under this stage of the sustained loading. The compression reinforcement strain was -0.000464 mm/mm, which was -7.72% of the total increase in compression strain in this stage.

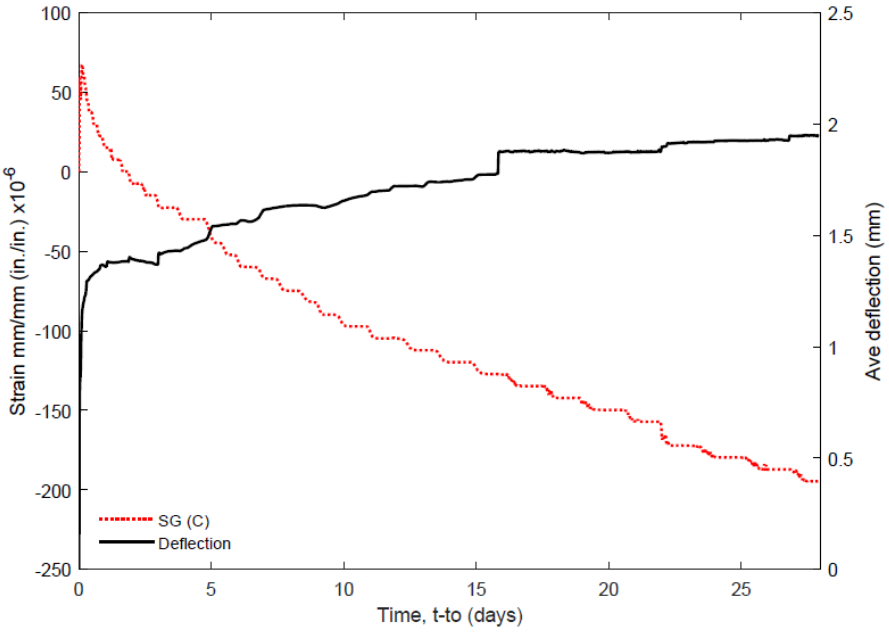

Figure 3-51. The increase in strains and deflection under 1st stage of SL (B9-SL).

As mentioned before, the compression strain decreased in the first 3.5 hours; then, it increased with time, which justified why the percentage here was negative. After seven days, the average deflection was 8.46 mm (0.333 in.). It increased by 1.61 mm (0.0636 in.), which was 82.63% of the total increase on the deflection under this first stage. The compression reinforcement strain increased to -0.00055 mm/mm. The percent increase was 34.45% of the total increase in compression strain. At the beginning of the 22nd day, the average deflection increased to 8.72 mm (0.343 in.). The increase percent was 95.85% of the total increase in the average deflection in this stage. The compression reinforcement

strain increased to -0.00064 mm/mm, and the increase percent was 80.52% of the total increase in this stage. At the end of the first stage of the sustained loading, the average deflection was 8.80 mm (0.346 in.). The total increase in the average deflection was 1.95 mm (0.0769 in.), which was 28.55% of the instantaneous deflection. The compression reinforcement strain at the end of the first stage of the sustained loading was -0.00067 mm/mm. The total increase in the compression strain was -0.00019 mm/mm, which was 40.62% of the instantaneous compression strain. The deflection was almost constant in the last seven days of this stage.

Table 3-8 The increase percent in strains and deflection under 1st stage of SL (B9-SL).

Time (days)	SG (C) (%)	Ave deflection (%)
1	-7.72	69.53
7	34.45	82.63
21	80.52	95.85
27.93	100	100

Figure 3-52 shows the increase in deflection under all sustained loading stages except the first stage. As can be seen, most of the increase took place in the first 6 hours except the second stage. At the end of the first day, the increase percent in deflection for the sustained loads of 17.93 kN (4030 lbs), 18.37 kN (4130 lbs), and 18.82 kN (43220 lbs) were 49%, 79%, and 95%, respectively. It is rational that increasing the sustained load led to an increase in deflection. The specimen failed after 15.84 minutes under the sustained load of 19.26 kN (4330 lbs), as can be noticed in Figure 3-52.

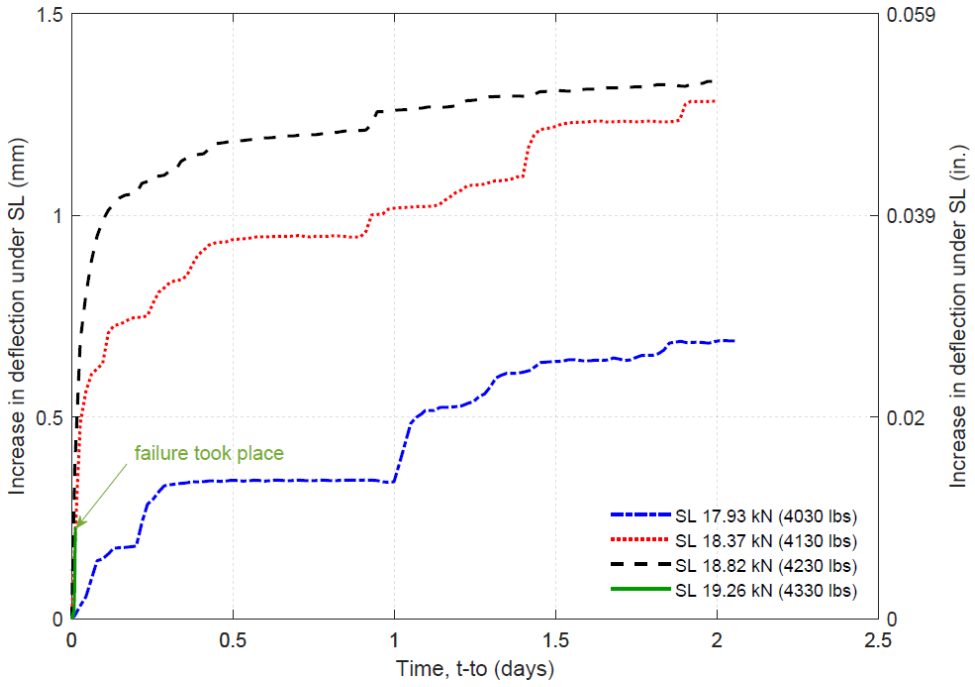

Figure 3-52. The increase in deflection under 2nd, 3rd, 4th, and 5th SL (B9-SL).

B9-SL failure is shown in Figure 3-53. The failure was shear, and it happened suddenly on the left side of the beam, deflecting less before the failure. The specimen had a branching crack. Flexural actions took place before the failure.

Figure 3-53. Beam 9 (B9-SL) failure.

Table 3-9 shows changes in the crack widths. All the cracks shown in the table were compared to the widths of the crack taken within an hour of the beginning of the sustained loading stages. All cracks widened in the first stage except crack #2 due to a new crack that took place between cracks #2 and #3. Redistribution of stresses due to the new crack caused

crack #2 to narrow. In the rest of the stages, crack widths varied between increasing and decreasing. The locations of the measured cracks are shown in Figure 3-54.

Table 3-9. Changes in crack width under SL (B9-SL).

	Loading stage	Sustained load kN (lbs)	Time	#2	#4	#6	#8	#9	#10
Change in crack widths (in)	1	17.48 (3930)	3 days	-0.0095	0.0013	0.0003	0.0013	0.0013	0.0010
			8 days	-0.0082	0.0012	0	0.0023	0.0015	0.0015
			28 days	-0.0072	0.0023	0.0005	0.0028	0.0018	0.0027
	2	17.93 (4030)	2 days	-0.0033	-0.0035	0.0027	0.0032	0.0062	-0.0003
	3	18.37 (4130)	2 days	0.0052	0	0.0008	-0.0053	0.0025	0.0016
	4	18.82 (4230)	2 days	0.001	-0.001	-0.0008	0.0020	-0.0008	0.0045

Figure 3-54. Locations of the measured cracks (B9-SL).

3.2.7.6 Beam 10 (B10–SL)

Beam 10 (B10-SL) was tested at the age of 543 days under sustained loading. The sustained load was 18.02 kN (4050 lbs), which is 98% of the BC5 ultimate load. B10-SL failed under the sustained load after 84.5 minutes of sustained loading. At the beginning of the sustained load, the average deflection was 5.87 mm. The average deflection at the

failure was 6.13 mm. The percent increase in deflection was 4.42% of the instantaneous average deflection.

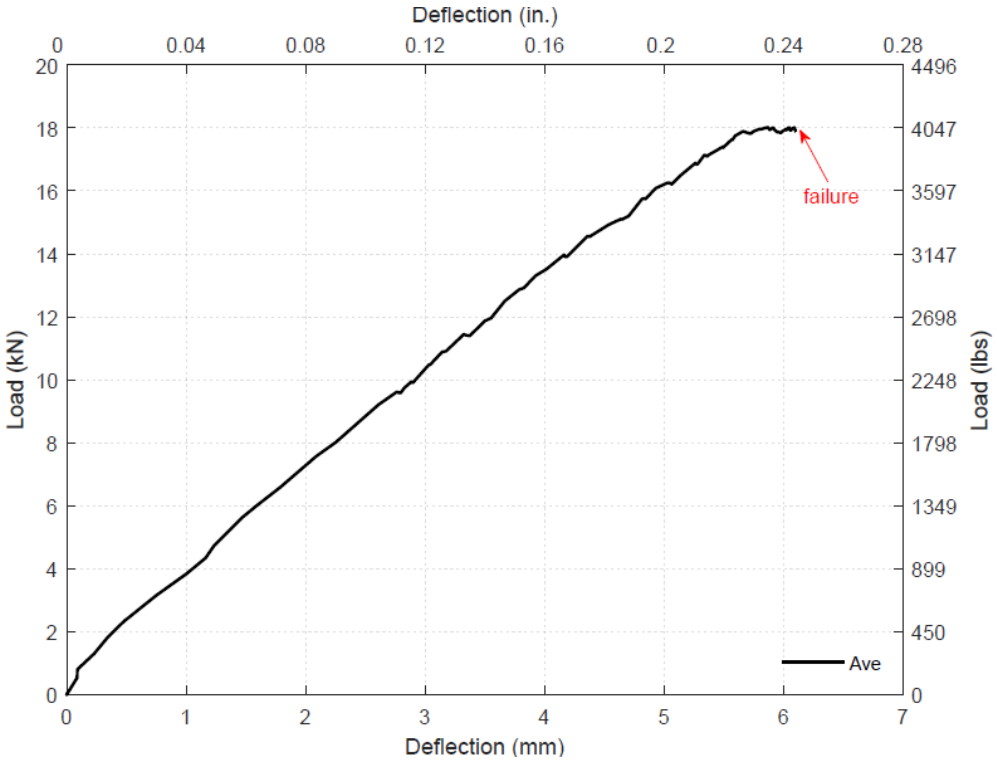

Figure 3-55. Load vs. deflection for B10-SL.

The percent increases in the left and right loading point deflections were 6.14% and 1.37%, respectively. The increase in the average deflection with time under sustained loading was shown in Figure 3-57. The large jumps in the deflection were due to load adjustment. About 72% of the deflection increase under the sustained load occurred in the first 60 minutes.

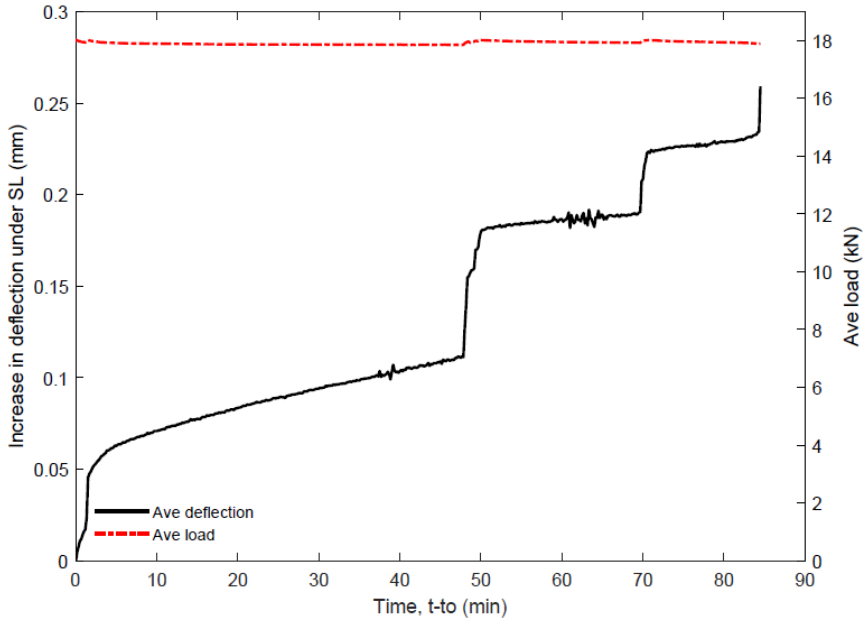

Figure 3-56. The increase in deflection under SL (B10-SL).

Magnification of Figure 3-55 for the part under sustained loading is shown in Figure 3-57. As can be seen, the load was adjusted three times before failure took place. The load dropped first from 18.02 kN (4050 lbs) to 17.94 kN (4033 lbs). Then, the load was increased to 18.01 kN (4049 lbs). After the adjustment, the load was decreasing with time simultaneously with an increase in the deflection. Then, the load was adjusted to 18.01 kN (4049 lbs). The load dropped again to 17.92 kN (4029 lbs), and this time was faster than the previous two reductions in load. Finally, the load was adjusted to 18.01 kN (4049 lbs). After that, the load reduced, and the reduction was the sharpest.

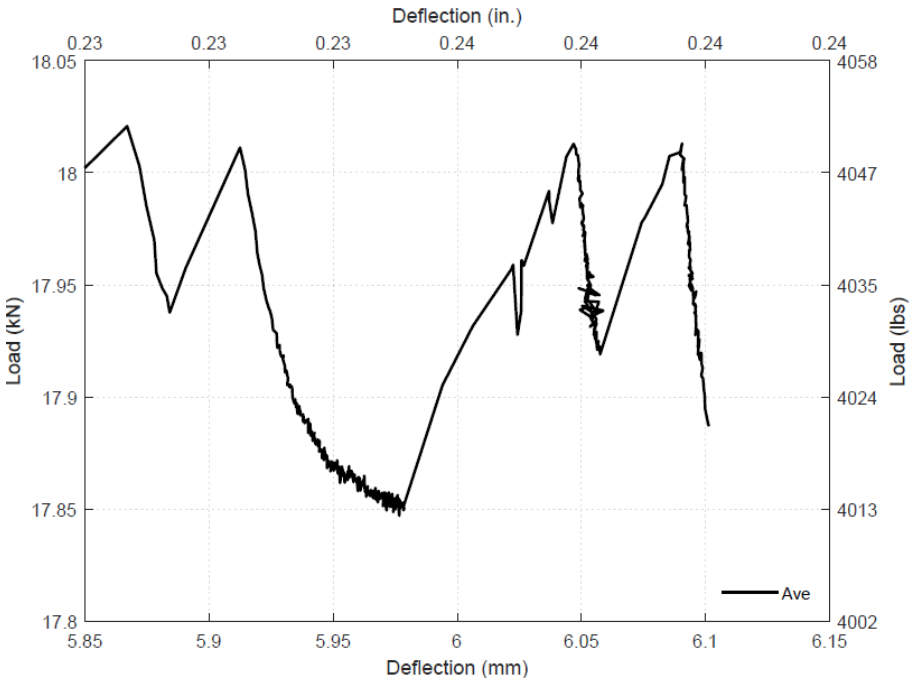

Figure 3-57. Load vs. deflection for B10-SL under SL.

The specimen was not capable of resisting the load. Thus, the specimen failed. The failure was shear, as shown in Figure 3-60, and it happened suddenly. The failure was on the right side, which deflected less before the failure took place. The left side deflection more than the right side, which means most of the energy dissipation occurred in the left of B10-SL. This justifies why the failure occurred on the right side. Like all beams of series II with an exception to B6-SL, the concrete crushed, and the reinforcement can be seen. The design depth of all the tension reinforcement was 119 mm. However, the average depth was found to be 114 mm.

Figure 3-58 shows the reinforcement strains. With the exception of the part that the load was less than 4 kN (899 lbs), the strains were linear with the load. Yield seemed not to take place in the specimen since the relationship between the strain, and the load was linear and there was no reduction in the stiffness as can be seen in Figure 3-55 and.

However, the strain in the tension reinforcement exceeded 0.0024 mm/mm. It could be due to that the tension strain gauge was attached to the middle rebar. Although the design depth of the tension reinforcement was 119 mm, the depth of the tension reinforcement was found to be less than this value. Also, the depth of the middle rebar was the largest of the three rebars.

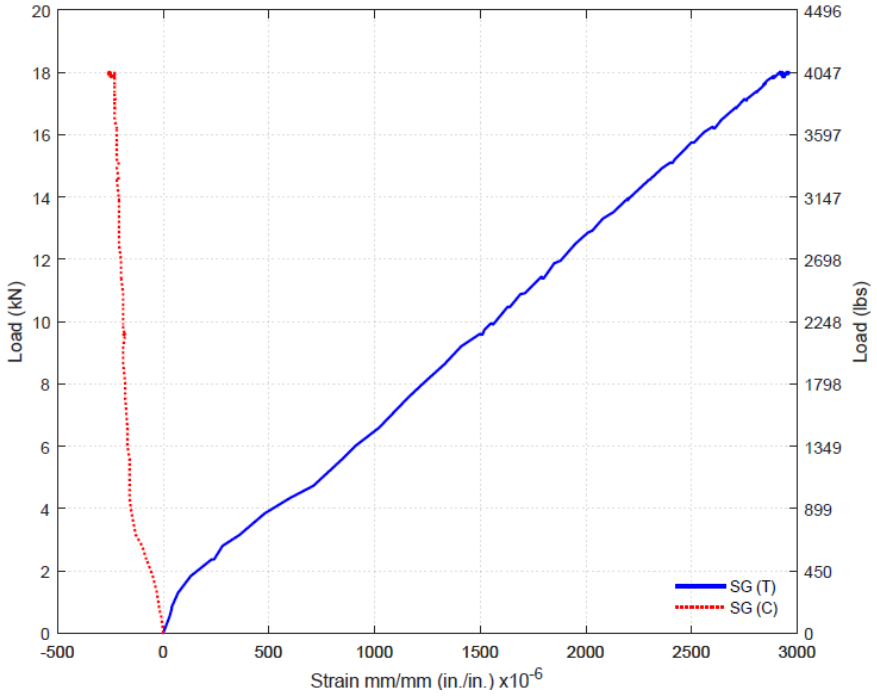

Figure 3-58. Load vs. SGs until just before failure (B10-SL).

In this specimen, the depth of the middle rebar was 117 mm, while the depths of the edge rebars were 115 mm and 109 mm. Figure 3-59 shows the increase in strains and deflection under the 1st stage of B10-SL. Both tension and compression strains increased under the sustained load. At the beginning of the sustained loading, the tension strain and the compression strain were 0.00292 mm/mm and 0.00023 mm/mm, respectively. They became 0.00294 mm/mm and 0.00025 mm/mm for tension and compression strains just

before the failure of B10-SL under the sustained load. The percent increases in strain under the sustained load were 0.68% for tension strain and 8.70% for compression strain.

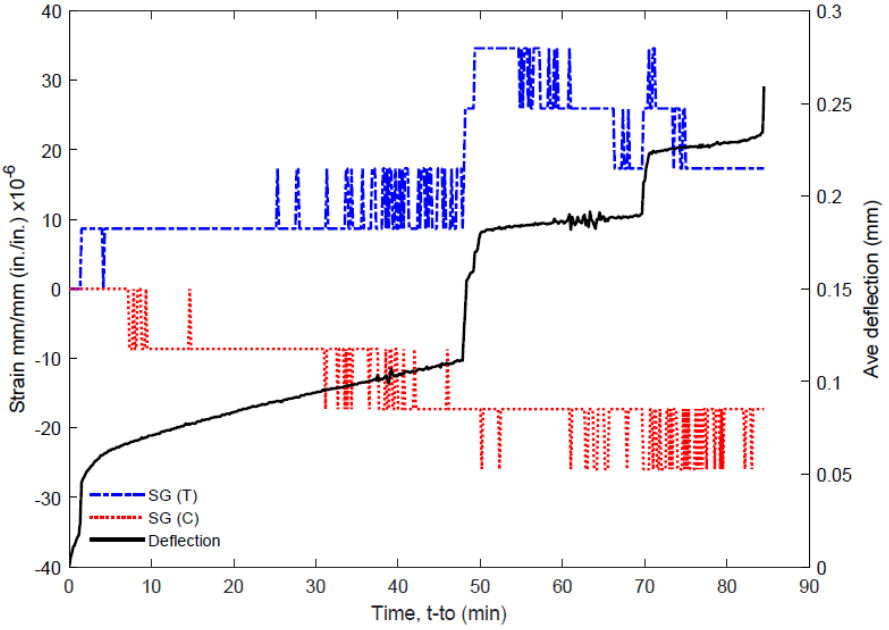

Figure 3-59. The increase in strains and deflection under 1st stage of SL (B10-SL).

Figure 3-60 exhibits the failure of B10-SL. Like BC5, the specimen failed due to a shear crack. The flexural actions were very small since the specimen failed in less than two hours. The flexural cracks just before the failure were narrow.

Figure 3-60. B10-SL failure.

3.2.7.7 Temperature

Temperature and relative humidity fluctuations during the tests of beam series II are shown in Figure 3-61. BC5 had an average temperature and average humidity of 74˚F and 77%, respectively. During the test of B6-SL, the temperature fluctuated between 68.5 ˚F and 89.6 ˚F, while the humidity fluctuated between 63.9% and 79%. The temperature ranged from 73 ˚F to 86 ˚F, and the humidity varied from 65% to 79% in the test duration of B7-SL. For B9-SL, the temperature range was between 52.1 ˚F and 73.4 ˚F, and the variation in the humidity was between 11% and 45.2%. The duration of the B10-SL was less than two hours, with an average temperature of 54.6 ˚F and average humidity of 22.6%.

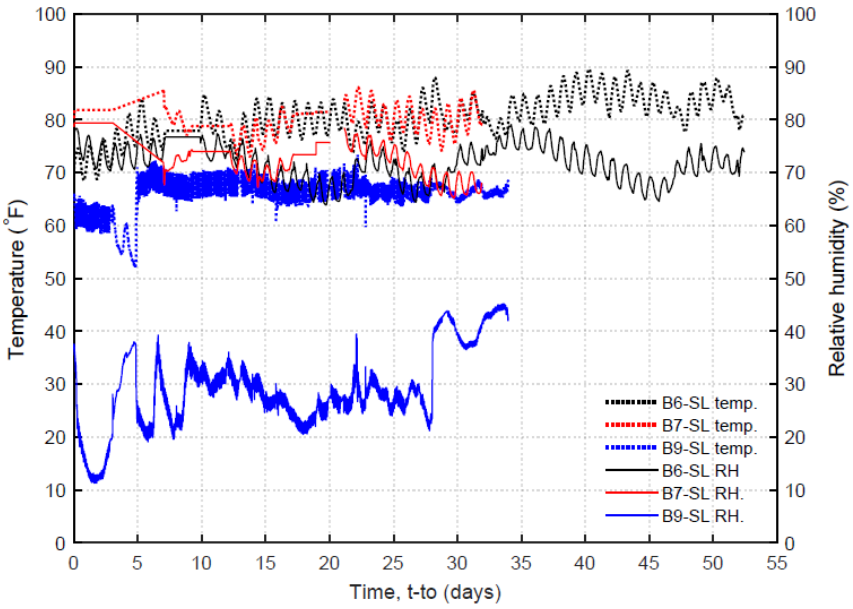

Figure 3-61. Temperature and humidity during the tests of beam series II.

3.2.8 Discussion

The load vs. deflection curves for beam series II are exhibited in Figure 3-62, and the beam series II results are summarized in Table 3-10. BC5 served as a control specimen

and was tested to failure at the age of 282 days. It failed at the load of 18.35 kN (4126 lbs) and the deflection of 5.52 mm (0.222 in.).

The second specimen, B6-SL, was tested at the age of 284 days under the sustained load of 15.38 kN (3457 lbs), which was 84% of the control specimen resistance for 28 days. As seen in Figure 3-62, B6-SL behaved more ductility than the other beams.

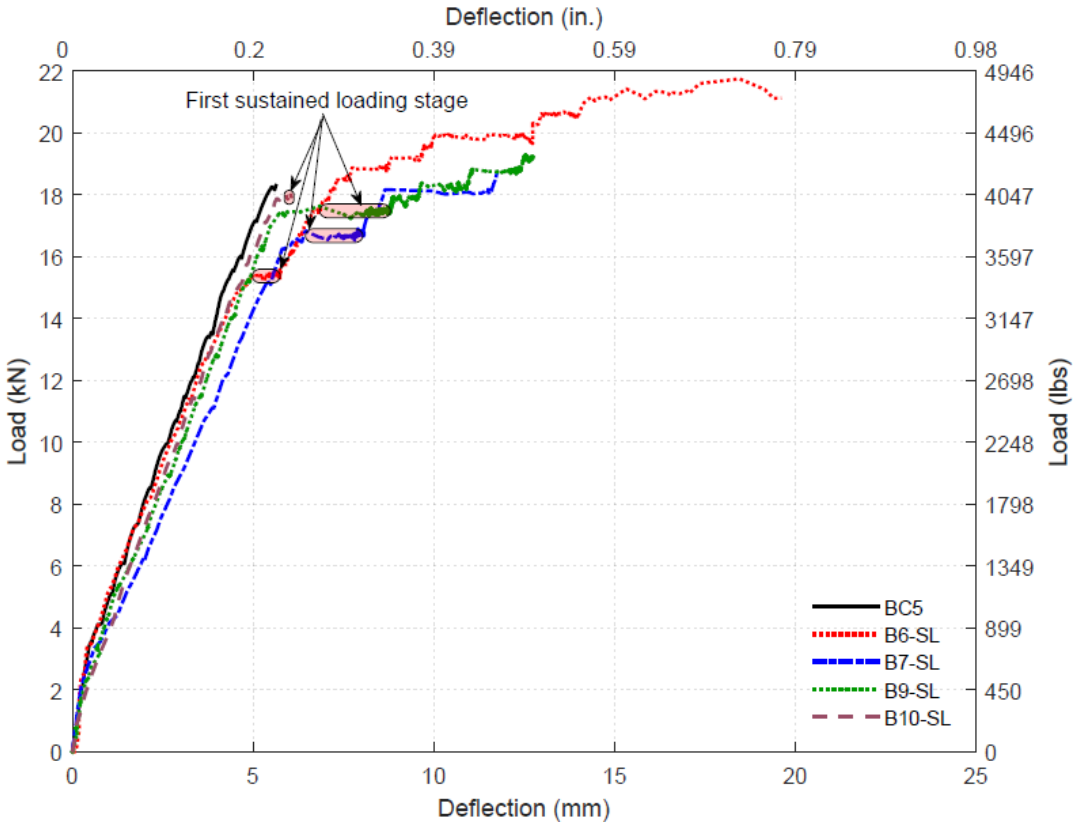

Figure 3-62. Load vs. deflection for beam series II.

B7-SL was loaded up to the sustained load of 16.68 kN (3750 lbs), which was 91% of the short-term resistance of BC5 at the age of 338 days. There were three additional loading stages. The specimen failed while trying to add an additional loading step at the load of 18.70 kN (4205 lbs) and at the deflection of 11.76 mm (0.463 in.).

B9-SL was tested at the age of 492 days under the sustained load of 17.48 kN (3930 lbs), which is 95% of the BC5 ultimate load for 28 days. There were four additional loading stages, and each stage lasted for two days. The specimen failed at 19.26 kN (4330 lbs) under the last stage of the sustained loading after about 16 minutes.

The last specimen in this series, B10-SL, was tested under the sustained load of 18.02 kN (4050 lbs), which was 98% of the short-term resistance of the control specimen, BC5. The specimen failed after about 85 minutes of the sustained load at the deflection of 6.13 mm (0.241 in.).

As seen from the data in Table 3-10, the application of sustained loads increased the deflection at failure for all specimens (B10-SL excluded) by an average of 1.5 times. The large increase in deflection shows the significant deformations that can occur under sustained loading. This large increase in deflection would allow for load redistribution in redundant systems or signs indicating problems in the structure.

Furthermore, in general, the sustained loads increased the strength of the specimens by an average of 6.1%. The failure mode of all specimens remained a shear failure. Unlike beam series I, this series did not experience flexural failure.

Specimens tested below 98% of the control specimen strength did not fail under sustained loading. Even specimen B9-SL, which was at 95% of the control strength of the control specimen did not fail in the first stage of sustained loading. The tests indicated that to fail under sustained load, that level of the load must be very close (within 2% in this case) to what would cause failure. However, based on concrete material tests, the load level may be as low as 80% in unreinforced specimens (Iravani and MacGregor 1998;

Rusch 1960). The results of these tests indicate that a reinforced concrete specimen had a significant ability to redistribute loads and survive under sustained loading.

Table 3-10. Series II test matrix.

Specimen	BC5	B6-SL	B7-SL	B9-SL	B10-SL
Sustained load intensity	-	0.84	0.91	0.95	0.98
Loading age t_o (days)	282	284	338	492	543
Duration $t_{d\text{-}s1}$ of the first loading stage	-	28 days	28 days	28 days	84.5 minutes
Duration $t_{d\text{-}t}$	-	52 days	32 days	34 days	84.5 minutes
Peak load kN (lbs)	18.35 (4126)	21.75 (4889)	18.70 (4205)	19.26 (4330)	18.02 (4050)
Increase in the peak load to BC5	-	0.185	0.019	0.049	-0.018
Deflection at the peak mm (in.)	5.64 (0.222)	18.45 (0.727)	11.76 (0.463)	12.52 (0.493)	6.13 (0.241)
Increase in deflection at peak to BC5	-	2.27	1.08	1.22	0.08
Reinf. depth mm (in.)	116 (4.573)	112 (4.412)	112 (4.423)	111 (4.357)	114 (4.473)

The increases in deflection and the sustained loads with time for the first stage of sustained loading are shown in Figure 3-63. All the specimens behaved similarly. As with previous creep tests of plain concrete under sustained compressive loading, the deflections increased rapidly in the primary stage and then linearly in the secondary stage. Adjustments of loads caused the sudden jumps in deflections. The increases in deflection during the first stage of the sustained loading were 0.77 mm (0.030 in.), 1.59 mm (0.062 in.), and 1.95 mm

(0.077 in.) for S6-SL, S7-SL, and S9-10, respectively. This amount of increase in deflection under sustained loading increased with higher levels of sustained loading.

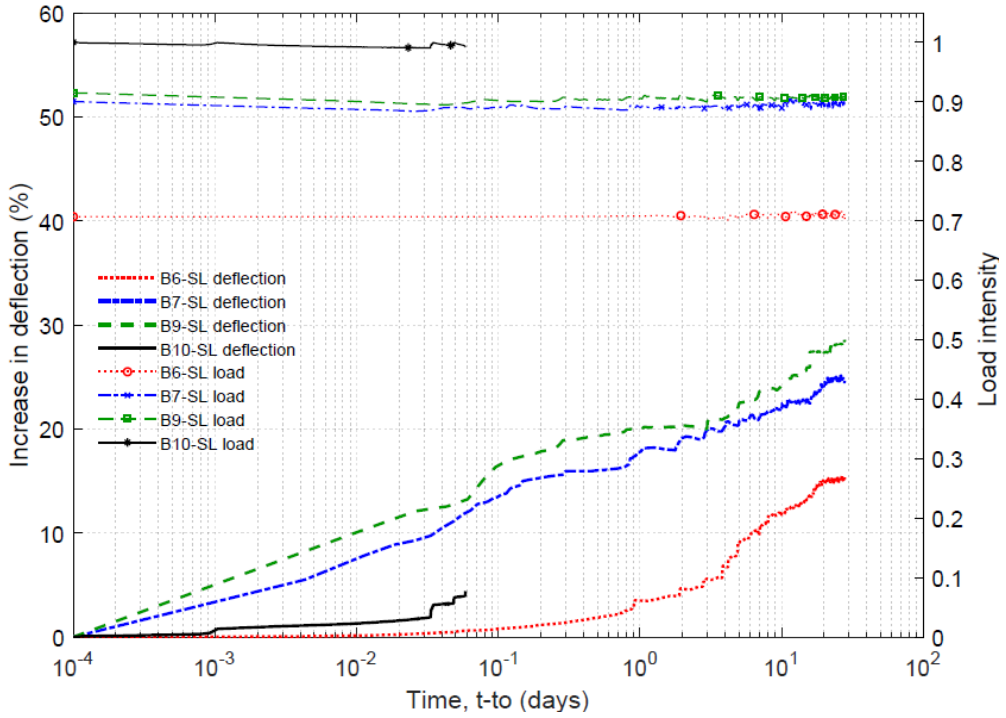

Figure 3-63. Sustained load & deflection with time of first stage (series II).

Figure 3-64 exhibits the percent increase in defection under sustained load (determined in reference to the deflection at the end of sustained loading). As can be seen, most increases in deflection took within the first day. Over 50% of the increase in B7-SL and B9-SL took place in less than 6 hours. The curves for B7-SL and B9-SL are very similar, while B6-SL is much lower overall. This difference is likely due to the lower ratio of sustained loading but may also be due to other differences in B6-SL that led to a slightly different failure mode.

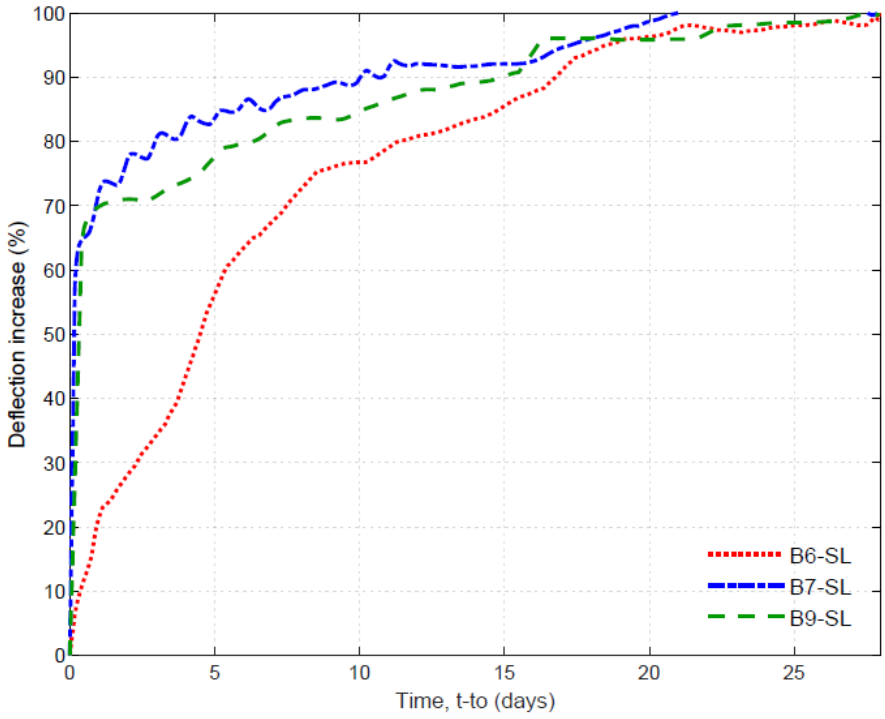

Figure 3-64. Percent increase in deflection with time Beam series II

Figure 3-65 exhibits the beam series II failures. With the exception of B6-SL, all specimens in this series failed in the same manner. Shear failure was dominant. They all had a branching shear crack. The first beam, BC5, failed in shear with small flexural actions. B7-SL and B9-SL failed in shear but at a higher level of displacement than BC5. B10-SL failed in shear, similar to BC5. B6-SL behaved differentially, and it failed in a different manner. The specimen seemed to reach flexural strength. After that, compression failure took place just above the support, which led to failure in the right release in load. As can be seen, the crack on the right side was not at the tips of the flexural crack. Two flexural cracks approached each other. They could increase the compression and eventually cause the compression failure above the support. All the specimens tested under the sustained loads had wider flexural cracks than B10-SL, which failed under the first stage

of the sustained loading. This indicated that widths of flexural cracks did not control the failure under sustained loading.

Figure 3-65. Beam series II failures.

3.3 Conclusions

In this chapter, two beam series were tested. The differences between the two series were the reinforcement and loading conditions. Beam series I had four specimens. Each specimen had two rebars in the tension zone and two rebars in the compression zone. One specimen served as a control specimen. Three specimens were tested under high sustained

loads ranging from 82% to 93% for periods of time between 24 days and 42 days. The specimens were tested under four-point bending (4PB). Beam series II had six specimens. Each specimen in this series had three rebars in the tension zone and two rebars in the compression zone. One specimen was served as a control specimen. Five specimens were tested under high sustained loads ranging from 83% to 98% for periods of time between 84.5 minutes and 52 days. The specimens were tested under three-point bending (3PB). The following points are main conclusions:

- No beam in series I failed under sustained loading. The applied sustained loading was not high enough to cause failure under sustained loading.
- In series II, one beam failed under a sustained loading intensity of 0.98 after about 85 minutes. Moreover, another beam failed during an additional loading stage after about 16 minutes. In both beams, the sustained load seemed close to the short-term shear capacity.
- The peak load carried by the specimen increased for specimens experiencing sustained loading. For beam series I, the increase was on average 3%, while for beam series II, the increase was 6.1%. While the increases in peak loads are within the range of inherent variability in concrete testing, the results show that sustained loading does not reduce the load-carrying capacity of the member.
- Sustained loading increased the deflection at peak load for all specimens. For beam series I, the increase in deflection was 41%. For beam series II, the increase in deflection was 1.5 times. The large increase in deflection shows the significant deformations that can occur under sustained loading. This large increase in

deflection would allow for load redistribution in redundant systems or provide warning signs of impending failure.

- Sustained loading changed the behavior of beams in series I. Beams tested under sustained loads showed a different mode of failure from the control specimen that was tested under monotonically increasing load to failure. Unlike the control specimen, which failed in shear, specimens tested under sustained loads experienced significant increases in deflection and flexural failure before the shear failure. Concrete creep under sustained load enabled flexural failure of the beam to occur before the shear failure. For beam series II the specimens under sustained load did not experience a flexural failure but did see increased deflections (1.5 times) at failure compared to the control specimen.
- Over 50% of the increase in deflection under sustained loading in series I took place in the first two days. For beam series II, 50% of the increase in deflection under sustained load took place in the first five days. The sharper increase in deflection early in the loading coincides with the primary stage of creep for reinforced concrete. After the sharper increase, the secondary stage exhibited nearly a linear increase in deflection with time. Only specimen B10-SL experienced a tertiary stage that showed a sharp increase in deflection with time just 10 seconds before failure.
- Both the tensile and compressive strains increased under sustained loading. The increase in strain shows that the reinforcement took more of the loading as the concrete softened under the sustained loading. The increase in the compression

strain was higher than in the tension strain, indicating that the creep of the concrete in compression.

- The curvature of the section where strains were measured increased throughout the sustained loading period. The increase in curvature occurred at a higher rate than the increase in deflection for most beams indicating that the distribution of curvature along the length of the beam was changing under sustained load as the concrete in the highly stressed locations (near the center of the beam) experienced creep deformations.

Chapter 4

FLAT PLATES UNDER HIGH SUSTAINED LOADING

4.1 Objectives

The experimental program aims to investigate the time-dependent behavior of half-scale reinforced concrete slabs under high sustained loading. The program consists of testing twelve isolated half-scale slab column connections, among which nine were tested under high sustained loading of periods ranging from 22 minutes to 84 days. Short-term and long-term deflections, strains, and loads were measured and recorded in addition to monitoring the width and propagation of existing cracks. The testing sought to evaluate the time-dependent strength and stiffness characteristics of flat-plate connections under high levels of sustained load. Specifically, the research sought to identify what level of loading will lead to eventual failure under sustained loading, the near-failure behavior of slab-column connections under high sustained loads and evaluate the effect of the reinforcement ratio in the sustained loading.

4.2 Specimens

The experimental work involved the testing of ten 0.47 scale isolated slab-column connections with two different steel reinforcement layouts. All the twelve slabs were identical with the same dimensions 2438× 2438 mm (8×8 ft) with an 89 mm (3.5 in.) slab thickness supported on a 152 mm (6 in.) square column, extending 140 mm (5.5 in.) above and 229 mm (9 in.) below the slab, located at the center of the slab, as shown in Figure 4-1.

Each specimen had four through holes at (0.22 L) for loading. The presence of the footing at the bottom of the column is to provide moment restraint in the eccentric test.

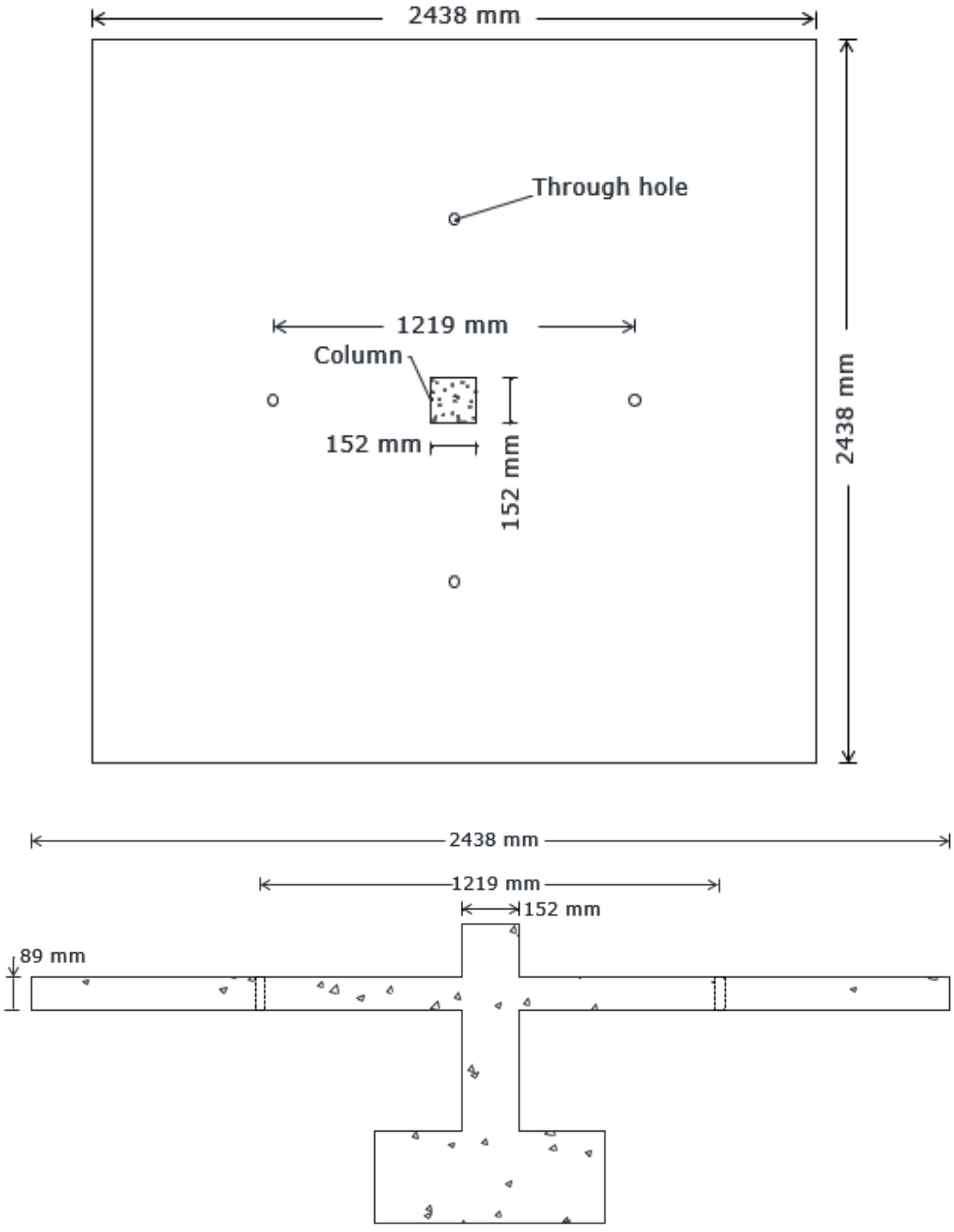

Figure 4-1. Slab specimen details: plan view (top) and elevation (bottom).

4.3 Reinforcement Layout

For all specimens, the reinforcement was designed based on Building Code Requirements for Structural Concrete (ACI Committee 318 2014). Each specimen had four layers of reinforcement: two layers at the bottom and the two layers at the top of the slab. The rebars in the south-north direction were the 1st, and 4th layers (near the extreme compression and tension fibers) and the rebars going west-east direction were in the 2nd and 3rd layers. Reinforcing bar No.10 (No.3) with 9.525 mm (3/8 in.) diameter, Grade 420 (Grade 60), was utilized to reinforce all specimens. Four slab specimens were fabricated with a flexural reinforcement ratio of 0.64% on the top in each principal direction, while a flexural reinforcement ratio on the top for the other four slab specimens was 1%. The reinforcement details of slab specimens with 0.64% are illustrated in Figure 4-2, while the reinforcement details of eight slab specimens with a 1% reinforcement ratio are exhibited in Figure 4-3. The center-to-center spacings of tension reinforcing bars were 152.4 mm (6 in.) (Slab 1, S2, S3, and S4) and 96.52 mm (3.8 in.) (Slab 5, S6, S7, and S8) for specimens with 0.64% and 1% reinforcement ratios, respectively. The average effective depth, d, was 73 mm (2.875 in.). All specimens had design clear covers of 6.35 mm (0.25 in.) for both the flexural tension and compression reinforcement. The column in each specimen was comprised of four No.13 (No.4) with 12.7 mm (1/2 in.) diameter longitudinal rebars with four transverse rebars.

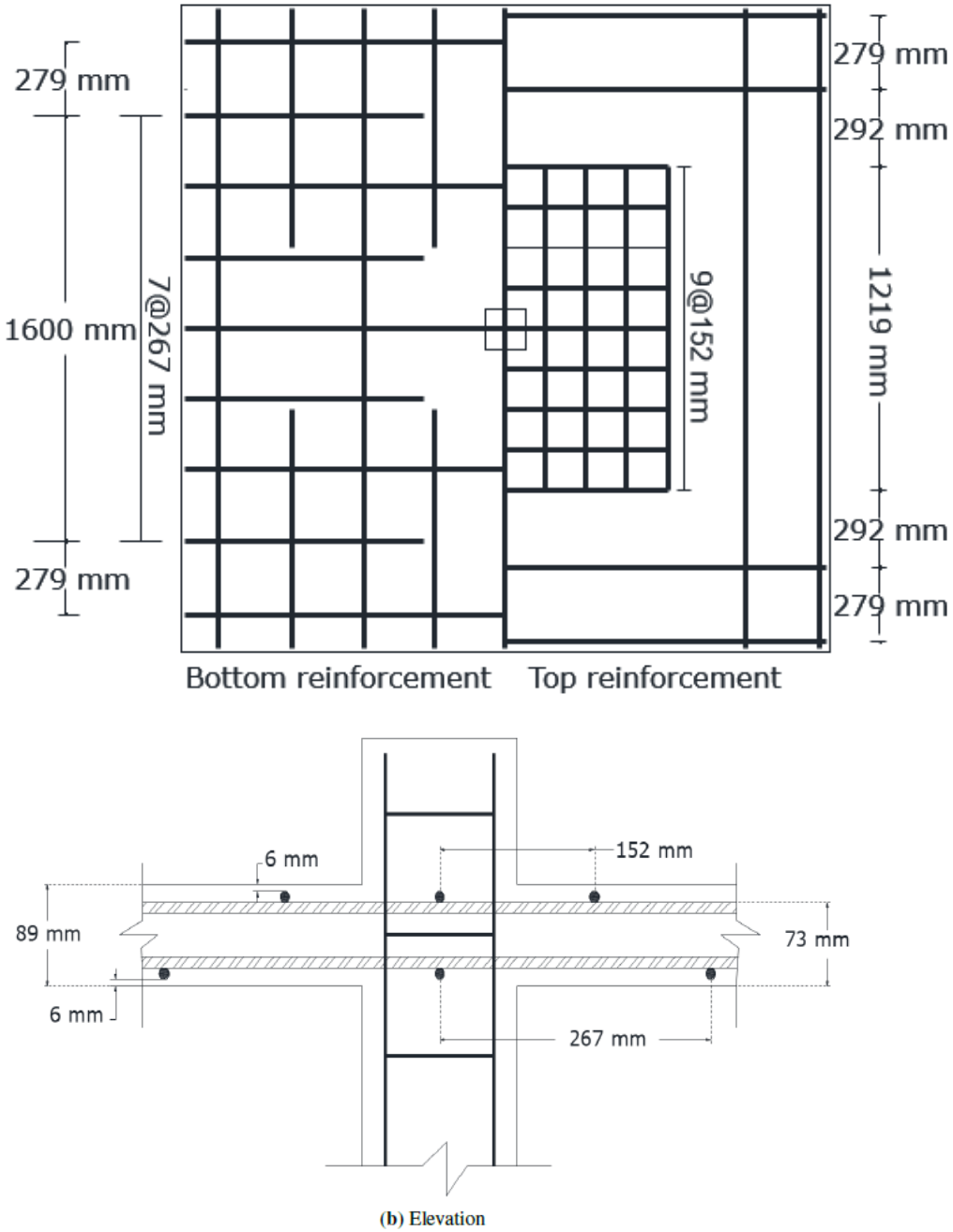

Figure 4-2. Slab reinforcement details (0.64%).

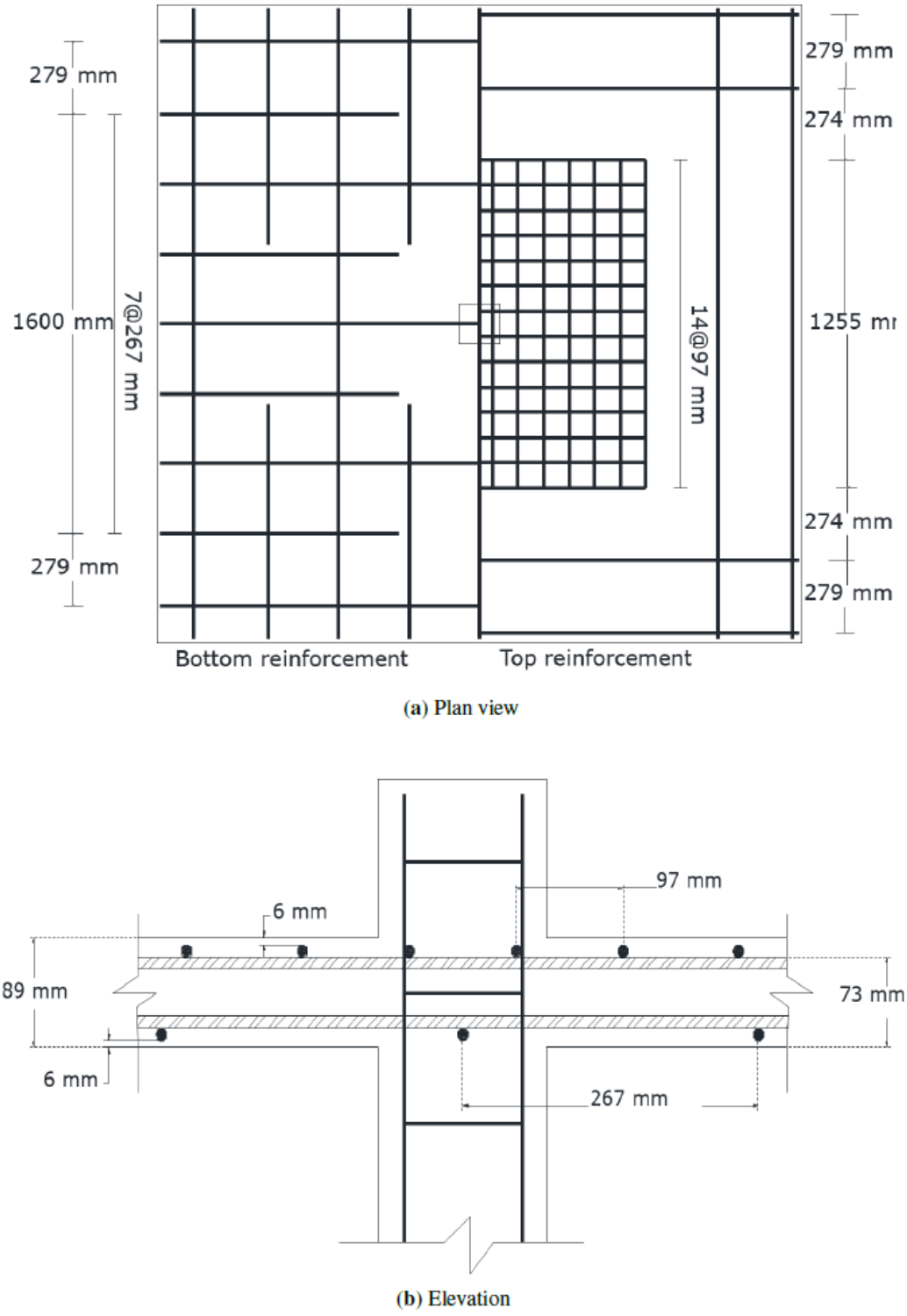

Figure 4-3. Slab reinforcement details (1%).

4.4 Experimental Setup

The test setup was designed to apply concentrated loading at eight points at a distance of 243 mm (25.30 in.) from the center of the column cross-section. Slab edges extended outside the loading points to simulate slab in-plane restraint that exists in a continuous flat plate structure. Peng et al. (2017) showed that the full panel specimens better simulated the restraint in actual structures. The edges of the slabs for all specimens were free to rotate and displace laterally. Figure 4-4 and Figure 4-5 illustrate the loading points and the testing setup. Each slab had four through holes at (0.22 L) created using PVC pipes to allow threaded rods to pass through and load the specimens.

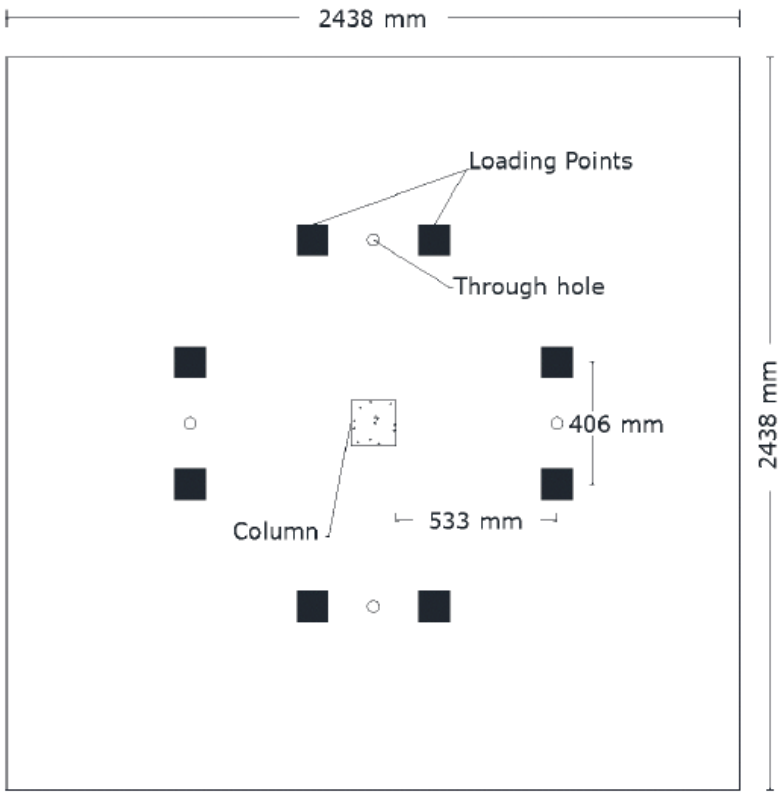

Figure 4-4. Loading points.

Each threaded rod was connected to a load cell to measure the applied load. Four spreader bars were used to divide the applied load into two loading points at a space of 406 mm (16 in.).

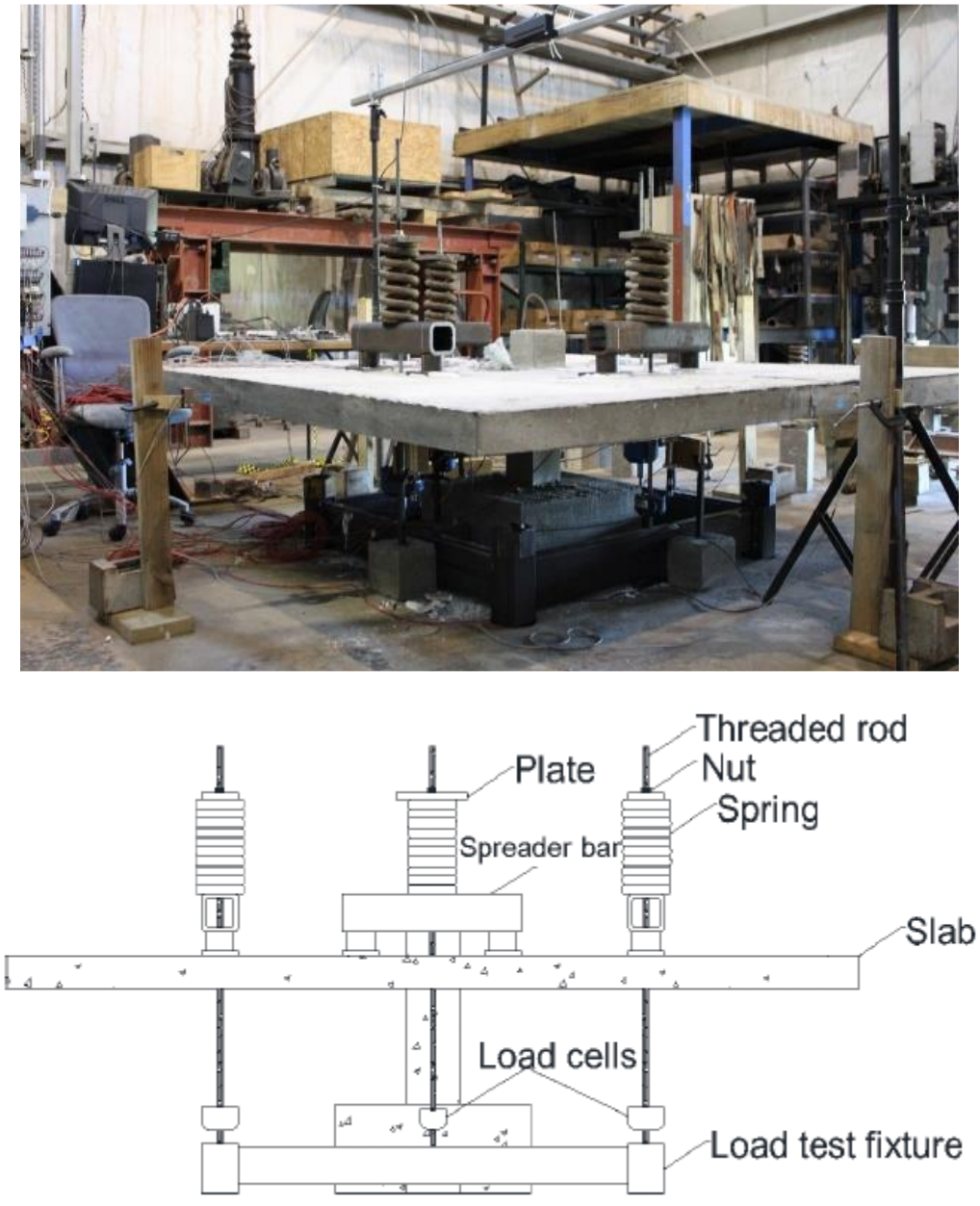

Figure 4-5. Slab test setup.

Springs were used to helping maintain consistency of load while the specimen deflected. The load was applied by tightening the nuts on the top of the threaded rods. Loading of the slab to the initial sustained load level occurred within approximately 30 min. Once the sustained load testing started, the load was checked and adjusted in a short period of time (~4-6 hours) for the first days of loading due to greater deflections in the early stages of sustained loading. Afterward, the load was checked and adjusted every 24 hours.

4.5 Constructions of Specimens

Prior to pouring the column and the slab, pad footings were constructed and poured. Then, the formwork was constructed, and reinforcement was placed and tied inside the forms. The footing dimensions were the same for all eight specimens 610 mm×610 mm×229 mm (24 in.×24 in.×9 in.). The column base was placed in the center of the footing. Appendix B shows the pad footing with column reinforcement. The lower layer of the slab bottom reinforcement was rested on 6.35 mm (1/4 in.) hardwood square dowels. The top rebars were placed on 63.5 mm (2.5 in.) high steel chairs. The chairs were placed away from the critical shear perimeter of the column to eliminate any beneficial effect on punching shear resistance of the slab. Each specimen had 4 through holes created using PVC pipes to allow the loading rod to pass through. One hole was made to half the slab depth and used to record temperature and humidity in the slab. Wood props were used for temporary scaffolds to support concrete formwork. Formwork with reinforcement for a slab specimen before casting the concrete is exhibited in Appendix B. After pouring the concrete, the top surfaces were leveled and finished. The top of the column was cast at the

same time as the slab. The slab specimens were covered by plastic sheets and moist cured for one week. The formwork was removed after two weeks. The props were kept in their locations to support slabs under self-weight until the time of testing.

4.6 Loading Histories

The loading histories of the slab-column specimens of slabs (0.64%) are shown in Figure 4-6. Slab 1, the control specimen, was initially tested under monotonically increasing loading to failure at the age of 175 days. For Slab 2, the load was applied at age 189 until the specified load, 89.32 kN (20080 lb). Then, this load was sustained for 70 days. After the sustained loading stage, the load was increased in increments of 4.45 kN (1000 lbs) and held for three days. The slab failed under sustained loading two days after the 4th addition of load at a load of 106.76 kN (24000 lbs).

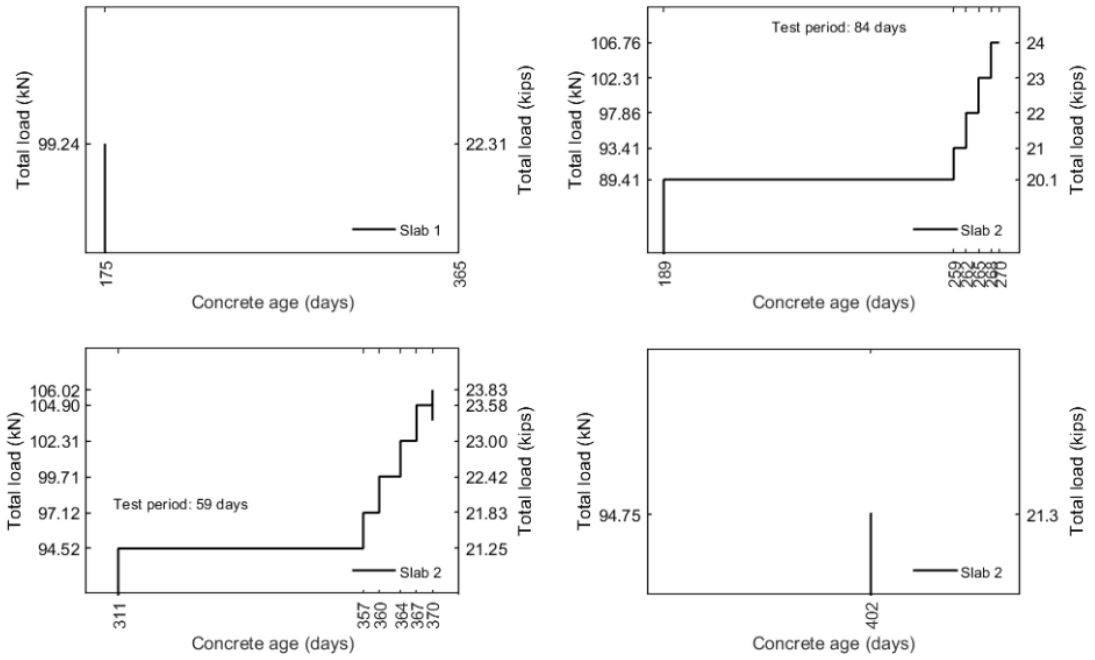

Figure 4-6. Loading histories (Slab 0.64%).

Slab 3 was first subjected to sustained load, 94.52 kN (21250 lbs), at age 311 days, and the load was held for 46 days. 1.59 kN (583 lbs) load was added at age 357 days and was kept for three days. The load was increased by 1.59 kN (583 lbs) increments and held for 3 to 4 days. The test was terminated by loading up the specimen to failure at the age of 370 days. The last slab with a 0.64% reinforcement ratio, Slab 4, failed at age 402 days while loading it up.

Figure 4-7 exhibits the loading histories of slabs (1%). Slab 5 was tested in a short time at the age of 200 days. Slab 6 was loaded up at the age of 281 days. The sustained load was 89.85 kN (20200 lbs), and it lasted for 45 days. After that, there were seven additional stages of the sustained loading. In each stage, the sustained load was increased by 2.67 kN (600 lbs), and the sustained load was kept for about ~ 3 days unless failure happens before that. The sustained load of 94.30 kN (21200 lbs) was applied to Slab 7 at the age of 345 days, and the sustained load was held for 45 days. Then, there were nine additional stages of the sustained loading. Like Slab 6, the increase in the load and the duration in each stage was 2.67 kN (600 lbs) and three days, respectively. Slab 8 was tested under the sustained load of 106.76 kN (24000 lbs) at the age of 441 days. The load was kept for 45 days; then, seven additional stages of the sustained loading were applied to the specimen. The sustained load in these additional stages last for three days, and the increment in the sustained load was 2.67 kN (600 lbs). For Slab 9, it was tested at the age of 197 days, and it failed under the sustained load of 103.64 kN (23300 lbs) after 21 minutes. The last specimen, Slab 10, was loaded up to the sustained load of 97.15 kN (21840 lbs) at the age of 203 days for 30 days. Then, the sustained load was increased by 1.78 (400 lbs) before the failure took place after 67 hours.

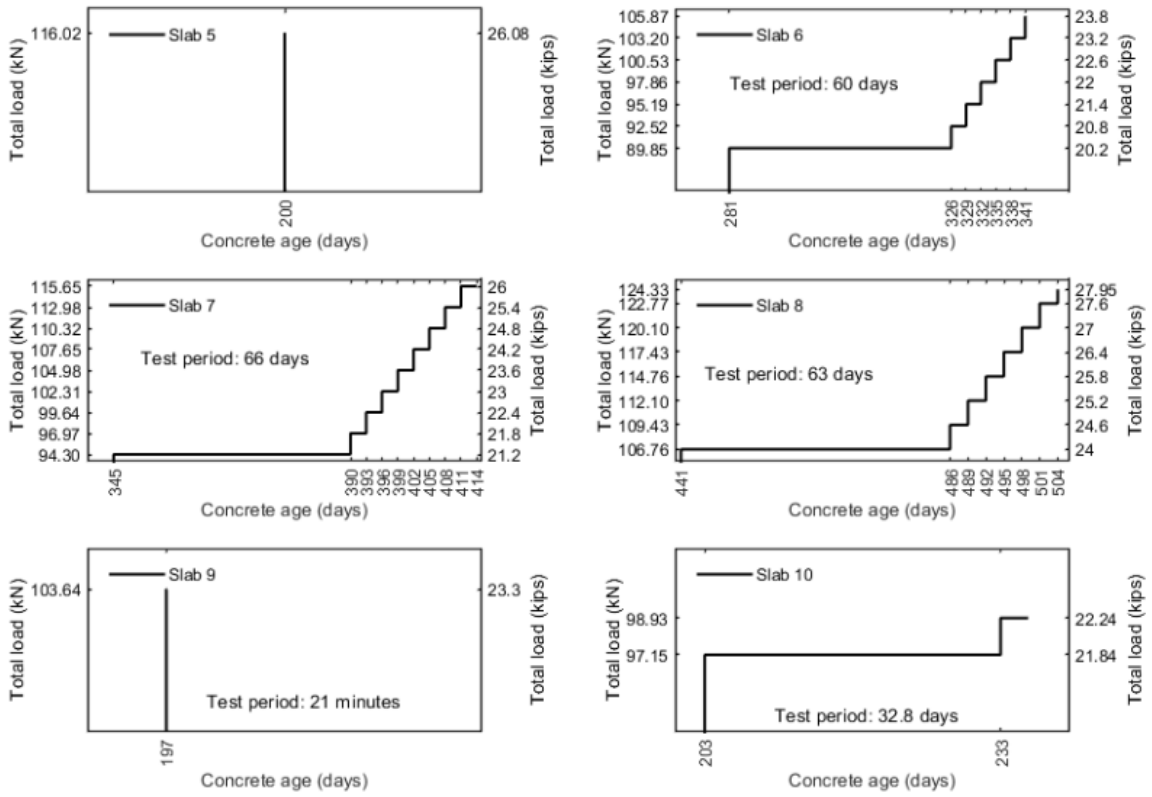

Figure 4-7. Loading histories (Slab 1%).

4.7 Instrumentation and Data Collection

Each specimen was instrumented to provide detailed data required to understand the behavior of the specimen during the entire loading history. The data were collected through a NI (National Instruments) data acquisition system. Measurements involved load, deflection, displacement, strains in reinforcement and concrete.

4.7.1 Load Measurement

Each slab specimen had four loading points through 15 7/8 mm (5/8 in.) threaded rods connected to four load cells. The east and west threaded rods were connected to 38 mm (1.50 in.) threaded rod extensions, and these extensions were linked to 222 kN (50 kips) capacity load cells. Those loading points in the north and south were attached to 44.50

kN (10 kips) capacity load cells. The load cells, as shown in Figure 4-8, were placed underneath the specimen and connected to a steel fixture attached to the lab floor. Since the slab specimens were set above the load cell, the self-weight was not included in the determined applied load.

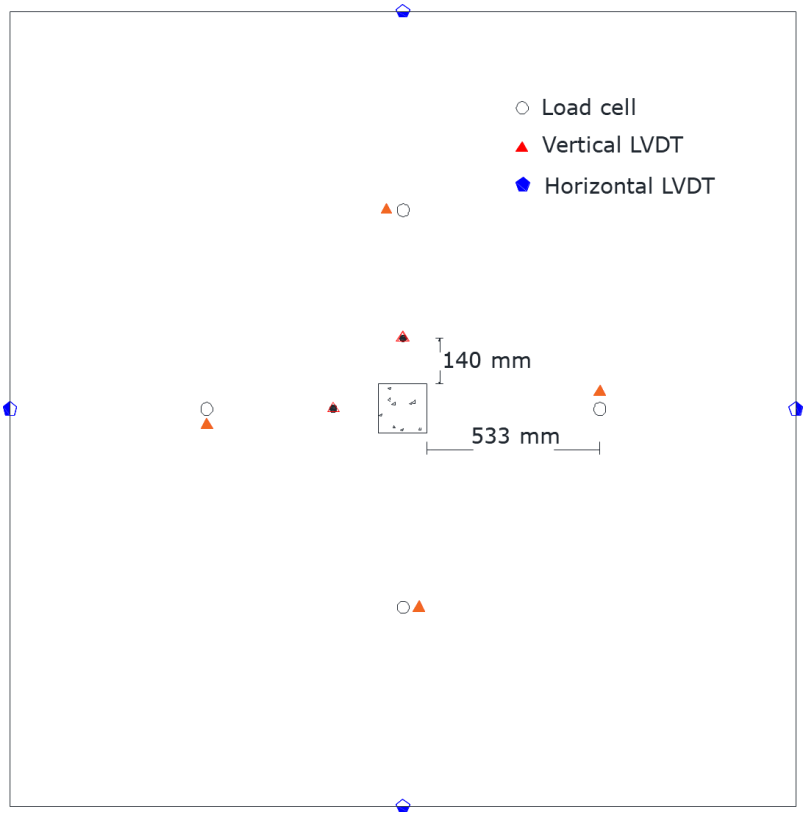

Figure 4-8. Load cells and LVDTs.

4.7.2 Deflection and Rotation Measurements

Four Linear Variable Differential Transformers (LVDTs) were used to determine the vertical deflections of the slab at 433 mm (21 in.) of the slab near the loading points, as shown in Figure 4.10. The LVDTs were placed underneath the slab closet to the loading points. The measured deflections were based on the measured applied load without self-weight. Slab rotations were measured by two LVDTs at two locations near the column

faces: north and west. The LVDTs were placed underneath the slab at a distance of 140 mm (5.5 in.), as shown in Figure 4-8. Slab lateral displacement was determined using four horizontal LVDTs located at the centers of the slab edges. Figure 4-8 shows the locations of the horizontal LVDTs.

4.7.3 Strain Measurements on Steel Reinforcement

Each specimen had eight 350-ohm electrical strain gauges attached at different locations to flexural tension reinforcement (i.e., to the top layer of reinforcement) to provide information on rebar strain distribution and redistribution near the column faces. The strain gauges were installed on the neutral plane of the rebar cross-section. The approximate locations of strain gauges placed on the steel of specimens with 0.64 percent reinforcement are shown in Figure 4-9. The approximate locations of strain gauges placed on the steel of specimens with 1.0 percent reinforcement for series I are shown in Figure 4-10, and for series II are shown in Figure 4-11.

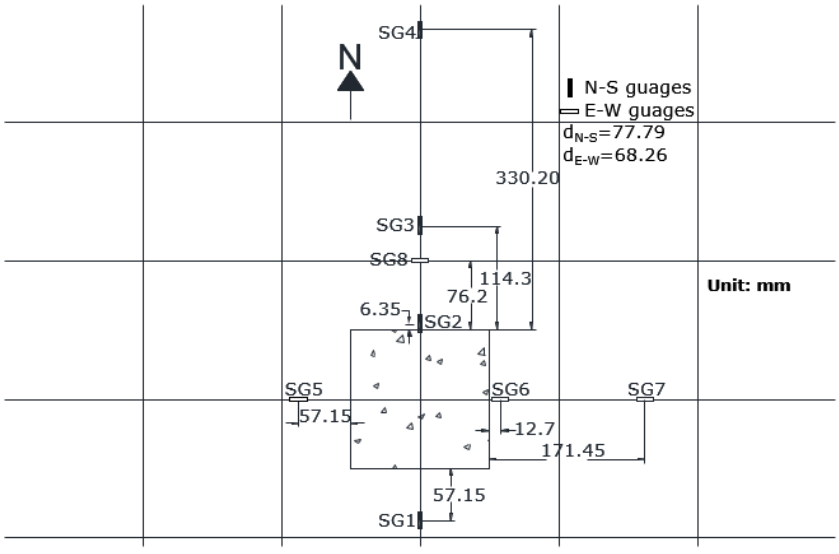

Figure 4-9. The locations of strain gauges (0.64%).

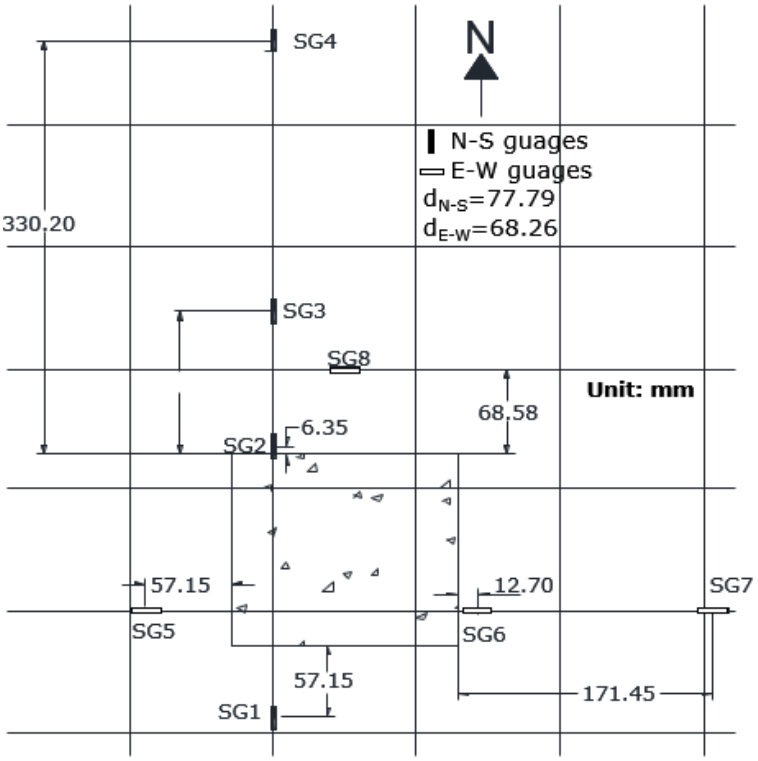

Figure 4-10. The locations of strain gauges (1%) series I.

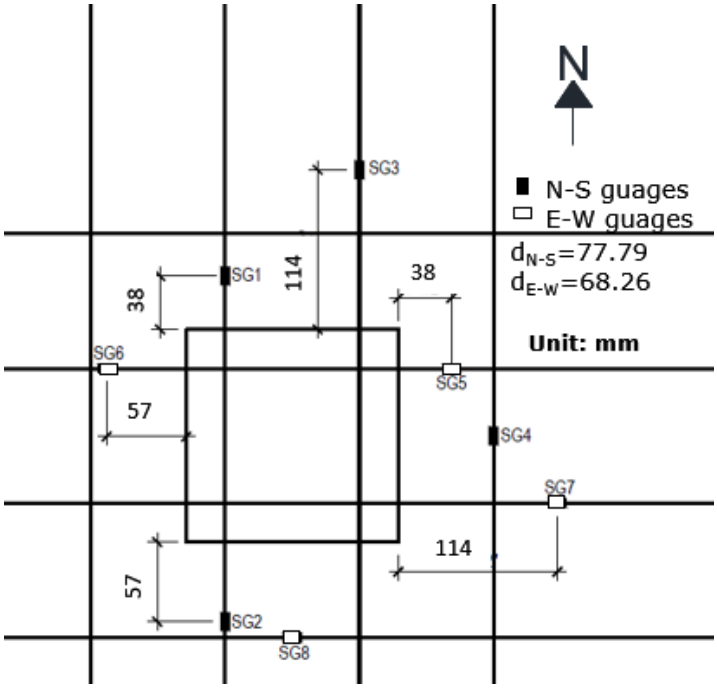

Figure 4-11. The locations of strain gauges (1%) series II.

4.7.4 Strain Measurements on Concrete

Four 3-inch-long steel strain transducers were mounted to the bottom of the slab to measure the strain in concrete near the column. Two strain transducers were attached perpendicularly in the east (PERP E) and the south (PERP S). The other transducers were mounted parallelly in the north (PAR N) and the west (PAR W). The distances between the column and the transducers were 13 mm (0.5 in.) for all perpendicular and parallel transducers. Figure 4-12 shows the locations of the strain transducers.

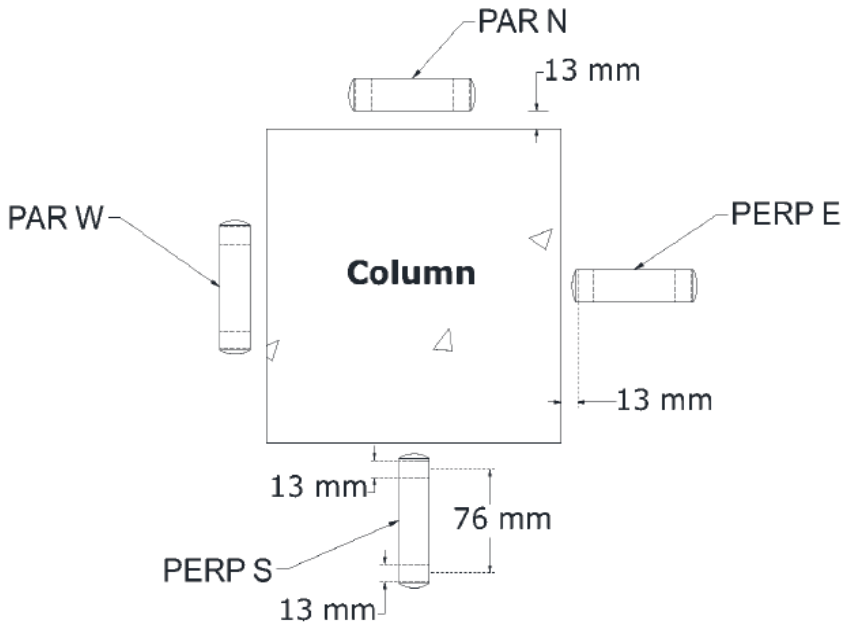

Figure 4-12. The locations of the strain transducers.

4.8 Mechanical Properties.

The following section provides an overview of the mechanical properties of materials used to build slab-column connections, including concrete and steel reinforcement.

4.8.1 Concrete

The concrete mixtures in all batches to build slab specimens were designed to have 27.58 MPa (4000 psi) compressive strength at the age of 28 days. Cylindrical specimens of dimensions 100 × 200-mm (4 × 8-in.) were tested under compressive axial loading to obtain the average compressive strength of the concrete. Table 4-1 shows the compressive strengths of the batches used to build slab specimens. The compressive strengths of the first four slabs (0.64%) at ages of 233 and 353 days were 38.75 MPa (5620 psi) and 38.61 MPa (5600 psi). Batch 2 used to build beams series II was the same batch used to build slabs (1%) series I. The compressive strength at the age of 206 days was 35.45 MPa (5141 psi). Batch 4 was used to build slab (1%) series II with compressive strength of 31 MPa (4492 psi) at the age of 197 days. Stress-strain curves from at least 2 of the tested cylindrical specimens are shown in Figure 4-13. The concrete mixtures of these batches are exhibited in appendix B.

Table 4-1. Compressive strength of batches (slabs).

Batch	Age (days)	Compressive strength, f'c	Specimen
3	233	38.75 MPa (5620 psi)	Slab 1, 2, 3, 4
	353	38.61 MPa (5600 psi)	
2	206	35.45 MPa (5141 psi)	Slab 5, 6, 7, 8
4	197	31 MPa (4492 psi)	Slab 9, 10

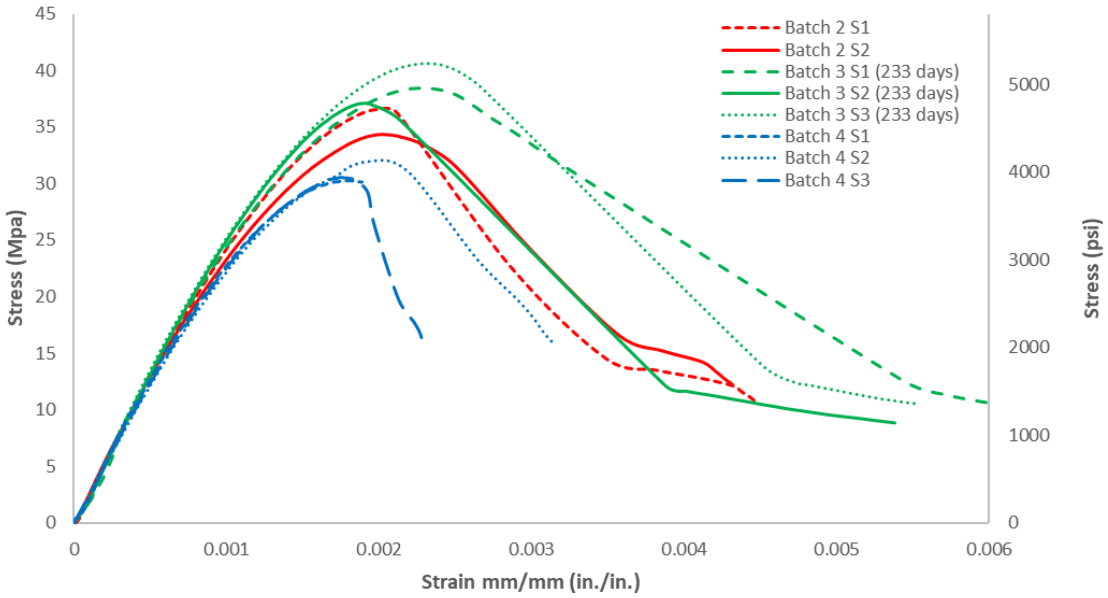

Figure 4-13. Stress-strain curves of concrete batches 2, 3, and 4.

4.8.2 Steel Reinforcement

Reinforcing bar No.10 (No.3) with 9.525 mm (3/8 in.) diameter, Grade 420 (Grade 60) were used in all specimens. Steel rebars were tested under uniaxial tension according to the specifications of ASTM A370. Table 4-2 summarizes the steel rebar properties. Stress-strain curves from tested reinforcement specimens are exhibited in Figure 3-5. Slabs 1 through 8 were made with steel bars from batch no. 1, and slabs 9 and 10 were made with bars from batch no. 2. Figure 4-13 shows stress-strain curves of batch 2.

Table 4-2. Material properties of steel rebars.

Batch	Yield strength MPa (ksi)	Tensile strength MPa (ksi)	Young's Modulus GPa (ksi)	Specimen
1	476 (69)	718 (104)	197 (28600)	Slab 1, 2, 3, 4, 5, 6, 7, and 8
2	468 (67.9)	712 (103)	205 (29716)	Slab 9, 10 ,11, and 12

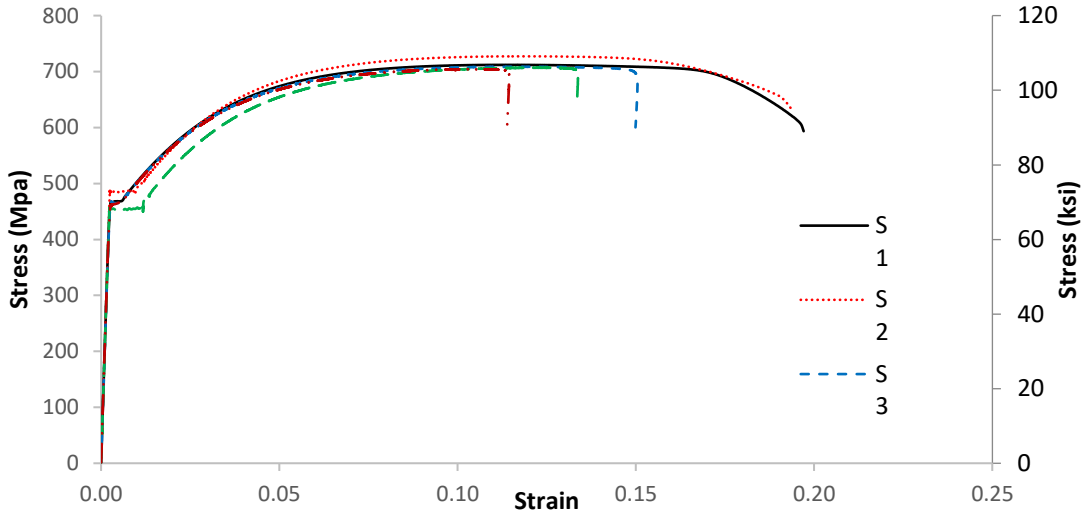

Figure 4-14. Stress-strain curves of reinforcement (batch 2).

4.9 Results

The results of the testing on the slab-column specimens are presented in this section. The first four slabs had a tensile reinforcement ratio of 0.64%. Slab 1 (SC1) served as a control specimen. S2-SL and S3-SL were tested under sustained loading, while S4 failed before being under sustained loading. The rest of the slabs had a tensile reinforcement ratio of 1%. Slab 5 served as the control specimen and we tested under short-term loading until failure. Slabs 6 through 12 were tested under sustained loading. Slabs 5 through 8 were part of series I and slabs 9 through 12 were part of series II (two specimens are currently being tested). Although the design of the two series was the same, there were differences in the concrete batch, strain gauge locations, and the concrete covers. The results include deflections, horizontal displacements, reinforcement strains, concrete

strains. The results for deflection are the average deflection of the four side deflections at 533 mm (21 in.) of the faces of the columns.

4.9.1 Slabs (0.64%)

Four specimens were tested in slabs with a 0.64% reinforcement ratio. The control specimen, SC1, was loaded to failure in a short time. Two slabs (S2-SL and S3-SL) were tested under sustained loading, and slab 4 (S4) was failed during loading up before reaching the sustained loading.

4.9.1.1 Initial Loading and Overall Response

Figure 4-15 shows total load vs. average deflections curves of slabs reinforcement ratio of 0.64%. As can be seen in Figure 4-15, cracks took place multiple times during the initial loading of the slabs that led to an increase in the average deflections with a decrease in the total loads, as is common in the testing of reinforced concrete.

Slab 1 (SC1) was loaded monotonically to failure in 58 minutes at the age of 175 days as a control specimen. The first crack took place in SC1 at the total load of 30.99 kN (6967 lbs), which led to an increase in the average deflection from 0.7429 mm to 1.102 mm. After this crack, the stiffness softened. The peak total load was 100.34 kN (22557 lbs) at the average deflection of 14.06 mm (0.553 in.). SC1 failed at the total load of 99.22 kN (22305 lbs) at the average deflection of 14.45 mm (0.569 in.). The slab thickness varied from 79.38 mm (3 1/8 in.) to 85.73 mm (3 3/8 in.), while the clear cover ranged from 9.53 mm (3/8 in.) to 15.88 mm (5/8 in.).

The second specimen, S2-SL, was loaded to 89.32 kN (20080 lbs) at the age of 189 days. The stiffness softened after the first crack took place at the total load of 30.07

kN (6760 lbs), which was very close to the total load of the first crack in SC1. The sustained load was selected when the specimen was not capable of maintaining the load while being loaded up. That happened when the average deflection increased rapidly in a short time with a reduction in the load. The initial loading stage took a total of 75 minutes. The sustained load was maintained for 73 days. After the sustained load, there were four additional sustained loading stages. S2-SL failed during the last stage of the sustained loading after 45 hours. The sustained load of the last stage was 106.76 kN (24000 lbs). The failure load was 106.37 kN (23913 lbs) at the average deflection of 15.15 mm (0.596 in.). The variation in the thickness of S2-SL was between 82.55 mm (3 1/4 in.) and 85.73 mm (3 3/8 in.). The range of S2-SL clear cover was between 9.53 mm (3/8 in.) to 12.7 mm (1/2 in.).

Slab 3 (S3-SL) was initially loaded to 94.52 kN (21250 lbs) in 117 minutes. The age of the specimen at the beginning of the test was 311 days, and the first stage of the sustained loading lasted for 46 days. S3-SL was the stiffest specimen in slabs (0.64%). The first crack, which resulted in a reduction in stiffness, occurred at the total load of 46.24 kN (10395 lbs). The first-crack load of S3-SL was over 1.5 times the first-crack loads of the first two specimens. This significant difference indicated superior strength over the first two specimens. Therefore, the first sustained load was higher than the sustained load of S2-SL. Similar to B2-SL, loading up was stopped when the specimen deflected rapidly with a reduction in the total load. There were four additional sustained loads after the first stage. S3-SL failed while being loaded up at an additional stage. The peak load was 106.17 kN (23868 lbs) at the average deflection of 14.60 mm (0.555 in.). The failure load was 106.17 kN (23868 lbs) when the average deflection was 14.60 mm (0.575 in.). The

thickness of S3-SL ranged from 88.9 mm (3 1/2 in.) to 90.49 mm (3 9/16 in.). The clear cover of S3-SL varied from 12.7 mm (1/2 in.) to 15.88 mm (5/8 in.). The extra thickness and cover in the slab contributed to its increased strength compared to the other slabs.

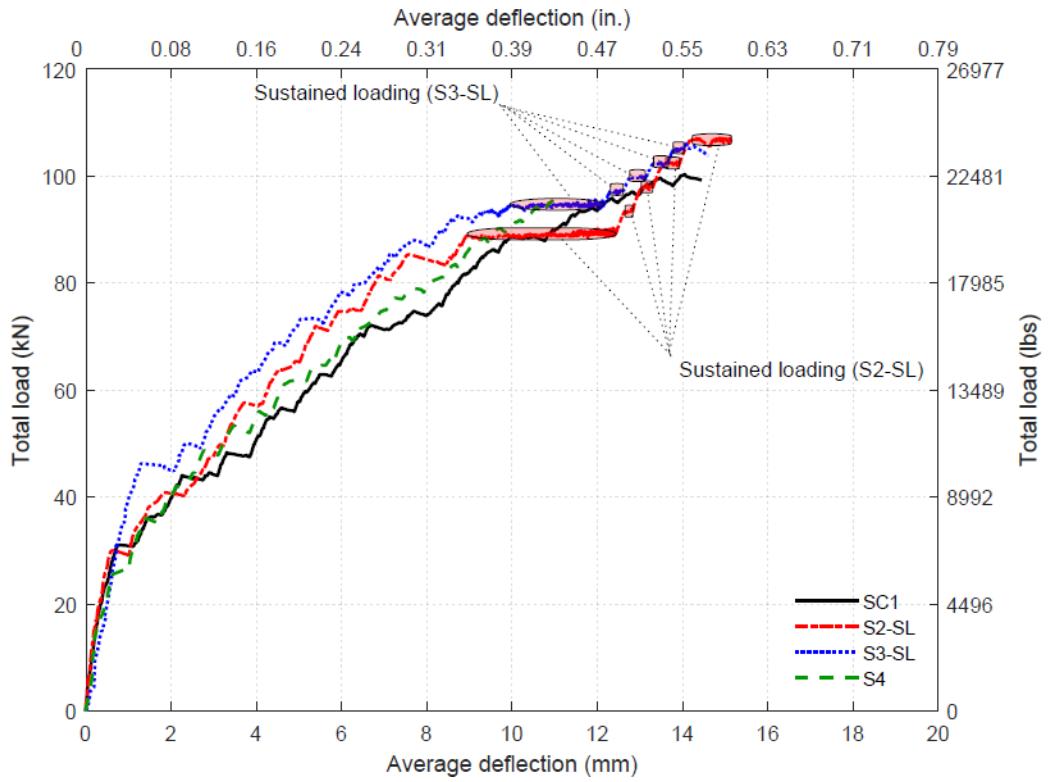

Figure 4-15 load vs deflection curves of slabs (0.64%).

The last specimen, S4, was intended to be loaded up under sustained loading, but it failed before reaching a specific sustained load. It could be due to possible eccentric loading. The east side deflected considerably more than any other side. To catch up this deflection, all sides were loaded up except the east side, which might eventually lead to failure. S4 was loaded up at the age of 402 days. The failure load was applied in 74 minutes. This specimen had the lowest stiffness of slabs (0.64%). The first crack that softened the stiffness occurred at the total load of 25.56 kN (5746 lbs). The peak load was 95.86 kN

(21551 lbs) at the average deflection of 11.01 mm (0.433 in.). The failure load occurred at the total load of 94.86 kN (21325 lbs) at the average deflection of 11.15 mm (0.439 in.).

Figure 4-16 shows reinforcement strains of slabs with a reinforcement ratio of 0.64%. The locations of the strain gauges were shown in section 4.7.3. The strain gauges very close to the faces of the column were influenced by the column rigidity and had small values of strains. As expected, during initial loading, the strain in the reinforcement increased with increasing load.

As seen in Figure 4-16 (SC1), SG4 had the lowest strain because its location was the furthest of the face of the column. In general, strain gauges SG5, SG6, and SG8 had the maximum strains. They all were attached to the extreme layer of tension reinforcement. Reinforcement at SG5, SG6, and SG8 yielded when the total load exceeded 96.97 kN, 88.57 kN, and 74.52 kN, respectively. The strain readings of the rest of the SGs showed that reinforcement at these strain gauge locations did not yield even at the failure. Failure strains are exhibited in Table 4-3. For those, which yielded, the one that yielded first had the highest strain at the failure.

For S2-SL, the lowest strain was read in SG4, just like the one in SC1. Similar to SC1, Strain gauges SG5, SG6, and SG8 had the maximum strains. SG8 yielded first before reaching the sustained load of 89.19 kN (20050 lbs), while SG7 yielded during the first stage of the sustained loading. As shown in Figure 4-16, the gauge with the highest strain at failure was SG5 since the failure was initiated in the east side where SG5 was placed. The three-reinforcement yielding in SC1 yielded in S2-SL. With the exception of SG5 and SG7, the failure strains of S2-SL were lower than the failure strains of SC1, although the failure load of S2-SL was higher than the one in SC1.

The first crack in S3-SL took place at a total load higher than the ones in the other specimens in slabs (0.64%), and the effect of that was seen in the reinforcement strains. No reinforcement strain exceeded 0.0025 mm/mm (in./in.) at the total load less than 93 kN (20907 lbs), which made it different from the other slabs. Reinforcement of SG6 yielded at the total load of about 92 kN (20682 lbs) and was the only one to reach yield before the beginning of the sustained loading. Reinforcement of SG5 and SG8 yielded under the first stage of the sustained loading.

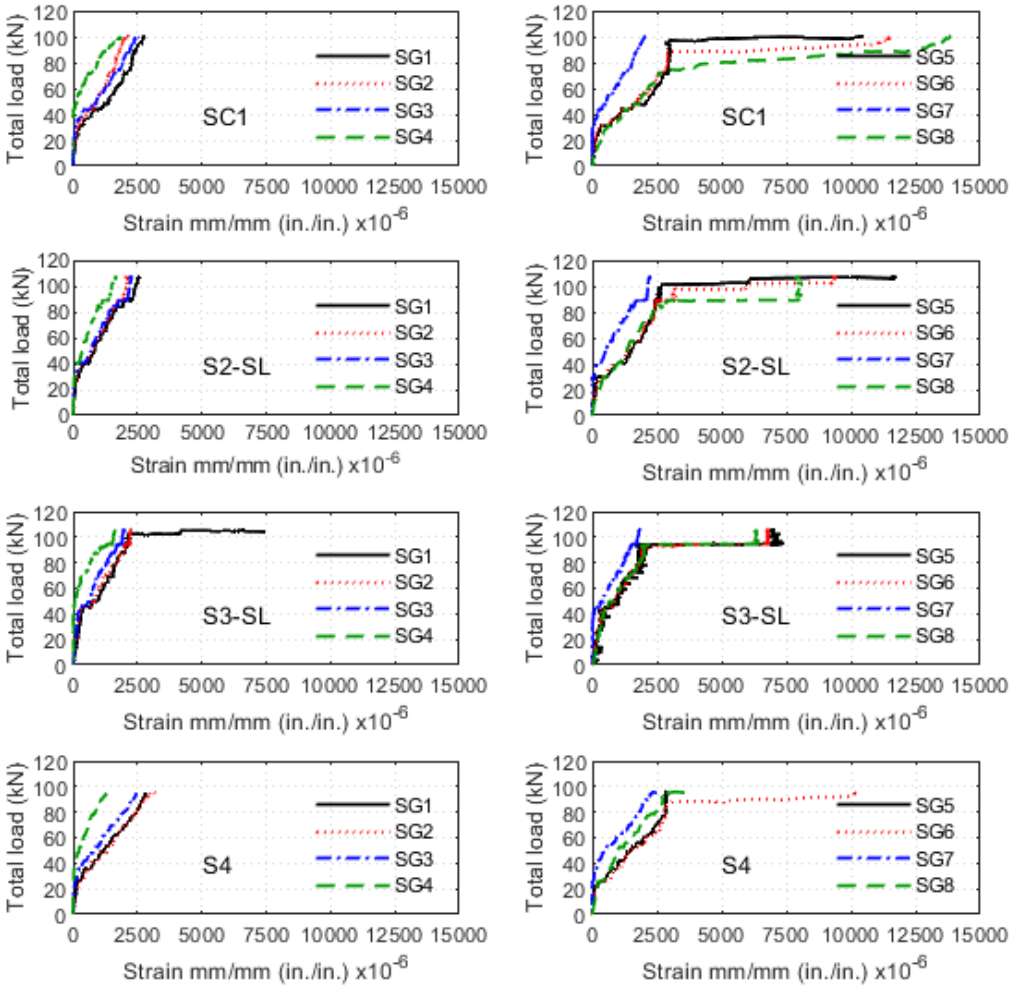

Figure 4-16. Reinforcement strain of slabs (0.64%).

The last specimen was S4, which failed before being under sustained loading. Reinforcement of SG6 yielded at the load of ~88 kN (19783 lbs). Reinforcement of SG8 yielded just before the failure. Only two reinforcement of SGs yielded in S4. This agreed that the before specimen failed. Reinforcement of SG5 did not yield like the other specimen. As can be seen in Table 4-3. , failure strain in SG6 exceeded 0.01 mm/mm (in./in.) at the failure.

In all specimens, only reinforcement of SG5, SG6, and SG8 yielded before the failure took place, except S3-SL, where the reinforcement of SG1 also yielded. The failure strains are shown in Table 4-3. In general, reinforcement of SG4 and SG7 had the lowest strain, and reinforcement of SG5, SG6, and SG8 had the highest strain at the failure.

Table 4-3. Failure strains of slabs (0.64%)

	Failure strain mm/mm (in./in.)			
Strain gauge	SC1	S2-SL	S3-SL	S4
SG1	0.0028	0.0026	0.0075	0.0028
SG2	0.0023	0.0022	0.0023	0.0032
SG3	0.0026	0.0023	0.0020	0.0025
SG4	0.0019	0.0017	0.0016	0.0014
SG5	0.0105	0.0116	0.0069	0.0028
SG6	0.0115	0.0093	0.0068	0.0101
SG7	0.0020	0.0022	0.0018	0.0025
SG8	0.0139	0.0079	0.0063	0.0037

The concrete strain of slabs (0.64%) is shown in Figure 4-17. As shown, there was a discrepancy in the values of concrete strain. Strain transducer locations are exhibited in Figure 4-9. There were huge differences in the concrete strain at failure. In all specimens of slabs (0.64%) except SC1, parallel strain transducers had the highest values because they

were close to the faces of the column. As seen in Peng et al. (2017) and Broms (2008), the parallel (or radial) strains decreased just before failure due to the generation of radial tension strains just before punching.

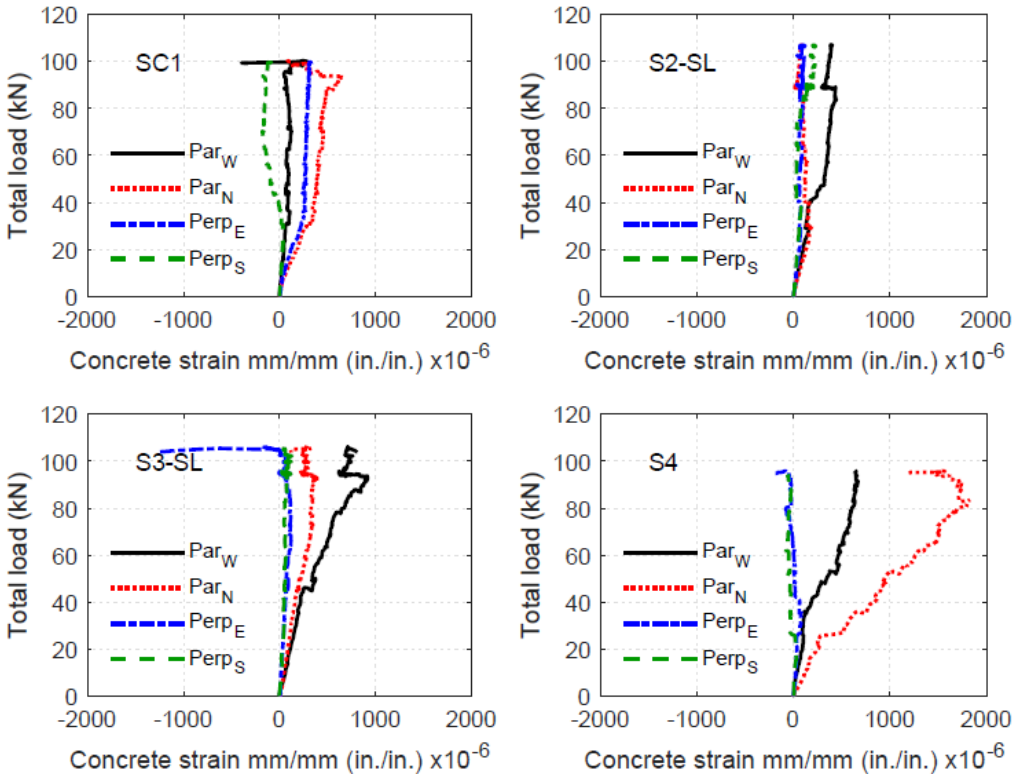

Figure 4-17. Concrete strain of slabs (0.64%)

At the total load of 93.3 kN (20974 lbs) of SC1, the concrete strain of Par_N was 0.00065 mm/mm (in/in.). Then, the concrete strain decreased with the increase of loading. At the failure, the concrete strain of Par_W decreased from 0.0003 mm/mm (in./in.) to a negative value. The highest concrete strain in S2-SL was 0.00044 mm/mm (in./in.) at the load 89.19 kN (20050 lbs). At the failure of S2-SL, the concrete strain of the same transducer was 0.00041 mm/mm (in./in.). It was less than the highest strain because the concrete strain decreased under sustained loading due to redistribution of stresses between the concrete and reinforcement. Similar to S2-SL, the highest concrete strain was in Par_W.

Also, the concrete strain of Par_W at the failure was less because of the distribution of stresses under sustained loading. The highest concrete strain of S4 took place in Par_N. The concrete strain was 0.0018 mm/mm (in./in.) at the total load of 83.25 kN (18715 lbs).

4.9.1.2 First Stage of Sustained Loading

Load and deflection vs. time curves of the first stage of the sustained loading for S2-SL and S3-SL are shown in Figure 4-18. As mentioned previously, the first stage of the sustained loading lasted 73 days for S2-SL and 46 days for S3-SL.

Table 4-4. shows the increase in deflection and increase percentage of S2-SL and S3-SL during the first stage of sustained loading.

At the beginning of the first stage of the sustained loads of S2-SL, the average deflection was 8.94 mm (0.352 in.) and became 12.44 mm (0.490 in.) at the end of the stage. The total increase in the average deflection was 3.50 mm (0.138 in.), which was 0.39 times the average instantaneous deflection. The increase in the average deflection at the beginning of the 4^{th} day was 1.43 mm (0.056 in.), which was 40.9% of the total increase in the average deflection. On the 46^{th} day, the increase in the average deflection was 3.26 mm (0.128 in.), which was 93% of the total increase in the average deflection of S2-SL.

The sustained load of the first stage in S3-SL was 94.52 kN (21250 lbs). The average deflection at the beginning and at the end of the first sustained load was 9.95 mm and (0.392 in.) and 12.13 mm (0.478 in.). Therefore, the increase in deflection was 2.18 mm (0.086 in.), which was 0.22 of the average instantaneous deflection. At the end of the 3^{rd} day, the increase in deflection was 0.74 mm (0.029 in.), which was 33.8% of the total increase in deflection of S3-SL in the first stage. This is a similar amount of early-term deflection as in S2-SL.

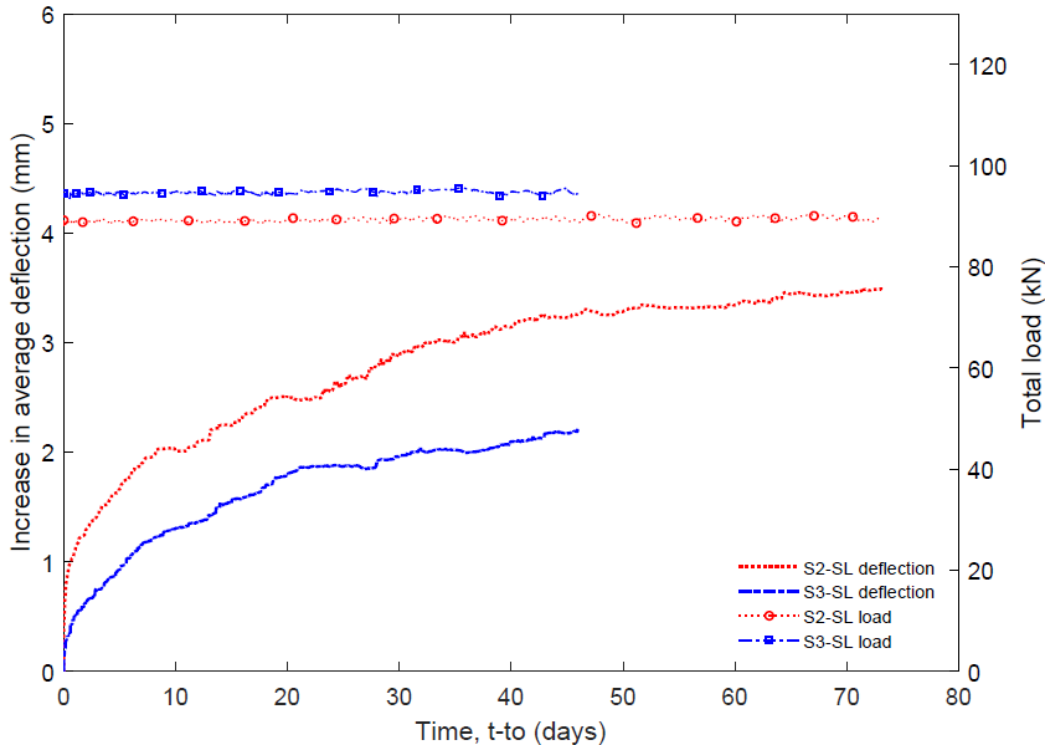

Figure 4-18. Load and deflection vs. time curves of 1st stage of SL loading (S2-SL and S3-SL).

As seen in Figure 4-17, the increase in deflection under sustained load has the same shaped curve as the beam and concrete cylinder tests. As Table 4-4 exhibits, over 50% of the deflection took place in the first week regardless of the duration of the sustained load. The primary stage of creep deformations lasted for approximately one week. The secondary stage of creep deformations lasted through the remainder of the loading period. The shape of both the curves for slab S2-SL and S3-SL are similar; however, S2-SL overall had a lower level of stiffness compared to S3-SL, which could have led to increase in deflection under sustained load.

Table 4-4. Increase in deflection and percentage during 1st stage (S2-SL & S3-SL)

	S2-SL		S3-SL	
Time	Increase in deflection mm (in.)	Increase percentage (%)	Increase in deflection mm (in.)	Increase percentage (%)
1	1.10 (0.043)	31.5	0.50 (0.020)	23
3	1.43 (0.056)	40.9	0.74 (0.029)	33.8
7	1.90 (0.075)	54.3	1.16 (0.046)	52.9
21	2.43 (0.097)	70.7	1.86 (0.073)	85.1
46	3.26 (0.128)	93	2.18 (0.086)	100
73	3.50 (0.138)	100	-	

Reinforcement strain under the first stage of the sustained loads (S2-SL and S3-SL) is exhibited in Figure 4-19. The increase in reinforcement strains here means the reinforcement strains under the sustained loading without instantaneous reinforcement strains that took place before the beginning of the sustained loading. Table 4-5 shows the total increase in reinforcement strains of S2-SL and S3-SL during the first stage of the sustained loading. As seen in Figure 4-19, for both S2-SL and S3-SL, the increase in the reinforcement strains of SG1, SG2, SG3, and SG4 was slight in comparison to the rest of the reinforcement strains. However, all the strains do show increasing throughout the period of sustained loading, indicating that the reinforcement was taking additional stress even though the load on the specimen remained constant. The jagged dropping in SG1 for specimen S3-SL is likely due to cracking in the concrete. Most increases in reinforcement strains took place in SG5, SG7, and SG8, which were also the location showing the highest strains during the initial loading.

For S2-SL, the minimum increase in reinforcement strain was in SG5. The increase was 0.00003 mm/mm (in./in.), which was 0.01 of instantaneous strain. Like SG5, the increase in reinforcement strain of SG2 was small, although both SG2 and SG5 were the

nearest SGs to the faces of the column. The reason for these small strains was that they were affected by the column rigidity. The maximum increase in reinforcement strain took place in SG8. The increase in strain and ratio to the instantaneous strain were 0.00497 mm/mm (in./in.) and 1.65, respectively. The increase in reinforcement strains of SG2 and SG4 was almost following what happened in the initial loading. As shown in Figure 4-19, the increase in reinforcement strain of SG3 was a little higher than the one in SG1, although based on their locations, the increase in SG3 should have been less. The increase in the deflections of each side could explain why the increase in SG3 was higher than SG1. The increase in the north side where SG3 was located had the highest increase in deflection under the first stage of the sustained loading. The same explanation could be applied to SG8, which had the highest increase in strain; besides that, the reinforcement of SG8 yielded before the beginning of the sustained loading. Most increases in reinforcement strain of SG3 took place during the first day under the sustained loading because the reinforcement yielded just before the beginning of the sustained loads. The sudden jump in the reinforcement strain of SG8 on the 4^{th} day took place in about 4 minutes. It could be due to aggregate breakage. The small jumps in the reinforcement strain of SG6 in the 30^{th} and 34^{th} days might be due to aggregate breakage. There were reductions in the reinforcement strain of SG5, as shown in Figure 4-19, and it became less than zero on the 52^{nd} day. That did not mean the reinforcement became in the compression zone because the instantaneous strain was subtracted. These reductions were due to the noise of the channel that SG5 was connected to. Even the reduction in strains was insignificant.

The reinforcement strains of SG1, SG2, and SG3 of S3-SL decreased in the first minutes; then, it increased with time under the first stage of sustained loading. SG5 had the

highest increase in strain under the first sustained loads. The reinforcement strain of SG5 was 0.0052 mm/mm (in./in.). The increase in strain was 2.63 of the instantaneous strain of SG5. The lowest increase in reinforcement strain occurred in SG1. The ratio of increase in the strain of SG1 at the end of the first stage to the instantaneous strain was 0.024. The reinforcement strains of SG2 and SG3 increased almost the same amount at the end of the stage. SG4, which was expected to have the lowest increase in strain, had the highest strain between the first four SGs. It could be just because the strain of SG4 was the smallest between all the eight SGs at the beginning of the sustained loading. Therefore, it increased more than SG1, SG2, and SG3 in this stage. However, the total strain of SG4 was the smallest at the end of the first sustained loading even though it increased more than the first three SGs. The reinforcement strain of SG1 of S3-SL fluctuated, and it became below and above zero many times, as seen in Figure 4-19. It could be due to the noise of the channel to which SG1 was connected because it happened one time at midnight when no one was around the specimen and two times around 8 AM when the light got on. The jumps in the strain of SG6 on the 6^{th} day and 30^{th} days were probably due to aggregate breakage. As mentioned, the highest increase in strain under the first stage of the sustained loading was in SG5. The highest increase in deflection took place on the west side in where SG5 was located. That gave an explanation for why the highest increase in the strain of SG5 under sustained loading. The reinforcement of SG5 and SG8 yielded during the first stage of the sustained loading, while the reinforcement of SG6 yielded before the beginning of the sustained loading.

In general, the highest increase in reinforcement strain under the first stage of the sustained loading happened in the bottom layer of tension reinforcement. Reinforcement

strains of SGs that were close to the yield stress or already yielded at the beginning of the sustained loading were more likely to have the highest increases in strain under sustained loading. The increases of strain in the first four SGs of S2-SL were higher than the ones in S3-SL even for the values of the first four SGs of S2-SL on the 46th day. Reinforcement could yield under the sustained loading as B2-SL and S3-SL showed. A side of slab deflected more under sustained loading was more likely to have the highest increase in a strain of an SG located in that side. Jumps in strain might take place due to concrete cracking, especially for reinforcement that yielded or close to yield.

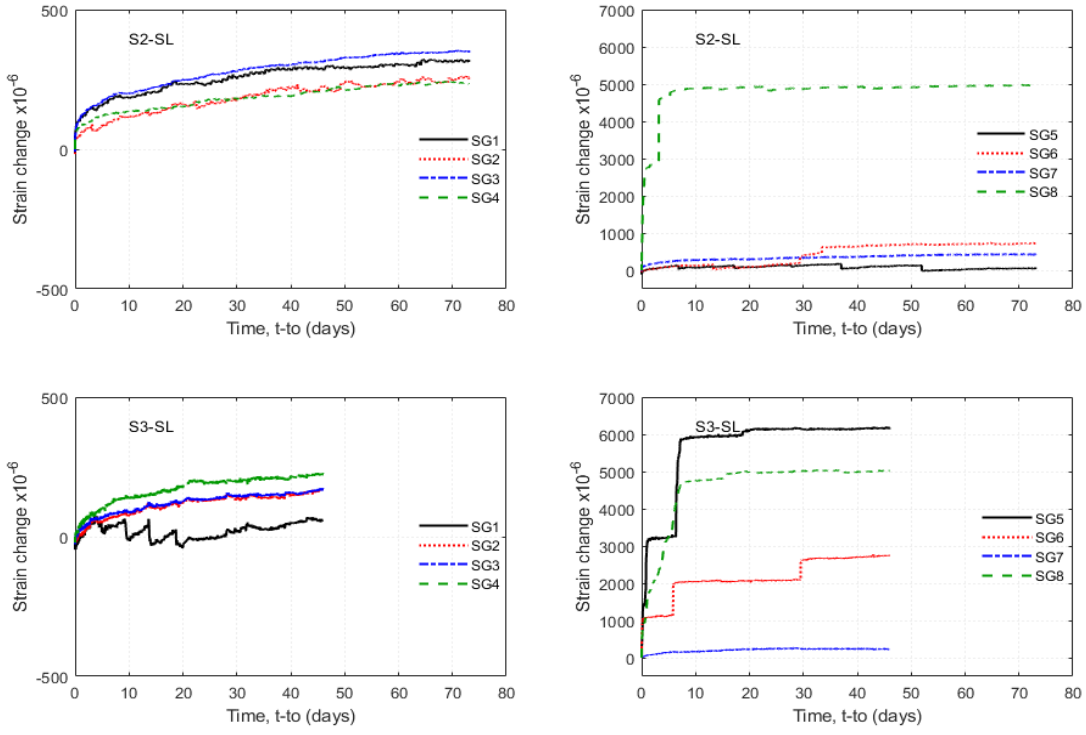

Figure 4-19. Increase in reinforcement strains under 1st sustained loading (S2-SL & S3-SL).

Table 4-5. Increases in strains during of 1st of SL (S2-SL & S3-SL)

	Increase in strain mm/mm (in./in.)							
	SG1	SG2	SG3	SG4	SG5	SG6	SG7	SG8
S2-SL	0.0003	0.0003	0.0003	0.0002	0	0.0007	0.0004	0.005
S3-SL	0.0001	0.0002	0.0002	0.0002	0.0052	0.0023	0.0002	0.0042

The increase percent in strain under the first stage of sustained loading of S2-SL and S3-SL is shown in Table 4-6. Yielding of reinforcement and concrete cracking may take place during sustained loading, as seen in Figure 4-19.

Table 4-6. Increase percent under 1st stage of S2-SL and S3-SL.

Time (days)	Increase percentage of S2-SL (%)							
	SG1	SG2	SG3	SG4	SG5	SG6	SG7	SG8
1	35.1	20.1	32.5	34.2	70.0	1.5	33.3	55.1
3	46.3	31.7	44.0	42.7	218.0	7.2	45.9	58.1
7	56.2	39.1	56.0	55.4	178.7	14.2	61.4	97.5
21	72.9	59.4	72.2	67.7	333.3	12.9	70.5	98.9
46	89.2	86.3	90.6	88.7	420.0	91.9	89.9	98.3
73	100	100	100	100	100	100	100	100
	Increase percentage of S3-SL (%)							
	SG1	SG2	SG3	SG4	SG5	SG6	SG7	SG8
1	7.3	2.8	18.6	22.8	47.8	39.3	28.1	29.5
3	83.0	32.4	39.8	40.1	51.2	41.1	49.1	44.2
7	63.3	38.2	48.3	61.8	87.8	74.4	69.2	90.3
21	-7.2	74.8	82.6	92.2	97.6	76.0	103.8	98.9
46	100	100	100	100	100	100	100	100

Strain gauges close to the face of the column may fluctuate around the zero or fluctuate in a small range as SG5 of S2-SL and SG1 of S3-SL, as shown in Figure 4-19. As a result, the increase percent may be negative or higher than 100%. The effect of that can be seen in SG6 of S2-SL in Table 4-6. The increase percent in the strains of S2-SL on

the 7th day varied from 14.2% to 178.7%, which the increase percent in the strains of S3-SL ranged between 38.6% and 88.4% on the same day. On the 21st day, the variations in the increase percent in the strains of S2-SL and S3-SL were between 12.9% and 333.3% between -6.8% and 98.3%, respectively.

Figure 4-20 shows changes in concrete strains under the first stage of sustained loading of S2-SL and S3-SL. In both tests, strains of Par_W and Par_N decreased under sustained loading due to redistribution of stresses between rebars and concrete. Strains of Par_W and Par_N in S3-SL decreased more than the ones in S2-SL because the concrete strains of S3-SL at the beginning of the first sustained load were higher. Strains of Perp_E and Prep_S increased in S2-SL, but they decreased in S3-SL. The increase and decrease in strains of Perp_E and Perp_S were small in compression to strains of Par_W and Par_N. Fluctutions in strains after the first days were due to load adjustment.

For S2-SL, the strain of Par_W decreased by 0.00014 mm/mm (in./in.) by the end of the 10th day; then, it fluctuated with time. It decreased by 0.00011 mm/mm (in./in.) at the end of the sustained loading. The strain of Par_N of S2-SL was reduced by 0.000068 mm/mm (in./in.) by the end of the 10th day. The total decrease in the strain of Par_N of S2-SL under the first stage was 0.000044 mm/mm (in./in.). The strain of Perp_S increased by 0.000078 mm/mm (in./in.) in the first two days; then, it fluctuated with time. Like the strain of Perp_S, the strain of Perp_E increased at first; after that, it fluctuated until the end of the first sustained load. Both strains of Perp_E and Prep_S increased under sustained loading, but the increases were less than 0.000037 mm/mm (in./in.) at the end of the first stage of sustained loading. The strain of Par_W in S3-SL sharply dropped in the first five hours. The strain decreased by 0.00024 mm/mm (in./in.) on the third day. The strain kept

increasing and decreasing. It decreased by 0.00017 mm/mm (in./in.) by the end of the 10th day. At the end of the first stage of sustained loading, the total reduction in the strain of Par_W was 0.00021 mm/mm (in./in.). The strain of Par_N followed the strain of Par_W in the change of strain. However, the reduction in the strain of Par_N was less than the reduction in Par_W. The strain of Par_N decreased by 0.000079 mm/mm (in./in.) by the end of the 10th day and by 0.00008 mm/mm (in./in.) at the end of the first stage of sustained loading. The strains of Perp_E and Perp_S were similar in fluctuations. Strains of Perp_E and Perp_S decreased by 0.00003 mm/mm (in./in.) and 0.000003 mm/mm (in./in.), respectively, at the end of the first stage of sustained loading of S3-SL.

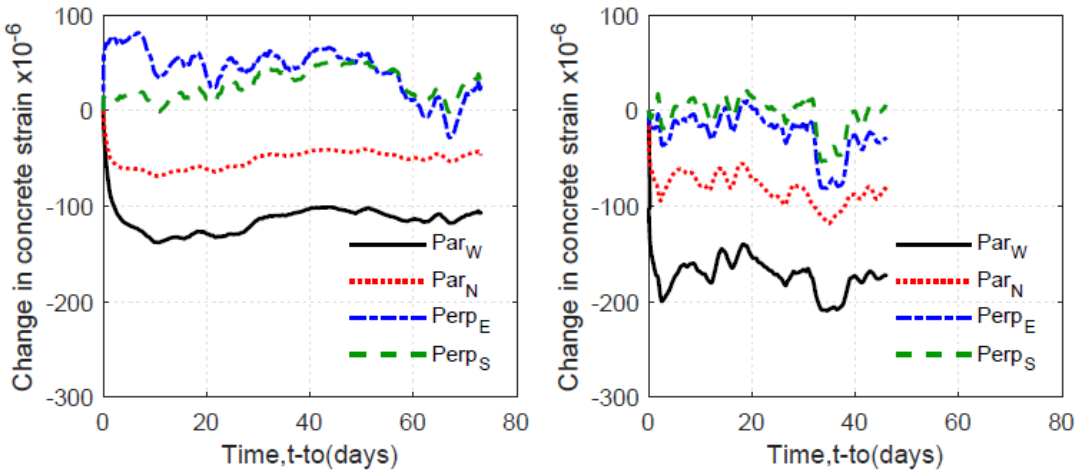

Figure 4-20. Changes in concrete strains under 1st sustained loading (S2-SL & S3-SL).

4.9.1.3 Additional Loading Stages

The specimens tested did not fail under the initial stage of sustained load; therefore, additional load was added and sustained for periods of 3 days. The additional stages of sustained loading sought to evaluate if the specimen could fail under a sustained load and how close that load level needed to be. Due to limitations in the time allowed for testing only stages of 3 days were used as the initial results showed a large percentage of the

deflections and strains happened in the early time period. Table 4-7 summarizes the increase in average deflection under the stages of the sustained loads (S2-SL and S3-SL).

Table 4-7. Increase in average deflection under sustained loads (S2-SL and S3-SL).

Stage		S2-SL	S3-SL
1	Total load kN (lbs)	89.32 (20080)	94.52 (21250)
	Period (days)	73.1	46
	Increase in average deflection mm (in.)	3.50 (0.1379)	2.18 (0.086)
2	Total load kN (lbs)	93.4 (21000)	97.12 (21833)
	Period (days)	3.1	2.7
	Increase in average deflection mm (in.)	0.18 (0.007)	0.30 (0.012)
3	Total load kN (lbs)	97.86 (22000)	99.71 (22417)
	Period (days)	3	4.1
	Increase in average deflection mm (in.)	0.27 (0.0104)	0.36 (0.014)
4	Total load kN (lbs)	102.31 (23000)	102.31 (23000)
	Period (days)	2.9	3.1
	Increase in average deflection mm (in.)	0.33 (0.0129)	0.34 (0.013)
5	Total load kN (lbs)	106.76 (24000)	104.90 (23583)
	Period (days)	1.9	2.89
	Increase in average deflection mm (in.)	0.92 (0.0361)	0.25 (0.010)

After 73 days under the first sustained load, S2-SL was subjected to four additional sustained loads for about ~3 days with the additional load in each stage of 4.45 kN (1000 lbs). The specimen failed under the fifth stage of sustained loading 45 hours after the additional load was applied. The sustained load of the fifth stage was 106.76 kN (24000 lbs).

S3-SL was under the sustained load of 94.52 kN (21250 lbs) for 46 days. Then, four additional stages were added to the specimen. The increased load in each stage was 2.594 kN (583.33 lbs). The duration of the four sustained loading stages was about ~ 3 days. The sustained load of the last stage was 104.90 kN (23583 lbs). S3-SL failed while adding the last additional load.

For S2-SL, the increase in deflection under the 3-day additional load stages became greater with higher levels of loading. The highest increase in the average deflection was in the 5th stage when the increase in the average deflection was 0.92 mm (0.0361 in.) just before the failure. For S3-SL the increase in the average deflection was highest in the 3rd and 4th stages. The increase in sustained load deflections with higher levels of loading matches the behavior of the beams theory that indicates the amount of creep deformations is dependent on the level of loading.

Table 4-8 shows the changes in reinforcement strain under all stages of the sustained loads for S2-SL and S3-SL. The duration of stages is shown in the table. As can be seen in Table 4-8, strains fluctuated during the additional stages of sustained loads in S2-SL and S3-SL. All strains in S2-SL increased with the exception of SG6 during the last stage of the sustained loading where the failure took place. The reinforcement strain of SG5 had the highest increase in strain at this stage. During this stage, the west side where SG5 was located had the highest increase in deflection. Some strains increased, and some strains decreased in the last stage of sustained loading in S3-SL. The highest increase in strain in this stage took place in SG1.

Table 4-8. Changes in reinforcement strain under sustained loads (S2-SL & S3-SL).

		S2-SL							
Stage	Time (days)	SG1	SG2	SG3	SG4	SG5	SG6	SG7	SG8
1	73.06	0.00032	0.00026	0.00035	0.00023	2.6E-05	0.00074	0.000424	0.00497
2	3.14	0.00001	-0.00005	-0.00003	0.00003	-0.00010	0.00000	0.00000	-0.00016
3	3.00	0.00002	0.00003	0.00001	0.00002	-0.00005	0.00267	-0.00003	0.00001
4	2.93	0.00003	-0.00003	-0.00001	0.00003	0.00069	0.00113	0.00000	-0.00005
5	1.91	0.00003	0.00013	0.00005	0.00004	0.00226	-0.00001	0.00002	0.00000
		S3-SL							
	Time (days)	SG1	SG2	SG3	SG4	SG5	SG6	SG7	SG8
1	45.95	0.00005	0.00015	0.00014	0.00017	0.00525	0.00228	0.000184	0.0042
2	2.71	-0.00002	-0.00003	-0.00002	-0.00001	-0.00001	0.00000	0.00003	-0.00013
3	4.10	-0.00013	-0.00004	-0.00001	-0.00002	-0.00014	-0.00003	0.00001	-0.00005
4	3.13	0.00203	0.00001	0.00000	0.00003	-0.00009	-0.00012	0.00002	-0.00005
5	2.89	0.00232	0.00000	-0.00001	0.00001	-0.00008	-0.00003	0.00001	-0.00004

The changes in concrete strain under all stages of sustained loading of S2-SL and S3-SL are exhibited in Table 4-9. As seen, the concrete strain of S2-SL increased in all additional stages except the fourth stage, where the perpendicular transducers read negative strain. The highest increase in the concrete strain of S2-SL under all five stages of sustained loads took place in the last stage, where the failure happened under sustained loading. This highest increase in concrete strain was 0.00005 mm/mm (in./in.). For S3-SL, concrete strain fluctuated under the additional stages of sustained loading. Like the first stage, all concrete strain decreased in the fourth stage.

Table 4-9. Changes in concrete strain under sustained loads (S2-SL & S3-SL).

Stage	Time (days)	S2-SL Concrete strain $\times 10^{-6}$ Parallel (west)	Parallel (north)	Perpendicular (east)	Perpendicular (south)
1	73.1	-106.9	-46.0	25.6	35.5
2	3.1	7.6	3.6	6.6	18.2
3	3.0	0.9	2.0	3.5	14.4
4	2.9	4.8	1.7	-16.8	-8.7
5	1.9	13.7	11.0	48.6	6.8
		S3-SL Concrete strain $\times 10^{-6}$ Parallel (west)	Parallel (north)	Perpendicular (east)	Perpendicular (south)
1	46.0	-172.0	-83.5	-30.8	3.7
2	2.7	27.4	-5.6	15.4	12.7
3	4.1	8.2	-28.0	-10.5	-4.5
4	3.1	-61.3	-51.5	-55.3	-33.5
5	2.9	8.0	-2.6	-114.4	-11.9

4.9.1.4 Failure Under Sustained Loading

The increase in deflection of the last stage of the sustained loading of S2-SL when the failure took place is shown in Figure 4-21. Over 50% of the increase in deflection took place in less than 5 hours. The specimen failed after 45 hours during the stage of increased loading. The curve leveled off, as shown in Figure 4-21, because the specimen deflected, and due to that, there was a reduction in the load. The load was adjusted at a time of 1 day, which led to a temporary steeper increase in deflection with time. The last adjustment of the load was about 37 minutes before the failure of the specimen.

As can be seen, the tertiary stage, as evidenced by a sudden increase in deflection, took place just before the failure. What happened just before the failure was that the north side deflected more than the rest three sides which caused a reduction in load. The west

side then deflected just two minutes before the failure. As a consequence, the specimen failed. The north side initiated the failure, and the west side caused the failure because it deflected more than any other side. The tertiary stage, as exhibited by rapidly increasing displacements, only lasted for about 2 minutes. The small amount of time for the tertiary phase limits the ability to warn and evacuate a structure before the collapse.

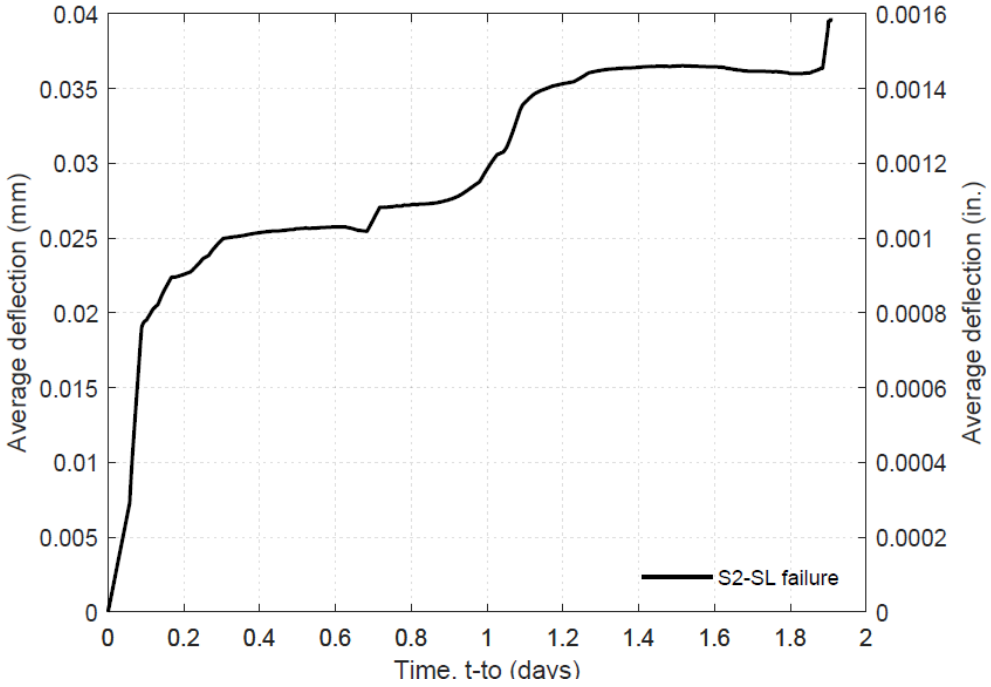

Figure 4-21. Increase in deflection of S2-SL in last stage of SL.

Figure 4-22 exhibits changes in the reinforcement strain of S2-SL in the last stage of the sustained loading. The fluctuations in strain around the first days were due to load adjustment. Most of the increase in reinforcement strain of SG2 and SG5 took place in the first hours of the sustained loading. SG5 yielded early in the stage. As can be seen in Figure 4-22, just before the failure, strains of SG1, SG2, SG3, and SG4 increased suddenly in the tertiary stage. In contrast, strains of SGs attached to the lower layer of tension reinforcement (SG5, SG6, SG7, and SG8) decreased slightly. The first four gauges were

attached to a bar in the N-S direction and was the topmost layer in the specimen. The other gages were mounted on bars in the E-W direction. The increase in strains in the N-S and reduction in the E-W indicates that the E-W direction was failing in the tertiary loading stage and transferring strain to the N-S. The failure in the E-W side of the slab first is reasonable as it has the lowest d, and thus the weaker faces.

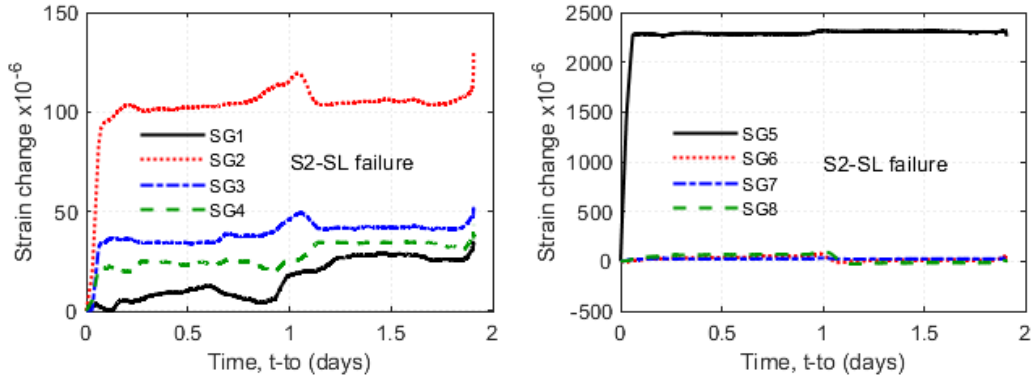

Figure 4-22. Changes in reinforcement strain of S2-SL in last stage of SL.

The changes in the concrete strain of the last stage of S2-SL where the failure occurred are shown in Figure 4-23. The concrete strain was fluctuating with time until the tertiary stage took place just two minutes, leading to failure of the specimen.

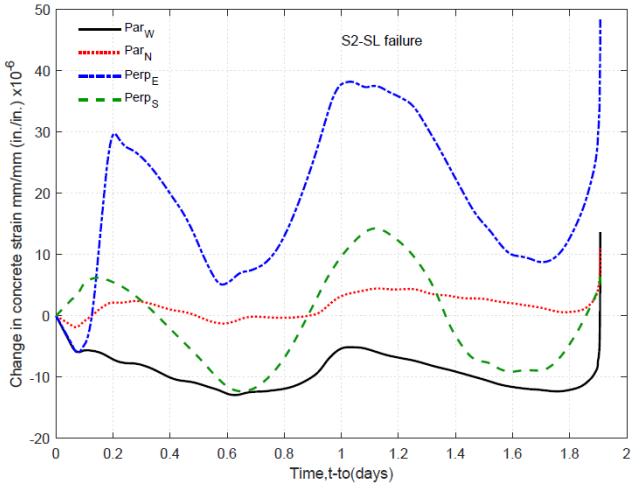

Figure 4-23. Changes in concrete strain of S2-SL in last stage of SL.

4.9.1.5 Failure Rotation

Failure rotation was calculated based on a deflection at 533 mm (21 in.) of the face of the column. Table 4-10 exhibits the average rotation and maximum rotation at the failure. As shown, S2-SL had the highest average rotation at the failure among slab (0.64%) specimens, while SC1 had the highest maximum rotation at the failure. As exhibited in Figure 4-15, SC1 was the softest specimen after the first crack took place. Therefore, it was expected to have the highest rotation. However, sustained loading increased both average and maximum rotation. The average rotation of S2-SL exceeded the average rotation of SC1 at failure due to sustained loading. The average rotations of SC1 and S3-SL were equal. If the duration of sustained loading of S3-SL was longer, as S2-SL had, probably the average and maximum rotation at the failure could be higher than the ones in SC1. S4 had the lowest average and maximum rotation at the failure because one side rotated more and led to the failure unexpectedly.

Table 4-10. Failure rotation of slabs (0.64%).

	Average rotation	Maximum rotation
SC1	0.027	0.035
S2-SL	0.028	0.032
S3-SL	0.027	0.033
S4	0.021	0.029

4.9.1.6 Temperature and Humidity

Figure 4-24 shows the fluctuations in temperature and relative humidity during the sustained loading of S2-SL and S3-SL. As seen, the temperature and relative humidity of S2-SL were higher than the ones in S3-SL. S2-SL was tested in the summer. The

temperature of S2-SL ranged from 72 ˚F to 90 ˚F, while the range relative humidity was between 61% and 76%. For S3-SL, the temperature range was between 52 ˚F to 73 ˚F, and the relative humidity ranged from 39% to 53%.

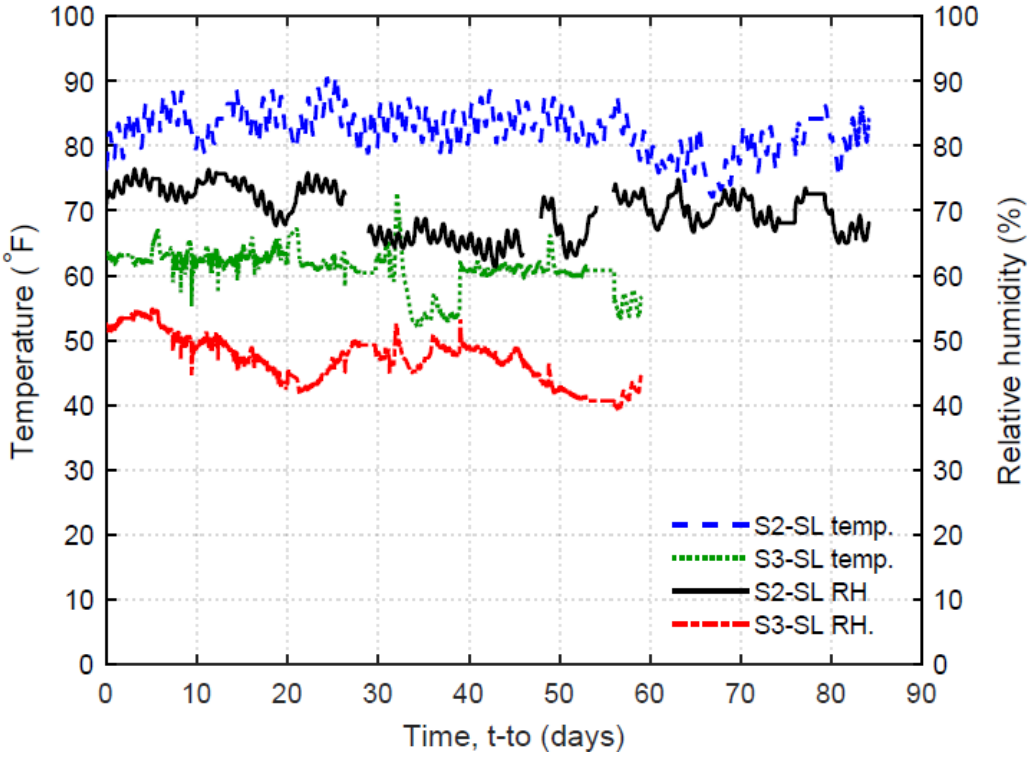

Figure 4-24. Temperature and RH of S2-SL and S3-SL.

4.9.2 Slabs (1%) Series I

In this slab series, four specimens were tested. One specimen (SC5) was tested under short-term loading serving as a controlled specimen, and three specimens (S6-SL, S7-SL, and S8-SL) were tested under sustained loading.

4.9.2.1 Initial Loading and Overall Response

Like slabs of 0.64% reinforcement ratio, the initial loading to the level of sustained load lasted for a time period of ~ 1 hour. Similar to slabs (0.64%), it was hard to establish

the sustained loading level that a specimen would be under based on the control specimen because of the inherent variability of concrete and the variation in slab covers. As a result, the level of the sustained load was selected when the deflection increased significantly after the addition of additional load.

Load vs. deflection curves of slab (1%) series I are exhibited Figure 4-25. The control specimen, SC5, was tested to failure at the age of 200 days in 58 minutes. The first crack took place at a load of 32.07 kN. The maximum total load was 116.02 kN (26081 lbs) at the average deflection of 7.36 mm (0.290 in.). The specimen failed shortly after the maximum total load took place at the total load of 115.43 kN (25949 lbs). The average deflection was 7.43 mm (0.292 in.). The thickness of the specimens at the slab column connection ranged between 91.28 mm (3.59 in.) and 93.37 mm (3.68 in.). The clear cover at the location of the first reinforcing bar out from the column varied from 9.14 mm (0.36 in.) to 19.56 mm (0.77 in.).

Slab 6 (S6-SL) was loaded up to the total sustained load of 89.85 kN (20200 lbs) in 54 minutes at the age of 281 days. This sustained load lasted for 45 days. The stiffness of S6-SL was softer than the stiffness of the control specimen (SC5). The first two cracks took place at the total loads of 27.16 kN and 30.55 kN. The increase in the average deflection after these cracks occurred was slight in comparison with the slabs (0.64%). Then, there were six additional loading stages. In each stage, the sustained load was increased by 2.67 kN (600 lbs), and the sustained load was kept for three days. The specimen failed under the sustained loading after 200 minutes of the last additional load at the total load of 105.47 kN (23710 lbs) when the average deflection was 9.45 mm (0.372 in.). The variations in the thickness of S6-SL were between 80.96 mm (3.19 in.) and 87.31

mm (3.44 in.). The clear cover was in the range of 16.26 mm (0.64 in.) to 23.88 mm (0.94 in.).

At the age of 345 days, slab 7 (S7-SL) was tested under the total sustained load of 94.30 kN (21200 lbs) for 45 days. The load was applied in 51 minutes. The stiffness of S7-SL was similar to the stiffness of S6-SL. The first concrete crack occurred at a total load of 29.75 kN. After the 45-day period of the sustained loading, there were eight additional loading stages. Like S6-SL, the increment in the sustained loading in each stage was 2.67 kN (600 lbs), and the specimen was under each of the additional stages for three days. The failure happened under the last stage of the sustained loads after 17 minutes at the total load of 115.67 kN (26003 lbs) at the average deflection of 9.72 mm (0.383 in.). The thickness of S7-SL ranged between 88.05 mm (3.47 in.) and 95.25 mm (3.75 in.), while the clear cover varied from 17.02 mm (0.67 in.) to 20.07 mm (0.79 in.).

The last specimen in slab (1%) series I, S8-SL, was loaded up the sustained load of 106.76 kN (24000 lbs) in 131 minutes at the age of 441 days. The sustained load lasted for 45 days. The stiffness of S8-SL was close to the stiffness of the control specimen (SC5). The first crack occurred at the total load of 53.06 kN. Six additional loading stages were applied to the specimen after the first stage. The increase in and duration of each stage were 2.67 kN (600 lbs) and three days, respectively. Due to mechanical failure (stripping of the threaded rod used to load the specimen), the test stopped while adding loading at the total load of 124.33 kN (27950 lbs) at the average deflection of 8.87 mm (0.349 in.). The thickness varied from 90.42 mm (3.56 in.) to 95.25 mm (3.75 in.). The variation in the clear cover was between 18.29 mm (0.72 in.) and 22.61 mm (0.89 in.).

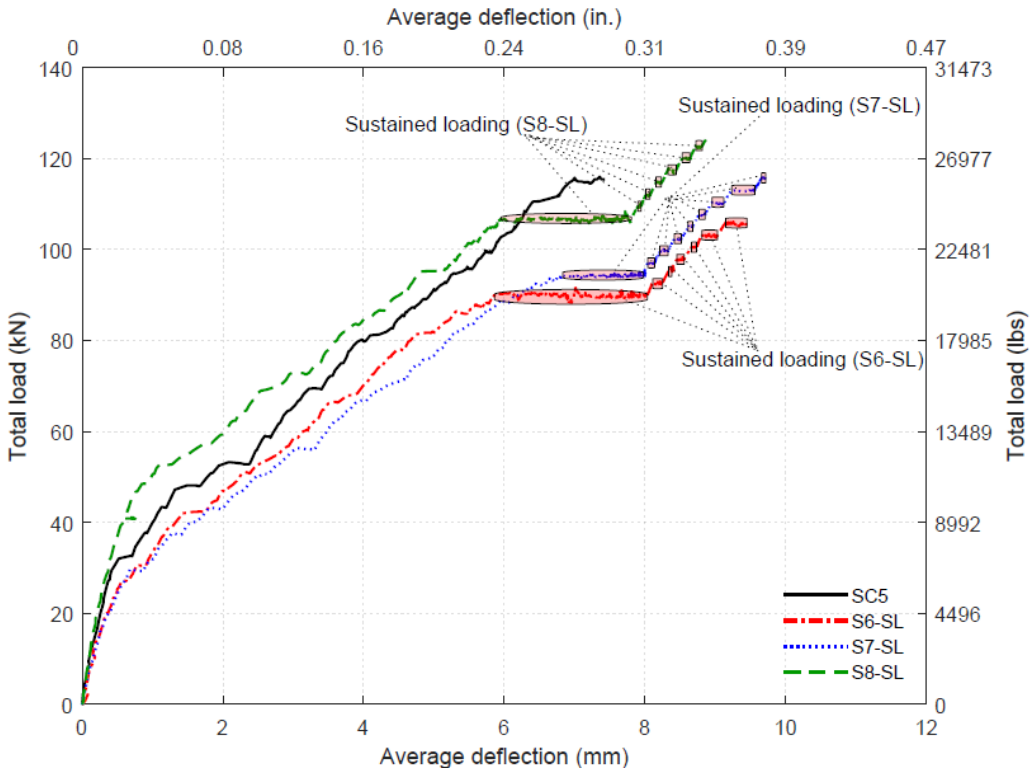

Figure 4-25. load vs deflection curves of slab (1%) series I.

The reinforcement strains of slab (1%) series I are shown in Figure 4-26. Strain gauge locations were exhibited in Figure 4-10. SG4, further away from the slab-column connection, had the lowest strain in all four slabs. Table 4-11 shows the failure strains of slab (1%) series I. In general, the reinforcement strains were less than the reinforcement strains of slabs (0.64%) as expected due to the higher reinforcement ratio. On average, S7-SL had the highest strains at the failure.

For the control specimen (SC5), SG1 yielded when the total load was 115.4 kN. The reinforcement strains of SG6 and SG8 were almost the same at the failure.

The highest reinforcement strain in S6-SL was the strain of SG6. It was the only reinforcement that yielded in S3-SL. SG1, SG2, and SG3 had the same strain at the failure.

The reinforcement strains of S7-SL were the highest in this slab series. The reinforcement strains of SG5 and SG8 at the failure were 0.0061 mm/mm (in./in.) and 0.0061 mm/mm (in./in.), respectively. The reinforcement of SG5 and SG8 yielded when the total load was 113 kN.

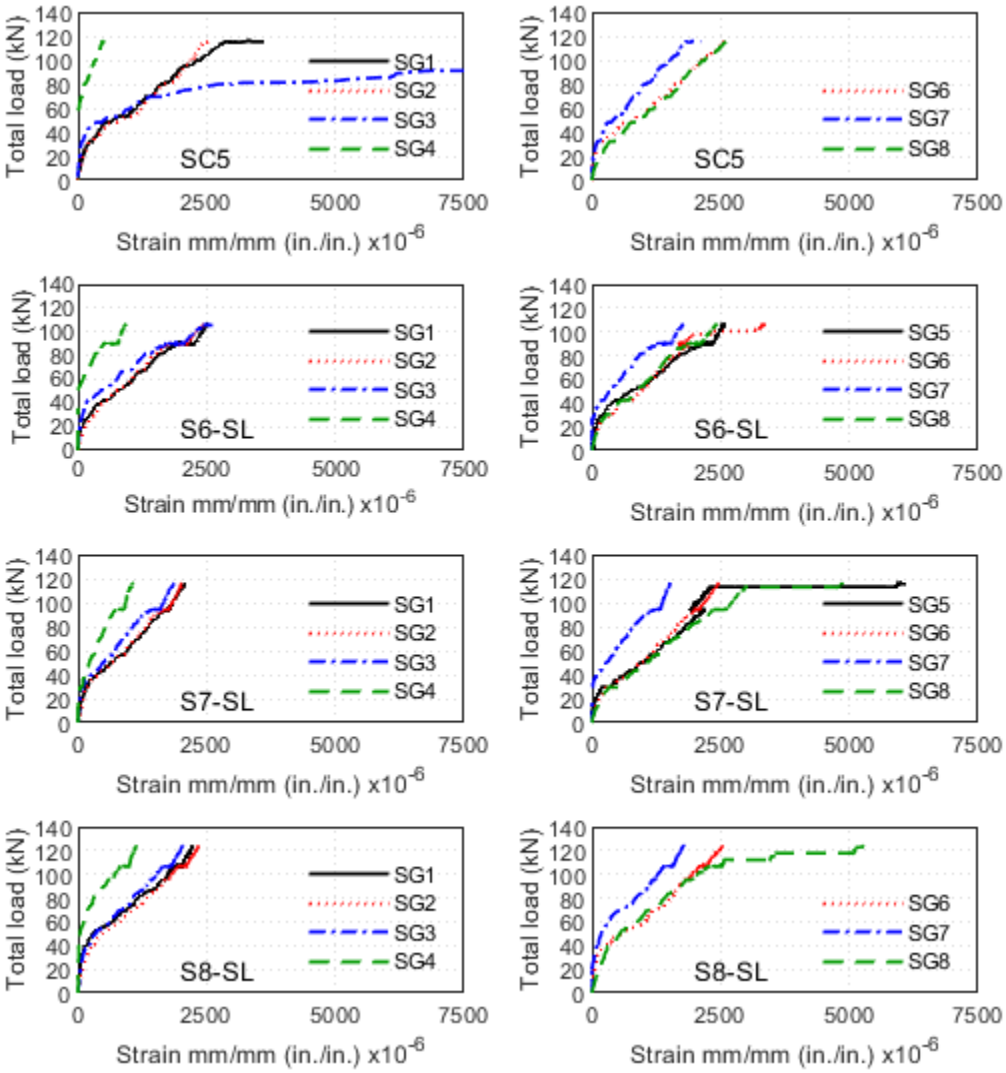

Figure 4-26. Reinforcement strain of slab (1%) series I.

For S8-SL, the reinforcement of SG8 was the only reinforcement yielding before the failure. At the mechanical failure, the strain of SG8 was 0.0052 mm/mm (in.in.). The

strains of the rest of the strain gauges were more minor than 0.0026 mm/mm (in./in.). Although the total load at the mechanical failure was the highest in this series, the strains were not the highest.

Table 4-11. Failure strains of slab (1%) series I.

	Failure strain mm/mm (in./in.)			
Strain gauge	SC5	S6-SL	S7-SL	S8-SL
SG1	0.0036	0.0025	0.0021	0.0022
SG2	0.0025	0.0025	0.0020	0.0023
SG3	0.0228	0.0026	0.0019	0.0020
SG4	0.0005	0.0009	0.0011	0.0011
SG5	NA	0.0026	0.0061	NA
SG6	0.0026	0.0034	0.0025	0.0026
SG7	0.0021	0.0018	0.0015	0.0018
SG8	0.0026	0.0024	0.0049	0.0053

Figure 4-27 shows the concrete strains of slab (1%) series I. Generally, concrete strains increased with the increase in the load during the initial loading. The magnitudes of the strains across the specimens differed because of the inherent variability of the concrete. The specimen of S6-SL had the lowest concrete strains due to poor consolidation.

For SC5, the concrete strain of Par_W was the highest at the failure. The concrete strain was 0.0014 mm/mm (in./in.). The concrete strain of Perp_S decreased when the total load exceeded 92.88 kN due radial tension strains. The same reduction took place in Perp_E when the total load exceeded 115.7 kN.

The concrete strains of S6-SL were very small even at the failure. Two reasons might cause that: poor consolidation and poor connection between the transducer and the

concrete. The highest strain at the failure took place in Par_N. The strain was 0.0001 mm/mm (in.in).

The concrete strain of Par_N was the highest strain in S7-SL at the failure. The strain failure of Par_N was less than the strain at the beginning of the first stage of the sustained loading because the concrete strain decreased under the sustained loading due to the redistribution of the stresses between reinforcement and concrete.

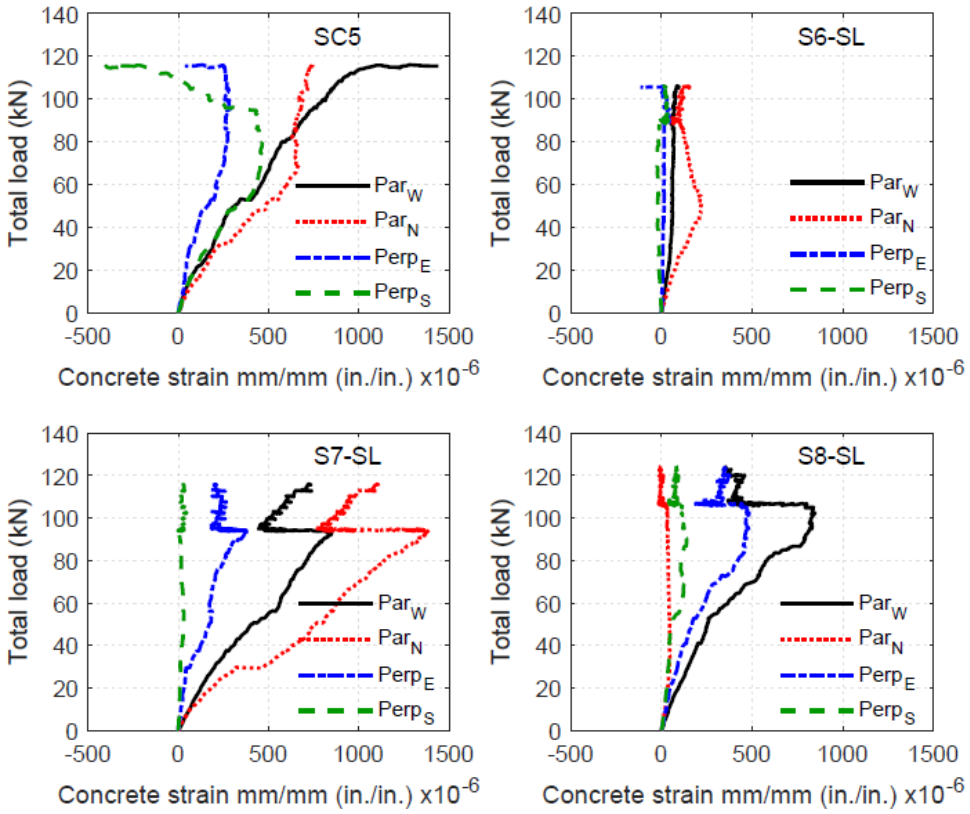

Figure 4-27. Concrete strains of slab (1%) series I.

For S8-SL, not like all specimens in this series, the concrete strain of Par_N was the lowest in the concrete specimen because the transducer was not attached firmly to the concrete. The strains of Par_W and Perp_E were close in the values at the mechanical failure.

4.9.2.2 First Stage of Sustained Loading

Figure 4-28 exhibits load and deflection vs. time curves of the first stage of the sustained loading for S6-SL, S7-SL, and S8-SL, which lasted 45 days. The sustained loads of the first stages of S6-SL, S7-SL, and S8-S were 89.85 kN (20200 lbs), 94.30 kN (21200 lbs), and 106.76 kN (24000 lbs). The increase in deflection and increase percentage of S6-SL, S7-SL, and S8-SL during the first stage of sustained loading are summarized in Table 4-12.

For S6-SL, the average deflection increased from 5.86 mm (0.231 in.) at the beginning of the first stage of the sustained loads to 8.03 mm (0.316 in.) at the end of the first stage. The ratio of the total increase in the average deflection under the first stage to the average instantaneous deflection was 0.37. Slightly above 45% of the total increase in the average deflection took place the first week. About 25% of the total increase in the average deflection occurred in the last 17 days.

The average deflection of S7-SL in the first stage of the sustained loading increased by 1.15 mm (0.045 in.), which was 0.17 times the average instantaneous deflection at the beginning of the first stage. The increase percent in average deflection of the total increase on the first week was close to 56%. Less than 6% of the total increase in the average deflection took place after the first 28 days.

At the beginning of the first stage of the sustained loads of S8-SL, the average deflection was 5.95 mm (0.234 in.) and then increased 7.81 mm (0.308 in.) at the end of the stage. The ratio of the total increase in the average deflection to the average instantaneous deflection was 0.31. About 30% of the total increase in the average deflection

happened in the first week of the sustained loading. The increase percent in average deflection of the total increase on the last 17 days was ~16%.

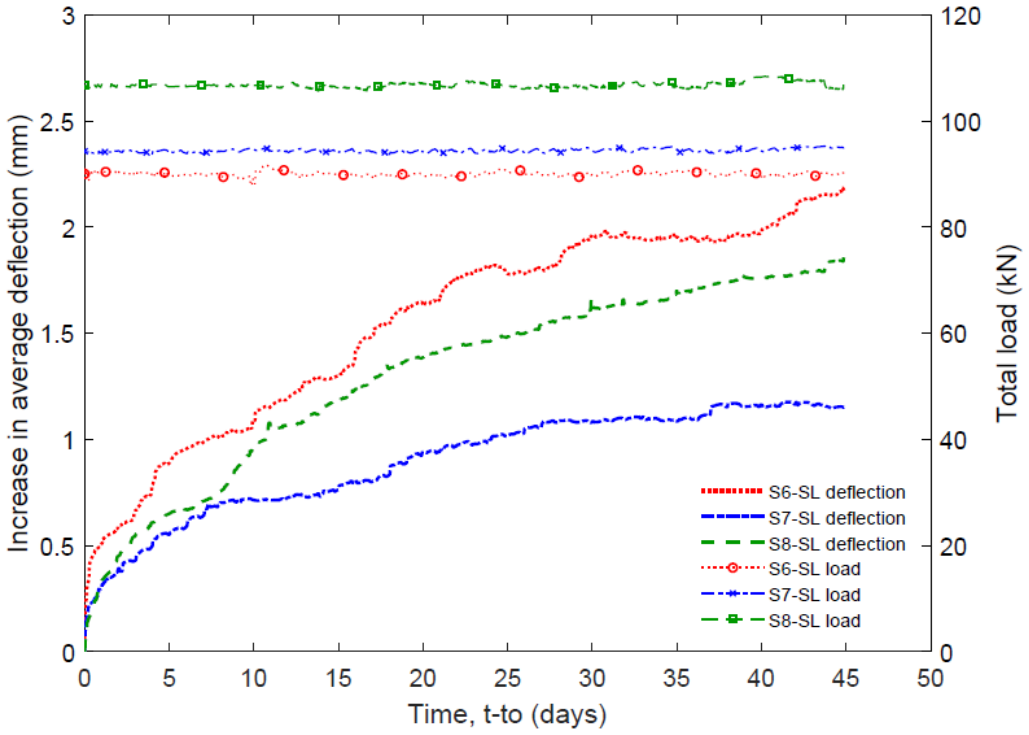

Figure 4-28. Load and deflection vs. time curves of 1st stage of SL loading (S6-SL, S7-SL, and S8-SL).

As shown in Table 4-12. , the total increase in the average deflection of S6-SL under the first stage of the sustained loads was the highest in this slab series. The percent increases in the average deflection of S6-SL and S8-SL were almost the same on the third and the fourth weeks. S7-SL had the highest percent increase in the average deflection of the total increase for the same duration, as seen in Table 4-12. The ratios of increases in the average deflection to the average instantaneous deflection of S6-SL, S7-SL, and S8-SL were 0.37, 0.17, and 0.31, respectively. The ratios of the sustained loads of the first stage of S6-SL, S7-SL, and S8-SL to the maximum load were 0.85, 0.81, and 0.86, respectively. The specimen of S8-SL reached the total load of 124.33 kN (27950 lbs) then mechanical failure

took place. Therefore, the load intensity could be less than 0.86. Based on the load intensity and the deflection ratios, the increases in deflections seemed reasonable compared to the load intensity. Also, the consolidation of B6-SL was not good, which led to higher deflection.

Table 4-12. Increase in average deflection and percentage during 1st stage (S6-SL, S7-SL, and S8-SL.)

	S6-SL		S7-SL		S8-SL	
Time (days)	Increase in deflection mm (in.)	Increase percentage (%)	Increase in deflection mm (in.)	Increase percentage (%)	Increase in deflection mm (in.)	Increase percentage (%)
1	0.51 (0.020)	23.38	0.30 (0.012)	25.90	0.33 (0.013)	17.80
3	0.67 (0.026)	30.74	0.43 (0.017)	37.34	0.55 (0.022)	29.51
7	0.99 (0.039)	45.38	0.64 (0.025)	55.65	0.71 (0.028)	38.09
21	1.66 (0.065)	76.52	0.95 (0.037)	82.46	1.42 (0.056)	76.22
28	1.83 (0.072)	84.25	1.09 (0.043)	94.47	1.57 (0.062)	84.29
45	2.17 (0.086)	100	1.15 (0.045)	100	1.86 (0.073)	100

Figure 4-29 shows the increases in reinforcement strains of S6-SL, S7-SL, and S8-SL under the first stage of the sustained loads. Table 4-13 exhibits the increases in reinforcement strain and the percentage of increase to instantaneous strain during the first stage of the sustained loading. The increases in reinforcement strain were small in comparison to the increase in strain in slabs (0.64%). Unlike the ρ=0.64% slabs, there was no reinforcement yielding under the first stage of the sustained loading.

For S6-SL, the increases in reinforcement strains of strain gauges, attached to the topmost layer of tension reinforcement, were higher the reinforcement strains of strain gauges mounted the lower layer of tension reinforcement with exception to the strain of SG4, as Figure 4-29 shows. The highest increase in the reinforcement strain took place in

SG1. The reinforcement strain of SG6 decreased under the first stage of sustained loading. It might be because it was very close to the column. The highest percent of the total increase in strain under the first stage to the instantaneous strain occurred in SG4, which increased by 59.69%.

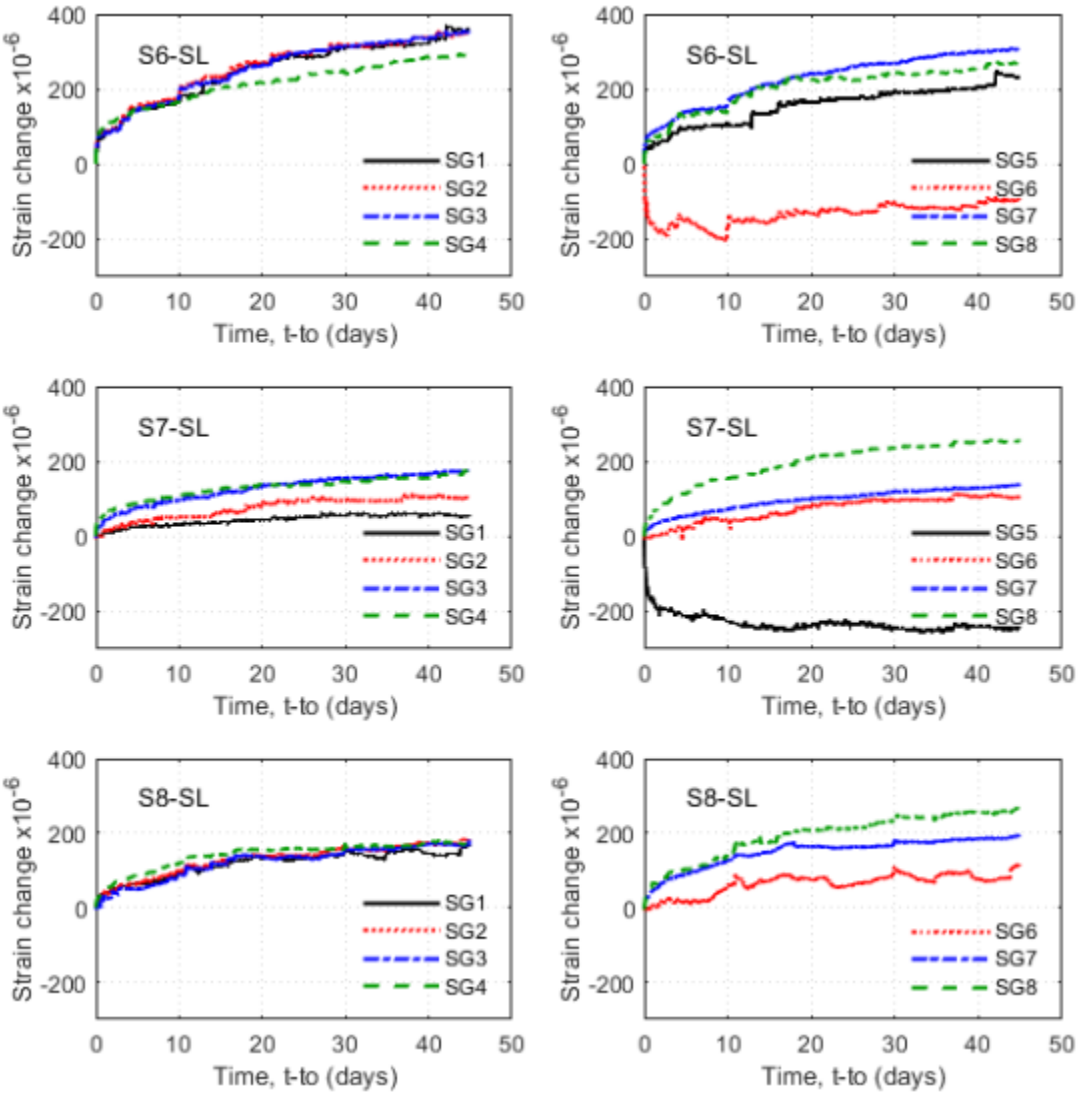

Figure 4-29. Increases in reinforcement strains under 1st sustained loading (S6-SL, S7-SL, and S8-SL).

All the reinforcement strains in S7-SL increased except the reinforcement strain of SG5, which decreased under the first stage of the sustained loads. The highest increase in

the reinforcement strain happened in SG8, which increased by 0.00026 mm/mm (in./in.). Similar to S6-SL, the highest increased percent to instantaneous strain took place in SG4, which increased by 25.15%.

For S8-SL, all reinforcement strains increase in the first stage of the sustained loads. The reinforcement strain of SG6 fluctuated under the first stage sustained loads, but it increased in general at the end. Like S7-SL, the reinforcement strain of SG8 was the highest. SG4 had the highest increase percent, similar to S6-SL and S7-SL.

Table 4-13. Increase in strain during of 1st of SL (S6-SL, S7-SL, and S8-SL).

		SG1	SG2	SG3	SG4	SG5	SG6	SG7	SG8
S6-SL	Change in strain	0.00036	0.00035	0.00035	0.00029	0.00023	-0.00009	0.00031	0.00027
	Change percentage of instantaneous strain (%)	18.84	19.71	20.73	59.69	10.97	-5.04	25.06	14.33
S7-SL	Change in strain	0.00005	0.00010	0.00018	0.00018	-0.00024	0.00010	0.00014	0.00026
	Change percentage of instantaneous strain (%)	3.09	6.22	12.36	24.15	-11.31	5.24	11.51	10.80
S8-SL	Change in strain	0.00017	0.00018	0.00018	0.00017		0.00012	0.00020	0.00028
	Change percentage of instantaneous strain (%)	9.08	9.55	11.05	21.05		5.73	14.11	12.26

Generally, reinforcement strains increased under the first stage of the sustained loading with the exception to SG6 in S6-SL and SG5 in S7-SL. These increases in strains were due to redistribution is stresses between concrete and reinforcement. The highest increase percent in strain to instantaneous strain took place in SG4 because the instantaneous strain of the initial loading stage was the smallest. In addition, SG4 was the gage located furthest from the column. The greater increase in this gauge indicates that the

stresses applied during the initial loading were being distributed further out in the specimen during the sustained loading. On average, S6-SL had the highest increase percent, and S7-SL had the lowest increase percent in the first stage of the sustained loads.

Table 4-14 exhibits the increase percent of S6-SL, S7-SL, and S8-SL under the first stage of the sustained loads. For a percentage over 100%, it means strain did not increase gradually. It fluctuated during the sustained loading. Similar to the average deflection of S7-SL, the highest increase percent in the strain on the 28th day was in S7-SL. In general, over 70% of the increase percent in strain happened in the first four weeks.

Table 4-14. Increase percent under 1st stage (S6-SL, S7-SL, and S8-SL).

	S6-SL							
Time (days)	SG1	SG2	SG3	SG4	SG5	SG6	SG7	SG8
1	20.37	24.70	22.04	32.39	19.71		27.40	24.86
3	29.37	34.20	31.83	41.15	30.72		35.32	35.82
7	40.99	47.02	44.07	52.55	43.14		47.54	50.88
21	74.23	79.83	76.69	74.54	73.57		78.07	85.08
28	81.16	88.30	85.70	83.06	78.18		86.55	87.35
45	100	100	100	100	100		100	100
	S7-SL							
	SG1	SG2	SG3	SG4	SG5	SG6	SG7	SG8
1	10.74	10.83	23.48	33.42	71.13	0.83	21.50	23.54
3	32.78	24.11	33.62	43.85	80.84	11.57	31.92	36.03
7	51.44	33.83	43.85	53.60	85.70	35.22	44.00	54.08
21	89.21	85.00	77.18	77.28	91.35	80.86	74.37	83.73
28	112.33	97.50	87.31	77.96	95.67	93.76	82.25	91.94
45	100	100	100	100	100	100	100	100
	S8-SL							
	SG1	SG2	SG3	SG4	SG5	SG6	SG7	SG8
1	24.33	23.46	17.49	26.67		4.91	23.84	23.88
3	32.46	32.98	27.37	41.27		21.89	40.02	34.19
7	41.69	42.85	33.81	55.30		18.47	53.61	41.00
21	80.81	75.64	73.33	89.10		65.53	83.82	75.44
28	82.66	84.00	77.81	90.80		65.67	84.09	82.00
45	100	100	100	100		100	100	100

The changes in concrete strains of S6-SL, S7-SL, and S8-SL during the first stage of the sustained loads are shown in Figure 4-30. In general, concrete strains decreased during the first stage due to the concrete creep. Decreases in strains of Par_N and Par_W were the highest because they were close to the column except for the strain of Par_N in S8-SL. The strain of Par_N in S8-SL was small since the strain transducer was not attached firmly to concrete due to the difference in the level of the slab at the two points that the edges of the transducer were attached to.

The lowest changes in concrete strains in slab (1%) series I during the first stage of the sustained loading happened in S6-SL. Poor consolidation could be the reason for these slight changes in strains. The decreases in concrete strains of Par_N and Par_W and the increase in the concrete strain of Perp_S were high in the first several hours; then, they leveled off. The highest decrease in concrete strain in S6-SL took place in Par_N. The concrete strain of Par_N decreased by 0.00003 mm/mm (in./in.) at the end of the first stage. The concrete strain of Perp_S increased by 0.00004 mm/mm (in./in.) at the end of the first stage.

The specimen of S7-SL had the greatest changes in concrete strains during the first stage of the sustained loading. The concrete strain of Par_W had the highest decrease on the first day. After the 10^{th} day, the concrete strain of Par_N decreased steeply. The decrease in the concrete strain of Par_N was 0.0006 mm/mm (in./in.) at the end of the first stage of the sustained loading. The concrete strain of Perp_S increased by 0.00002 mm/mm (in./in.) at the end of the first stage.

For S8-SL, the concrete strains of Par_W and Perp_E decreased until the 8^{th} day; after that, they fluctuated with time. The concrete strain of Par_W decreased by 0.00037

mm/mm (in./in.) at the end of the first stage of the sustained loading. The concrete strains of Par_N and Perp_S were reduced by 0.000025 mm/mm (in./in.) at the end of the first stage of the sustained loading.

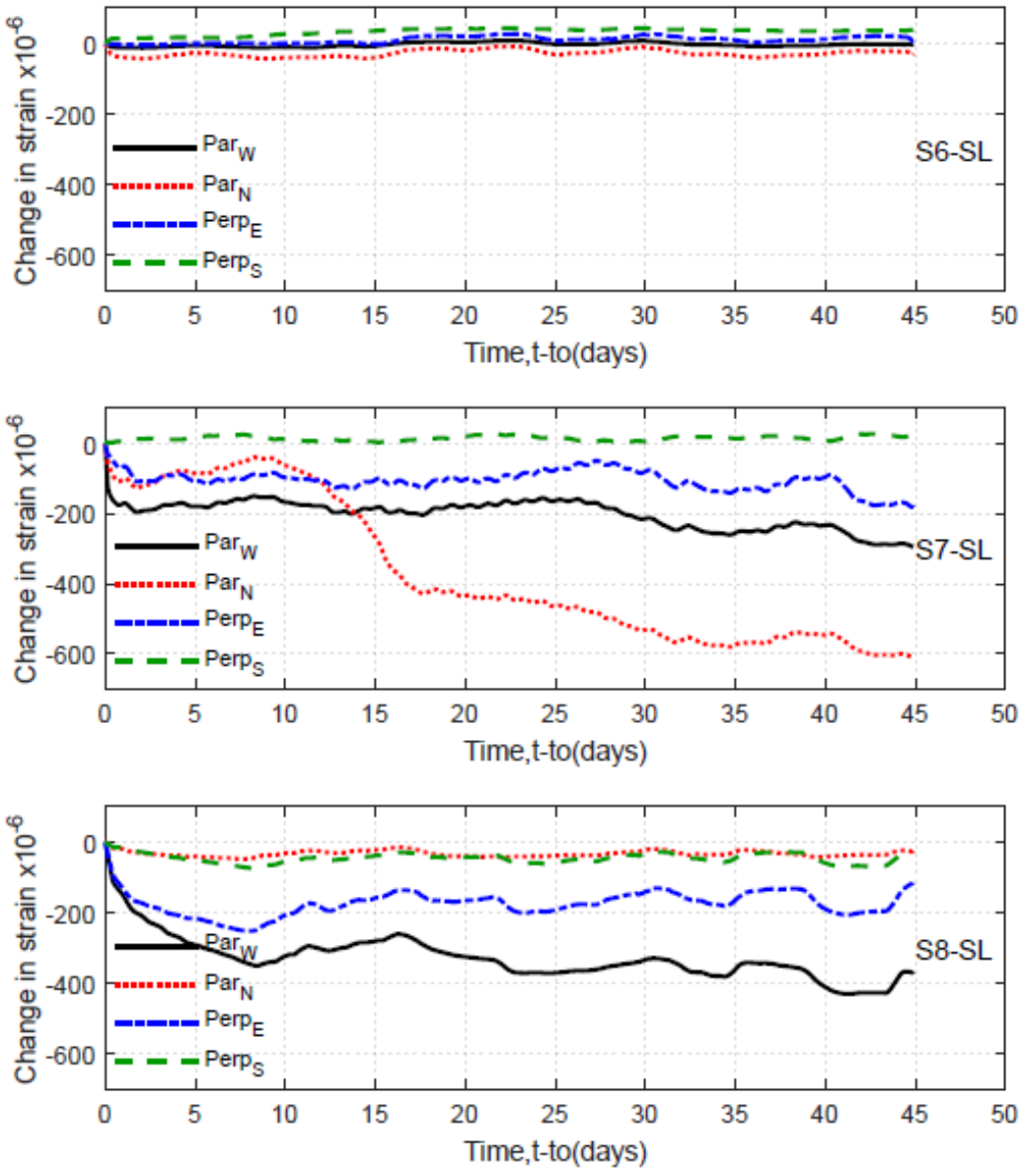

Figure 4-30. Changes in concrete strains under 1st sustained loading (S6-SL, S7-SL, and S8-SL).

4.9.2.3 Additional Loading Stages

For all specimens tested under sustained loading, the duration of the first stage of the sustained loads was 45 days. After that, specimens were subjected to additional sustained loads for about ~3 days with the additional load in each stage of 2.69 kN (600 lbs). Table 4-15 summarizes the durations, load intensities, and increase in average deflections of S6-SL, S7-SL, and S8-SL, for all stages. Failure under additional sustained loads took place in S6-SL and S7-SL after 200 minutes and 17 minutes. Load intensity is the ratio of a sustained load to the maximum load.

For S6-SL, there were six additional stages of sustained loading. The sustained load of the last stage, where the specimen failed under the sustained load, was 105.87 kN (23800 lbs). Even though the specimen failed after 200 minutes of the last additional sustained load, the increase in deflection in this was the highest among additional stages of sustained loads. The average deflection increased by 0.30 mm (0.012 in.) during the last stage. The load intensity of the 6^{th} stage, the stage that took place before the last stage, was 0.97. Therefore, the specimen was under the load intensity of 0.97 for about three days and it did not occur.

Nine additional stages of sustained loading took place in S7-SL. The sustained load of the last stage was 115.65 kN (26000 lbs). The failure happened after 17 minutes of the sustained loading, and the increase in the average deflection was 0.06 mm (0.002 in.). The highest increase in deflection under the additional stages occurred in the 8^{th} stage, where the deflection increased by 0.33 mm (0.013 in.). The load intensity was 0.98. It seemed like if the duration of the sustained load had increased, the specimen might have failed under this sustained load.

There were 6th additional stages of the sustained load. The mechanical failure took place after the 7th stage while adding additional loads. The highest increase in deflection was in the 5th stage, where the average deflection increased by 0.12 mm (0.005 in.). The load intensity of the 7th stage was 0.99. However, the peak load is higher than 124.33 kN (27950 lbs).

Table 4-15. Increase in average deflection under sustained loads (S6-SL, S7-SL, and S8-SL).

	S6-SL			S7-SL			S8-SL		
Stage	Duration (days)	Load intensity	Deflection mm (in.)	Duration (days)	Load intensity	Deflection mm (in.)	Duration (days)	Load intensity	Deflection mm (in.)
1	44.86	0.85	2.17 (0.086)	44.87	0.82	1.15 (0.045)	44.85	0.86	1.86 (0.073)
2	3.03	0.87	0.14 (0.005)	3.01	0.84	0.10 (0.004)	2.99	0.88	0.05 (0.002)
3	2.92	0.90	0.04 (0.002)	3.00	0.86	0.12 (0.005)	3.01	0.90	0.06 (0.002)
4	3.06	0.92	0.11 (0.004)	3.12	0.88	0.10 (0.004)	3.00	0.92	0.08 (0.003)
5	3.00	0.95	0.08 (0.003)	2.83	0.91	0.07 (0.003)	3.00	0.94	0.12 (0.005)
6	2.98	0.97	0.22 (0.009)	2.97	0.93	0.09 (0.003)	3.02	0.97	0.11 (0.004)
7	0.14	1	0.30 (0.012)	3.02	0.95	0.17 (0.007)	2.93	0.99	0.09 (0.004)
8				3.00	0.98	0.33 (0.013)			
9				0.01	1	0.06 (0.002)			

The changes in reinforcement strains under all stages of the sustained loads for S6-SL, S7-SL, and S7-SL are summarized in Table 4-16. In general, reinforcement strains fluctuated during the additional stages, but most of the reinforcement strains increased.

For S6-SL, all reinforcement strains increased in the 2nd and 6th stages of the sustained loads. The reinforcement strain of SG6 had the highest increase in strain under the additional stages. The reinforcement strain of SG6 increased by 0.0008 mm/mm (in./in.) in the 5th stage of the sustained loading. Also, on average, the highest increase in reinforcement strain occurred in the 5th stage.

Table 4-16. Changes in reinforcement strains under sustained loads (S6-SL, S7-SL, and S8-SL).

		S6-SL							
Stage	Time (days)	SG1	SG2	SG3	SG4	SG5	SG6	SG7	SG8
1	44.86	0.00036	0.00035	0.00035	0.00029	0.00023	-0.00009	0.00031	0.00027
2	3.03	0.00001	0.00001	0.00003	0.00001	0.00000	0.00003	0.00003	0.00001
3	2.92	0.00001	0.00000	0.00003	0.00002	-0.00003	0.00003	0.00003	0.00000
4	3.06	0.00002	0.00003	0.00003	0.00002	-0.00001	0.00034	0.00003	0.00003
5	3.00	0.00002	-0.00001	0.00003	0.00003	0.00000	0.00080	0.00002	0.00000
6	2.98	0.00002	0.00005	0.00006	0.00003	0.00001	0.00007	0.00007	0.00004
7	0.14	0.00000	0.00004	0.00016	0.00002	0.00002	0.00001	0.00004	-0.00003
		S7-SL							
	Time (days)	SG1	SG2	SG3	SG4	SG5	SG6	SG7	SG8
1	44.87	0.00005	0.00010	0.00018	0.00018	-0.00024	0.00010	0.00014	0.00026
2	3.01	0.00001	0.00002	0.00002	-0.00001	0.00003	0.00002	0.00000	0.00003
3	3.00	0.00002	0.00000	0.00001	0.00001	-0.00004	0.00002	0.00001	0.00003
4	3.12	0.00001	0.00000	0.00002	0.00001	0.00001	0.00002	0.00001	0.00001
5	2.83	0.00002	0.00000	0.00001	0.00001	-0.00003	0.00001	0.00002	0.00001
6	2.97	0.00001	0.00001	0.00001	0.00001	0.00005	0.00000	0.00002	0.00002
7	3.02	0.00001	0.00001	0.00002	0.00001	-0.00001	0.00000	0.00002	0.00005
8	3.00	0.00003	-0.00002	0.00003	0.00003	0.00363	0.00000	0.00002	0.00183
9	0.01	0.00001	-0.00001	0.00000	0.00001	0.00007	0.00001	-0.00001	0.00002
		S8-SL							
	Time (days)	SG1	SG2	SG3	SG4	SG5	SG6	SG7	SG8
1	44.85	0.00017	0.00018	0.00018	0.00017		0.00012	0.00020	0.00028
2	2.99	-0.00001	0.00000	0.00000	0.00001		-0.00001	0.00001	-0.00001
3	3.01	0.00000	0.00001	0.00001	0.00000		0.00000	0.00001	0.00087
4	3.00	0.00002	0.00001	0.00002	0.00002		0.00002	0.00002	0.00004
5	3.00	0.00003	0.00003	0.00003	0.00001		0.00003	0.00002	0.00151
6	3.02	0.00000	-0.00001	0.00000	0.00002		0.00002	0.00002	-0.00003
7	2.93	0.00001	0.00002	0.00001	0.00001		0.00002	0.00001	0.00011

All reinforcement strains of S7-SL increased during the 4th and 6th stages of the sustained loading. SG5 had the highest increased in strain by 0.0036 mm/mm (in./in.) in the 8th stage of the sustained load. Moreover, the 8th stage had the highest increase in strain on average.

All reinforcement strains in the 3rd, 4th, 5th, and 7th stages of the sustained loads increased in S8-SL. The reinforcement strain of SG8 increased by 0.0015 mm/mm (in./in.) in the 5th stage, which was the highest increase in strain during the additional stages. Also, the highest increase in reinforcement strains on average took place during the 5th stage.

4.9.2.4 Failure Under Sustained Loading

Figure 4-31 shows the increase in the average deflections of S6-SL and S7-SL during the last stages where the failure under the additional stage of sustained loading took place. The tertiary stage leading to failure, as shown by rapidly increasing displacements, only lasted for about two minutes for both specimens. The tertiary phase restricts the ability to warn and evacuate a structure before collapse since it happened in about two minutes.

The failure of S6-SL occurred after 200 minutes of the last stage of the sustained loading. The average deflection increased gradually when the time exceeded 150 minutes, and it kept increasing until the tertiary stage happened about two minutes before the failure. What happened before the failure was that the load was adjusted at the time of 149 minutes; then, the east and north deflections increased gradually with almost the same amount of deflection. Two minutes before failure, the tertiary stage took place just in the east and north deflections. The increases in the east and north deflections during the last stage were between 3.37 times and 4.31 times of the increases in west and south deflections.

For S7-SL, the failure happened about 17 minutes after adding the last additional load. Warning of failure took place just two minutes before failure. The increase in deflections was slight before the last two minutes. The increase in deflection during the last stage happened at the load adjustment. The highest increases in deflection before the failure were in the east and south deflections. Two minutes before the failure, the load of the south side decreased very rapidly, and the south deflection increase quickly. After that, the west deflection increased rapidly, leading to the failure specimen. The tertiary stage happened on all sides except the north side.

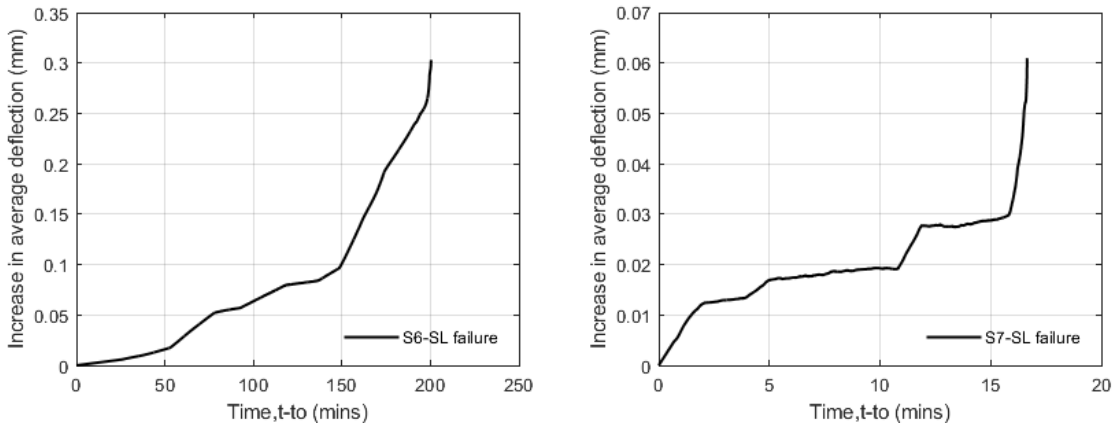

Figure 4-31. Increase in average deflection of S6-SL and S7-SL in the last stage of SL.

The changes in the reinforcement strains of S6-SL and S7-SL during the last stages of the sustained loads are exhibited in Figure 4-32. Similar to deflection, the tertiary stage took place very quickly, just before failure.

Overall, the changes in reinforcement strains of S3-SL were slight except for the reinforcement strain of SG3, which could be an indicator of failure. The reinforcement strain of SG3 kept increasing for the beginning of the last stage of the sustained loading; then tertiary stage occurred in about two minutes. The changes in the reinforcement strains

of SG1, SG2, and SG5 were insignificant even at the failure. The strain of SG8 decreased in the tertiary stage, while the strains of SG5, and SG6, and SG7 increased.

For S7-SL, the reinforcement strains changed slightly in the last stage, especially for strain gauges attached to the top layer of the tension reinforcement. The reinforcement strain of SG5 decreased first; then, it increased with time when time exceeded 11 minutes. Just before the failure, the reinforcement strains of SG4 and SG5 increased rapidly. The rest of the strain gauges seemed not affected in the tertiary stage.

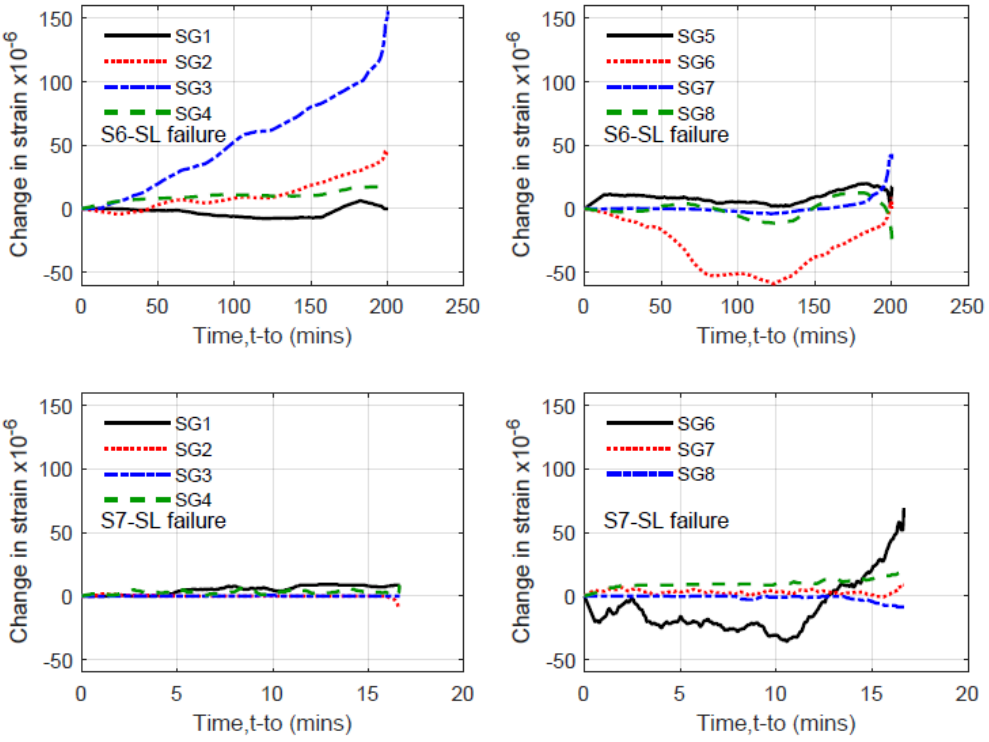

Figure 4-32. Changes in reinforcement strain of S6-SL and S7-SL in last stages of SL.

4.9.2.5 Failure Rotation

Table 4-17 shows failure rotations of the slab (1%) series I. The average rotation was calculated based on the average deflection at 533 mm (21 in.) of the face of the column at the failure, while the maximum rotation was determined based on the maximum

deflection of the four sides at 533 mm (21 in.) of the face of the column. The control specimen had the lowest average and maximum rotations at the failure. Therefore, sustained loading increased the rotation. S6-SL and S7-SL had an average rotation of 0.018 at the failure, and S8-SL had an average rotation of 0.017. The maximum rotation at failure varied from 0.016 to 0.024. The specimen of S8-SL had the thickest thickness in this series, and as expected, it had the lowest rotation at failure among the specimens tested under sustained loading.

Table 4-17. Failure rotation of slab (1%) series I.

	Average rotation	Maximum rotation
SC5	0.014	0.016
S6-SL	0.018	0.022
S7-SL	0.018	0.024
S8-SL	0.017	0.019

4.9.2.6 Temperature and Humidity

The fluctuations in temperature and relative humidity during the sustained loading of S6-SL, S7-SL, and S8-SL are shown in Figure 4-33. The temperature of S6-SL varied from 68 ˚F to 90˚F, while the range relative humidity was between 64% and 79%. For S7-SL, the temperature ranged between 62 ˚F to 90 ˚F, and the relative humidity varied from 58% to 78%. Temperature and relative humidity of S8-SL were not recorded during the entire test. The variation in temperature in the first 20 days was between 57 ˚F to 72 ˚F, and the range of the relative humidity was between 51% and 64%.

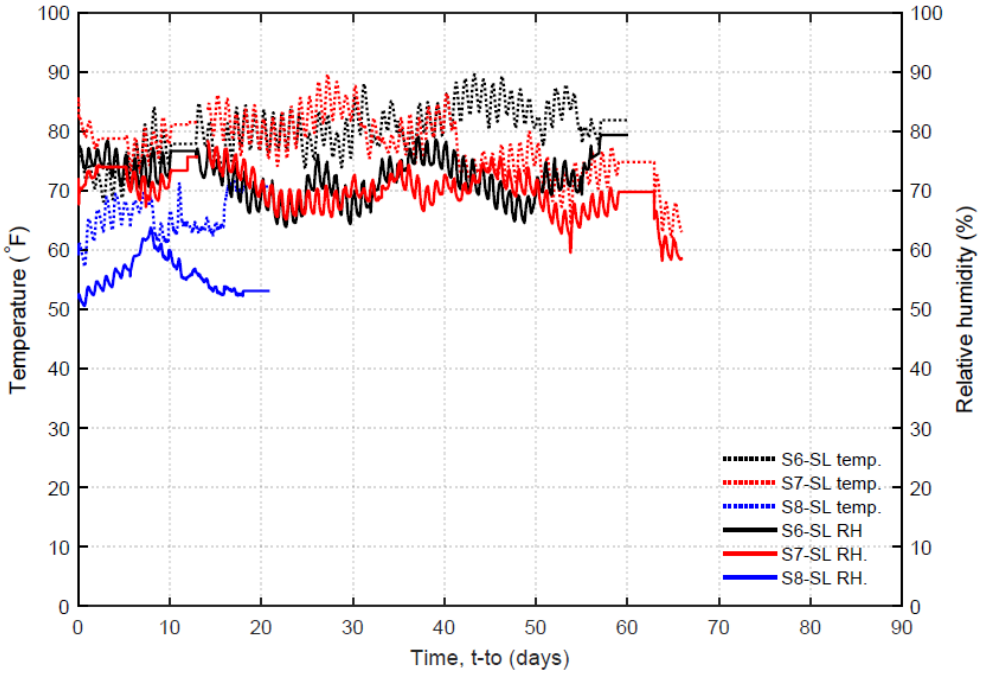

Figure 4-33. Temperature and RH of S6-SL, S7-SL, and S8-SL.

4.9.3 Slabs (1%) Series II

Two specimens were tested under sustained loading in the slab (1%) series II. The thickness and clear cover were controlled in this series, which led to more consistency in the strength. Also, the locations of the strained gauges were different from the locations of the ones in series I.

4.9.3.1 Initial Loading and Overall Response

Load vs. deflections curves of the slab (1%) series II are shown in Figure 4-34. Sustained loading was applied in a short time of ~ 1 hour. The slab covers were controlled by a plywood sheet placed above the slab during pouring. The control of the slab cover helped to reduce the variability in strength seen in the earlier tests.

Slab 9 (S9-SL) was tested at the age of 197 days under the sustained load of 103.64 kN (23300 lbs) in 66 minutes. The first crack occurred when the total load was 26.77 kN.

The specimen failed after 21 minutes at the total load of 103.41 kN (23248 lbs) at the average deflection of 6.88 mm (0.271 in.). The thickness and the clear cover were 88.9 mm (3.5 in.) and 6.35 mm (0.25 in.), respectively.

The second specimen in this series, S10-SL, was loaded up to the sustained load of 97.15 kN (21840 lbs) in 57 minutes at the age of 203 days. The sustained load lasted for 30 days. Then, the sustained load was increased by 1.78 kN (400 lbs). The first concrete crack took place at a total load of 32.84 kN. The failure took place under the sustained load after 67 hours. The total load at the failure was 98.73 kN (22195 lbs) at the average deflection of 7.78 mm (0.306 in.). Like S9-SL, the thickness was 88.9 mm (3.5 in.), and the clear cover was 6.35 mm (0.25 in.).

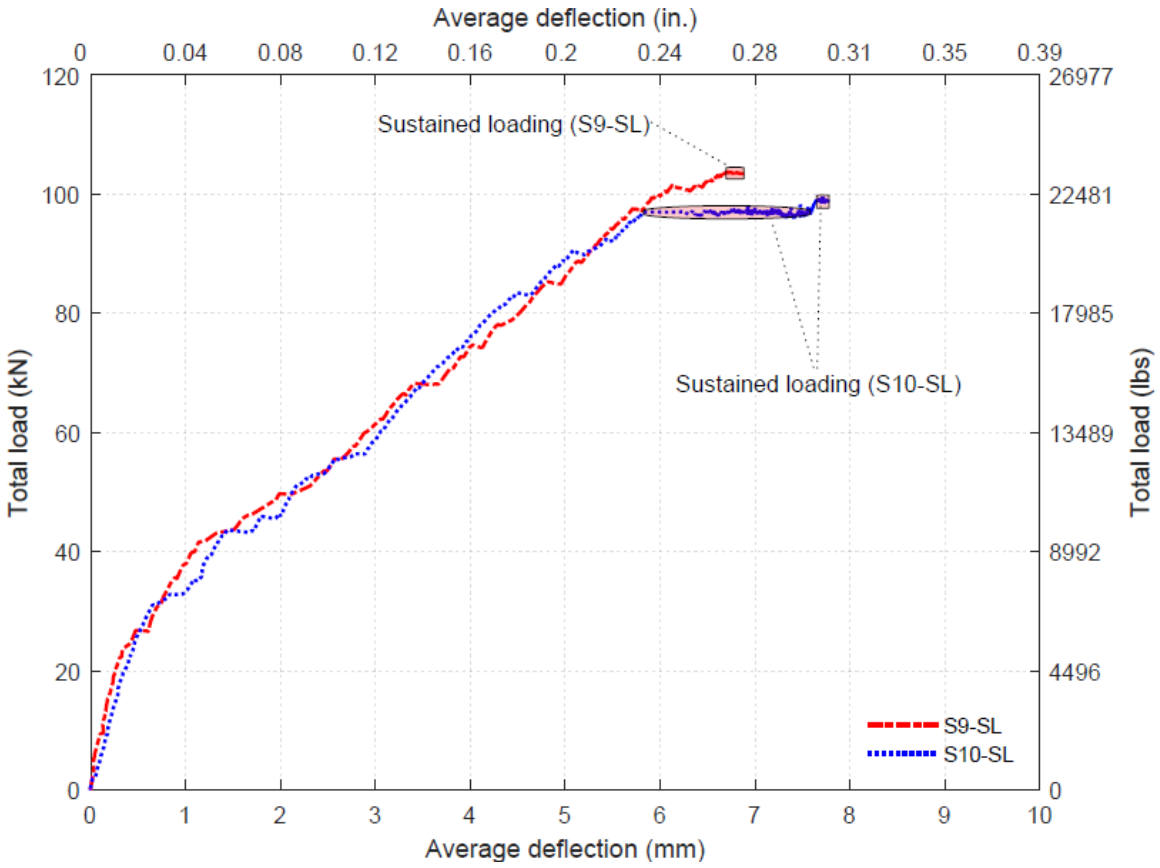

Figure 4-34. Load vs deflection curves of slab (1%) series II.

Figure 4-35 shows the reinforcement strains of the slab (1%) series II. Some strain gauges were damage in this series. The reinforcement strain of SG3 was the lowest because it was located further away from the slab-column connection. No reinforcement strain exceeded 0.0025 mm/mm (in./in.) because the total load was not high at failure. The failure strains are exhibited in Table 4-18. On average, the reinforcement strains of S9-SL were higher than the reinforcement strains of S10-SL. One reason could be that the load reached in S9-SL was higher than that in S10-SL. Another reason was that some of the reinforcement strains of S10-SL decreased when the total load approached the failure load.

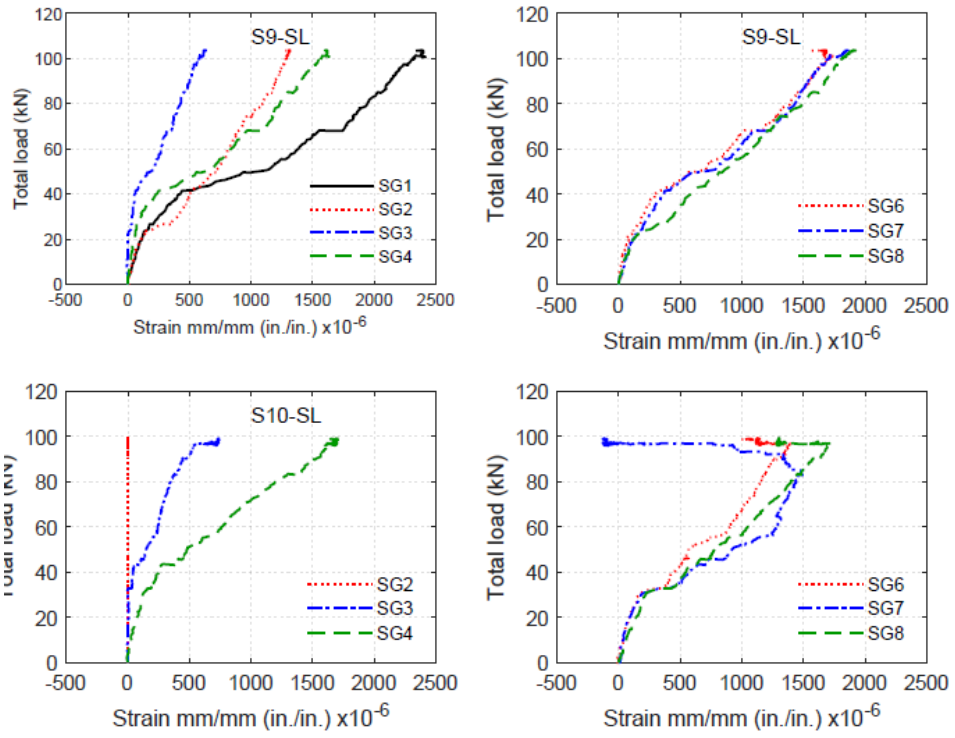

Figure 4-35. Reinforcement strain of slab (1%) series II.

For S9-SL, the reinforcement strain of SG3 was the lowest because of its locations, while the reinforcement strain of SG1 was the highest. The reinforcement strain of SG1 was 0.0023 mm/mm (in./in.) at the failure. SG6 and SG7 were located at the same distance

of the slab-column connection, but they were in opposite sides. Therefore, they almost had the same strain until the total load was close to the failure load.

Some of the reinforcement strains of S10-SL decreased when the total load was high. Like S9-SL, SG3 had the lowest reinforcement strain. SG2 seemed damaged since its value was zero during the test. The highest reinforcement strain at failure took place in SG4. The reinforcement strain of SG7 was negative at the failure, although it was 0.0015 mm/mm (in./in.) when the total load was 83.03 kN before it decreased with the increase of the load.

Table 4-18. Failure strains of slab (1%) series II.

	Failure strain mm/mm (in./in.)	
Strain gauge	S9-SL	S10-SL
SG1	0.0023	NA
SG2	0.0013	NA
SG3	0.0006	0.0007
SG4	0.0016	0.0016
SG5	NA	NA
SG6	0.0015	0.0010
SG7	0.0019	-0.0001
SG8	0.0019	0.0013

Load vs. concrete strain curves are shown in Figure 4-36. The concrete strain of Par_W was the highest in both specimens. The concrete strain of Perp_E increased at first with an increase in the load. Then, it decreased with the increase in the load.

For S9-SL, the specimen failed under the first stage of the sustained loading. The failure occurred due to the increase in the east deflection. What the figure shows is that the considerable increase in the east deflection caused the concrete strain of Perp_E to decrease, while the concrete strain of Par_W increased. These decrease and increase in the

concrete strains of Perp_E and Par_W became sharper when the specimen was near to failure. In the tertiary stage, all strains increased, but it is difficult to see it in the is figure. The concrete strain of Par_W was 0.0014 mm/mm at the failure.

Similar to S9-SL, the failure of S10-SL happened because of the increase in the east deflection. Therefore, all concrete strains behaved similarly to the concrete strains of S9-SL. The concrete strain of Perp_E increased then decreased with the increase in the load, and the concrete strain of Par_W increased with the increase in the load. At the failure, the concrete strain was 0.00099 mm/mm.

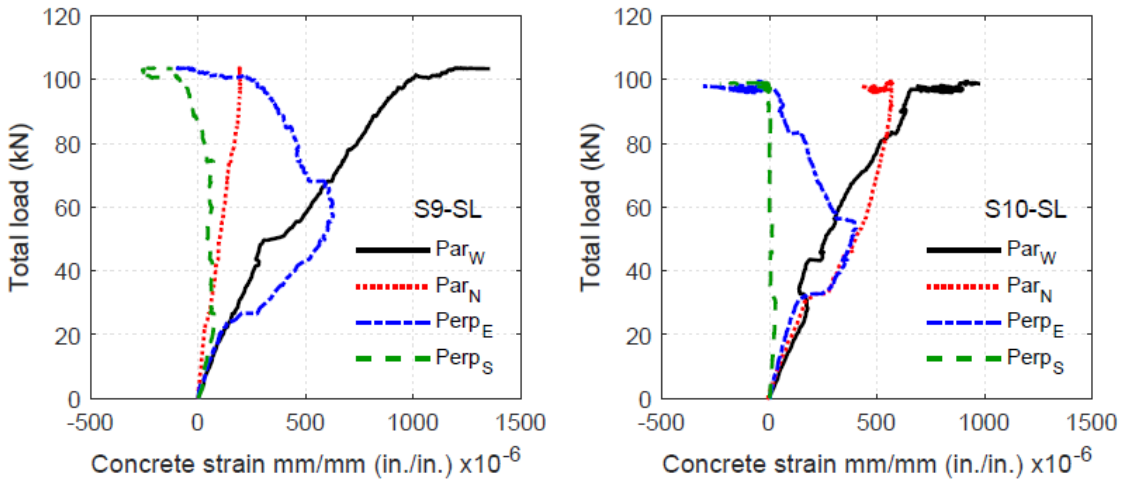

Figure 4-36. Concrete strains of slab (1%) series II.

4.9.3.2 First Stage of Sustained Loading

Load and deflection vs. time curves of the first stage of the sustained loading of S9-SL and S10-SL are shown in Figure 4-37. The sustained load of S9-SL was 103.64 kN (23300 lbs), and it lasted for 21 minutes because the specimen failed in this period. For S10-SL, the sustained load of the 1st stage was 97.15 kN (21840 lbs), and it was kept for 30 days. Slab 9 (S9-SL) was the only specimen that failed during the first stage of the sustained loading. The average deflection was 6.70 mm (0.264 in.) at the beginning of the

first stage, and it was 6.88 mm (0.271 in.) at the end when the failure took place. The increase in the average deflection was 0.19 mm (0.007 in.), which was 0.028 times the average instantaneous deflection. This ratio seemed very small in comparison with all ratios of slabs during the first stage. However, slabs were tested under the first sustained loading for at least 30 days except for S9-SL, which failed before reaching a 30-day time frame. Therefore, the ratio of increase in average deflection of S9-SL in the first stage to the average instantaneous deflection seems reasonable based on the time frame.

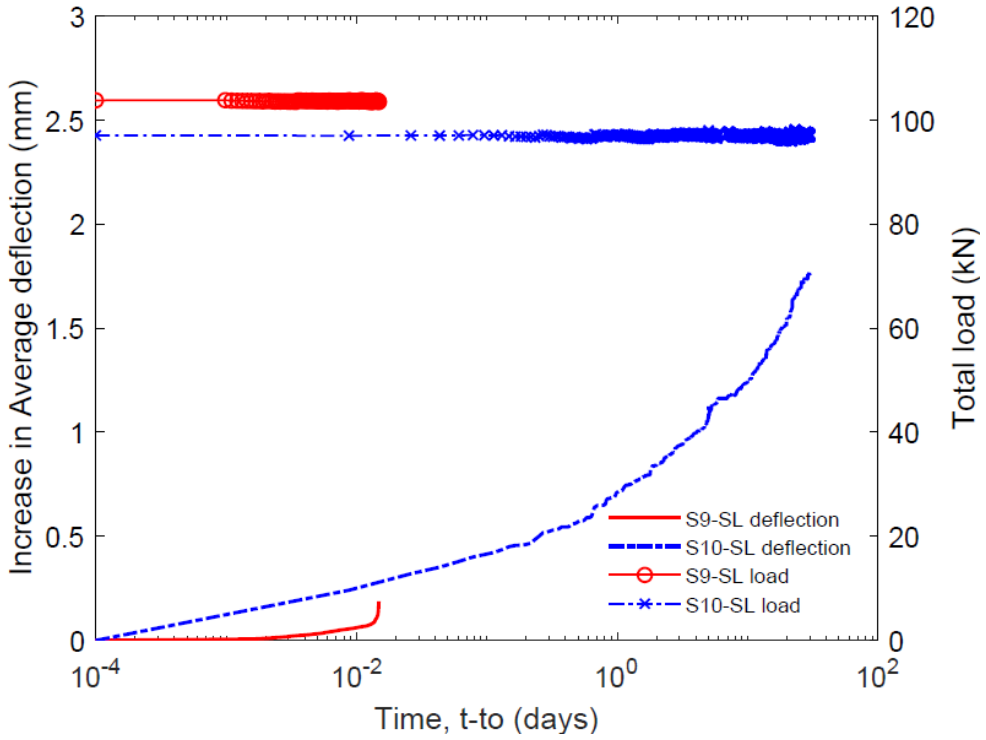

Figure 4-37. Load and deflection vs. time curves of 1st stage of SL loading (S9-SL and S10-SL).

The average deflection of S10-SL rose from 5.82 mm (0.229 in.) to 7.58 mm (0.299 in.) during the first stage of the sustained loading. The ratio of increase in average deflection of S10-SL to the average instantaneous was 0.30. Above 53% of the increase in

the average deflection took place in the first three days. The percent increase in the average deflection was about 89% in the first three weeks.

The changes in reinforcement strains of S9-SL and S10-SL under the first stage of the sustained loads are shown in Figure 4-38. The changes in reinforcement strain and the percentage of increase to instantaneous strain during the first stage of the sustained loading are exhibited in Table 4-19. Most of the reinforcement strains in both specimens decreased under the first sustained loads. The decrease percent to the instantaneous strain of S10-SL was high, as Table 4-19 shows.

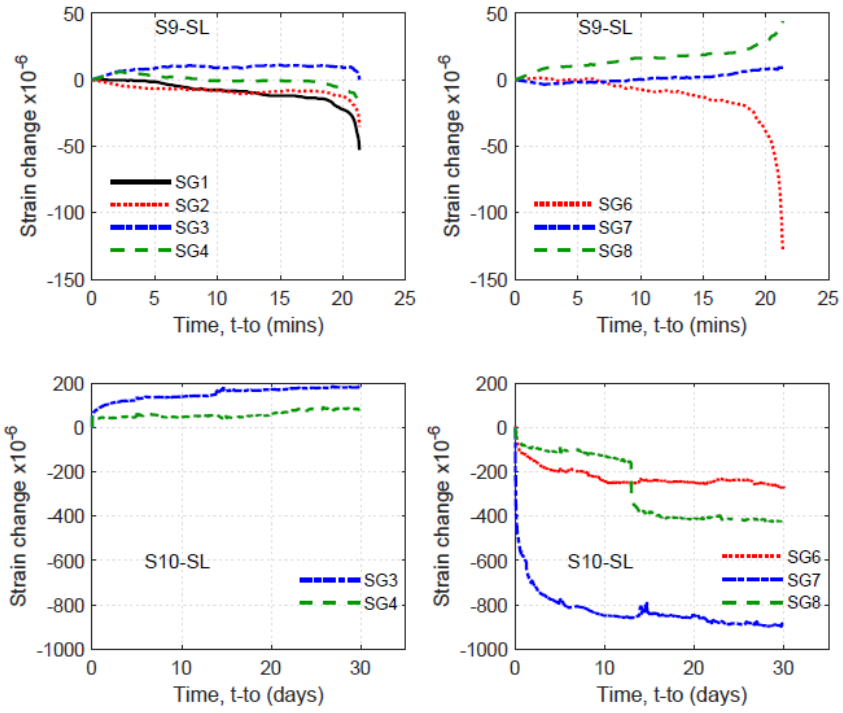

Figure 4-38. Increases in reinforcement strains under 1st sustained loading (S9-SL and S10-SL).

The changes in reinforcement strains of S9-SL were small. The tertiary stage took place during this stage, and some strain gauges changed sharply in the tertiary stage. The highest decrease in reinforcement strain took place in SG6. The strain increased sharply

just before the failure of the specimen. The strain of SG3 increased first and returned to zero at the failure. The only strains that increased under the sustained load were SG7 and SG8.

For S10-SL, the strains of the strain gauges attached to the bottom layer of the tension reinforcement decreased under the sustained load, while the strains of the ones attached to the top layer of tension reinforcement increased slightly. There was a sudden decrease in the strain of SG8 in the 13th day due to load adjustment. The strain of SG7 decreased by 0.0009 mm/mm at the end of the first stage, which was -105% of the instantaneous strain.

Table 4-19. Increase in strain during of 1st of SL (S9-SL and S10-SL)

		SG1	SG2	SG3	SG4	SG5	SG6	SG7	SG8
S9-SL	Changes in strain	-0.00005	-0.00004	0	-0.00002		-0.00013	0.00001	0.00004
	Change percentage to the instantaneous strain	-2.21	-2.68	0	-1.08		-7.65	0.49	2.33
S10-SL	Changes in strain			0.00018	0.00008		-0.00027	-0.00089	-0.00043
	Change percentage to the instantaneous strain			33.33	4.84		-19.08	-115.48	-25.26

Figure 4-39 exhibits the changes in concrete strains of S9-SL and S10-SL during the first stage of the sustained loading. Under the first stage of the sustained loads, the concrete strain of Par_W increased, the concrete strains of Par_N and Perp_E decreased for both specimens.

The first stage of S9-SL was the failure stage. The concrete strains of Par_W and Perp_S increased with time, and the concrete strain of Perp_E, located in the side that deflected more, decreased with time. In previous specimens, concrete strain decreased under the first stage of the sustained loads. Here, two concrete strains increased, which probably a warning of failure. The tertiary stage took place, leading to the failure. In this tertiary stage, all strains increased.

The concrete strains of Par_N and Perp_E in S10-SL decreased even though the east side deflected more than the west. The concrete strain of Par_W in S10-SL was the only strain that increased that much under the first stage of the sustained loading, and the specimen did not fail during the first stage. It could be that this increased a warning that the specimen near to failure.

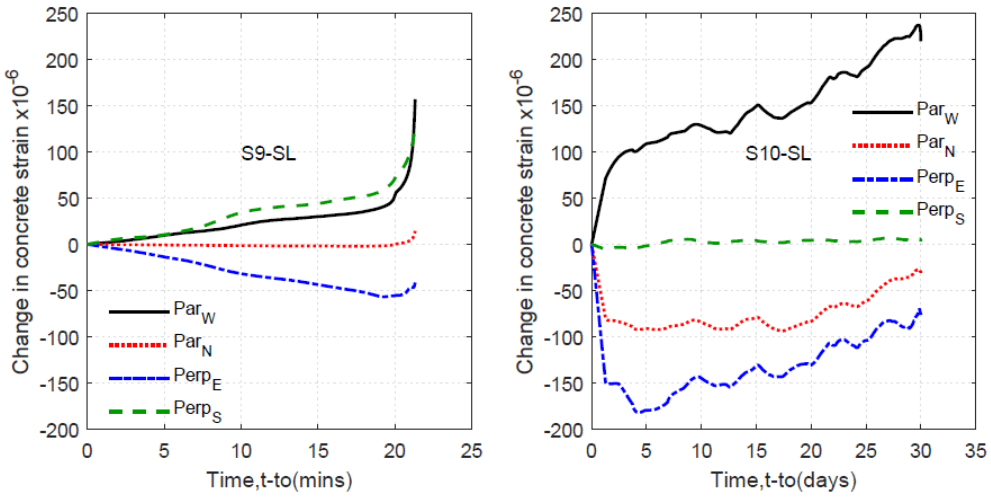

Figure 4-39. Changes in concrete strains under 1st sustained loading (S9-SL and S10-SL).

4.9.3.3 Additional Loading Stages

S9-SL had one stage of sustained loading since it failed under this stage. S10-SL was under the first stage of the sustained loading for 30 days; then, there was one additional

load stage lasting for 67 hours because the specimen failed under the sustained load. Since there was one additional stage of the sustained loading and the failure took place during this stage, the discussion of this stage will be in 4.9.3.4.

4.9.3.4 Failure Under Sustained Loading

The increases in the average deflections of S9-SL and S10-SL in the failure stages are exhibited in Figure 4-40. The failure occurred with a little warning. The tertiary stage took place and lasted for about 2 minutes in both specimens before the failure.

S9-SL was the only slab specimen failing under the first stage of the sustained loading. As Figure 4-37 shows, the specimen failed under the sustained load of 103.64 kN (23300 lbs) after 21 minutes. The failure load was 103.41 kN (23248 lbs). The sustained load seemed near to the strength capacity of the specimen. The specimen resisted the sustained load in the first four minutes. After that, the south side deflected more than any other side leading to a reduction in the south load. The north deflection decreased simultaneously with the increase in the south deflection. At a time of 8 minutes, the east side started deflecting at the rate close to the rate of the increase in deflection of the south side. About two minutes before the failure, the tertiary stage took place on the south side and then on the east side. The failure of the specimen initiated on the south side and eventually happened due to the increase in the east deflection. At the beginning of the sustained load stage, the east side deflected more than any other side. Therefore, this side caused the failure after the south side triggered that. The deflection of the north increased first, then it decreased under the sustained load.

The failure of S10-SL happened in the second stage of the sustained loading after 67 hours. As seen in Figure 4-40, the increase in average deflection was high in the first five

hours. Then, it increased slowly. Based on the average deflection, the specimen seemed not going to fail. However, the tertiary stage took place leading to failure. About 12 minutes before the failure, the south side was not able to resist the load with an increase in the south deflection. This behavior continued until the tertiary stage occurred on the east side.

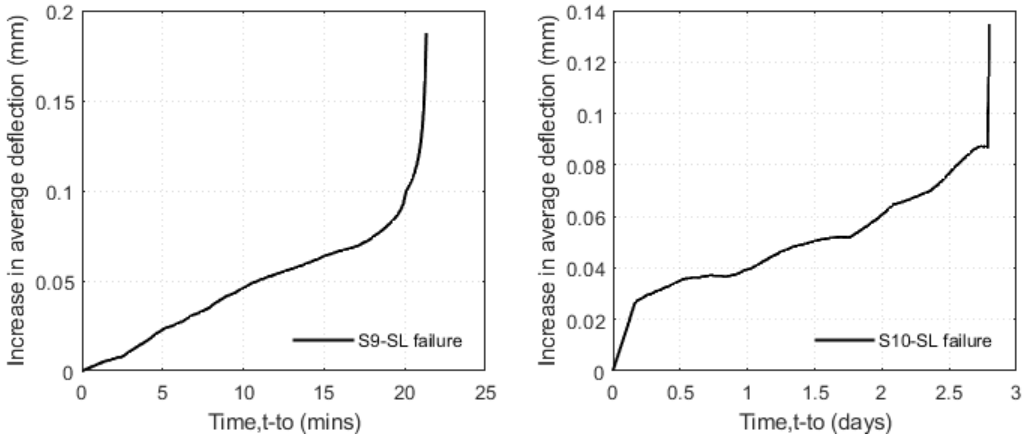

Figure 4-40. Increase in deflection of S9-SL and S10-SL in failure stage.

Figure 4-41 shows the changes in the reinforcement strains of S9-SL and S10-SL during the failure stages. Tertiary stages happened in some of the reinforcement strains before the failure.

The reinforcement strains of S9-SL changed slightly during the failure stage. Just before the failure, all reinforcement strains decreased except the reinforcement strains of SG7 and SG8. The highest decrease in the reinforcement strain took place in SG6, which decreased by 0.00013 mm/mm just before the failure.

For S10-SL, the reinforcement strains of SG3 and SG8 changed very slightly. The changes were almost zero. The reinforcement strains of SG4, SG6, and SG7 decreased sharply in the tertiary stage just before the failure.

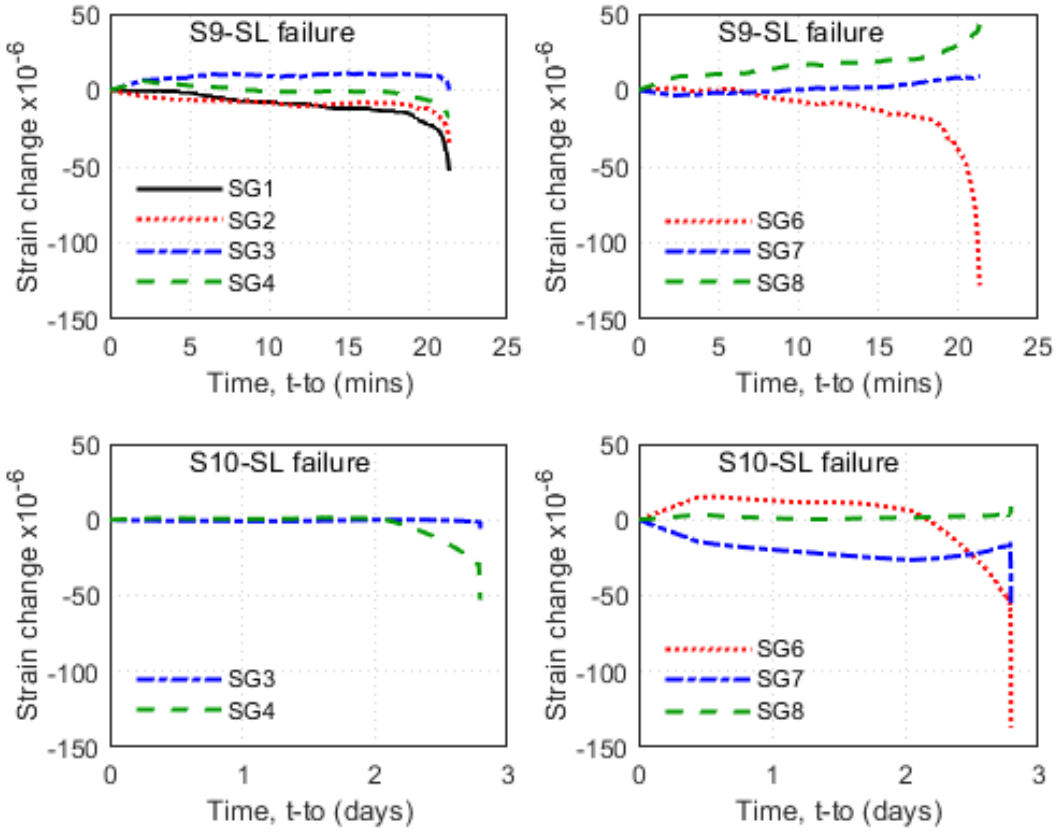

Figure 4-41. Changes in reinforcement strain of S9-SL and S10-SL in failure stages.

The changes in the concrete strains of S9-SL and S10-SL in failure stages are shown in Figure 4-42. All concrete strains increased in the tertiary stage except the concrete strain of Perp_E of S10-SL. The tertiary stages took place in a short time (~2 minutes). The changes in the concrete strains of S9-SL in the failure stage were discussed in section 4.9.3.2. For S10-SL, the concrete strain of Par_W kept increasing, as happened in the first stage. The concrete strain of Perp_S decreased in the failure stage, although it almost did not change in the first stage of the sustained loading.

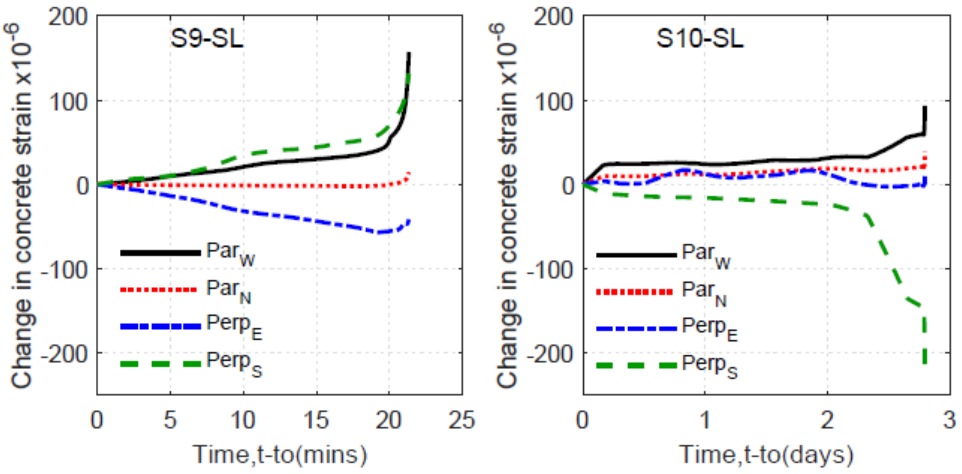

Figure 4-42. Changes in concrete strains of S9-SL and S10-SL in failure stage.

4.9.3.5 Failure Rotation

The failure rotations of the slab (1%) series II are exhibited in Table 4-20. Similar to the previous slabs, the average rotation was determined based on the average deflection at 533 mm (21 in.) of the face of the column at the failure, and the maximum rotation was calculated based on the maximum deflection of the four sides at 533 mm (21 in.) of the face of the column. Both S9-SL and S10-SL had the same maximum rotation. The thickness and the clear cover were controlled in this series. Therefore, the maximum rotation agreed with Muttoni's critical shear crack theory. The average rotation at the failure of S10-SL was higher than the one of S9-SL due to the duration of the sustained loading.

Table 4-20. Failure rotation of slab (1%) series II.

	Average rotation	Maximum rotation
S9-SL	0.013	0.017
S10-SL	0.015	0.017

4.9.3.6 Temperature and Humidity

The fluctuations in the temperature and humidity of S10-SL are shown in Figure 4-43. S9-SL failed in small duration. The average temperature and humidity were 62 ˚F and 38.3%, respectively. The temperature in S10-SL varied from 53.6 ˚F to 70.5 ˚F, and the humidity ranged from 17.2% to 47.7%.

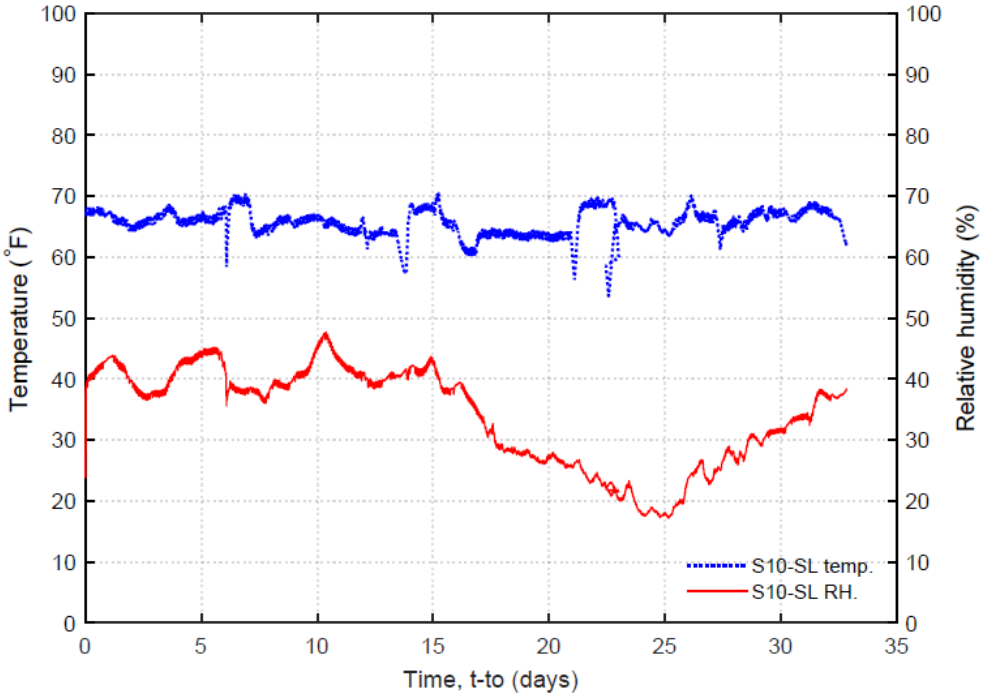

Figure 4-43. Temperature and RH of S10-SL

4.9.4 Overall Comparison

A total of 10 slab-column specimens were tested to evaluate the time-dependent strength and stiffness characteristics under high levels of sustained load.

Table 4-21shows an overall matrix from the slab-column testing. All specimens were between 175 days and 441 days of concrete age. The duration of the tests were at least 30 days unless failure of the specimen occurred. The sustained load intensities (sustained

load / peak load) of the first stages ranged from 81% to 97.6%, except for S9-SL whose sustained load intensity was close to 1.

Under sustained, loading the specimens experienced an increase in displacement that was on average 30% more than the instantaneous deflection at the start of the sustained loading. The increase in deflection under sustained load exhibits the continued deformation of the connection due to creep in the concrete.

There were additional loading stages after the first stage that varied from one to eight stages until failure of the specimen. The during the additional loading stages addition load of 1.78 kN to 4.45 kN (400 lbs to 1000 lbs) was placed on the specimen and sustained for thre- days to determine the short term sustained loading behavior at higher levels of loading. One specimen (S9-SL) failed under the first stage of the sustained loading, and four failed during additional stages. Sustained load intensities were between 95.4% and 98.8% in stages just before the last stage in which failure occurred during or while loading the specimen. Although given more time in the additional load stages some specimens may have reached failure, this high level of load that can be withstood for three days indicates that the load for which failure would occur under sustained load is a high percentage of the capacity of the specimen.

Table 4-21. Overall results of slab-column tests

Reinforcement ratio (%)	0.64%				1%					
Specimen	SC1	S2-SL	S3-SL	S4	SC5	S6-SL	S7-SL	S8-SL	S9-SL	S10-SL
Loading condition	Short time (control)	Sustained loading	Sustained loading	Short time	Short time (control)	Sustained loading	Sustained loading	Sustained loading	Sustained loading	Sustained loading
Loading age t_o (days)	175	189	311	402	200	281	345	441	197	203
Duration t_d	-	84 days	59 days	-	-	60 days	66 days	63 days	21 minutes	32.8 days
Duration of first stage t_d	-	73 days	46 days	-	-	45 days	45 days	45 days	21 minutes	30 days
Sustained load of 1st stage kN, (lbs)	-	89.32 (20080)	94.52 (21250)	-	-	89.85 (20200)	94.30 (21200)	106.76 (24000)	103.64 (23300)	97.15 (21840)
Sustained load intensity	-	0.833	0.890	-	-	0.846	0.813	0.859	-	0.976
Increase percent under 1st SL to average instantaneous deflection, %	-	39	22	-	-	37	17	31	3	30
Increase percent under 1st SL to average instantaneous deflection (30 days), %	-	32	20	-	-	33	16	28	-	30
Peak load, kN (lbs)	100.34 (22557)	107.25 (24110)	106.17 (23868)	95.86 (21551)	116.02 (26081)	106.17 (23868)	116.04 (26086)	124.33 (27950)	103.76 (23326)	99.52 (22373)
Load at failure, kN (lbs)	99.22 (22305)	106.37 (23913)	103.82 (23340)	94.86 (21325)	115.43 (25949)	105.47 (23710)	115.67 (26003)	124.33 (27950)	103.41 (23248)	98.73 (22195)
Increase in average deflection 1st stage mm (in.)	-	3.50 (0.1379)	2.18 (0.086)	-	-	2.17 (0.086)	1.15 (0.045)	1.86 (0.073)	0.19 (0.007)	1.76 (0.069)
average deflection at failure mm (in.)	14.45 (0.569)	15.15 (0.596)	14.60 (0.575)	11.15 (0.439)	7.43 (0.292)	9.45 (0.372)	9.72 (0.383)	9.72 (0.383)	6.88 (0.271)	7.78 (0.306)
Average rotation at failure at 533 mm (21 in.)	0.027	0.028	0.027	0.021	0.014	0.018	0.018	0.017	0.013	0.015
Maximum rotation at failure at 533 mm (21 in.)	0.035	0.032	0.033	0.029	0.016	0.022	0.024	0.019	0.017	0.017
Load at final stage of SL	-	102.31 (23000)	104.90 (23583)	-	-	103.20 (23200)	112.98 (25400)	122.77 (27600)	-	97.15 (21840)
Load intensity at last stage of SL	-	0.954	0.988	-	-	0.972	0.974	0.998	-	0.976
Average temperature, ˚F	NA	82	61	57	71	80	76	66	67	66
Average RH, %	NA	65	47	43	58	72	69	56	34	34

Load vs. deflection curves for all slabs are shown in Figure 4-44. As seen, slabs with a 0.64% reinforcement ratio failed at the average deflection higher than the one of slabs constructed at a 1% reinforcement ratio as would be expected. As is typical with slab-column tests, there is variability in the strength and stiffness of the specimens. Also, the stiffness of slabs (0.64%) was softer than the stiffness of slabs (1%). Small differences ~9.53 mm (3/8 in.) in the slab cover and thickness led to some variability of the slab stiffness and strengths. Similar variability in cover would be expected in actual construction. However, due to the scale of the specimen the % change was high and affected the results of the tests.

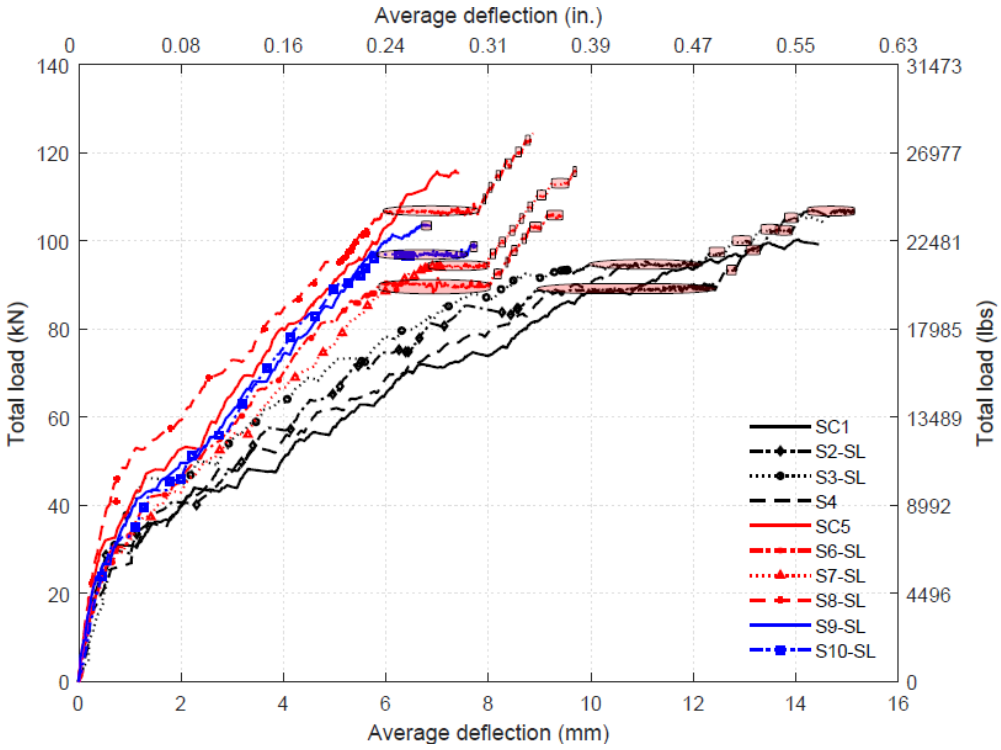

Figure 4-44. Load vs. deflection curves for all slabs.

Overall, the load vs. deflection curves show the significant continued deflection of the specimens that experienced sustained loading. For the 0.64% specimens, the failure

deflection was on average only 3% higher than the control specimen. However, for the 1% reinforcement, specimens the failure deflection was on average 18% higher than the control deflection. The greater increase in the 1% specimens indicates that more flexural response is enabled in those specimens due to thecreep of the concrete under sustained load. As was seen in the beams, specimens that would normally perform brittlely under short-term loading can see increased flexural response under sustained loading. As the 0.64% reinforcement specimens already had significant flexural actions under short-term loading, the increase in deflection is not as significant under sustained loading.

Figure 4-45 exhibits the deflection ratio (deflection under sustained load / short-term deflection at start of sustained load) vs. time for the 1st stage of sustained load. The results show similar behavior in all slabs. S10-SL had the highest sustained load intensity, which is almost 1, and therefore saw greater increases in deflection at earlier times than the other slabs.

The sustained load intensities of S2-SL and S6-SL were 0.833 and 0.846, respectively, yet had some of the highest increases in deflection. One contributing factor was the average temperatures of S2-SL and S6-SL at the test periods were the highest. The average temperature during the tests exceeded 80˚F just in these two specimens that were tested in the summer. The sustained load intensity of S7-SL was the lowest at 0.81 and had the lowest increase percent in the average deflection.

In fact, the S9-SL failed in a time more than 21 minutes since it took over 15 minutes to bring the load intensity from 0.979 to 0.991. The reason for that was that the average deflection increased considerably. Therefore, there was time to make the specimen stabilized.

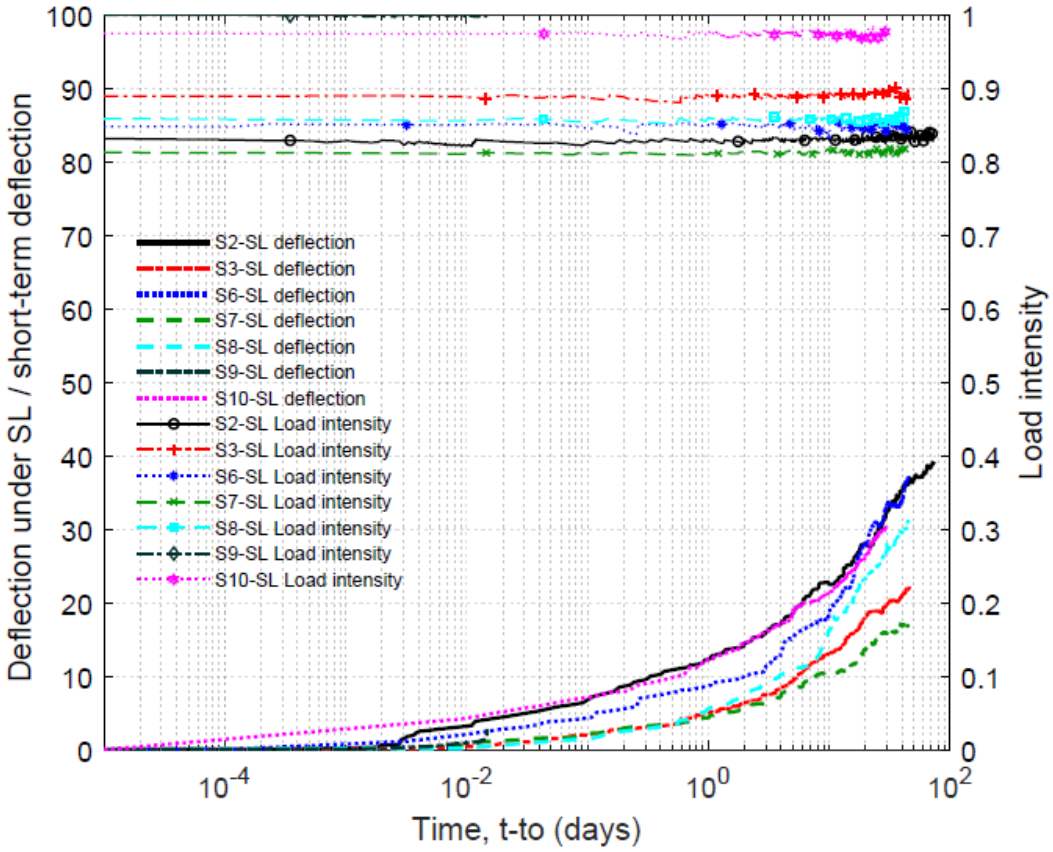

Figure 4-45. First stage of the sustained loading (all slabs).

Table 4-22 shows the percent increase in deflection under sustained load to the deflection at 30 days. As can be seen, S2-SL and S10-SL had the highest increase percent on the first day. By the end of the first week, the increase percent in all specimens exceeded 50% except S8-SL. The increase percent in the average deflection of S6-SL and S8-SL occurring in late days was higher than other specimens. The increase percent in the first three weeks was 85% or more.

Table 4-22. Increase percent of the total increase in average deflection under SL.

Time (days)	Increase percent of the total increase in average deflection under SL (%)					
	S2-SL	S3-SL	S6-SL	S7-SL	S8-SL	S10-SL
1	38	26	26	27	20	40
3	50	38	34	40	33	53
7	66	59	50	59	43	66
14	78	78	66	68	69	79
21	86	95	85	88	86	89

The increases in the average deflection during the stages in which failure occurred are exhibited in Figure 4-46, and the summary of the failure stages is shown in Table 4-23. As can be seen, the tertiary stage, as exhibited by a sudden increase in deflection, took place in a short time (~2 min) prior to punching of the slab-column connections. The short duration of the tertiary stage would provide a little warning prior to the failure of a structure.

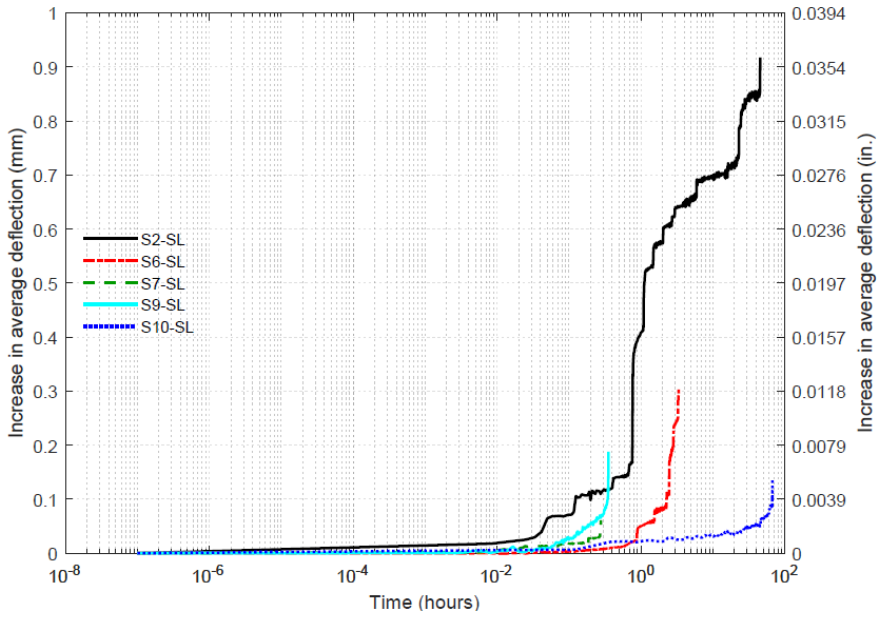

Figure 4-46. Increase in average deflection during failure stages.

S7-SL failed just in 17 minutes after adding the last sustained load, while S10-SL failed about 67 hours after the beginning of the second stage of the sustained loads. The specimen, having the highest increase in the average deflection in the first stage of the sustained loads, had the highest increase in the average deflection during the failure stage. The increase in the average deflection of S2-SL in the failure stage was at least three times the increases in the average deflections of the other specimens in failure stages.

Table 4-23. Summary of failure stages.

Specimen	Stage of the sustained loading	Increase in the average deflection during the failure stage mm (in.)	Time to failure
S2-SL	5	0.917 (0.0361)	46 hours
S6-SL	7	0.303 (0.0119)	200 minutes
S7-SL	9	0.061 (0.0024)	17 minutes
S9-SL	1	0.188 (0.0074)	21 minutes
S10-SL	2	0.135 (0.0053)	67 hours

Reinforcement strains of the slabs were discussed previously. In general, the reinforcement strains of the specimens with a 0.64% reinforcement ratio were higher than the ones of the specimens with a 1% reinforcement ratio. Table 4-24 shows the reinforcement strains at the failure for all slabs.

Table 4-24. Failure strains of slabs.

	Reinforcement ratio	Strain gauge	SG1	SG2	SG3	SG4	SG5	SG6	SG7	SG8
Failure strain mm/mm (in./in.)	0.64%	SC1	0.0028	0.0023	0.0026	0.0019	0.0105	0.0115	0.002	0.0139
		S2-SL	0.0026	0.0022	0.0023	0.0017	0.0116	0.0093	0.0022	0.0079
		S3-SL	0.009	0.0027	0.0024	0.002	0.0083	0.0081	0.0021	0.0075
		S4	0.0028	0.0032	0.0025	0.0014	0.0028	0.0101	0.0025	0.0037
	1%	SC5	0.0036	0.0025	0.0228	0.0005	NA	0.0026	0.0021	0.0026
		S6-SL	0.0025	0.0025	0.0026	0.0009	0.0026	0.0034	0.0018	0.0024
		S7-SL	0.0021	0.002	0.0019	0.0011	0.0061	0.0025	0.0015	0.0049
		S8-SL	0.0048	0.0007	0.0006	0.0008	NA	0.0022	0.0024	0.0049
		S9-SL	0.0023	0.0013	0.0006	0.0016	NA	0.0015	0.0019	0.0019
		S10-SL	NA	NA	0.0007	0.0016	NA	0.0010	-0.0001	0.0013

The percent increases in reinforcement strains at 30 days to instantaneous strains are exhibited in Table 4-25. Slabs with a 0.64% reinforcement ratio (S2-SL and S3-SL) had the highest increase percent in the reinforcement strains, as the table shows. The bottom layer of the tension reinforcement of S2-SL and S3-SL had the highest increase in strain. Some of the reinforcement of S2-SL and S3-SL yielded under the first stage of the sustained loading. Some of the strain gauges of S10-SL were not attached to the center of the rebars. Therefore, some reinforcement strain decreased under the first stage of the sustained loading.

Table 4-25. Increase percent in strain to instantaneous strain.

		SG1	SG2	SG3	SG4	SG5	SG6	SG7	SG8
Increase percent to instantaneous	S2-SL	13	10	16	16	5	15	20	161
	S3-SL	1	6	7	13	256	49	13	190
	S6-SL	16	18	18	49	9	-6	22	13
	S7-SL	3	6	11	20	-11	5	10	10
	S8-SL	9	9	10	20	17	5	13	11
	S10-SL			33	5		-19	-115	-25

Table 4-26 shows normalized increase percent of the total increase in reinforcement strain under the first stage of sustained loading.

Table 4-26. Increase percent of the total increase in reinforcement strain under 1st SL.

Time	S2-SL							
(days)	SG1	SG2	SG3	SG4	SG5	SG6	SG7	SG8
1	44	29	40	44	14	3	42	56
3	58	46	55	55	45	14	58	59
7	71	57	70	72	36	28	77	100
14	78	70	79	80	85	11	84	100
21	92	87	90	88	69	25	89	101
Time	S3-SL							
(days)	SG1	SG2	SG3	SG4	SG5	SG6	SG7	SG8
1	28	3	22	23	49	41	27	30
3	322	40	47	41	53	43	47	44
7	245	48	57	63	90	77	66	91
14	-125	76	82	78	97	79	85	96
21	-28	93	98	94	100	79	99	99
Time	S6-SL							
(days)	SG1	SG2	SG3	SG4	SG5	SG6	SG7	SG8
1	24	27	25	39	24	157	32	27
3	34	38	36	50	37	155	41	39
7	47	52	49	64	52	166	55	56
14	69	74	70	82	70	146	78	84
21	86	89	86	91	89	120	90	94
Time	S7-SL							
(days)	SG1	SG2	SG3	SG4	SG5	SG6	SG7	SG8
1	11	12	27	40	72	1	25	26
3	32	26	38	53	81	13	36	39
7	50	37	50	65	86	39	50	59
14	64	55	70	82	100	47	73	73
21	87	93	88	94	92	88	85	91
Time	S8-SL							
(days)	SG1	SG2	SG3	SG4	SG5	SG6	SG7	SG8
1	25	26	20	28	5	5	26	27
3	34	36	31	43	104	24	43	39
7	44	47	38	57	101	20	58	47
14	66	73	74	84	103	67	82	72
21	85	84	82	92	91	72	91	86
Time	S10-SL							
(days)	SG1	SG2	SG3	SG4	SG5	SG6	SG7	SG8
1			51	61		45	66	18
3			63	60		67	85	23
7			75	71		75	91	23
14			91	61		88	91	87
21			95	90		95	97	95

In general, the strain in the reinforcement increased with time as the concrete experienced creep deformations and the specimen deflected. As with the deflection, most

of the increase in strain occurred early in the sustained loading period. However, the difficulty of reading strain and the influence of cracking lead to more variability in the strain readings.

4.10 Conclusions

In this chapter, ten 0.47 scale aged, isolated slab-column connections with two different steel reinforcement layouts were tested. Four specimens were constructed at a reinforcement ratio of 0.64%, and six specimens were constructed at a 1% reinforcement ratio.

Slab-column connections with a 0.64% reinforcement ratio were tested at ages ranging between 175 days and 402 days. SC1 served as a control specimen, and S4 failed before being under sustained loading. The sustained load intensities of S2-SL and S3-SL were 83% and 89% for periods of 73 days and 46 days. There were four additional stages of sustained loading in each specimen, and each additional stage lasted for about three days.

Slabs (1%) series I (SC5, S6-SL, S7-SL, and S8-SL) were loaded up at the age between 200 days and 441 days. SC5 was a control specimen. The rest were tested under the sustained load intensity between 81% and 86% for periods of 45 days. Each specimen had several additional stages of sustained loading lasting for three days.

Slabs (1%) series II had two specimens, tested at the ages of 197 days and 203 days under sustained load intensities of ~ 1 and for about 21 minutes and 97.6% for 21 minutes and 30 days. Then, there was an additional stage of sustained loads added to S10-SL.

The following are the main conclusions from the slab-column tests:

- The load level to cause failure under sustained load is very close to the short-term capacity of the slab-column connection.
    - Only one specimen (S9-SL) failed under the first stage of the sustained loading after 21 minutes. This specimen was loaded very close (~1) to the short-term capacity.
    - Four specimens (S2-SL, S6-SL, S7-SL, and S10-SL) failed during additional stages of the sustained loads. These failures occurred 45 hours, 200 minutes, 17 minutes, and 67 hours, respectively, after the last addition of load. The specimens were able to carry sustained loads for three days at a load level ~4.45 kN (1000 lbs) (~5% of capacity) less than the load they eventually failed at. The sustained load intensities seem close to the ultimate capacity of the slabs.
    - The sustained load intensities of S2-SL, S3-SL, S6-SL, S7-SL, and S10-SL in the last stage before the failure took place due to additional loading or due to additional stage sustained load were 0.954, 0.988, 0.972, 0.974, and 0.976, respectively. Based on that, the sustained load intensity should be above 0.98 to lead to failure.
    - S10-SL first stage lasted for 30 days with a sustained load intensity of 97.6%. The slab was loaded with only 1.78 kN (400 lbs) and failed 67 hours after the last addition of loading.
- The average deflection and rotation at failure for specimens under sustained load are similar to the short-term value with more increase in the slabs with a 1% reinforcement ratio.

  - For the specimens with the 0.64% reinforcement ratio, the changes in deflection at failure compared to SC1 were 5% and 1% higher for slabs S2-SL and S3-SL, respectively.
  - For specimens with a 1% reinforcement ratio, the change in deflection at failure compared to SC5 was 27%, 31%, 31%, -7%, 4% for slabs S6-SL, S7-SL, S8-SL, S9-SL, and S10-SL, respectively. The smaller increase for the last two slabs is likely due to reduced cover in these slabs.
  - The greater increase in the 1% slabs is likely due to greater flexural deformation under sustained load. Under short-term load, slabs with a reinforcement ratio of 1% see little flexural deformation, while greater amounts are seen at a reinforcement ratio of 0.64%. The sustained loading seemed to increase the flexural response of the slabs with a higher reinforcement ratio.

- The rate of increase in deflection of the slabs is consistent with the material level behavior of concrete under creep, with over 50% of the sustained load deflection occurring in the first seven days.
- The increase in deflection under sustained load is similar for all slabs, as seen in Figure 4-43. Slightly higher rates were seen in slabs with higher loading intensities or in slabs that were tested at higher ambient temperatures.
- S6-SL, S7-SL, S8-SL, S9-SL, and S10-SL experienced a tertiary phase of deformation characterized by a sudden increase in the rate of deflection just

before failure. For these slabs, the tertiary stage lasted for less than 2 min giving little warning time for impending failure.

- Strains in the reinforcement also increased at a similar rate as the deflection of the slabs. Greater increases in strain were seen in gauges placed within the punching perimeter of the slab, and less increase in gauges places further from the column.
- Crack widths were monitored during testing of slabs 3 and 7. The increase in the crack width size could not be measured during the sustained loading.

Chapter 5

CONCLUSIONS AND RECOMMENDATIONS

5.1 Summary

The objective of this research was to understand the impact of high sustained gravity loads on the evolution of large-scale collapse in reinforced concrete (RC) elements. In particular, this research investigated the time-dependent behavior of ten RC beams and ten flat-plate connections under high sustained stresses. The research program evaluated the time-dependent strength and stiffness characteristics to determine what level of high sustained load would lead to eventual failure (collapse) in these systems and what are the characteristics of impending failure.

5.2 Conclusion

Two beam series were tested with differences in the reinforcement and loading conditions. Beam series I were under high sustained loads ranging from 82% to 93% for periods of time between 24 days and 42 days. Beam series II were tested under high sustained loads ranging from 83% to 98% for periods of time between 84.5 minutes and 52 days.

Ten 0.47 scale aged-isolated slab-column connections with two different steel reinforcement layouts (0.64% and 1%) were tested. Slab-column connections with a 0.64% reinforcement ratio were tested at ages ranging between 175 days and 402 days at sustained load intensities of 83% and 89% for periods of 73 days and 46 days. Slabs (1%) series I were tested at the ages between 200 days and 441 days under the sustained load intensity

between 81% and 86% for periods of 45 days. Slabs (1%) series II had two specimens, tested at the ages of 197 days and 203 days under sustained load intensities of ~ 1 and 97.6% for time periods of 21 minutes and 30 days.

The following are the main conclusions from the testing series:

- The level of sustained loaded must be very close (~5%) to the short-term capacity in order to initiate failure under sustained loads. While plain concrete may experience failure at load levels as low as 80% (Iravani and MacGregor 1998; Rusch 1960), the ability of reinforced concrete structures to withstand sustained load is much higher due to the contribution of the reinforcement. The variance in sustained load capacity to short-term capacity is within the inherent variability of concrete structures. Therefore, the use of the short-term capacity would be suitable for design.
    - No beam in series I failed under sustained loading. In series II, one beam failed under a sustained loading intensity of 98% after about 85 minutes. Moreover, another beam failed during an additional loading stage after about 16 minutes. In both beams, the sustained load seemed close to the short-term shear capacity.
    - Only one specimen (S9-SL) failed under the first stage of the sustained loading after 21 minutes. This specimen was loaded very close (~1) to the short-term capacity.
    - Four specimens (S2-SL, S6-SL, S7-SL, and S10-SL) failed during additional stages of the sustained loads. These failures occurred 45 hours, 200 minutes, 17 minutes, and 67 hours, respectively, after the last addition

of load. The specimens were able to carry sustained loads for three days at a load level ~4.45 kN (1000 lbs) (~5% of capacity) less than the load they eventually failed at. The sustained load intensities seem close to the ultimate capacity of the slabs.

  - The sustained load intensities of S2-SL, S3-SL, S6-SL, S7-SL, and S10-SL in the last stage before the failure took place due to additional loading or due to additional stage sustained load were 0.954, 0.988, 0.972, 0.974, and 0.976, respectively. Based on that, the sustained load intensity should be above 0.98 to lead to failure.
  - S10-SL first stage lasted for 30 days with a sustained load intensity of 97.6%. The slab was loaded with only 1.78 kN (400 lbs) and failed 67 hours after the last addition of load.

- Sustained loading increased the deflection at peak load for all beam specimens, with a greater increase in the specimens that were more shear controlled. While for the slab-column specimens, deflection at failure remained similar for the 0.64% reinforcement ratio specimen and increased for the 1% reinforcement ratio specimens. Sustained loading seems to cause more flexural response in the specimens. For those specimens that are strongly shear controlled (shear capacity much lower than flexural capacity), the greater flexural response led to much greater ultimate deflections in the specimen. For specimens that had flexural capacity at or near the shear capacity, the change in deflection was lower. The increase in deflection under sustained loading may allow for load redistribution and

halting of collapse in redundant structures and may give warning signs of structural distress.

  - For beam series I, the increase in deflection was 41%. For beam series II, the increase in deflection was 1.5 times. The large increase in deflection shows the significant deformations that can occur under sustained loading. This large increase in deflection would allow for load redistribution in redundant systems or provide warning signs of impending failure.
  - For the specimens with the 0.64% reinforcement ratio, the changes in deflection at failure compared to SC1 were 5% and 1% higher for slabs S2-SL and S3-SL, respectively.
  - For specimens with a 1% reinforcement ratio, the change in deflection at failure compared to SC5 was 27%, 31%, 31%, -7%, 4% for slabs S6-SL, S7-SL, S8-SL, S9-SL, and S10-SL, respectively. The smaller increase for the last two slabs is likely due to reduced cover in these slabs.
  - The greater increase in the 1% slabs is likely due to greater flexural deformation under sustained load. Under short-term load, slabs with a reinforcement ratio of 1% see little flexural deformation, while greater amounts are seen at a reinforcement ratio of 0.64%. The sustained loading seemed to increase the flexural response of the slabs with a higher reinforcement ratio.

- Sustained loading changed the behavior of beams in series I but not for the other specimens. Beams tested under sustained loads showed a different mode of failure from the control specimen that was tested under monotonically increasing load to

failure. Unlike the control specimen, which failed in shear, specimens tested under sustained loads experienced significant increases in deflection and flexural failure before the shear failure. Concrete creep under sustained load enabled flexural failure of the beam due to concrete crushing to occur before the shear failure.

- The rate of increase in deflection is consistent with the material level behavior of concrete under creep, with higher rates of deflection in the primary stage and a nearly linear rate with time in the secondary stage.
    - For beam series I, over 50% of the increase in deflection under sustained loading in series I took place in the first two days. For beam series II, 50% of the increase in deflection under sustained load took place in the first five days.
    - For the slab-column connections, over 50% of the sustained load deflection occurred in the first seven days.
    - The rate of increase in deflection under sustained load is similar for all slabs and beams. Slightly higher rates were seen in slabs and beams with higher loading intensities or in slabs that were tested at higher ambient temperatures.
- Failure under a stage of sustained loading due to the tertiary phase of creep, as characterized by the sudden increase in the rate of deformation just before failure, occurred in a short time (less than two minutes) before failure of the specimen. The short time frame of the tertiary creep would give a little warning prior to the failure of a structural system.

  - Only specimen B10-SL experienced a tertiary stage that showed a sharp increase in deflection with time just 10 seconds before failure.
  - S6-SL, S7-SL, S8-SL, S9-SL, and S10-SL experienced a tertiary phase of deformation less than 2 min before failure.

- Reinforcement strains increased under sustained loading. The increase in strain shows that the reinforcement took more of the loading as the concrete softened under the sustained loading.
  - For the beams, the increase in the compression strain was higher than in the tension strain, indicating that the creep of the concrete in compression. This also led to an increase in curvature in the locations of the highest moments. The increase in curvature occurred at a higher rate than the increase in deflection for most beams indicating that the distribution of curvature along the length of the beam was changing under sustained load as the concrete in the highly stressed locations (near center of the beam) experienced creep deformations.
  - Strains in the reinforcement also increased at a similar rate as the deflection of the slabs. Greater increases in strain were seen in gauges placed within the punching perimeter of the slab, and less increases in gauges placed further from the column.
- Crack widths increased at a similar rate to the deflection increase for the beams. Crack widths were monitored during testing of slabs 3 and 7. The increase in the crack width size could not be measured during the sustained loading.

The overall main conclusions of this experimental research that address the original objectives are:

- The level of sustained load that would lead to eventual failure (collapse) is very close (~5%) to the short-term capacity of the system.
- Characteristics of impending failure are increased deflections, especially for systems that are normally controlled by brittle shear failure, and sudden rapid increase in deflection due to tertiary creep very close (~2 min) to failure of the specimen.

5.3 Recommendations

The following are recommendations for future work in the area of the time-dependent response of RC beams and slab-column connections under high sustained loading.

- Additional experiments need to be conducted. Differences in concrete strength, aggregate, age, reinforcement, and load intensity need to be evaluated. In addition, redundant systems (multiple members) need to be evaluated.
- Longer durations of sustained load. During the additional load stages, the load was only sustained for three days due to time constraints of the testing. Additional time may have resulted in failure of the specimen under sustained load.
- Analysis and constitutive modeling of reinforced concrete behavior under creep. Additional tests on reinforcement bar to concrete bond and plain concrete are being conducted. These results, together with these tests results, need to be analyzed, and

a robust model for reinforced concrete members under sustained loads be developed.

- Analysis of the probability of collapse and progression of collapse in an entire concrete building is needed to inform code developers on the safety of concrete buildings under sustained loads.

REFERENCES

ACI Committee 318. (2014). *Building Code Requirements for Structural Concrete*. *American Concrete Institute*.

Alwis, W. A. M. (1999). "Long-term deflection of RC beams under constant loads." *Engineering Structures*, Elsevier, 21(2), 168–175.

Bakoss, S. L., Gilbert, R. I., Faulkes, K. A., and Pulmano, V. A. (1982). "Long-term deflections of reinforced concrete beams." *Magazine of Concrete Research*, Thomas Telford Ltd , 34(121), 203–212.

Bažant, Z. P. (1975). "Theory of Creep and Shrinkage in Concrete Structures: A Précis of Recent Developments." *Mechanics Today*, 2, 1–93.

Bazant, Z. P., and Gettu, R. (1992). "Rate Effects and Load Relaxation in Static Fracture of Concrete." *ACI Materials Journal*, 89(5), 456–468.

Bažant, Z. P., and Jirásek, M. (2018). *Creep and hygrothermal effects in concrete structures*. *Solid Mechanics and its Applications*.

Bažant, Z. P., and Xiang, Y. (1997). "Crack growth and lifetime of concrete under long time loading." *Journal of Engineering Mechanics*, 123(4), 350–358.

Bugalia, N., and Maekawa, K. (2017). "Time-dependent capacity of large scale deep beams under sustained loads." *Journal of Advanced Concrete Technology*.

CEB. (2013). "CEB-FIP Model Code 2010." *fib Model Code for Concrete Structures 2010*.

Dekoster, M., Buyle-Bodin, F., Maurel, O., and Delmas, Y. (2003). "Modelling of the flexural behaviour of RC beams subjected to localised and uniform corrosion." *Engineering Structures*, Elsevier BV, 25(10), 1333–1341.

Du, Y., Martin, C., and Li, C. (2013). "Structural Performance of RC Beams under

Simultaneous Loading and Reinforcement Corrosion." *Construction and Building Materials*, 38, 472–481.

Eldukair, Z. A., and Ayyub, B. M. (1991). "Analysis of recent U.S. structural and construction failures." *Journal of Performance of Constructed Facilities*, 5(1), 57–73.

Espion, B., and Halleux, P. (1990). "Long-Term Deflections of Reinforced-Concrete Beams- Reconsideration of Their Variability." *ACI Structural Journal*, 87(2), 232–236.

Ferguson, P. M., Breen, J. E., and Jirsa, J. O. (1988). *REINFORCED CONCRETE FUNDAMENTALS. FIFTH EDITION*.

Gabrielle Lucivero. (2015). "Structural Engineer: Ramp Likely Showed Signs of Deterioration Prior to Collapse." *Spectrum News*, Johnson City.

Gardner, N. J., Huh, J., and Chung, L. (2002). "Lessons from the Sampoong department store collapse." *Cement and Concrete Composites*, Elsevier, 24(6), 523–529.

Gilbert, R. I., Guo, X. H., and Gamble, W. L. (2006). "Time-dependent deflection and deformation of reinforced concrete flat slabs - An experimental study." *ACI Structural Journal*, 103(2), 304.

Green R, and Breen JE. (1969). "Eccentrically Loaded Concrete Columns Under Sustained Load." *ACI JOURNAL*, 66(11), 866–874.

Han, L. H., Tao, Z., and Liu, W. (2004). "Effects of sustained load on concrete-filled hollow structural steel columns." *Journal of Structural Engineering*, 130(9), 1392–1404.

Hill, B., Kuykendall, R., and Moore, M. (2011). *Final report to Merlin Law Group on 4th floor Distress of Dolphin Towers WJE No. 2010.3594, Wiss, Janney, Elstner*

Associates, Inc, Duluth, GA.

Iravani, S., and MacGregor, J. G. (1998). "Sustained load strength and short-term strain behavior of high-strength concrete." *ACI Materials Journal*, 95(5), 636–647.

Kim, C. S., Park, H. G., Choi, I. R., and Chung, K. S. (2017). "Effect of sustained load on ultimate strength of high-strength composite columns using 800-MPa steel and 100-MPa concrete." *Journal of Structural Engineering (United States)*, 143(3), 1–16.

Liu, Y., Jiang, N., and Deng, Y. (2016). "Flexural Experiment and Stiffness Investigation of Reinforced Concrete Beam under Chloride Penetration and Sustained Loading." *Construction and Building Materials*, 302–310.

Maekawa, K., Soltani, M., Ishida, T., and Itoyama, Y. (2006). "Time-dependent space-averaged constitutive modeling of cracked reinforced concrete subjected to shrinkage and sustained loads." *Journal of Advanced Concrete Technology*, 4(1), 193–207.

Mazzotti, C., and Savoia, M. (2002). "Nonlinear creep, Poisson's ratio, and creep-damage interaction of concrete in compression." *ACI Materials Journal*, 99(5), 450–457.

Morrill, K. B., Sheffield, C. S., Kersul, A. M., Crawford, J. E., Brewer, T. R., and Lan, S. (2016). "Calculations of the Response of a Flat Plate Structure To a Column Removal." *The 24th International Symposium on Military Aspects of Blast and Shock*.

Ozden, S., Erdogan, O., and Akpinar, E. (2013). "Punching Shear Behavior under Sustained Load." *International Journal of Engineering and Technology*, 5(6), 671–674.

Paulson, K. A., Nilson, A. H., and Hover, K. C. (1991). "Long-Term Deflection of High-Strength Concrete Beams." *ACI Material Journal*, 88(2), 197–206.

Peng, Z., Orton, S. L., Liu, J., and Tian, Y. (2017). "Experimental Study of Dynamic

Progressive Collapse in Flat-Plate Buildings Subjected to Exterior Column Removal." *Journal of Structural Engineering (United States)*.

Qiuning, Y., Mingjie, M., and Wenbo, Z. (2014). "Effects of Cover Thickness on the Punching Shear Strength of Reinforced Concrete Slabs." *Science & Technology Review*, 93–97.

Rankin, G. I. B., and Long, A. E. (1987). "Predicting the Enhanced Punching Strength of Interior Slab-Column Connections." *Proceedings of the Institution of Civil Engineers (London)*, 82(February), 1165–1186.

Reybrouck, N., Criel, P., Caspeele, R., and Taerwe, L. (2015). "Modelling of Long-Term Loading Tests on Reinforced Concrete Beams." *10th International Conference on Mechanics and Physics of Creep, Shrinkage, and Durability of Concrete and Concrete Structures*, American Society of Civil Engineers, Reston, VA, 745–753.

Richart, F. E., and Heitman, R. H. (1938). "Tests Of Reinforced Concrete Columns Under Sustained Loading." *ACI Journal Proceedings*, 35(9), 33–38.

Ruiz, M. F., Muttoni, A., and Gambarova, P. G. (2007). *Relationship between Nonlinear Creep and Cracking of Concrete under Uniaxial Compression*. *Journal of Advanced Concrete Technology*.

Rusch, B. H. (1960). "Researches Toward a General Flexural Theory for Structural Concrete." *ACI Journal Proceedings*, 57(7).

Saifullah, H. A., Nakarai, K., Piseth, V., Chijiwa, N., and Maekawa, K. (2017). "Shear creep failures of reinforced concrete slender beams without shear reinforcement." *ACI Structural Journal*, 114(6), 1581–1590.

Samra, R. M. (1997). "Time-dependent deflections of reinforced concrete beams

revisited.” *Journal of Structural Engineering*, 123(6), 823–830.

Sarkhosh, R., Walraven, J., and Den Uijl, J. (2015). “Shear-critical reinforced concrete beams under sustained loading Part I: Experiments.” *Heron*, 60(3), 181–205.

Shah, S. P., and Chandra, S. (1970). “Fracture of Concrete Subjected To Cyclic and Sustained Loading.” *J Amer Concrete Inst*, 67(10), 816–827.

Tasevski, D., Muttoni, A., and Ruiz, M. F. (2019). “Time-dependent strength of concrete in compression and shear.”

Tasevski, D., Ruiz, M. F., and Muttoni, A. (2020). “Influence of load duration on shear strength of reinforced concrete members.” *ACI Structural Journal*, 117(2), 157–170.

Viest, I. . M. ., Elstner, R. C., and Hognestad, E. (1956). “Sustained Load Strength of Eccentrically Loaded Short Reinforced Concrete Columns.” *ACI Journal Proceedings*, 52(3).

Wardhana, K., and Hadipriono, F. C. (2003). “Analysis of recent bridge failures in the United States.” *Journal of Performance of Constructed Facilities*, 17(3), 144–150.

Washa, G. W., and Fluck, P. G. (1953). “Effect of Sustained Overload on the Strength and Plastic Flow of Reinforced Concrete Beams.” *ACI Journal Proceedings*, 50(9), 65–72.

Wood, J. G. M. (2003). *Pipers Row Car Park Wolverhampton: Quantitative Study of the Causes of the Partial Collapse on 20th March 1997. Brit. HSE, Final Report*.

Yu, L., Francois, R., and Vu Hiep, D. (2015). “Structural Performance of RC Beams Damaged by Natural Corrosion under Sustained Loading in a Chloride Environment.” *Engineering Structures*, 96, 30–40.

Zhou, F. P. (1992). “Time-dependent crack growth and fracture in concrete.” *Division of*

Building Materials, 132.

APPENDIX A

More Details (Beams)

Formworks with the reinforcement of beams (series I).

Formwork with the reinforcement of beams (series II).

Batch 1

Date: 9/12/2018
Design Water: 54 gal
Design W/C: 0.40**0**
Actual Water: 54 gal
Actual W/C: 0.398
Design Slump: 4”

Concrete mix design quantities.

Material	Design Quantity (per yd^3)	Batch Quantity (per yd^3)	Var
3/8" Coarse Aggregate	1800 lbs	1820 lbs	1.11%
Sand	1400 lbs	1400 lbs	0%
Cement	564 lbs	580 lbs	2.34%
Air entrainer	3.5 oz	3.5 oz	0
Retarder	21.8 oz	22 oz	0.92%
Water	27 gal	27 gal	0%

Batch 2

Date: 8/19/2019
Design Water: 101.3 gal
Design W/C: 0.40**0**
Actual Water: 101 gal
Actual W/C: 0.396
Design Slump: 4”

Concrete mix design quantities.

Material	Design Quantity (per yd^3)	Batch Quantity (per yd^3)	Var
3/8" Coarse Aggregate	1800 lbs	1792 lbs	-0.44%
Sand	1400 lbs	1397.33 lbs	-0.19%
Cement	564 lbs	569.6 lbs	0.99%
Air entrainer	3.5 oz	3.47 oz	-0.95%
Retarder	21.8 oz	21.87 oz	0.31%
Water	27 gal	26.92 gal	-0.25%

APPENDIX B

More Details (Flat Plates)

Pad footing with column reinforcement.

Formwork with reinforcement (Flat plates).

Batch 2

Date: 8/19/2019
Design Water: 101.3 gal
Design W/C: 0.40**0**
Actual Water: 101 gal
Actual W/C: 0.396
Design Slump: 4”

Concrete mix design quantities.

Material	Design Quantity (per yd^3)	Batch Quantity (per yd^3)	Var
3/8" Coarse Aggregate	1800 lbs	1792 lbs	-0.44%
Sand	1400 lbs	1397.33 lbs	-0.19%
Cement	564 lbs	569.6 lbs	0.99%
Air entrainer	3.5 oz	3.47 oz	-0.95%
Retarder	21.8 oz	21.87 oz	0.31%
Water	27 gal	26.92 gal	-0.25%

Batch 3

Date: 12/18/2018
Design Water: 94.5 gal
Design W/C: 0.400
Actual Water: 95 gal
Actual W/C: 0.398
Design Slump: 4”

Concrete mix design quantities.

Material	Design Quantity (per yd^3)	Batch Quantity (per yd^3)	Var
3/8" Coarse Aggregate	1800 lbs	1771.43 lbs	1.59%
Sand	1400 lbs	1394.29 lbs	0.41%
Cement	564 lbs	569.14 lbs	0.91%
Air entrainer	3.5 oz	3.43 oz	2.04%
Retarder	21.8 oz	21.71 oz	0.39%
Water	27 gal	26.86 gal	0.53%

Batch 4

Date: 7/1/2020
Design Water: 131.8 gal
Design W/C: 0.459
Actual Water: 140.5 gal
Actual W/C: 0.485
Design Slump: 6”

Concrete mix design quantities.

Material	Design Quantity (per yd^3)	Batch Quantity (per yd^3)	Var
3/8" Coarse Aggregate	1689 lbs	1684.76 lbs	-0.25%
Sand	1400 lbs	1396.33 lbs	-0.27%
Cement	564 lbs	568.47 lbs	0.79%
Air entrainer	3.5 oz	3.53 oz	0.84%
Retarder	21.8 oz	21.88 oz	0.38%
Water	31 gal	31.08 gal	0.24%

Vita

Mohammed Shubaili was born in Gizan, Saudi Arabia. He earned his bachelor's degree in Civil Engineering in King Saud University in 2009. He received his master's degree in Structural Engineering in University of Pittsburgh in 2015. He started work toward his Ph.D. in Structural Engineering at the University of Missouri in 2017, and he received his doctoral degree in 2021.